



University  
of Antwerp

Faculty of Applied Engineering  
Research group Biochemical Wastewater Valorization and  
Engineering  
(BioWAVE)

**Improving and characterising  
solid-state fungal pretreatment  
by *Phanerochaete chrysosporium*  
for sugar production from poplar wood**

PhD thesis submitted for the  
degree of doctor in applied engineering at the University of  
Antwerp to be defended by ir. Nikolett Wittner

Supervisors:

Prof. dr. ir. Iris Cornet

Prof. dr. ir. Siegfried E. Vlaeminck

Antwerp, 2023

## Disclaimer

The author allows to consult and copy parts of this work for personal use. Further reproduction or transmission in any form or by any means, without the prior permission of the author is strictly forbidden.



University  
of Antwerp

Faculty of Applied Engineering

Biochemical Wastewater Valorization and Engineering (BioWAVE) research group

**Improving and characterising solid-state fungal pretreatment**

**by *Phanerochaete chrysosporium***

**for sugar production from poplar wood**

**Ir. Nikolett Wittner**



## Doctoral jury

Prof. dr. Serge Tavernier	President of the jury University of Antwerp Faculty of Applied Engineering
Prof. dr. ir. Pieter Billen	Secretary of the jury University of Antwerp Faculty of Applied Engineering
Prof. dr. ir. Iris Cornet	Promoter University of Antwerp Faculty of Applied Engineering
Prof. dr. ir. Siegfried. E. Vlaeminck	Promoter University of Antwerp Faculty of Applied Engineering
Prof. dr. ir. Szilveszter Gergely	External member of the jury Budapest University of Technology and Economics Faculty of Chemical Technology and Biotechnology
Dr. ir. Frederik Vaningelgem	External member of the jury International Flavors & Fragrances, Inc.
Prof. dr. ir. Eveline Peeters	External member of the jury Free University of Brussels Department of Bio-engineering Sciences

## Acknowledgements

I would like to express my deepest gratitude to all those who have supported me throughout my journey to complete this PhD.

First and foremost, I am immensely grateful to my supervisors, Prof. Iris Cornet and Prof. Siegfried Vlaeminck for their guidance, mentorship and unwavering support throughout this research endeavour. Their expertise, encouragement, and insightful feedback have been instrumental in shaping this dissertation and enhancing the quality of my work.

I would also like to thank the members of my doctoral committee (Prof. Serge Tavernier, Prof. Szilveszter Gergely, Prof. Pieter Billen, Prof. Eveline Peeters and Dr Frederik Vaningelgem) for their valuable insights, constructive criticism and suggestions, which have contributed immensely to the improvement of my research.

I would like to express my gratitude to my fellow researchers, who have not only been supportive colleagues but have also become dear friends. Their encouragement and shared experiences have made this journey more enjoyable and memorable.

I would like to thank the academic staff and researchers at the University of Antwerp for providing a conducive research environment and access to resources that were essential for the conduct of this study.

My sincere appreciation goes to my family, friends and loved ones for their unwavering support, understanding and encouragement throughout this challenging academic journey. Their love, belief in me and constant motivation have been invaluable.

Finally, I would like to acknowledge the financial support provided by the University of Antwerp (project number 36691) which made it possible for me to carry out this research and pursue my academic goals.

To all those who have contributed directly or indirectly to the completion of this dissertation, I would like to express my sincere gratitude. Your support and contributions have been instrumental in shaping my academic and personal growth.

Thank you all.

## Abstract

Pretreatment is a critical step in the conversion of lignocellulose into biofuels and biochemicals. During pretreatment, the recalcitrance of lignocellulose is reduced, e.g. by removing lignin, thereby making the carbohydrates more accessible for enzymatic saccharification. Fungal delignification by white-rot fungi is a biotechnological alternative to chemical/physicochemical methods, which is carried out in solid-state fermentation with mild reaction conditions and without the formation of microbial inhibitors. However, fungal pretreatment presents some challenges, such as long pretreatment time, non-selective and low delignification, low enzymatic digestibility and feedstock sterilisation requirement, making its commercial implementation challenging compared to conventional methods.

This study investigates the possibility of improving and characterising the solid-state fungal pretreatment of poplar wood by *Phanerochaete chrysosporium*. The individual and combined effects of  $\text{MnSO}_4$  and  $\text{CuSO}_4$  supplements on the delignification of sterilised wood are investigated using response surface methodology to improve the degree and selectivity of fungal delignification. Spore-inoculated solid-state fermentations are carried out for 4 weeks in sterile vented bottles. The mechanism of the concerted action of the metal ions on lignin degradation is then elucidated by relating fungal growth and ligninolytic enzyme activities to lignocellulose degradation as a function of pretreatment time. The optimised metal-supplemented system is then applied to the pretreatment of non-sterilised wood using different inoculation techniques (spores and pre-colonised substrate), nutrients (metal ions with or without glucose and sodium nitrate) and cultivation environments (sterile aerated bottles and open trays). The fermentations are then characterised using infrared spectroscopy, in particular NIR and ATR-FTIR spectroscopy, with the aim of developing rapid lignin quantification methods as an alternative to conventional wet chemical methods. Finally, the feasibility of producing fermentable sugars from sterilised and non-sterilised poplar wood using fungal pretreatment is evaluated through a techno-economic analysis.

Supplementing the pretreatment system with  $2.01 \mu\text{mol CuSO}_4$  and  $0.77 \mu\text{mol MnSO}_4 \text{ g}^{-1}$  wood resulted in 1.9-fold higher lignin degradation, 2.3-fold higher delignification selectivity value and 2.9-fold higher glucose yield. The improved delignification could be explained by the concerted action of  $\text{Mn}^{2+}$  and  $\text{Cu}^{2+}$  ions, with  $\text{Mn}^{2+}$  ions inducing and  $\text{Cu}^{2+}$  prolonging manganese peroxidase production responsible for delignification.

Fungal pretreatment at non-sterile conditions was obtained using trays in a simple solid-state fermentation set-up without sterile aeration. A 1:3 ratio of pre-colonised and untreated wood was applied for inoculation and only  $\text{Cu}^{2+}$ ,  $\text{Mn}^{2+}$  and sodium nitrate as supplements. Remarkably, this technology resulted in a comparably high glucose yield ( $28.51 \pm 0.28\%$ ) to the traditional method using sterilised wood, sterile aeration and spores as inoculum, while reducing the amount of wood to be sterilised by 71.2%.

Infrared spectroscopy-based methods with high coefficients of determination ( $R_{CV}^2 \geq 0.87$ ) were developed for the fast and reliable prediction of lignin in fungus-treated wood.

The techno-economic study showed that using non-sterilised wood as substrate and pre-colonised wood as inoculum resulted in a 14.5% reduction in sugar production costs (€2.15/kg) compared to using sterilised wood. This cost reduction can be attributed to the lower utility costs associated with the reduced need for sterilisation.

Although the evaluation of non-sterilised wood pretreatment showed promising cost reductions, fungal pretreatment remained more expensive than conventional chemical and physicochemical methods due to high capital costs caused by factors such as long pretreatment time and low sugar yields. To overcome these challenges, it is crucial to prioritise further research focusing on screening and engineering fungal strains with fast growth rates, high optimum growth temperature and selective lignin degradation capabilities as well as process optimisation and scale-up. The research of simple reactor designs, such as a pretreatment hall inspired by composting halls, could potentially improve the economics of the process. By combining advances in fungal strain development with innovative reactor designs, it is possible to improve the overall economic feasibility and large-scale applicability of solid-state fungal lignocellulose pretreatment.



## Samenvatting

Voorbehandeling is een kritieke stap bij de omzetting van lignocellulose in biobrandstoffen en biochemicalïen. Tijdens de voorbehandeling wordt de recalcitrantie van lignocellulose verminderd, bijvoorbeeld door lignine te verwijderen, waardoor de koolhydraten toegankelijker worden voor enzymatische versuikering. Schimmeldelignificatie door witrotschimmels is een milieuvriendelijk alternatief voor chemische en fysicochemische methoden, dat wordt uitgevoerd in fermentatie in vaste toestand met milde reactieomstandigheden en zonder de vorming van microbiële remmers. De voorbehandeling door schimmels kent echter een aantal uitdagingen, zoals de lange voorbehandelingstijd, de niet-selectieve en geringe delignificatie, de lage enzymatische verteerbaarheid en de vereiste sterilisatie van de grondstof, waardoor de commerciële toepassing ervan een uitdaging vormt in vergelijking met conventionele methoden.

Deze studie onderzoekt de mogelijkheid om de vaste-stof schimmelvoorbehandeling van populierenhout door *Phanerochaete chrysosporium* te verbeteren en te karakteriseren. De individuele en gecombineerde effecten van  $MnSO_4$  en  $CuSO_4$  supplementen op de delignificatie van gesteriliseerd hout worden onderzocht met behulp van response surface methodologie om de mate en selectiviteit van schimmeldelignificatie te verbeteren.

Met sporen geïnoculeerde vastestoffermentaties worden gedurende 4 weken uitgevoerd in steriele geventileerde flessen. Het mechanisme van de gecoördineerde werking van de metaalionen op de lignineafbraak wordt vervolgens opgehelderd door de schimmelgroei en de ligninolytische enzymactiviteit te relateren aan de lignocelluloseafbraak als functie van de voorbehandelingstijd.

Het geoptimaliseerde systeem met metaalsupplementen wordt vervolgens toegepast op de voorbehandeling van niet-gesteriliseerd hout met behulp van verschillende inoculatietechnieken (sporen en geprekoloniseerd substraat), voedingsstoffen (metaalionen met of zonder glucose en natriumnitraat) en kweekomgevingen (steriele flessen met luchttoevoer en open bakken). De fermentaties worden vervolgens gekarakteriseerd met behulp van infraroodspectroscopie, in het bijzonder NIR- en ATR-FTIR-spectroscopie, met het doel om snelle kwantificeringsmethoden voor lignine te ontwikkelen als alternatief voor conventionele natchemische methoden. Ten slotte wordt de haalbaarheid van de productie van fermenteerbare suikers uit gesteriliseerd en niet-gesteriliseerd populierenhout met behulp van een schimmelvoorbehandeling geëvalueerd door middel van een technisch-economische analyse.

Het aanvullen van het voorbehandelingssysteem met 2,01  $\mu\text{mol}$   $\text{CuSO}_4$  en 0,77  $\mu\text{mol}$   $\text{MnSO}_4 \text{ g}^{-1}$  hout resulteerde in een 1,9-voudig hogere lignineafbraak, een 2,3-voudig hogere selectiviteitswaarde voor delignificatie en een 2,9-voudig hogere glucoseopbrengst. De verbeterde delignificatie kan worden verklaard door de gezamenlijke werking van  $\text{Mn}^{2+}$  en  $\text{Cu}^{2+}$  ionen, waarbij  $\text{Mn}^{2+}$  ionen de productie van mangaanperoxidase, verantwoordelijk voor delignificatie, stimuleren en  $\text{Cu}^{2+}$  deze verlengt. Schimmelvoorbehandeling onder niet-steriele omstandigheden werd verkregen met behulp van trays in een eenvoudige vaste stof fermentatieopstelling zonder steriele beluchting. Een 1:3 verhouding van voorgekoloniseerd en onbehandeld hout werd toegepast voor inoculatie, en alleen  $\text{Cu}^{2+}$ ,  $\text{Mn}^{2+}$  en natriumnitraat als supplementen. Opmerkelijk genoeg resulteerde deze technologie in een vergelijkbaar hoge glucoseopbrengst ( $28,51 \pm 0,28\%$ ) als de traditionele methode waarbij gesteriliseerd hout, steriele beluchting en sporen als inoculum werden gebruikt, terwijl de hoeveelheid te steriliseren hout met 71,2% werd verminderd.

Op infraroodspectroscopie gebaseerde methoden met hoge determinatiecoëfficiënten ( $R_{CV}^2 \geq 0.87$ ) werden ontwikkeld voor een snelle en betrouwbare voorspelling van lignine in schimmelig voorbehandeld hout.

De technisch-economische studie toonde aan dat het gebruik van niet-gesteriliseerd hout als substraat en voorgekoloniseerd hout als inoculum resulteerde in een verlaging van de suikerproductiekosten met 14,5% (€2,15/kg) in vergelijking met het gebruik van gesteriliseerd hout. Deze kostenverlaging kan worden toegeschreven aan de lagere gebruikskosten in verband met de verminderde noodzaak tot sterilisatie.

Hoewel de evaluatie van niet-gesteriliseerde houtvoorbehandeling veelbelovende kostenreducties liet zien, bleef schimmelvoorbehandeling duurder dan conventionele chemische en fysicochemische methoden vanwege de hoge kapitaalkosten veroorzaakt door factoren zoals lange voorbehandelingstijd en lage suikeropbrengsten. Om deze uitdagingen te overwinnen, is het cruciaal om prioriteit te geven aan verder onderzoek dat zich richt op het screenen en ontwikkelen van schimmelstammen met snelle groeisnelheden, een hoge optimale groeitemperatuur en selectieve lignineafbraakcapaciteiten, evenals procesoptimalisatie en opschaling. Het onderzoek van eenvoudige reactorontwerpen, zoals een voorbehandelingshal geïnspireerd op composteringshallen, zou de economische aspecten van het proces kunnen verbeteren. Door vooruitgang in de ontwikkeling van schimmelstammen te combineren met innovatieve reactorontwerpen, is het mogelijk om de algemene economische haalbaarheid en de toepasbaarheid op grote schaal van schimmelpreparaten voor lignocellulose in vaste vorm te verbeteren.

## Table of contents

Doctoral jury.....	I
Acknowledgements.....	II
Abstract .....	III
Samenvatting .....	V
Table of contents.....	VII
List of figures .....	XIII
List of tables .....	XVII
List of abbreviations .....	XIX
Introduction, objectives and thesis outline.....	21
Chapter 1. Literature overview .....	27
1.1 Lignocellulose-based bioeconomy .....	28
1.2 Lignocellulosic biomass .....	29
1.2.1 Structure and recalcitrance of lignocellulose.....	29
1.2.2 Anatomy of plant cell walls .....	31
1.2.3 Poplar wood .....	32
1.3 Lignocellulose pretreatment for enhanced enzymatic saccharification .....	33
1.3.1 Purpose of pretreatment .....	33
1.3.2 Pretreatment methods.....	33
1.3.3 The evaluation of fungal pretreatment efficiency .....	36
1.3.4 Enzymatic saccharification .....	36
1.4 Fungal pretreatment by white-rot fungi .....	37
1.4.1 Mechanism of fungal delignification .....	38
1.4.2 Delignification selectivity .....	42
1.4.3 <i>Phanerochaete chrysosporium</i> , a non-laccase-producing WRF .....	43
1.5 Solid-state fermentation (SSF) for fungal pretreatment.....	45
1.5.1 General aspects of SSF .....	45
1.5.2 Factors influencing the fungal SSF.....	45
1.5.2.1 Moisture content.....	46

## Table of contents

---

1.5.2.2	Temperature .....	46
1.5.2.3	Aeration .....	46
1.5.2.4	Particle size .....	47
1.5.2.5	Pretreatment time .....	47
1.5.2.6	pH.....	47
1.5.2.7	Decontamination .....	48
1.5.2.8	Inoculum .....	48
1.5.2.9	Supplements .....	49
1.5.2.9.1	Metal supplements.....	50
1.5.3	Bioreactors for fungal SSF.....	51
1.5.3.1	Tray fermenters .....	53
1.5.3.2	Packed bed bioreactors .....	54
1.5.3.3	Rotary drum bioreactors .....	55
1.6	Monitoring lignin degradation during fungal pretreatment .....	55
1.6.1	Conventional methods .....	55
1.6.2	Infrared spectroscopy-based methods.....	56
1.6.2.1	Mid-infrared spectroscopy .....	56
1.6.2.1.1	FTIR spectroscopy.....	58
1.6.2.1.2	Attenuated total reflectance .....	59
1.6.2.2	Near-infrared spectroscopy.....	60
1.6.2.2.1	Diffuse reflectance mode .....	60
1.6.2.3	Pre-processing and multivariate analysis of spectral data .....	61
1.6.2.3.1	Standard normal variate.....	62
1.6.2.3.2	Derivatives .....	62
1.6.2.3.3	Principle component analysis.....	64
1.6.2.3.4	Partial Least Squares Regression.....	65
1.6.2.4	Application for lignin quantification in fungus-treated wood.....	66
1.7	Techno-economic feasibility of fungal pretreatment.....	66
Chapter 2.	Enhanced fungal delignification and enzymatic digestibility of poplar wood by combined CuSO <sub>4</sub> and MnSO <sub>4</sub> supplementation .....	69

---

2.1	Introduction.....	71
2.2	Materials and Methods.....	72
2.2.1	Fungal strain and spore suspension preparation.....	72
2.2.2	Lignocellulose substrate.....	72
2.2.3	Medium.....	73
2.2.4	Fungal pretreatment.....	73
2.2.5	Experimental design and statistical analysis.....	75
2.2.5.1	Influence of metal supplementation by Response Surface Methodology.....	75
2.2.5.2	Effect of metal supplementation on ligninolytic enzyme production.....	76
2.2.6	Analytical methods.....	76
2.2.6.1	Enzyme extraction.....	76
2.2.6.2	Ligninolytic enzyme assays.....	77
2.2.6.3	Total protein determination.....	77
2.2.6.4	Composition analysis of lignocellulose.....	77
2.2.6.5	Fungal growth measurement.....	79
2.2.6.6	Enzymatic saccharification of pretreated biomass.....	80
2.2.6.7	Characterization of pretreated biomass by FTIR.....	80
2.3	Results and discussion.....	81
2.3.1	Effect of metal supplements based on RSM.....	81
2.3.1.1	Degradation of biomass.....	81
2.3.1.2	Enzymatic saccharification by a commercial enzyme complex.....	85
2.3.2	The concerted actions of Mn <sup>2+</sup> and Cu <sup>2+</sup> on improved delignification.....	91
2.3.3	Characterization of biomass by FTIR spectroscopy.....	93
2.4	Conclusions.....	94
Chapter 3.	To sterilise or not to sterilise? Comparable saccharification yields obtained after fungal pretreatment of non-sterilised poplar wood.....	95
3.1	Introduction.....	97
3.2	Materials and Methods.....	98
3.2.1	Lignocellulose substrate.....	98

## Table of contents

---

3.2.2	Fermentation media .....	99
3.2.3	Inoculum preparation .....	99
3.2.4	Solid-state fungal pretreatment .....	100
3.2.5	Analytical methods .....	101
3.2.5.1	Compositional analysis .....	101
3.2.5.2	Enzymatic saccharification .....	102
3.2.6	Statistical analysis .....	102
3.3	Results and discussion .....	102
3.3.1	Spore-inoculated solid-state fermentation .....	102
3.3.2	Pre-colonised wood as inoculum .....	105
3.3.3	Application on new sawdust feedstock .....	110
3.4	Conclusion .....	113
Chapter 4.	Rapid lignin quantification for fungal wood pretreatment by ATR-FTIR spectroscopy	115
4.1	Introduction .....	117
4.2	Materials and Methods .....	118
4.2.1	Lignocellulose substrate and white-rot fungi .....	118
4.3	Fermentation media .....	118
4.4	Solid-state fungal pretreatment .....	119
4.5	Analytical methods .....	122
4.5.1	Removal of water-soluble substances .....	122
4.5.2	Total protein determination .....	122
4.5.3	Analysis of phenolic compounds .....	122
4.5.4	Fungal biomass estimation .....	123
4.5.5	Acid-insoluble lignin determination .....	123
4.5.6	Milling .....	123
4.5.7	ATR-FTIR analysis .....	124
4.5.8	Spectral data processing and multivariate analysis .....	124
4.6	Results and Discussion .....	125
4.6.1	Interpretation of ATR-FTIR spectra and PCA .....	125

---

4.6.2	Estimation of lignin content from ATR-FTIR.....	130
4.7	Conclusions.....	132
Chapter 5.	Follow-up of solid-state fungal wood pretreatment by a novel near-infrared spectroscopy-based lignin calibration model.....	133
5.1	Introduction.....	135
5.2	Materials and Methods.....	136
5.2.1	Poplar wood substrate and white-rot fungi.....	136
5.2.2	Solid-state fungal pretreatment.....	136
5.2.3	Analytical methods.....	137
5.2.3.1	Removal of water-soluble substances.....	137
5.2.3.2	Lignin quantification.....	137
5.2.3.3	Milling.....	138
5.2.3.4	NIR analysis.....	138
5.2.3.5	Spectral data processing and multivariate analysis.....	138
5.3	Results and Discussion.....	139
5.3.1	NIR spectra of fungus-treated wood.....	139
5.3.2	Development of PLSR models for lignin quantification.....	141
5.4	Conclusions.....	148
Chapter 6.	Techno-economic evaluation of fungal pretreatment for sugar production from sterilised and non-sterilised wood.....	149
6.1	Introduction.....	151
6.2	Materials and Methods.....	152
6.3	Techno-economic assessment.....	152
6.3.1	Process design and modelling.....	152
6.3.2	Data sources.....	153
6.3.3	Process description.....	153
6.3.4	Economic analysis.....	156
6.3.5	Economic global sensitivity analysis.....	157
6.4	Results and discussion.....	158
6.4.1	Economic performance of process scenarios.....	158

Table of contents

---

6.4.2 Global sensitivity analysis ..... 163

6.5 Conclusion ..... 164

Chapter 7. General conclusions and outlook for future work..... 165

7.1 General conclusions..... 166

7.2 Outlook for future work ..... 169

7.2.1 Fundamental research..... 169

7.2.2 Applied research..... 171

Appendix..... 173

References ..... 175

Curriculum vitae ..... 203



## List of figures

<b>Fig. 0.1</b> Thesis overview.....	23
<b>Fig. 1.1</b> Conversion of lignocellulosic biomass to biofuel [26].....	28
<b>Fig. 1.2</b> Structure of lignocellulosic biomass and its biopolymers cellulose, hemicellulose and lignin [30] .....	29
<b>Fig. 1.3</b> Structure of lignin [31].....	31
<b>Fig. 1.4</b> Different layers of the plant cell wall [37] .....	32
<b>Fig. 1.5</b> Overview of the main pretreatment methods available for lignocellulosic biomass [53]. SPORL = sulfite pretreatment to overcome recalcitrance of lignocellulose .....	34
<b>Fig. 1.6</b> A simplified schematic representation of the enzymatic action of cellulase on cellulose [57]. .....	37
<b>Fig. 1.7</b> Catalytic cycle of lignin peroxidase [71] .....	40
<b>Fig. 1.8</b> The catalytic cycle of manganese peroxidase [73].....	41
<b>Fig. 1.9</b> Schematic diagram of lignin degradation by white-rot fungi [62]. Lac: laccase, LMS: laccase-mediator system, LiP: lignin peroxidase, MnP: manganese peroxidase, VP: versatile peroxidase, H <sub>2</sub> O <sub>2</sub> -GO: H <sub>2</sub> O <sub>2</sub> -generating oxidases, AAO: aryl-alcohol oxidase, GLOX: glyoxal oxidase, ADD: aryl-alcohol dehydrogenases, QR: quinone reductases .....	42
<b>Fig. 1.10</b> Wood degradation by <i>P. chrysosporium</i> [84] .....	43
<b>Fig. 1.11</b> Life cycle of Basidiomycota [90] .....	44
<b>Fig. 1.12</b> Schematic diagram of tray reactor [98].....	54
<b>Fig. 1.13</b> Schematic diagram of packed bed bioreactor [130] .....	54
<b>Fig. 1.14</b> Schematic representation of rotary drum bioreactor (Adapted from Ref. [127]) .....	55
<b>Fig. 1.15</b> Vibrations modes [137] .....	57
<b>Fig. 1.16</b> Group frequencies and fingerprint region of the MIR spectrum [136] .....	57
<b>Fig. 1.17</b> Schematic diagram of Fourier transform infrared spectrometer [139] .....	58
<b>Fig. 1.18</b> Schematic diagram of the ATR measuring mode [141] .....	59
<b>Fig. 1.19</b> NIR bands [144] .....	60
<b>Fig. 1.20</b> Schematic diagram of diffuse reflectance [146].....	61
<b>Fig. 1.21</b> Effect of first and second derivative on the spectra: (A) original spectra, (B) first-derivative spectra, and (C) second-derivative spectra. 1, zero baseline; 2, linear sloping baseline; 3, curved (quadratic) baseline with offset [150]. .....	63
<b>Fig. 2.1</b> Graphical abstract.....	70
<b>Fig. 2.2</b> Cumulative percentage of wood passing through the sieves .....	73
<b>Fig. 2.3</b> Fermentation bottles placed on a bottle roller .....	74
<b>Fig. 2.4</b> Moisture content of poplar wood during SSF under different metal supplementation, i.e. (●) without supplement, (→) with 2.18 μmol CuSO <sub>4</sub> g <sup>-1</sup> DW	

wood, (—■—) 1.09  $\mu\text{mol MnSO}_4 \text{ g}^{-1}$  DW wood, and (—✕—) 2.18  $\mu\text{mol CuSO}_4$  and 1.09  $\mu\text{mol MnSO}_4 \text{ g}^{-1}$  DW substrate. The orange-coloured vertical lines show the time of the water addition. .... 74

**Fig. 2.5** Response surface plot of interactions between  $\text{Cu}^{2+}$  and  $\text{Mn}^{2+}$  dosages for (a) acid-insoluble lignin degradation and (b) increase of acid-soluble lignin content after pretreatment of poplar wood ..... 82

**Fig. 2.6** Response surface plot of interactions of  $\text{Cu}^{2+}$  and  $\text{Mn}^{2+}$  variables and total lignin degradation after pretreatment of poplar wood ..... 82

**Fig. 2.7** Response surface plot of interactions of  $\text{Cu}^{2+}$  and  $\text{Mn}^{2+}$  variables and total lignin degradation under 0–4.36  $\mu\text{mol metal ion g}^{-1}$  DW wood supplement dosages . 84

**Fig. 2.8** (a) Xylan consumption and (b) xylan/glucan consumption ratio after pretreatment of poplar wood as a function of  $\text{MnSO}_4$  and  $\text{CuSO}_4$  supplements ..... 84

**Fig. 2.9** Selectivity value in the function of  $\text{MnSO}_4$  and  $\text{CuSO}_4$  pretreatment variables after pretreatment of poplar wood..... 85

**Fig. 2.10** Response surface plot of interactions between  $\text{Cu}^{2+}$  and  $\text{Mn}^{2+}$  supplements and reducing sugar yield..... 86

**Fig. 2.11** Positive linear correlation between glucose yield and acid-insoluble lignin degradation ..... 87

**Fig. 2.12** Degradation of (■) lignin; (▨) glucan and (▩) xylan using different pretreatment time..... 87

**Fig. 2.13** Glucose yield obtained for SSFs performed for different time..... 88

**Fig. 2.14** Time course of the important responses for the SSF mechanism, with (a) MnP activities, (b) total lignin degradation, (c) fungal growth, and (d) glucan degradation (—●—) without supplement, (—▲—) with 2.18  $\mu\text{mol CuSO}_4 \text{ g}^{-1}$  DW wood, (—■—) 1.09  $\mu\text{mol MnSO}_4 \text{ g}^{-1}$  DW wood, and (—✕—) 2.18  $\mu\text{mol CuSO}_4$  and 1.09  $\mu\text{mol MnSO}_4 \text{ g}^{-1}$  DW substrate. STD values are obtained for analytical replicates (duplicate-MnP activity, triplicate-biomass degradation, fixed standard deviation of fungal growth determination (as described in 2.2.6.5) ..... 92

**Fig. 2.15** FTIR characterization of (—) untreated and pretreated poplar wood (—) without supplements; (—) with 2.18  $\mu\text{mol CuSO}_4 \text{ g}^{-1}$  DW wood; (—) 1.09  $\mu\text{mol MnSO}_4 \text{ g}^{-1}$  DW wood and (—) 2.18  $\mu\text{mol CuSO}_4$  and 1.09  $\mu\text{mol MnSO}_4 \text{ g}^{-1}$  DW substrate ..... 94

**Fig. 3.1** Graphical abstract..... 96

**Fig. 3.2** Pre-colonised wood prepared in the 1 L Schott bottle. The white spots indicate the growth of *P. chrysosporium* ..... 99

**Fig. 3.3** Poplar wood pretreated in a tray. The white spots indicate the growth of *P. chrysosporium*. ..... 100

**Fig. 3.4** Lignocellulose degradation after spore-inoculated pretreatment of (■) sterilised and (▩) non-sterilised wood in the presence of metal salts (M), metal salts with glucose (M+G), metal salts with  $\text{NaNO}_3$  (M+N), metal salts with glucose and  $\text{NaNO}_3$  (M+G+N) or metals salts with a complex medium (M+CM)..... 103

<b>Fig. 3.5</b> Degradation of (■) lignin; (▨) glucan and (▩) xylan after spore-inoculated pretreatment of sterilised wood in the presence of metal salts (M), metal salts with glucose (M+G), metal salts with glucose and NaNO <sub>3</sub> (M+G+N) and metals salts with a complex medium (M+CM) .....	104
<b>Fig. 3.6</b> The obtained (■) glucose and (▩) xylose yield after the enzymatic saccharification of previously sterilised wood pretreated in the presence of metal salts alone (M), with glucose (M+G), with NaNO <sub>3</sub> (M+N), with glucose and NaNO <sub>3</sub> (M+G+N) and with a complex medium (M+CM).....	104
<b>Fig. 3.7</b> Glucose yield after pretreatment of non-sterilised wood inoculated with pre-colonised wood in bottles, without any supplements (None) and in the presence of metal salts alone (M), with NaNO <sub>3</sub> (M+N), with glucose or with glucose and NaNO <sub>3</sub> (M+G+N). Supplements were used with the dosages of 10.9 mg glucose, 1.6 mg NaNO <sub>3</sub> , 0.10 mg MnSO <sub>4</sub> ·H <sub>2</sub> O and 0.38 mg CuSO <sub>4</sub> ·5H <sub>2</sub> O per g wood.....	106
<b>Fig. 3.8</b> Degradation of (■) lignin; (▨) glucan and (▩) xylan after pretreatment of sterilised wood in bottles (B_sterile), non-sterilised wood in bottles (B_non-sterile) and in trays (T_non-sterile) in the presence of metal salts (M) or metal salts with NaNO <sub>3</sub> (M+N) .....	107
<b>Fig. 3.9</b> (a) Glucose and (b) xylose yield after the enzymatic saccharification of (■) sterilised wood pretreated for 4 weeks in bottles and non-sterilised wood pretreated for 4 weeks (▩) in bottles or (▨) in trays in the presence of metal salts (M) and metal salts with NaNO <sub>3</sub> (M+N). .....	107
<b>Fig. 3.10</b> The obtained (■) glucose and (▩) xylose yield after the enzymatic saccharification of wood pretreated in bottles applying different mixing ratios of pre-colonised and untreated wood (mixing ratios are indicated in brackets) in the presence of metal salts (M) and metal salts with NaNO <sub>3</sub> (M+N).....	109
<b>Fig. 3.11</b> The obtained (■) glucose and (▩) xylose yield after the enzymatic saccharification of wood pretreated in trays for different pretreatment times .....	110
<b>Fig. 3.12</b> Composition of Sawdust Optimised (■) and Sawdust New (■) .....	111
<b>Fig. 3.13</b> Comparison of glucose yields obtained after the enzymatic saccharification of two different sawdust batches with and without pretreatment and metal supplementation .....	112
<b>Fig. 3.14</b> The obtained (■) glucose and (▨) xylose yield after the enzymatic saccharification of Sawdust New pretreated in trays for different pretreatment times .....	112
<b>Fig. 4.1</b> Graphical abstract.....	116
<b>Fig. 4.2</b> FTIR characterization of (—) manganese peroxidase (MnP), (—) <i>P. chrysosporium</i> , (—) untreated poplar wood, and pretreated poplar wood (—) with and (—) without washing.....	125
<b>Fig. 4.3</b> The individual variance ((▨) calibration; (▨) validation) and cumulative variance ((■) calibration; (●) validation) explained by principal component analysis	128

<b>Fig. 4.4</b> PCA scores of the first two principal components for (●) washed and (■) non-washed fungus-treated poplar wood samples .....	129
<b>Fig. 4.5</b> PCA loading plot of the first principal component.....	129
<b>Fig. 4.6</b> The predicted vs. reference acid-insoluble lignin (AIL) values of (■) calibration and (●) validation.....	131
<b>Fig. 4.7</b> Regression coefficients of PLSR factor-4 for acid-insoluble lignin determination .....	132
<b>Fig. 5.1</b> Raw (a) and Savitzky-Golay second derivative ( $D_2$ , 11 smoothing points) of SNV-treated NIR spectra (b) of (—) untreated poplar wood and pretreated poplar wood (—) with and (—) without washing .....	140
<b>Fig. 5.2</b> The predicted vs. reference acid-insoluble lignin (AIL) values of (■) calibration and (●) validation based PLSR30 model <b>Table 5.1</b> .....	143
<b>Fig. 5.3</b> Regression coefficients of the PLSR30 model ( <b>Table 5.1</b> ) for acid-insoluble lignin determination .....	143
<b>Fig. 6.1</b> Process flow diagrams and mass balances are presented for a fungal pretreatment-based wood biorefinery producing 135,000 tonnes of sugar per year (16.9 tonnes per hour) in two scenarios: (A) Scenario I and (B) Scenario II. The feedstock is sterilised by autoclaving. Fungal mycelium is prepared in an air-lift fermenter. Solid-state fungal pretreatment and pre-colonised wood preparation are performed in a packed bed bioreactor. Wet mass flows are shown in italics, with the equivalent dry mass values in brackets. Please note that values may not add up exactly due to rounding. Aeration flows are not included in the graphs. ....	158
<b>Fig. 6.2</b> (A) The contribution of (■) fixed capital investment, (■) working capital, (■) land cost, (■) variable operating and (■) fixed operating cost to the levelised sugar production cost. (B) Annual variable operating costs in (■) Scenario I and (■) Scenario II. ....	161
<b>Fig. 6.3</b> Global sensitivity analysis results for (■) Scenario I and (■) Scenario II .....	164

## List of tables

<b>Table 1.1</b> Composition of different lignocellulosic biomass [27].....	30
<b>Table 1.2</b> The main advantages and disadvantages of the common pretreatment methods [25,48–50] .....	35
<b>Table 1.3</b> Features of the fungal ligninolytic enzymes (Adapted from Ref. [63]) .....	39
<b>Table 1.4</b> Performance parameters of the common solid-state fermenters used for fungal pretreatment. Adapted from Ref. [127] by presenting only the three SSF reactors discussed in this section.....	52
<b>Table 1.5</b> Comparison of different pretreatment methods on the basis of techno-economic and environmental parameters (Adapted from Ref. [164]) .....	67
<b>Table 2.1</b> Central Composite Design 1 (CCD1) .....	76
<b>Table 2.2</b> Composition of raw feedstock, autoclaved (control) poplar wood from CCD1, and autoclaved (initial) wood from experiments described in 2.5.2. ....	79
<b>Table 2.3</b> Heavy metal content of poplar wood .....	81
<b>Table 2.4</b> Central Composite Design 2 (CCD2) .....	83
<b>Table 2.5</b> Biomass degradation and sugar yields after fungal pretreatment of hardwood by white-rot fungi .....	89
<b>Table 2.6</b> Degradation of lignin in relation to fungal growth, MnP activity and specific MnP activity measured after 27 days of fermentation with and without $\text{Cu}^{2+}$ and $\text{Mn}^{2+}$ supplementation .....	93
<b>Table 4.1</b> Fermentation conditions and the corresponding acid-insoluble lignin content .....	120
<b>Table 4.2</b> ATR-FTIR peak assignment in poplar wood with and without fungal pretreatment.....	126
<b>Table 5.1</b> Results of NIR spectroscopy-based PLSR models for lignin quantification ..	142
<b>Table 5.2</b> Regression coefficients (line plots) and predicted vs reference data (scatter plots) of NIR spectroscopy-based PLSR models for lignin quantification .....	144
<b>Table 6.1</b> Feedstock properties.....	153
<b>Table 6.2</b> Fungal pretreatment conditions, lignocellulose degradation and enzymatic digestibility in Scenario I and II.....	155
<b>Table 6.3</b> Main techno-economic assessment assumptions. (FCI: Fixed Capital Investment; ISBL: Inside the Battery Limits) .....	157
<b>Table 6.4</b> Energy requirements of the main units for Scenario I and II .....	159
<b>Table 6.5</b> Size, quantity and installation cost of major equipment used in Scenario I and II.....	162



## List of abbreviations

<b>AIL</b>	Acid-insoluble lignin
<b>ANOVA</b>	Analysis of variance
<b>ASL</b>	Acid-soluble lignin
<b>ATR</b>	Attenuated total reflectance
<b>B</b>	Bottle
<b>C</b>	Calibration
<b>CAPEX</b>	Capital expenditure
<b>CCD</b>	Central composite design
<b>CV</b>	Cross-validation
<b>CRISPR</b>	Clustered regularly interspaced short palindromic repeats
<b>DW</b>	Dry weight
<b>FCI</b>	Fixed capital investment
<b>FTIR</b>	Fourier transform infrared
<b>G-S</b>	Gap-segment
<b>HPLC</b>	High-performance liquid chromatography
<b>LiP</b>	Lignin peroxidase
<b>M</b>	Metal salts
<b>MIR</b>	Mid-infrared
<b>MnP</b>	Manganese peroxidase
<b>M+CM</b>	Metal salts and complex medium
<b>M+G</b>	Metal salts and glucose
<b>M+G+N</b>	Metal salts, glucose and sodium nitrate
<b>M+N</b>	Metal salts and sodium nitrate
<b>NF</b>	Number of factors
<b>NIR</b>	Near-infrared
<b>NREL</b>	National Renewable Energy Laboratory
<b>OPEX</b>	Operating expenditure
<b>PC</b>	Principal component
<b>PCA</b>	Principal component analysis
<b>PCR</b>	Polymerase chain reaction
<b>PBB</b>	Packed bed bioreactor
<b>PLSR</b>	Partial least squares regression
<b>RDB</b>	Rotary drum bioreactor
<b>RMSE</b>	Root mean square error

## List of abbreviations

---

<b>RSM</b>	Response surface methodology
<b>SG</b>	Savitzky-Golay
<b>SNV</b>	Standard normal variate
<b>SSF</b>	Solid-state fermentation
<b>STD</b>	Standard deviation
<b>SV</b>	Selectivity value
<b>T</b>	Tray
<b>TIC</b>	Total indirect cost
<b>TDC</b>	Total direct cost
<b>UV-Vis</b>	Ultraviolet-visible
<b>VP</b>	Versatile peroxidase
<b>WRF</b>	White-rot fungi
<b>YM</b>	Yeast mould



## Introduction, objectives and thesis outline

### Introduction and research gaps

Using lignocellulosic biomass as a renewable resource is a critical component of the growing bio-based economy for producing biofuels and biochemicals. Among the lignocellulosic biomasses, poplar wood is considered a promising feedstock due to its fast growth rate, in the Northern Hemisphere its availability for harvest over the whole year and higher bulk density compared to herbaceous feedstock [1]. The first step in many lignocellulose valorisation processes is the pretreatment [2–4]. The aim of biomass pretreatment is to reduce biomass recalcitrance, e.g. by removing lignin and to improve the accessibility of the structural carbohydrates, cellulose and hemicellulose, to hydrolytic enzymes during enzymatic saccharification. These (hemi)cellulolytic enzymes release sugars that microorganisms can convert into biofuels and biochemicals.

Chemical and physicochemical pretreatments have been extensively studied, but they often use harsh reaction conditions and harmful chemicals and release inhibitory compounds that can interfere with the later fermentation process. Fungal pretreatment is a promising alternative due to its mild reaction conditions and the absence of microbial inhibitory by-products [5]. White-rot fungi are considered to be the most efficient lignin-degrading microorganisms due to their ability to mineralise lignin via their unique ligninolytic enzyme system efficiently. *Phanerochaete chrysosporium* is one of the most widely studied fast-growing white-rot fungi, which produces manganese peroxidase (MnP) and lignin peroxidase (LiP) but no laccase to degrade lignin [6–9]. White-rot fungi mainly degrade lignin at the expense of cellulose and hemicellulose consumption, reducing the carbohydrate content of the feedstock available for the production of biofuels and biochemicals. The delignification selectivity of fungal pretreatment is commonly measured by the selectivity value (SV), which is determined by the ratio of lignin degradation to cellulose degradation. Besides non-selective delignification, fungal pretreatment also suffers from the drawbacks of longer pretreatment time (several weeks), lower sugar yields due to low and non-selective delignification, and feedstock sterilisation requirements [10].

Further research is needed to improve our understanding of the process and overcome its challenges to enable the large-scale implementation of the fungal pretreatment process. One of the approaches to improve fungal pretreatment is the use of supplements. Several studies have focused on the use of  $\text{Cu}^{2+}$  and  $\text{Mn}^{2+}$  to enhance the

ligninolytic enzyme activities of *P. chrysosporium* in liquid cultures [11–13]. While trace amounts of metal ions can be beneficial for fungal growth, in excess, they can inhibit growth [14]. Additionally, when used in excess, oxidising metal ions such as  $\text{Cu}^{2+}$  can modify cellulose, resulting in decreased enzymatic digestibility in their optimal amount to avoid adverse effects. The combined effect and optimal dosage of  $\text{Mn}^{2+}$  and  $\text{Cu}^{2+}$  ions in the solid fungal pretreatment of poplar wood by *P. chrysosporium* is unknown (Research gap 1).

Most fungal pretreatment studies have been carried out using sterilised feedstock directly inoculated with fungal spores or mycelia. Direct inoculation of non-sterilised feedstock often resulted in low pretreatment efficiency due to the outcompetition of the white-rot fungus by the indigenous microorganisms [15,16]. However, a few studies have reported effective fungal pretreatment using a different inoculation strategy, i.e. first growing the white-rot fungi on sterilised feedstock and then using the pre-colonised substrate as inoculum during fungal pretreatment [15,17]. This inoculation technique has not yet been investigated for the fungal pretreatment of non-sterilised poplar wood by *Phanerochaete chrysosporium* to reduce the energy requirements of the process (Research gap 2).

Delignification during fungal pretreatment significantly improves the enzymatic digestibility of pretreated biomass. Moreover, a positive linear correlation between the achievable enzymatic saccharification yield and lignin degradation has been reported, emphasising the importance of monitoring the lignin degradation during fungal pretreatment [18]. However, the most commonly used method for lignin quantification, which involves a two-step acid hydrolysis of the biomass, is very laborious and time-consuming. Attenuated Total Reflectance Fourier transform mid-infrared spectroscopy (ATR-FTIR) and near-infrared spectroscopy (NIR) in reflectance mode have been used as rapid and simple alternatives to quantify lignin in wood [19–23]. However, these spectroscopic techniques have not yet been applied to the determination of lignin in wood pretreated with white-rot fungi for the purpose of a biorefinery concept (Research gap 3).

Solid-state fungal pretreatment is a biotechnological method with great potential and is often considered to be cost-effective. However, only a very few studies assessed the techno-economic feasibility of fungal pretreatment on a commercial scale, and they reported significantly higher fermentable sugar production costs than those obtained by conventional chemical and physicochemical pretreatment methods [10,24]. These

outcomes emphasise the importance of further process optimisation and performing techno-economic assessment enabling the large-scale application of solid-state fungal pretreatment. The techno-economic performance of fungal pretreatment of poplar wood by *P. chrysosporium* has not yet been evaluated (Research gap 4).

The main research goal of the present PhD research was to improve and characterise the solid-state fungal pretreatment of poplar wood by *Phanerochaete chrysosporium* by addressing the above-described research gaps.

### **Thesis outline and research objectives**

The PhD manuscript is divided into seven chapters. The first chapter comprehensively reviews the scientific literature relevant to the PhD study. Chapters 2-6 describe the PhD research and its findings. The thesis ends with the main conclusions of this work and provides some suggestions for future research (Chapter 7).

The research articles in Chapters 2-5 have been published or are under review in peer-reviewed journals, while Chapter 6 will form the basis of a future publication. These chapters follow the same structure, with a concise abstract of the chapter, followed by a literature review on the subtopic, a section describing the experimental design and methodology, and finally, a conclusion summarising the main findings of the given chapter. The objectives of each chapter are summarized below, with **Fig. 0.1** showing an overview of the PhD thesis.

### **Chapter 1. Literature overview**

Chapter 1 provides general information on lignocellulosic biomass and its conversion to fermentable sugars through pretreatment and enzymatic saccharification. An overview of the various pretreatment techniques is given, emphasising solid-state fungal pretreatment using white-rot fungi. The mechanism of fungal delignification, culture parameters, advantages, disadvantages and reactor designs associated with solid-state fungal pretreatment are discussed. The fungal delignification monitoring methods are introduced, starting with conventional wet-chemical methods and moving on to infrared spectroscopy coupled with multivariate analysis as a fast and simple alternative.

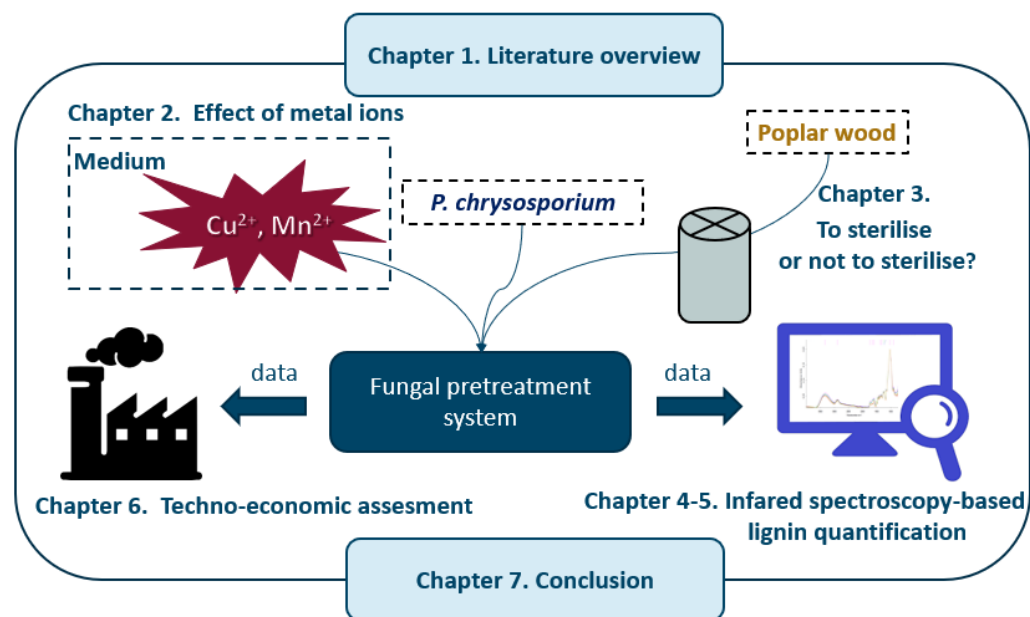


Fig. 0.1 Thesis overview

## Chapter 2. Enhanced fungal delignification and enzymatic digestibility of poplar wood by combined CuSO<sub>4</sub> and MnSO<sub>4</sub> supplementation

Since some of the main drawbacks of lignocellulose pretreatment by white-rot fungi are the low and non-selective lignin degradation, improving the efficiency and selectivity of fungal delignification by combined metal supplementation with Mn<sup>2+</sup> and Cu<sup>2+</sup> is the main objective of this chapter. Better knowledge and insight into the effects of metal ions on solid-state fungal pretreatment of poplar wood by *P. chrysosporium* will be gained by measuring fungal growth and the production of ligninolytic enzymes and relating these to lignocellulose degradation.

## Chapter 3. To sterilise or not to sterilise? Comparable saccharification yields obtained after fungal pretreatment of non-sterilised poplar wood

One of the main bottlenecks in the applied fungal pretreatment is the need for substrate sterilisation, contributing to low techno-economic performance. The main objective of the chapter is to investigate the use of pre-colonised wood to inoculate non-sterilised poplar wood, thereby reducing the sterilisation requirement of the process. This main research goal includes the comparison of inoculation with spores and with pre-colonised wood and the evaluation of different fermentation supplements (metal ions with or without glucose and sodium nitrate) and cultivation methods (sterile vented

bottles and open trays) to optimise the fungal pretreatment process of non-sterilised substrate.

#### **Chapter 4. Rapid lignin quantification for fungal wood pretreatment by ATR-FTIR spectroscopy**

Monitoring lignin degradation during solid fungal pretreatment requires a laborious and time-consuming compositional analysis by two-step acid hydrolysis. Therefore, a fast and simple alternative method using ATR-FTIR coupled with multivariate analysis, such as Partial Least Squares Regression (PLSR), is to be developed. This method development requires a large amount of experimental data, i.e. pretreated wood samples with known lignin content measured by conventional two-step acid hydrolysis as a reference method, obtained in Chapters 2-3.

#### **Chapter 5. Follow-up of solid-state fungal wood pretreatment by a novel near-infrared spectroscopy-based lignin calibration model**

Similar to Chapter 4, this chapter aims to develop a quick and easy method for lignin quantification, but using NIR spectroscopy in reflectance mode instead of ATR-FTIR. Comparing the predictive performance of the ATR-FTIR and NIR spectroscopy-based methods using the same fungal-treated sample set provides important information regarding the correct choice of IR instrumentation, spectral data processing and modelling.

#### **Chapter 6. Techno-economic evaluation of fungal pretreatment for sugar production from sterilised and non-sterilised wood**

The purpose of Chapter 6 is to compare the techno-economic feasibility of commercial-scale fungal pretreatment for the production of fermentable sugars from sterilised and non-sterilised poplar wood using the experimental data obtained in Chapters 2-4. The two scenarios, one using sterilised wood inoculated with mycelia and the other non-sterilised wood inoculated with pre-colonised wood, are compared on the basis of the cost of sugar production and the capital and operating expenditure to assess their techno-economic feasibility.

#### **Chapter 7. General conclusions and outlook for future work**

The results of the present PhD research are summarised, and possible future research directions are suggested.



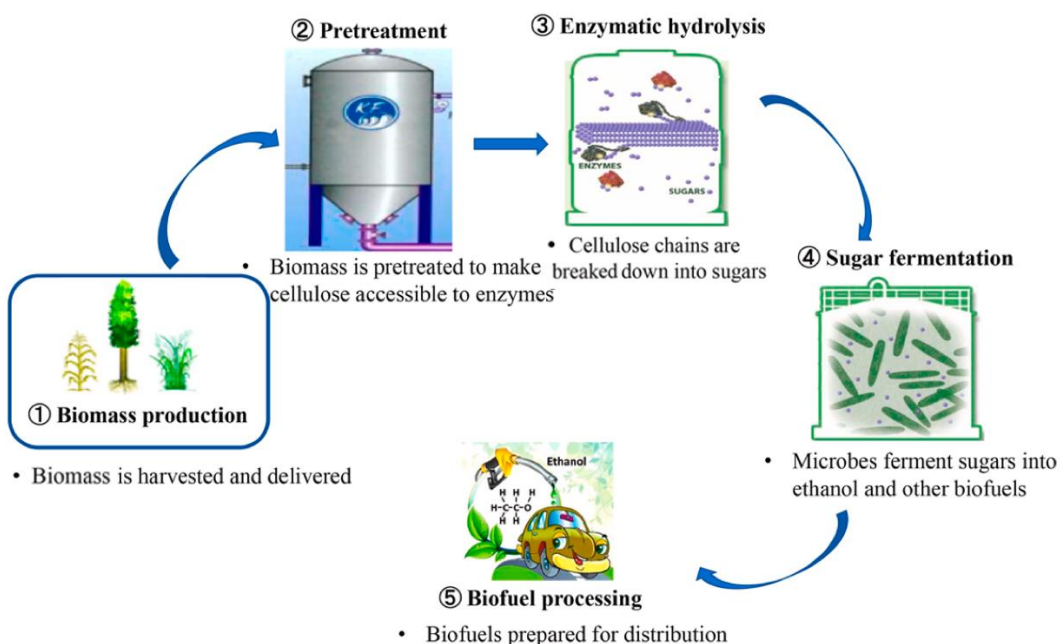
## **Chapter 1. Literature overview**

---

## 1.1 Lignocellulose-based bioeconomy

With a rapidly growing population and rising living standards, the demand for energy is increasing worldwide. The commonly used non-renewable fossil fuels contribute to environmental challenges such as air pollution, global warming and climate change. In contrast, lignocellulosic biomass from plant cell walls is an inexpensive and abundantly available renewable resource with an annual production of  $15 - 17 \times 10^{10}$  t and can be used to produce biofuels and high-value biochemicals [25].

Lignocellulose mainly comprises the polysaccharides cellulose and hemicellulose and the polyaromatic compound lignin. In order to obtain sugars from lignocellulose in a biorefinery, lignocellulose must undergo the process steps of pretreatment and subsequent enzymatic hydrolysis (**Fig. 1.1**). The pretreatment reduces the recalcitrance of lignocellulose and thus improves the accessibility of the carbohydrates to (hemi)cellulolytic enzymes, while during the subsequent enzymatic saccharification, the carbohydrates are hydrolysed to sugars. These sugars can be used for the fermentative production of biofuels, organic acids or sugar alcohols. The economic viability of sugar-based lignocellulosic biorefineries heavily depends on the pretreatment methods used [2–4].



**Fig. 1.1** Conversion of lignocellulosic biomass to biofuel [26]



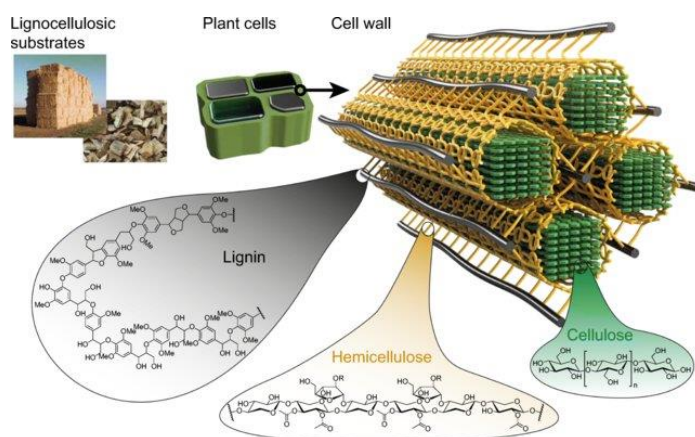
## 1.2 Lignocellulosic biomass

### 1.2.1 Structure and recalcitrance of lignocellulose

Lignocellulosic biomass from plant cell walls consists of three main compounds, i.e. the carbohydrate polymers cellulose and hemicellulose, and the aromatic polymer lignin (**Fig. 1.2**). The composition of lignocellulosic biomass varies with the lignocellulose source (e.g. forest residues, agricultural residues and energy crops) and with the plant species (**Table 1.1**) [27]. In addition, it is also affected by age, origin, cultivation and storage conditions [28]. As poplar wood is used as lignocellulosic biomass in this thesis, a greater emphasis will be placed on this type of feedstock in the next sections.

Cellulose is a polysaccharide composed of D-glucose subunits linked together via  $\beta$ -1,4 glycosidic bonds forming long, linear, unbranched polysaccharide chains, each containing 500 to 14 000 glucose molecules. The glucan chains are linked together by hydrogen bonds to form cellulose microfibrils creating a crystalline structure. Cellulose also has amorphous regions which are less compact and more easily hydrolysed by cellulase enzymes.

Hemicellulose is an amorphous, short-chain branched, heterogeneous polymer of hexoses (mannose, galactose, glucose), pentoses (xylose and arabinose) and sugar acids (glucuronic acid, 4-O-methyl-D-glucuronic acid, galacturonic acid) with a polymerization degree of 70 to 200 [28]. In hemicellulose, the hydroxyl groups of sugars can be partially substituted with acetyl groups. The composition of hemicellulose is highly dependent on the plant species. In hardwood, hemicellulose is predominantly glucuronoxylan, whereas glucomannan is more prevalent in softwood [29].



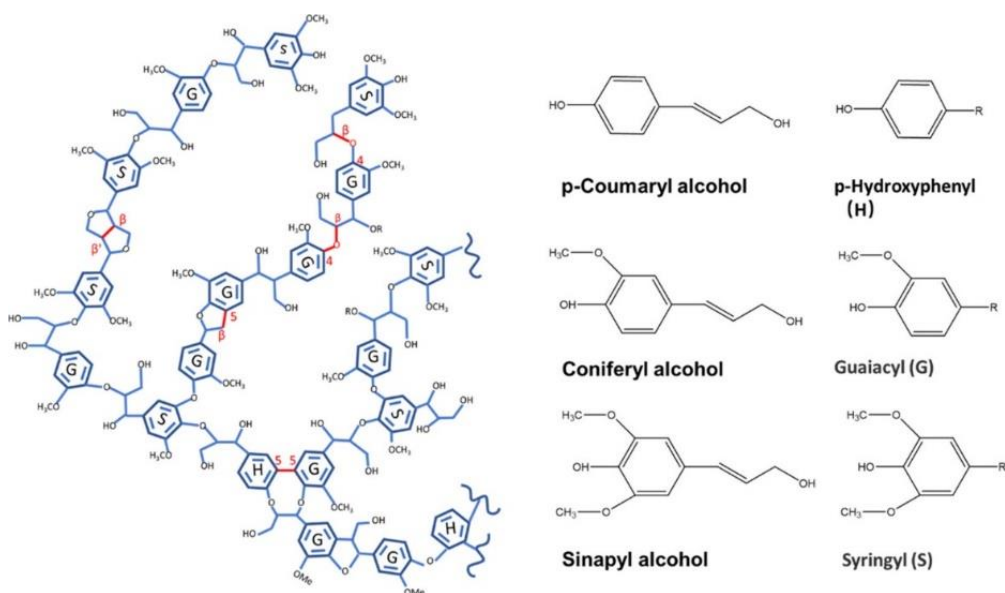
**Fig. 1.2** Structure of lignocellulosic biomass and its biopolymers cellulose, hemicellulose and lignin [30]

**Table 1.1** Composition of different lignocellulosic biomass [27]

<b>Biomass</b>	<b>Cellulose [%]</b>	<b>Hemicellulose [%]</b>	<b>Lignin [%]</b>
Switchgrass	5–20	30–50	10–40
Miscanthus	38–40	18–24	24–25
General grasses	25–40	25–50	10–30
Municipal solid waste	33–49	9–16	10–14
Newspapers	40–55	25–40	18–30
Corn cob	42–45	35–39	14–15
Corn stover	38–40	24–26	7–19
Sugarcane bagasse	42–48	19–25	20–42
Rice straw	28–36	23–28	12–14
Wheat straw	33–38	26–32	17–19
Barley straw	31–45	27–38	14–19
Sweet sorghum bagasse	34–45	18–27	14–21
Oat straw	31–37	27–38	16–19
Rye straw	33–35	27–30	16–19
Rice husk	25–35	18–21	26–31
Softwood	27–30	35–40	25–30
Hardwood	20–25	45–50	20–25

Lignin is an amorphous heteropolymer consisting of three phenylpropanoid units: p-hydroxyphenyl (H), guaiacyl (G) and syringyl (S). These units are derived from the monolignols p-coumaryl, coniferyl and sinapyl alcohol, respectively [31] (**Fig. 1.3**). Softwood lignin contains mainly G units (~ 90%) with a small number of H-units, whereas hardwood lignin consists mainly of G and S units [32,33].

Different types of linkages connect the phenylpropanoid units, mainly ethers (e.g.  $\alpha$ -O-4,  $\beta$ -O-4 and 4-O-5) and C-C linkages (e.g.  $\beta$ - $\beta$ ,  $\beta$ -5 and 5-5), which can vary between species. The most common type of linkage in the lignin structure is the  $\beta$ -O-4 aryl ether, which contributes to its highly branched aromatic structure [32]. Compared to the  $\beta$ -O-4 linkages, C-C bonds are less abundant and more difficult to cleave [34]. The complex and highly branched aromatic structure, stabilised by various covalent bonds, make lignin highly resistant to chemical and microbial degradation. Carbohydrates in plant cell walls are protected by lignin through covalent and non-covalent bonds, reducing their accessibility to enzymatic attack [35,36].

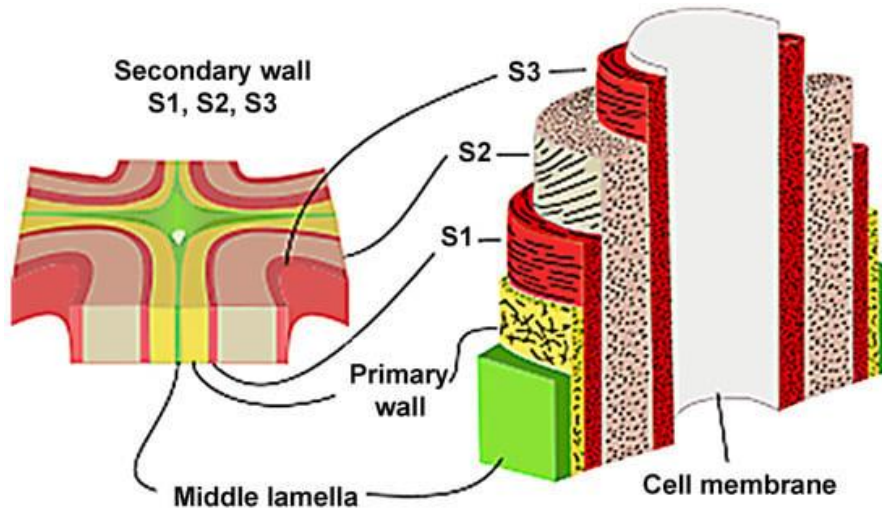


**Fig. 1.3** Structure of lignin [31]

### 1.2.2 Anatomy of plant cell walls

The construction of the plant cell wall is layered and heterogeneous, typically consisting of the middle lamella, primary wall, and secondary wall (**Fig. 1.4**). The primary cell wall consists of randomly arranged cellulose microfibrils and is usually non-lignified, whereas the secondary cell walls are highly lignified [27]. The secondary cell wall is made up of three sub-layers, namely the outer (S1), middle (S2) and inner (S3) layers, with the S2 layer generally being the thickest and crucial for maintaining the mechanical strength of wood [37]. The microfibrils are arranged horizontally in the S1 layer, vertically in the S2 layer and horizontally again in the S3 layer. The mechanical and physical properties of

the cell wall are mainly due to the vertical orientation of the microfibrils in the cell wall. The adjacent cells are connected to each other by the highly lignified middle lamella.



**Fig. 1.4** Different layers of the plant cell wall [37]

### 1.2.3 Poplar wood

The operating costs of a biorefinery are significantly influenced by the availability and price of feedstock [38]. Hybrid poplar wood is considered one of the most important wood feedstocks for the production of biofuels and biochemicals due to its excellent characteristics, including high carbohydrate and low ash content and high growth rate [1]. Poplar wood belongs to the hardwood family. Hardwoods are angiosperms (flowering plants with enclosed seeds), while softwoods are gymnosperms (plants with naked seeds) [39].

Poplar wood is native to the Northern Hemisphere. The nominal yield (including moisture content) of hybrid poplar species in North America is estimated to be 14 tonnes per hectare per year [1].

Poplars are highly suitable for various applications, including the production of biofuels, pulp and paper, but can also be used for lacquered furniture, mouldings or plywood.

Approximately 42-49% cellulose, 16-23% hemicellulose and 21-29% lignin are commonly found in poplar wood [1]. The study by Krutul et al. found that the lignin

content of poplar trees increased slightly with age, while no change in cellulose content was observed [40]. Most studies on lignocellulose conversion used debarked wood as a substrate, as the composition of bark differs from that of wood, with significantly higher levels of extractives and higher lignin and lower carbohydrate contents, which can affect the efficiency of the conversion process [41].

Poplar sawdust is a by-product of the wood manufacturing process and is therefore considered a waste material. Although often discarded, sawdust can be used for a variety of applications, including composting, water remediation, composites or as a lignocellulosic feedstock in biorefineries [42,43]. Every year up to 24.2 million m<sup>3</sup> of sawdust is produced worldwide [44].

### **1.3 Lignocellulose pretreatment for enhanced enzymatic saccharification**

#### **1.3.1 Purpose of pretreatment**

In recent decades, there has been growing interest in using lignocellulosic biomass as a potential raw material for producing biochemicals and biofuels. However, due to the recalcitrant structure of lignocellulose, pretreatment is required to break down the cross-linked fractions and improve the accessibility of cellulose and hemicellulose to (hemi)cellulolytic enzymes during enzymatic saccharification (Section 1.3.4). The ideal pretreatment can (1) break the lignin-carbohydrate linkages, (2) reduce cellulose crystallinity, (3) partially depolymerise cellulose and hemicellulose, (4) improve enzymatic digestibility, (5) avoid carbohydrate degradation or loss (6) prevent the formation of by-products inhibiting the subsequent fermentation, (7) avoid the use of chemical reagents polluting the environment and/or highly corroding the equipment, (8) reduce the generation of solid residues and, (9) be cost-effective [25,45–47].

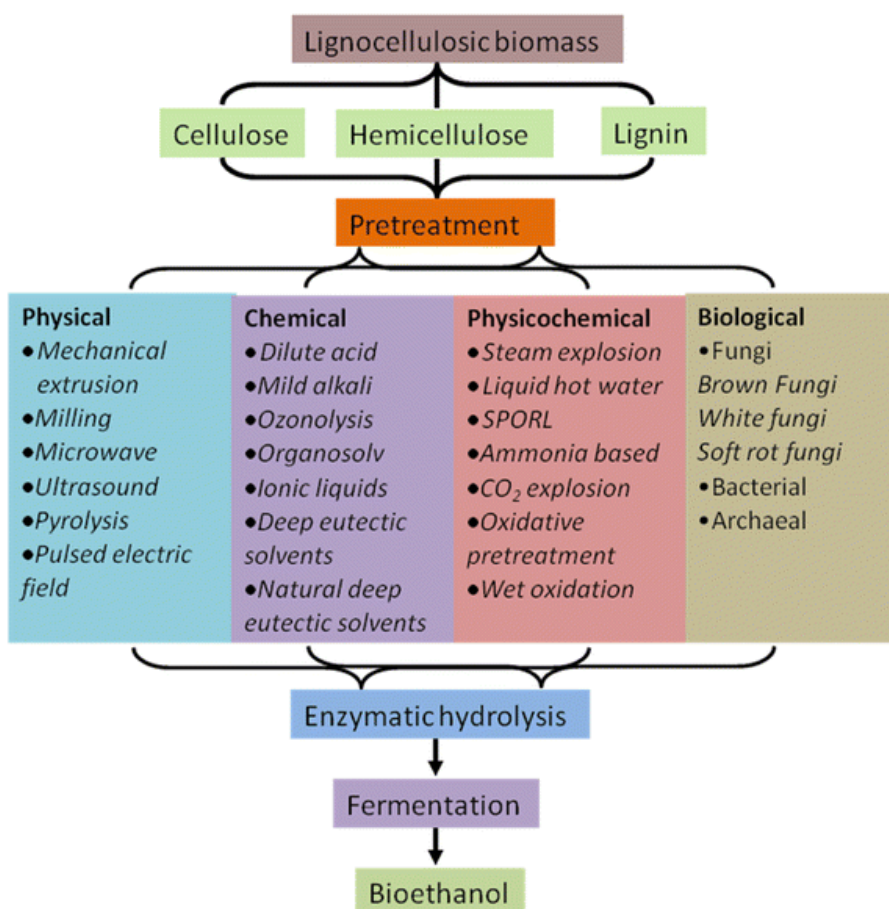
However, the pretreatment approach depends on the desired end product. While this study aims to utilise the carbohydrate fraction of lignocellulose, it should be noted that lignin valorisation is the objective of many other studies and is of great importance [48].

#### **1.3.2 Pretreatment methods**

The pretreatment approaches can be classified into physical, chemical, physicochemical and biotechnological methods and work in different ways to break down the complex structure of lignocellulose (**Fig. 1.5**). Each method has advantages and limitations, summarised in **Table 1.2** [25,48–50]. Physical pretreatments typically involve mechanical disruption to increase the surface area. Chemical pretreatment uses substances such as acids, bases and ionic liquids and is often carried out at high temperatures and/or pressures. Physicochemical pretreatments combine both

chemical and physical processes. Biotechnological pretreatment uses microorganisms or enzymes that can degrade the lignin and make the carbohydrates more susceptible to hydrolytic enzymes. Fungi, including white-, brown- and soft-rot fungi, can degrade lignocellulosic biomass. Among these, basidiomycetes white-rot fungi are considered the most effective for delignification due to their unique ligninolytic enzyme systems and are therefore discussed in this study [51]. Brown- and soft-rot fungi, on the other hand, have different enzyme systems and primarily target cellulose and hemicellulose, leaving behind a significant amount of lignin, and are therefore not as well suited to lignocellulose pretreatment as white-rot fungi.

Combining these pretreatment methods is also explored to integrate the benefits of each pretreatment method [25,52].



**Fig. 1.5** Overview of the main pretreatment methods available for lignocellulosic biomass [53]. SPORL = sulfite pretreatment to overcome recalcitrance of lignocellulose

**Table 1.2** The main advantages and disadvantages of the common pretreatment methods [25,48–50]

Pretreatment method		Advantage	Disadvantage
Physical	Milling	Reduce the particle size and crystallinity	High energy consumption
Chemical	Acid	Enzymatic hydrolysis is sometimes not required as the acid itself may hydrolyse the biomass to yield fermentable sugars	High cost of the reactors, chemicals are corrosive and toxic, and the formation of inhibitory by-products
	Alkaline	Cause less sugar degradation than acid pretreatment	Generation of inhibitors
	Organosolv	Produce low residual lignin substrates that reduce unwanted adsorption of enzymes and allow their recycling and reuse.	High capital investment, handling of harsh organic solvents, formation of inhibitors
	Ionic liquid	Low vapour pressure designer solvent, working under mild reaction conditions	Costly, the complexity of synthesis and purification, toxicity, poor biodegradability and inhibitory effects on enzyme activity
Physicochemical	Steam explosion	Low chemical consumption, hemicellulose and lignin disruption, an increase of the assessable surface area	Degradation products may inhibit further processes and need high pressure
Biotechnological	Fungal	Mild reaction conditions, lack of production of inhibitory by-products	Slow process, partial degradation of carbohydrates

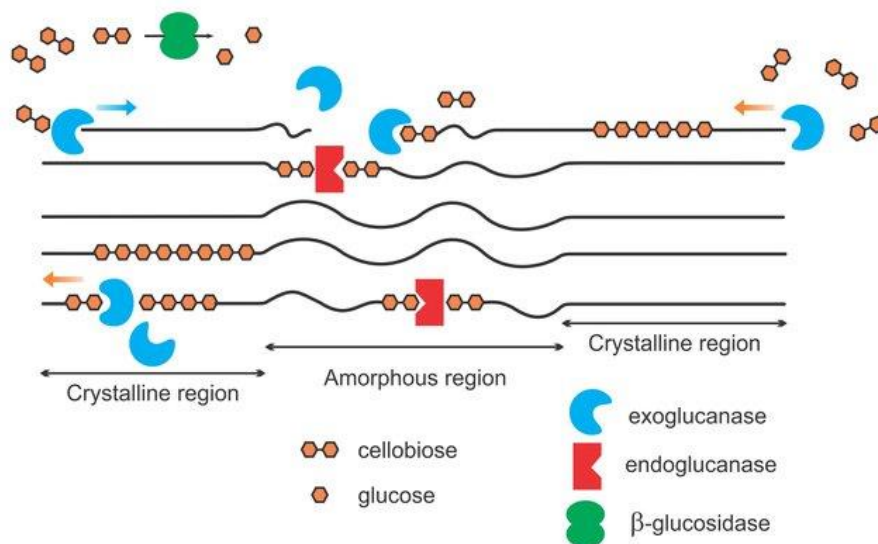
### 1.3.3 The evaluation of fungal pretreatment efficiency

The effectiveness of the fungal pretreatment is mainly evaluated by determining (1) the lignin reduction, (2) the selectivity of lignin degradation, and (3) the enzymatic saccharification yield. The enzymatic hydrolysis is necessary to assess the potential usefulness of fungal pretreatment for lignocellulose conversion. An efficient fungal pretreatment provides substantial and selective lignin degradation and consequently enhanced enzymatic digestibility.

### 1.3.4 Enzymatic saccharification

Saccharification of the polysaccharides into fermentable sugars can be achieved by acid or enzymatic hydrolysis. Enzymatic hydrolysis is an alternative to chemical hydrolysis that uses milder and non-corrosive reaction conditions (the temperature of 40–50°C and pH of 4–5) and does not produce fermentation inhibitors [54]. Enzymatic saccharification involves the action of (hemi)cellulolytic enzymes to break down (hemi)cellulosic polymers into fermentable hexoses and pentoses. This process requires the action of several synergistic enzymes, including endo- $\beta$ -1,4-glucanases, exo- $\beta$ -1,4-glucanases and  $\beta$ -glucosidases. The endo- $\beta$ -1,4-glucanases catalyse random cleavage of the internal glycosidic bonds, reducing the degree of polymerization. The exo- $\beta$ -1,4-glucanases (cellobiohydrolases) catalyse cleavage at the reducing or non-reducing ends of the cellulose chain, releasing cellobiose. The  $\beta$ -glucosidases are specifically active on cello-oligosaccharides and cellobiose and catalyse the hydrolysis of non-reducing chain ends with the release of glucose [55]. The enzymes work in synergy: endo-acting enzymes create new reducing, and non-reducing chain ends for the exo-acting enzymes, which release cellobiose. Cellobiose is then converted to glucose by  $\beta$ -D-glucosidases (**Fig. 1.6**) [56,57]. Commercially available cellulases are often produced by filamentous fungi such as *Trichoderma reesei* and *Aspergillus niger* [54,56]. Hemicellulases that are responsible for the degradation of hemicellulosic polymers and side chains of hemicellulose include arabinofuranosidases, mannanases, galactomannase, esterases, xylanases and xylosidases [54].





**Fig. 1.6** A simplified schematic representation of the enzymatic action of cellulase on cellulose [57].

Several factors can influence the degradation of lignocellulosic materials by enzymatic hydrolysis. These factors can be divided into two categories: enzyme-related and substrate-related factors [58]. Enzyme-related factors are primarily concerned with the enzyme activity by dealing with end-product inhibition and improving thermal stability, synergism and adsorption. Meanwhile, substrate-related factors aim to improve enzyme accessibility to cellulose, which can be influenced by factors such as decreasing cellulose crystallinity, lignin and hemicellulose content and distribution, and increasing the available surface area.

#### 1.4 Fungal pretreatment by white-rot fungi

White-rot fungi (WRF) are most commonly applied for fungal pretreatment of lignocellulosic biomass for the purpose of a biorefinery concept. However, they can also be used for biopulping [59], animal feed upgrading [60], and soil and wastewater bioremediation [61] by oxidising lignin and various lignin-analogous compounds.

Compared to chemical/physical pretreatment methods, fungal pretreatment is considered a biotechnological method. It requires less energy due to its mild reaction conditions and does not use harsh chemicals or produce inhibitory by-products that negatively affect the subsequent fermentation [5]. Fungal pretreatment can remove

11.6-41.7% of lignin from lignocellulosic biomass in 5-120 days, resulting in a 1.5-10 times increase in saccharification yield after subsequent enzymatic hydrolysis compared to the untreated raw feedstock [62]. However, the main limitations to the widespread application of fungal pretreatment are the long pretreatment time (several weeks), the feedstock sterilisation requirement and the partial consumption of hemicellulose and cellulose by fungal growth and metabolism, resulting in carbohydrate loss that negatively affects the achievable saccharification yield [10].

### 1.4.1 Mechanism of fungal delignification

The hyphae of white-rot fungi secrete numerous ligninolytic enzymes to degrade lignin. These extracellular enzymes are collectively known as ligninases. Four ligninolytic enzymes are produced by WRT, including laccase, lignin peroxidase (LiP), manganese peroxidase (MnP) and versatile peroxidase (VP). These enzymes belong to two families: polyphenol oxidases (laccase) which use molecular oxygen as an electron acceptor, and heme peroxidases (LiP, MnP and VP), which use hydrogen peroxide as a co-substrate [63]. In each case, the ultimate product of lignin degradation by these enzymes is carbon dioxide [64]. The white-rot fungus can secrete one or more of the ligninase enzymes. *Phanerochaete chrysosporium*, i.e. the white-rot fungus used in this study, produces manganese and lignin peroxidase but not laccase or versatile peroxidase [9,65,66]. Therefore, this section will discuss the mechanism of MnP and LiP in more detail, with less emphasis on laccase and VP.

The ligninolytic enzymes are generally too large to penetrate the wood cell wall [67]. Therefore, the enzymes first oxidise low-molecular weight diffusible reactive oxidative compounds. The oxidised compounds move to the substrate and catalyse the removal of an electron from the phenolic hydroxyl or aromatic groups, producing free phenoxy and aromatic radicals, respectively. These radicals then initiate the decomposition of lignin polymers. Examples of mediators are organic acids, simple phenols or veratryl alcohol, depending on the type of ligninase enzyme [62,63,68]. The mediators, molecular weight, optimal temperature and pH range of the four ligninase enzymes are included in **Table 1.3**.

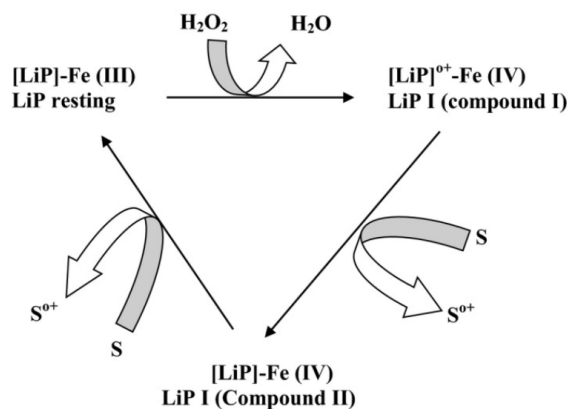
**Table 1.3** Features of the fungal ligninolytic enzymes (Adapted from Ref. [63])

Type of enzymes	Cofactor	Mediators	Subunits & molecular mass (kDa)	Optimum temperature/ pH range
Laccase	-	Phenols, aniline, 3-HAA, NHA, syringaldehyde, hydroxybenzotriazole and ABTS	Monomeric (43-100), dimeric, trimeric & oligomeric	20-80°C/2-10
LiP	Heme	Veratryl alcohol	Monomeric (37-50)	35-55°C/1-5
MnP	Heme	Organic acids as chelators, thiols, and unsaturated fatty acids	Monomeric (32-62.5)	30-60°C/ 2.5-6.8
VP	Heme	Veratryl alcohol, Compounds similar to LiP and MnP mediators	Monomeric (Unkown)	Unknown/3-5

3-HAA: 3- hydroxyanthranilic acid; NHA: N-hydroxyacetanilide; ABTS: 2,2'-azinobis(3-ethylbenzthiazoline-6-sulphonate).

Lignin peroxidases use H<sub>2</sub>O<sub>2</sub> to catalyse the oxidative depolymerisation of various non-phenolic lignin compounds and the oxidation of phenolic compounds (e.g. guaiacol, vanillyl alcohol and syringic acid) [63]. LiPs utilise multi-step electron transfers to oxidise the substrates and produce intermediate radicals, including phenoxy radicals and veratryl alcohol radical cations. These intermediates undergo non-enzymatic reactions such as radical coupling and polymerisation, side chain cleavage, demethylation, and intramolecular addition and rearrangement [63].

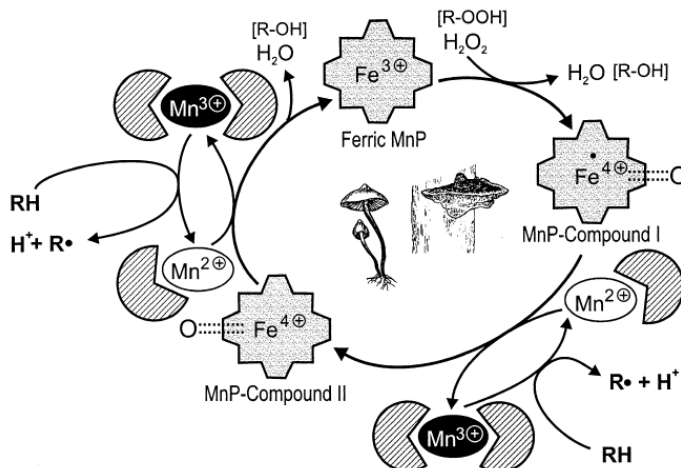
In the LiP-catalysed reaction, (1) the resting ferric state of the enzyme is oxidised by H<sub>2</sub>O<sub>2</sub> to form the oxo-ferryl intermediate I (Compound I), which is a radical cation. (2) It is reduced by the electron-donating substrate, such as veratryl alcohol (VA), a secondary metabolite of the fungal metabolism, to form the oxo-ferryl intermediate II (Compound II). Finally, (3) the reduced substrate gives an additional electron to compound II, allowing LiP to return to its resting ferric state [69,70] (**Fig. 1.7**).



**Fig. 1.7** Catalytic cycle of lignin peroxidase [71]

Manganese peroxidase facilitates the oxidation of  $\text{Mn}^{2+}$  to  $\text{Mn}^{3+}$  using  $\text{H}_2\text{O}_2$ . Subsequently, the  $\text{Mn}^{3+}$  is released from the enzyme surface and chelated with oxalate or with other chelators. The chelated  $\text{Mn}^{3+}$  acts as a diffusible redox mediator in the oxidation process of several phenolic compounds. For the oxidation of non-phenolic compounds, reactive radicals must be formed in the presence of a second mediator. Organic acids are the primary second mediators in producing reactive radicals such as acetic acid, peroxy, and formate radicals [63].

The catalytic cycle of MnP begins with (1)  $\text{H}_2\text{O}_2$  binding to the resting ferric enzyme form, resulting in an iron-peroxide complex. An unstable intermediate MnP compound I ( $\text{Fe}^{4+}$ oxo-porphyrin radical complex) is formed by the cleavage of the peroxide enzyme O–O bond with two-electron transfer from the heme-porphyrin (**Fig. 1.8**). Consequently, the dioxygen bond is cleaved, releasing one water molecule. (2)  $\text{Mn}^{3+}$  is produced by the oxidation of the porphyrin intermediate using a mono-chelated  $\text{Mn}^{2+}$  ion as a one-electron donor, forming the unstable intermediate MnP compound II ( $\text{Fe}^{4+}$ oxo porphyrin complex). (3) The reduction of compound II proceeds in a similar way, i.e. another  $\text{Mn}^{3+}$  is formed from  $\text{Mn}^{2+}$ , returning the resting state of the enzyme with the release of a second water molecule [68,72].

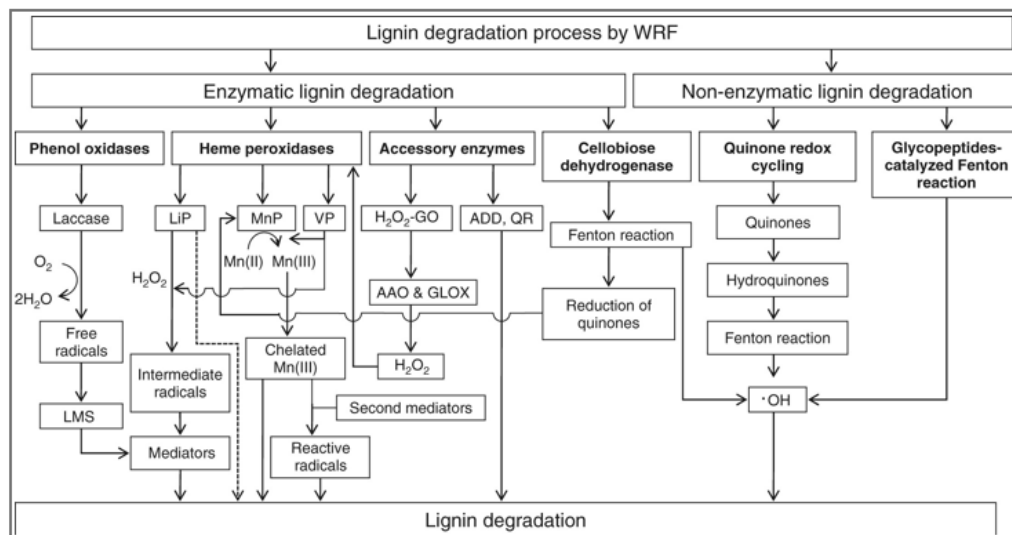


**Fig. 1.8** The catalytic cycle of manganese peroxidase [73].

Versatile peroxidases show the properties of both lignin peroxidases and manganese-dependent peroxidases and, thereby, the ability to attack both non-phenolic and phenolic sites in lignin.

Laccases are Cu<sup>2+</sup>-containing phenol oxidases that catalyse the oxygen-mediated oxidation of lignin and other phenol-containing compounds.

The fungal lignin degradation process relies on the coordinated activities of the ligninase and the accessory enzymes (e.g. the H<sub>2</sub>O<sub>2</sub>-producing glyoxal and aryl alcohol oxidases), as it was visually summarised in the study of Tian et al. (**Fig. 1.9**) [62]. Non-enzymatic mechanisms are also involved in the degradation of plant cell walls by generating free hydroxyl radicals. White-rot fungi produce hydrogen peroxidase, which participates in the Fenton reaction ( $Fe^{2+} + H_2O_2 \rightarrow Fe^{3+} + OH^- + OH^\bullet$  [67]) that ultimately leads to the release of hydroxyl radicals. The non-specific nature of these radicals allows them to attack both polysaccharides and lignin in the plant cell wall, causing various cleavages that facilitate the penetration of lignocellulolytic enzymes into the wall [63]. Fungi generate free hydroxyl radicals via several pathways, including cellobiose dehydrogenase-catalysed reactions, low molecular weight peptide/quinone redox cycling, and glycopeptide-catalysed Fenton reactions (**Fig. 1.9**) [62,63].



**Fig. 1.9** Schematic diagram of lignin degradation by white-rot fungi [62]. Lac: laccase, LMS: laccase-mediator system, LiP: lignin peroxidase, MnP: manganese peroxidase, VP: versatile peroxidase,  $H_2O_2$ -GO:  $H_2O_2$ -generating oxidases, AAO: aryl-alcohol oxidase, GLOX: glyoxal oxidase, ADD: aryl-alcohol dehydrogenases, QR: quinone reductases

Compared to the direct use of ligninolytic enzymes for pretreatment, fungal pretreatment also has several additional positive effects, including (1) increasing the hydrophilicity of lignin by modifying lignin molecules, (2) increasing the surface area through hyphal penetration-forming pore structures, and (3) reducing the concentration of inhibitors caused by mycelial metabolism [62].

### 1.4.2 Delignification selectivity

White-rot fungi can be divided into two groups based on their degradation patterns. Most WRFs are non-selective (simultaneous) lignin degraders and degrade all lignocellulosic components simultaneously, while selective lignin degraders preferentially degrade lignin and hemicellulose [5,74,75]. The cellulose and hemicellulose degradation occurs due to the cellulolytic and hemicellulolytic enzymes produced by the fungi. These enzymes play an important role in providing easily digestible carbon sources for fungal growth and metabolism. However, carbohydrate consumption during fungal pretreatment reduces the amount of polysaccharide substrates available for enzymatic saccharification [76]. Therefore, it is desirable to remove lignin while leaving the cellulose and hemicellulose intact selectively.

The delignification selectivity of the fungal pretreatment is indicated by the selectivity value (SV), which is defined as the ratio of lignin degradation and cellulose consumption [77–79]. Lignin degradation and cellulose consumption are both calculated as the ratio of the amount of lignin and cellulose degraded to the initial amount of lignin and cellulose, respectively. The SV during pretreatment depends not only on the ligninolytic ability of the fungal strains but also on the substrate used and, more importantly, on the culture conditions [79,80].

#### 1.4.3 *Phanerochaete chrysosporium*, a non-laccase-producing WRF

Based on the latest taxonomic classification, *Phanerochaete chrysosporium* belongs to the Fungi kingdom, *Basidiomycota* phylum, *Agaricomycetes* class, *Polyporales* order, *Phanerochaetaceae* family and *Phanerochaete* genus [81,82].

*Phanerochaete chrysosporium* is one of the most extensively studied WRFs due to its ability to remove a wide range of pollutants and effectively degrade lignin in hardwood and softwood (Fig. 1.10). *P. chrysosporium* can be found in temperate forests throughout North America, Europe, and Iran [83] and has an optimum pH of 3.5–5 and an optimum growth temperature of 37–39 °C, with the latter being uniquely high among WRF, which may be beneficial for ligninase activities (Table 1.3) [84]. The reported specific growth rate of *P. chrysosporium* during submerged fermentation of poplar wood is 0.90 d<sup>-1</sup> between 5 and 6 days [85].

*P. chrysosporium* is considered a non-selective lignin degrader, which can simultaneously attack lignin, cellulose and hemicellulose. Depending on the fungal pretreatment system, delignification selectivity values between 0.59 and 1.2 were reported in the literature for *P. chrysosporium* [77,86–88].

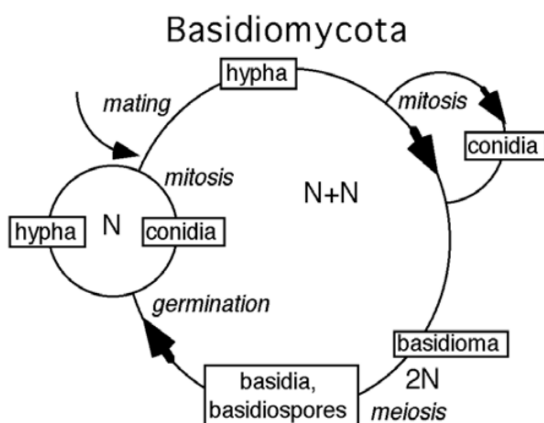


Fig. 1.10 Wood degradation by *P. chrysosporium* [84]

This fungus produces flat, crust-like fruiting bodies containing basidia on the surface of a smooth or wrinkled hymenium and asexual conidiospores called conidia [89]. The sexual spores of *P. chrysosporium* are called basidiospores and are produced by the fruiting body. Basidiospores undergo germination to produce monokaryotic hyphae characterised by haploid nuclei [90] (**Fig. 1.11**). Fusion of the hyphae gives rise to dikaryotic hyphae. The fusion of dikaryotic nuclei within the basidium produces a zygote, which then undergoes meiosis, forming basidiospores. As the basidiospores are formed by meiosis, they have a different genotype than the parent strain.

Conidia are haploid cells which are produced through mitosis on the ends of specialised hyphae called conidiophores. They are genetically identical to their haploid parents, making them a good inoculum type for fermentation [91]. The ability to reproduce asexually allows the fungi to exist and multiply in the vegetative state [92].

The genome of *P. chrysosporium* was the first Basidiomycota genome to be sequenced. The genes of *P. chrysosporium* encode many lignocellulose degrading enzymes, including 10 LiPs, 5 MnPs, 1 glyoxal oxidase, 7 copper radical oxidases, 4 multicopper oxidases, 1 cellobiose dehydrogenase and approximately 440 putative carbohydrate-active enzymes [6–9]. However, no laccase coding sequences were found in its genome.



**Fig. 1.11** Life cycle of Basidiomycota [90]

In conclusion, although *Phanerochaete chrysosporium* does not produce laccase, it is widely used in lignin degradation and bioremediation studies due to its intricate ligninolytic enzyme network, rapid growth rate, relatively high optimum temperature and spore production. These characteristics together make it a valuable organism.



## **1.5 Solid-state fermentation (SSF) for fungal pretreatment**

### **1.5.1 General aspects of SSF**

Solid-state fermentation (SSF) has been defined as a fermentation process which involves a solid matrix and is carried out in the absence or near-absence of free water [93]. However, the substrate must possess enough moisture to support the growth and metabolism of the microorganism and to enable substrate transport. Fungi are considered the most suitable organisms for SSF due to their ability to grow on particle surfaces, penetrate interparticle spaces and grow in an environment with relatively low moisture content. However, there have been several successful applications of SSF using bacterial cultures as well [94].

Solid-state fermentation is also the method of choice for fungal delignification, where the production of ligninolytic enzymes and therefore the delignification is higher than in submerged fermentation [95,96]. In submerged fermentation, fungi grow under conditions different from their natural habitat, which may contribute to the observed lower ligninolytic activity in liquid culture [97]. SSF offers several advantages over submerged fermentation, lower energy requirements, water savings, adequate aeration, less substrate inhibition, higher product yields and lower sterility requirements due to the low water activity [98,99]. However, due to the heterogeneous nature of the media and poor mixing capabilities, it is difficult to monitor and control the process parameters such as moisture content, temperature and pH and to scale up the process. Additionally, SSF often requires complicated downstream processing [100]. Fungal biomass estimation is another major challenge of SSF because the biomass is embedded in the solid substrate and cannot be quantitatively separated from it, making direct methods of biomass measurement impossible. Indirect methods such as measuring oxygen uptake rate, carbon dioxide evolution, or a specific fungal cell component not present in the substrate, such as glucosamine, ergosterol, protein or nucleic acid, are used to determine biomass in SSF [100].

### **1.5.2 Factors influencing the fungal SSF**

Several factors influence the efficiency of fungal pretreatment. These include physical factors (e.g. temperature, moisture content, pretreatment time, aeration, particle size and substrate sterilisation), chemical factors (e.g. culture media and supplements), and biological factors (e.g. used microorganisms and interaction/competition of microorganisms). The most critical factors are reviewed below, with a particular emphasis on the effect of metal ion supplements which was extensively researched in this study.

### **1.5.2.1 Moisture content**

The moisture content of the biomass is critical for fungal growth, enzyme production and lignin degradation. Previous studies have shown that 70-80% initial moisture content is optimal for lignin degradation and ligninase activities of most white-rot fungi [76]. However, the optimum moisture content varies depending on the type of biomass and microorganism used. Higher moisture content is favourable for the formation of fungal mycelia but does not necessarily improve the delignification process and will result in a lower level of solid loading and a higher chance of bacterial contamination. Too low moisture content can reduce nutrient availability, fungal growth and delignification [5,76].

### **1.5.2.2 Temperature**

Temperature is a critical factor in the fungal pretreatment process. However, the optimal temperature varies with the fungi used [5,76]. Most white-rot basidiomycetes grow best in a temperature range of 25-30°C, whereas most white-rot ascomycetes grow optimally around 39°C [51]. The metabolism of these fungi generates heat which can lead to temperature gradients in the solid-state fermentation media. Excessive heat accumulation can negatively affect fungal growth and metabolic activity.

### **1.5.2.3 Aeration**

Fungal pretreatment requires sufficient oxygen for the production and activity of ligninolytic enzymes, as lignin degradation is an oxidative process [95]. Aeration also plays an important role in removing CO<sub>2</sub> and heat, distributing water vapour to regulate humidity and dispersing volatile compounds produced by fungal metabolism [94,95]. While passive air diffusion through cotton plugs was found to be as effective as forced air circulation for delignification in small flasks (< 500 ml), reactors containing packed feedstock require active aeration to ensure uniform air diffusion throughout the substrate [76]. The porosity of the substrate determines the aeration rate, and therefore optimisation is required for each type of substrate and process [95]. While high oxygen levels can increase the delignification rate, they do not necessarily improve delignification selectivity [76].

#### 1.5.2.4 Particle size

Reducing the size of solid substrate particles increases the surface area, making it easier for hyphae and air to penetrate the centre of the particles. Smaller particle size also increases the packing density, thus the amount of material that can be accommodated in a fermenter. However, the increased packing density reduces the size of interparticle channels which hinders gas circulation [101].

In the study by Reid et al., similar lignin degradation and saccharification yield were achieved by *Phlebia tremellosa* using 0.42 mm and 1.68 mm aspen wood particles and active aeration, while the lowest delignification was observed with the bigger aspen chips and shavings [16]. In the study of Wan and Li on corn stover pretreatment with *Ceriporiopsis subvermispora*, particle size reduction from 15 to 10 mm resulted in increased lignin degradation and saccharification yield with passive aeration. However, further particle size reduction from 10 to 5 mm did not significantly increase the sugar yield [102]. As particle size reduction is costly, the largest size that allows good fermentation is recommended.

#### 1.5.2.5 Pretreatment time

The low delignification rate of the fungal pretreatment is a major challenge to the widespread application of this method. Several weeks to months are typically required to achieve high levels of lignin degradation depending on the microorganism, substrate and conditions used. While *P. chrysosporium* can achieve vigorous lignocellulose degradation within days to weeks, its high lignin degradation is often associated with low delignification selectivity [76]. In contrast, *Pleurotus ostreatus* provides good delignification selectivity but low lignin degradation after several weeks of pretreatment [103]. Pretreatment time also affects the delignification selectivity. Longer than optimal pretreatment can result in high cellulose losses and, thus, reduced delignification selectivity [18,104,105].

#### 1.5.2.6 pH

White-rot fungi typically thrive at slightly acidic pH levels, with the optimum range between 4 and 5 [106]. White-rot fungi can lower the pH of their environment during growth through the production of various acidic compounds, including phenolic acids and simple organic acids [107]. However, a too low pH can be detrimental to fungal growth and bioconversion [108]. Maintaining optimal pH levels in solid-state fermentation is particularly difficult due to the inherent heterogeneity of the system, and it is therefore rarely attempted in practice.

### 1.5.2.7 Decontamination

Decontamination of the lignocellulosic feedstocks with steam or chemicals (e.g. sodium meta-bisulfite and sodium hydrosulfite) is necessary to prevent the growth of indigenous microorganisms (bacteria and fungi) naturally present in the feedstock [76]. This process is particularly important before fungal pretreatment, especially when using white-rot basidiomycetes, which are often vulnerable to microbial (fungal and bacterial) contamination. However, the need for feedstock sterilisation contributes to increased sugar production costs in a biorefinery that relies on fungal pretreatment.

Few attempts have been made in research to use non-sterilised feedstocks for fungal pretreatment. Direct inoculation of non-sterilised feedstock with fungal mycelium, which has been shown to be effective for sterilised feedstock, often resulted in low pretreatment efficiencies [16,109,110]. However, some studies have reported successful fungal pretreatment using an unusual inoculation strategy where white-rot fungi are first grown on sterilised feedstock, and then the obtained pre-colonised substrate is used as inoculum during fungal pretreatment. Zhao et al. found that pre-colonised yard trimmings with *Ceriporiopsis subvermispota* as inoculum resulted in comparable degradation of lignocellulosic components as the sterilised system inoculated with fungal mycelium [15]. Vasco-Correa et al. also reported fungal pretreatment of unsterilised miscanthus, softwood and hardwood being successful using pre-colonised feedstock as inoculum, but not for maize stover [17].

### 1.5.2.8 Inoculum

Various techniques can be used to prepare the inoculum for solid fungal pretreatments, such as growing mycelium in liquid or agar medium, preparing spawn (mycelium-coated grains) on cereal grains, or using pre-colonised substrate as mentioned above. *Phanerochaete chrysosporium* is advantageous as it produces spores, which are reproductive structures designed to ensure the survival and spread of the fungus. Spores have specialised structures and mechanisms that increase their genetic stability and enable them to withstand harsh environmental conditions. On the other hand, other white-rot basidiomycetes do not produce spores, and mycelium must be used for inoculation [76].

The use of pre-inoculated substrate has several advantages. This inoculation technique has several important advantages. Firstly, the fungus is already adapted to the wood substrate. Secondly, the pre-inoculated wood contains fully developed white-rot fungi, eliminating the need for spore germination. In addition, the lignin-degrading enzymes are also already present. These combined effects effectively promote faster fungal

growth and lignocellulose utilisation. However, too many transfers of pre-colonised substrate can lead to fungal degeneration [111]. The use of fungi grown on cereals (spawn) is another inoculation approach but would result in a preference for carbohydrate utilisation rather than lignin degradation.

In general, a minimum inoculum is required for effective colonisation and subsequent delignification. However, larger inoculum sizes do not necessarily improve pretreatment efficiency [76]. In the study by Kuijk et al., the amount of inoculum (0.5, 1.5 or 3%) had no significant effect on the treatment of wood chips by *C. subvermispora*, while the addition of 1.5% *L. edodes* inoculum instead of 0.5% resulted in more selective delignification of wheat straw [112].

#### 1.5.2.9 Supplements

Lignin degradation generally occurs under nitrogen- or carbon-deficient conditions [83]. However, the effect of nitrogen varies between species and strains of white-rot fungi [95]. A previous study found that the concentration of nitrogen, regardless of its source ( $NO_3^-$ ,  $NH_4^+$ , amino acids), is a critical factor for ligninase production by *P. chrysosporium* [113]. While nitrogen should be limited, too low a concentration inhibits both LiP and MnP production, probably because the mould requires a nitrogen source for enzyme expression [12].

Several studies have reported an improvement in ligninolytic enzyme production by *P. chrysosporium* in the presence of Tween 80 surfactant, which can increase the availability of less soluble substrates to fungi, promote fungal spore growth and increase ligninase activity [12,83]. MnP and LiP activities were significantly increased when veratryl alcohol, a by-product of the fungal metabolism of *P. chrysosporium* and a mediator of LiP, and both a preservative and a stimulator of lignin-degrading peroxidases, was added to the liquid culture medium.

Many studies have shown that phenolic supplements such as ferulic, vanillic and gallic acids can significantly increase laccase activities through their mediator function, but this does not apply to *P. chrysosporium* [79,114,115]. The study by Nousiainen et al. concluded that phenolic mediators enhance MnP-catalysed oxidation of recalcitrant lignin model compounds and synthetic lignin [116]. In the study of Mishra et al., phenolic supplements greatly enhanced the laccase activities and had less effect on MnP and LiP activities [79].

### **1.5.2.9.1 Metal supplements**

Metal supplementation can influence fungal pretreatment by affecting fungal growth, lignocellulolytic enzyme production and activities, and cellulose digestibility. The literature on these individual effects is discussed below, particularly emphasising the most crucial metal ions, i.e.  $Mn^{2+}$  and  $Cu^{2+}$ , that can positively influence fungal pretreatment. Whilst the effect of these metal ions has been well researched in liquid cultures using a basal medium without lignocellulosic biomass, there are significantly fewer studies where they have been applied in the complex solid-state fungal pretreatment of lignocellulose.

#### **1.5.2.9.1.1 Effect of on fungal growth**

White-rot fungi have the ability to adsorb and accumulate heavy metals. While trace amounts of metal ions can be beneficial for fungal growth, in excess, they can inhibit growth, cause morphological and physiological changes and affect reproduction [14].

In the study of Singhal et al.,  $CuSO_4$  concentrations of 0.06-63.84 mg/L resulted in increased fungal biomass in liquid culture. However, further elevation of  $Cu^{2+}$  resulted in a decline in fungal growth [13]. In the study of Wang et al.,  $Mn^{2+}$  levels between 0.1 and 9 mg/L did not increase the mycelium dry weight in liquid culture [12]. In the study of Falih., high metal ion concentrations (400 mg/L of  $Cu^{2+}$  and  $Mn^{2+}$ ) considerably decreased the fungal growth; however, even at this concentration, the fungal growth was still detectable [117].

#### **1.5.2.9.1.2 Effect on the ligninolytic enzyme system**

Several studies have shown that the absence of  $Mn^{2+}$  ions in the culture inhibits MnP production [83]. Wang et al. reported that adding  $Mn^{2+}$  not only increases the production of MnP by *P. chrysosporium* in liquid culture but, to a lesser extent, of LiP as well [12]. On the other hand, in the research of Mester et al., the addition of  $Mn^{2+}$  promoted the production of MnP while reducing the secretion of LiP and veratryl alcohol, suggesting that  $Mn^{2+}$  act as a regulator in the production of ligninolytic enzymes [118]. In addition to being a substrate for MnP and thus directly involved in the MnP catalytic cycle,  $Mn^{2+}$  enhances the production of the MnP enzyme by activating the transcription of the MnP-encoding genes [119].

Copper ions are essential for the activity and production of copper-containing laccase and are also inducers of laccase gene expression [115,120].  $Cu^{2+}$  and  $Zn^{2+}$  were proven to increase both LiP and MnP activities in the liquid culture of *P. chrysosporium* [13]. The study of Mishra et al. showed that the addition of  $CuSO_4$  increases both MnP and

LiP activities during solid-state fungal pretreatment [121]. However, the exact mechanism by which copper ions increase LiP and MnP activities in the cultures of *P. chrysosporium* is not yet fully investigated and understood. The study of Zeng et al. confirmed that  $\text{Cu}^{2+}$  enhance the activities of purified LiP and MnP enzymes of *Phanerochaete chrysosporium* [122]. However, the effect of copper on the expression of MnP- and LiP-encoding genes in *P. chrysosporium* has not yet been researched. The study of Álvarez et al. showed that  $\text{Cu}^{2+}$  ions increase the transcript levels of Mn-encoding genes in *C. subvermispota* [123].

It should be noted that excessive amounts of heavy metals, even those that are essential, can act as inhibitors of enzymatic reactions. Extracellular enzymes are particularly susceptible to inhibition because they are not protected by the metal detoxification system present in fungi [14].

#### **1.5.2.9.1.3 Effect on cellulase activities and cellulose digestibility**

In liquid culture, cellulase enzymes of *P. chrysosporium* were inhibited in the presence of 50-150 mg/L  $\text{Cu}^{2+}$  and  $\text{Mn}^{2+}$  [14]. Inhibition of cellulolytic enzyme activities by  $\text{Cu}^{2+}$  and  $\text{Mn}^{2+}$  was also reported in studies focusing on the enzymatic saccharification of cellulose [124,125]. Moreover, the study of Xu et al. showed that  $\text{Cu}^{2+}$  ions at a concentration of 140  $\mu\text{mol Cu}^{2+} \text{g}^{-1}$  Avicel (microcrystalline cellulose) could oxidise the reducing ends of cellulose, resulting in a structurally modified cellulose with reduced enzymatic digestibility [126].

### **1.5.3 Bioreactors for fungal SSF**

The most commonly used bioreactors for solid-state fungal pretreatment are packed bed, tray and rotatory drum reactors, with their performance parameters summarised in **Table 1.4** [127]. Mixing in bioreactors is beneficial to ensure the effective distribution of spore suspension, moisture and nutrient solutions, to help to distribute airflow evenly and to improve heat dissipation [128]. However, for fungal fermentation, where hyphal bridges are formed between particles on the substrate, mixing can be detrimental to bioreactor performance due to the disruption of the hyphae between particles and the shear force generated by mixing [76,129]. For this reason, static operation in tray fermenters and packed bed bioreactors, or low-speed rotation in rotary drum reactors, is recommended when performing fungal SSF.

**Table 1.4** Performance parameters of the common solid-state fermenters used for fungal pretreatment. Adapted from Ref. [127] by presenting only the three SSF reactors discussed in this section.

Performance parameter	Bioreactors Types		
	Tray	Packed bed bioreactor (PBB)	Rotary drum bioreactor (RDB)
<b>Heat transfer capability</b>	Primarily through conduction, low thermal conductivity of substrate often leads to inefficient heat dissipation.	Conductive, convective and evaporative heat transfer at play, but at large scale the process is often confronted with bed compaction & air channelling. Therefore, maintenance of optimum bed temperature and moisture is challenging.	Heat transfer is achieved through conduction, convection and evaporative cooling. At high substrate bed loading temperature control is off limits.
<b>Scalability</b>	Mostly done by increasing the surface area and the number of trays	Due to issues of bed compaction, air channelling, heterogeneity, traditional PBB are not suited for scale-up.	The working volume is usually 30% of the reactor volume. RDBs are generally not suited for scale-up.
<b>Sterilisation/ Containment issues</b>	Not suited for sterile applications and the process is not contained.	In-situ sterilisation may be achieved by injecting high pressure steam, however this may not be feasible with high bed loading.	In situ sterilisation may be achieved by injecting high pressure steam. The process can be operated in a contained environment.
<b>Loading Capacity</b>	Low substrate bed loading due to limitations in operational bed heights.	High substrate loading coefficients are generally not possible due to problems of bed compaction and air channelling.	Low substrate bed loading. Usually useful space for fermentation comprises only around 30% of total volume.



<b>Modularity</b>	A single tray may serve as a module so the system can be modular in nature.	Zymotis among PBB is partly modular in nature.	RDBs are not modular in nature.
<b>In-situ product recovery</b>	May not be feasible	May not be feasible.	Has been possible in some reactor types.
<b>In-situ residue treatment</b>	May not be feasible.	May not be feasible.	Has been possible in some reactor types.
<b>Maintenance requirements</b>	Generally, maintenance is not intensive.	Due to its simple design, maintenance is generally not intensive.	Generally, not intensive but may be required in large-scale RDB with mixers.
<b>Damage to fungal mycelia</b>	No damage to the fungal mycelia due to shear.	No damage to the fungal mycelia due to shear.	Shear forces come into play. Trade-off between the rotational speed and fermentation.

### 1.5.3.1 Tray fermenters

Tray fermenters are the simplest reactors of solid-state fungal pretreatment. These reactors consist of stacked shallow trays loosely filled with solid substrates and inoculated with microorganisms in an aerated and controlled environment (**Fig. 1.12**) [98]. The top surface of the trays is exposed to air, while the bottom surface is usually perforated but without forced air circulation. Temperature is controlled by regulating the temperature of the gas flow into the chamber, and moisture saturation is maintained by spraying sterilised water into the chamber to maintain an optimum moisture content for fermentation. Tray reactors are the most commonly used SSF bioreactors in industrial applications, but they have several unresolved problems, such as insufficient heat removal, high risk of contamination, and low substrate utilisation efficiency due to low heat and mass transfer rates.

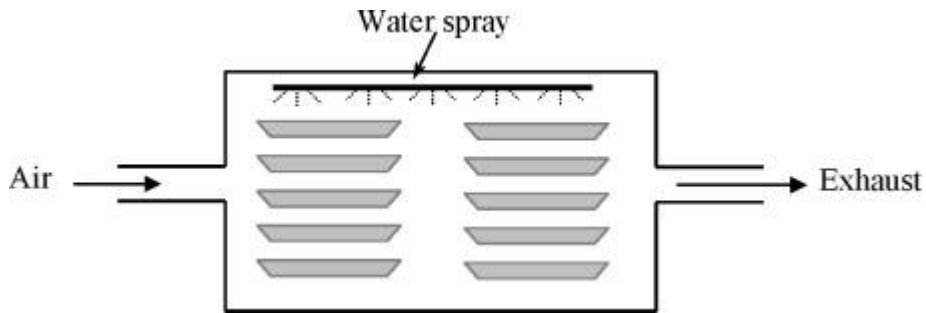


Fig. 1.12 Schematic diagram of tray reactor [98]

### 1.5.3.2 Packed bed bioreactors

A packed bed solid-state fermentation bioreactor is a vertical column that allows forced aeration through a perforated bottom (Fig. 1.13). Heat transfer is usually achieved by using a water jacket or by installing heat transfer plates inside the reactor (Zymotis packed bed) [130]. Temperature and gas concentration gradients are still observed but are smaller than in the tray fermenter [98]. However, the axial temperature gradients in the packed bed reactors result in high temperatures and significant water evaporation at the bed outlet drying out the substrate and reducing water activity to undesirable levels leading to poor microbial growth, even when saturated air is supplied [76].

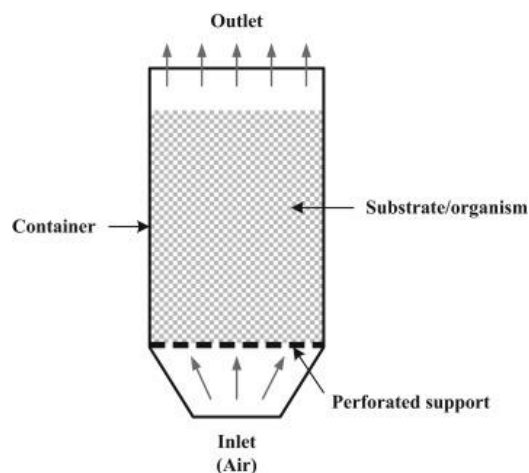
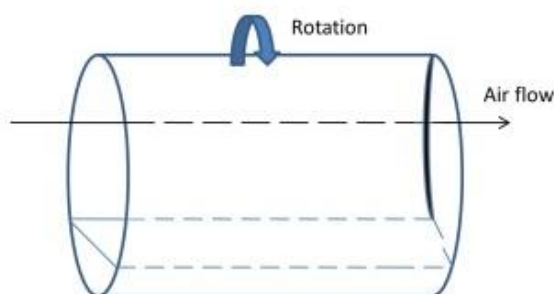


Fig. 1.13 Schematic diagram of packed bed bioreactor [130]

### 1.5.3.3 Rotary drum bioreactors

In the rotary drum bioreactor configuration, a horizontal or inclined cylinder rotates around its own longitudinal axis, causing constant movement of the substrate inside to facilitate gentle mixing **Fig. 1.14** [127,131]. A low rotation speed (1–15 rpm) has been recommended in this type of bioreactor [132]. The tumbling motion of the rotating drum allows efficient heat and mass transfer. However, there are drawbacks, such as the tendency for particles to agglomerate over time, and the rotational speed can damage shear-sensitive mycelia. Inner wall baffles within the rotating drum can help by lifting and lowering the substrate, increasing the maximum oxygen uptake rate by 60% compared to runs without baffles [133].



**Fig. 1.14** Schematic representation of rotary drum bioreactor (Adapted from Ref. [127])

## 1.6 Monitoring lignin degradation during fungal pretreatment

In the pursuit of the development of technologies that utilise plant biomass as a renewable source of feedstock for the production of biofuels and biochemicals, considerable attention has been paid to the understanding of how lignin content affects the accessibility of cell wall carbohydrates to cellulolytic enzymes, as well as the potential utilisation of the lignin itself. In the study of Nazarpour et al., a positive linear correlation between achievable enzymatic saccharification yield and lignin degradation was reported underlying the importance of following up the lignin degradation process during fungal pretreatment [18].

### 1.6.1 Conventional methods

The most commonly used methods for measuring lignin are the acetyl bromide, thioglycolic acid and Klason methods [134,135]. The acetyl bromide and thioglycolic acid

methods both involve solubilising lignin and measuring absorbance at 280 nm. These methods are invasive, laborious and lengthy. The Klason method, described by the National Renewable Energy Laboratory (NREL), is the oldest and most widely used method for quantifying lignin content [135]. This method involves a two-step acid hydrolysis of lignocellulose using concentrated sulfuric acid at 30°C for 1 hour, followed by dilution with water to 4% w/w sulfuric acid and autoclaving at 121°C for 1 hour to convert polysaccharides to monomeric sugars. The acid-insoluble lignin is determined gravimetrically, while the acid-soluble lignin is measured by UV spectrometry, usually at 240 nm. Although this traditional wet-chemical method has been effective for quantifying lignin in lignocellulose, it is time-consuming, laborious and requires the use of hazardous concentrated sulphuric acid and a relatively large amount of biomass (300 mg).

### 1.6.2 Infrared spectroscopy-based methods

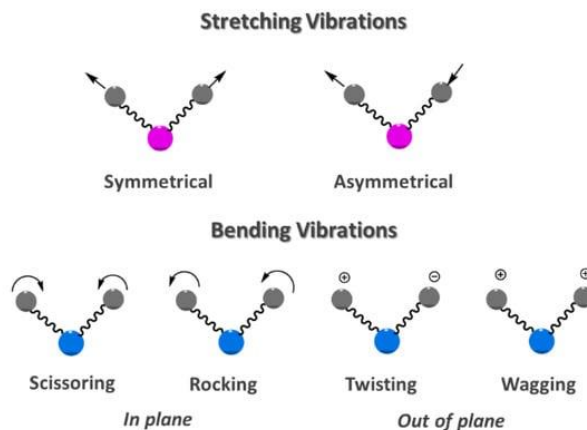
Infrared spectroscopy in the near-infrared (NIR; 14,000-4000  $\text{cm}^{-1}$ ) and mid-infrared (MIR; 4000-400  $\text{cm}^{-1}$ ) regions has gained interest in determining lignin in lignocellulose in a rapid, simple and non-destructive manner with this addressing the drawbacks of the traditional wet-chemistry based lignin quantification methods.

In infrared spectroscopy, a vibrational transition involving a change in the dipole moment results in the absorption of an infrared photon. The energy of the absorbed photon is equal to the energy difference between the two vibrational states of the molecule [136]. As covalent bonds vibrate, they absorb energy from IR light, with the absorbed wavelength depending on the type of bond (e.g. C=O or N-H), the type of vibration (bending, stretching, etc.) and the environment of the bond [136].

The following sections outline the principles, advantages and disadvantages of these techniques and their application to lignin quantification in fungus-treated wood.

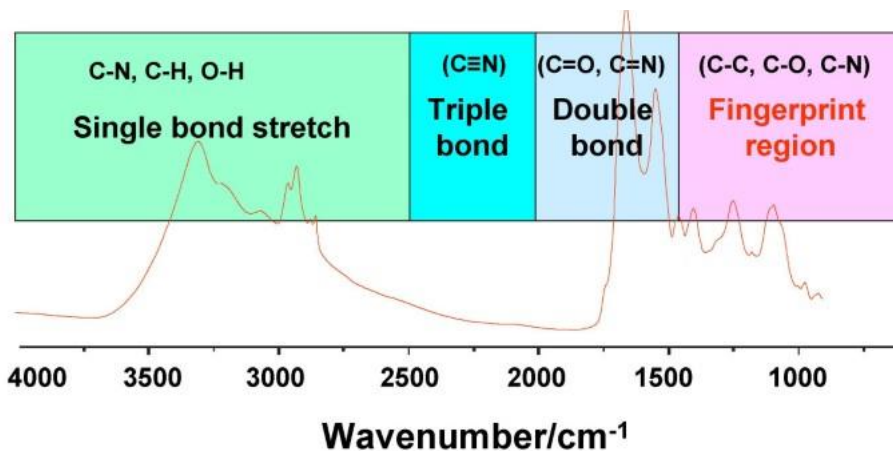
#### 1.6.2.1 Mid-infrared spectroscopy

The mid-infrared spectral region spans from 4000 to 400  $\text{cm}^{-1}$  (2.5 to 25  $\mu\text{m}$ ). MIR radiation is absorbed when chemical bonds undergo fundamental vibrations, i.e. transition from the ground state vibration to the first excited state, resulting in a change in bond length (stretching vibration) or bond angle (bending vibration). Certain bonds can stretch either in phase (symmetric stretching) or out of phase (asymmetric stretching) and bend in the plane or out of the plane (**Fig. 1.15**) [137].



**Fig. 1.15** Vibrations modes [137]

The mid-infrared spectral range can be partitioned into the fingerprint and the functional group region. The fingerprint region, which extends from 1500 to  $400\text{ cm}^{-1}$ , greatly differs for every molecule, but it is challenging to evaluate this region because of its high complexity **Fig. 1.16** [136]. The functional group region, on the other hand, covers the frequencies corresponding to the fundamental vibrations of most organic compounds.



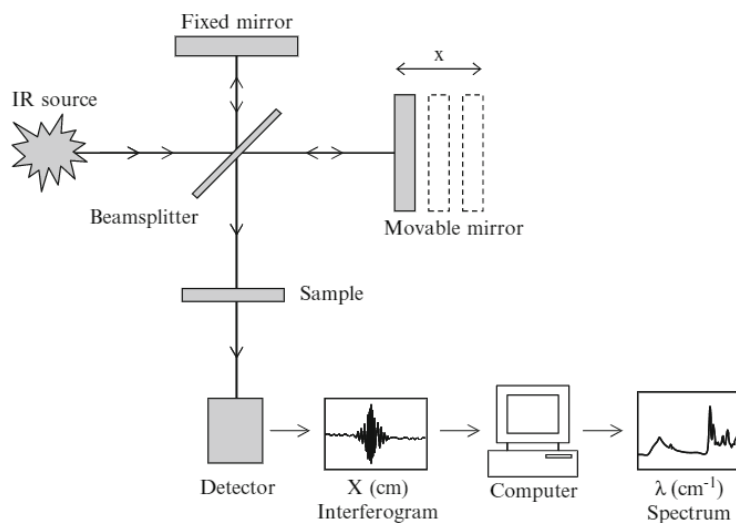
**Fig. 1.16** Group frequencies and fingerprint region of the MIR spectrum [136]

Most mid-IR instruments on the market today use an interferometer, which differs from earlier dispersive IR spectrometers in which the light transmitted through a sample is dispersed by a diffraction grating and the intensity at each wavelength is measured

sequentially, one wavelength at a time [138]. FTIR spectroscopy measures the entire spectrum simultaneously, and as a result, FTIR spectroscopy is generally faster and more sensitive than dispersive IR spectroscopy.

#### 1.6.2.1.1 FTIR spectroscopy

The heart of the FTIR instrument is the Michelson interferometer, which consists of a light source, a beam splitter, two mirrors (fixed and movable mirrors), a laser and a detector (**Fig. 1.17**) [139]. This optical device uses the beam splitter to split the incoming infrared beam in two. Half of the radiation is transmitted to the fixed mirror, and the other half is reflected to the movable mirror. After reflection from the mirrors, the two beams are recombined at the beam splitter, creating an interference pattern. The recombined beam passes through the sample, which absorbs the different wavelength components of the beam. The beam is then focused on the detector. The two beams recombine with varying degrees of optical path difference, depending on the position of the movable mirror, which moves back and forth at a constant speed, controlled by the response of the calibration laser.



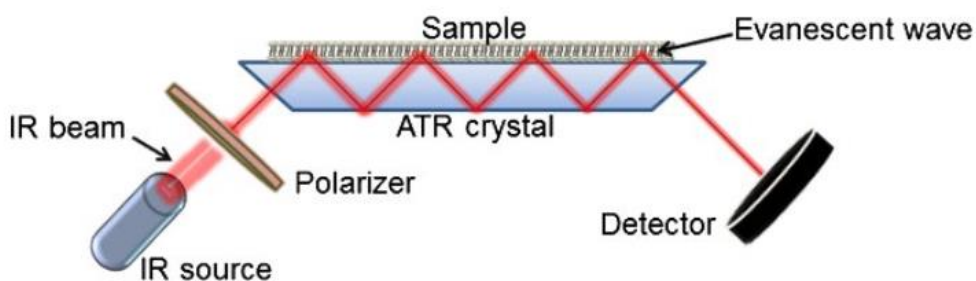
**Fig. 1.17** Schematic diagram of Fourier transform infrared spectrometer [139]

The optical path ( $\delta$ ) difference causes the two beams to interfere constructively or destructively on recombination. Constructive interference occurs when the optical path length difference is an integer multiple ( $n = 0, \pm 1, \pm 2, \pm 3, \dots$ ) of the wavelength ( $\delta = n \cdot \lambda$ ), while destructive interference occurs when the optical path length difference is

half an integer multiple of the wavelength ( $\delta = (n+0.5) \cdot \lambda$ ). The detector measures the variation of light intensity with optical path difference to produce the interferogram. The Fourier transform is then used to decode this intensity information and produce a spectrum. FTIR in MIR can be used in a variety of modes, including transmission, attenuated total reflectance (ATR), and diffuse reflectance mode. Each of them has its advantages and disadvantages. The ATR mode, i.e. the technique used in this study, is introduced in detail in the following section.

#### 1.6.2.1.2 Attenuated total reflectance

ATR mode is a powerful and widely used technique in FTIR spectroscopy for the analysis of a wide range of materials. ATR is based on a total internal reflection. In ATR mode, the sample is in contact with an internal reflection element (IRE, e.g. ZnSe, diamond, silicon or germanium) with a high refractive index [140–142]. The IR beam is passed through the IRE at an angle greater than the critical angle for total internal reflection to occur, resulting in the formation of an evanescent wave. The evanescent wave penetrates only a few microns into the sample, where it can be absorbed [143]. When the attenuated beam exits the crystal, it is directed to the detector and measured, creating the IR spectrum (**Fig. 1.18**) [141].



**Fig. 1.18** Schematic diagram of the ATR measuring mode [141]

FTIR in ATR sampling mode has gained a lot of attention as it allows the reproducible analysis of solid and liquid samples with minimal or no sample preparation [134–136] in contrast to the transmission mode, which often requires compression of the powdered samples and potassium bromide into a pellet [136].

### 1.6.2.2 Near-infrared spectroscopy

NIR spectra differ from MIR spectra in that MIR identifies fundamental vibrational modes, whereas NIR spectra detect subtle overtones and combination bands [136,144]. Overtones refer to higher-energy vibrational transitions ( $\Delta v > \pm 1$ ) than the fundamental vibrations. The first overtone involves a  $v = 0$  to  $v = 2$  transition, while the second overtone is a transition from  $v = 0$  to  $v = 3$  [145]. Combination bands are formed when two or more fundamental vibrations absorb energy simultaneously. These bands are mainly caused by stretching vibrations of C-H, N-H and O-H.

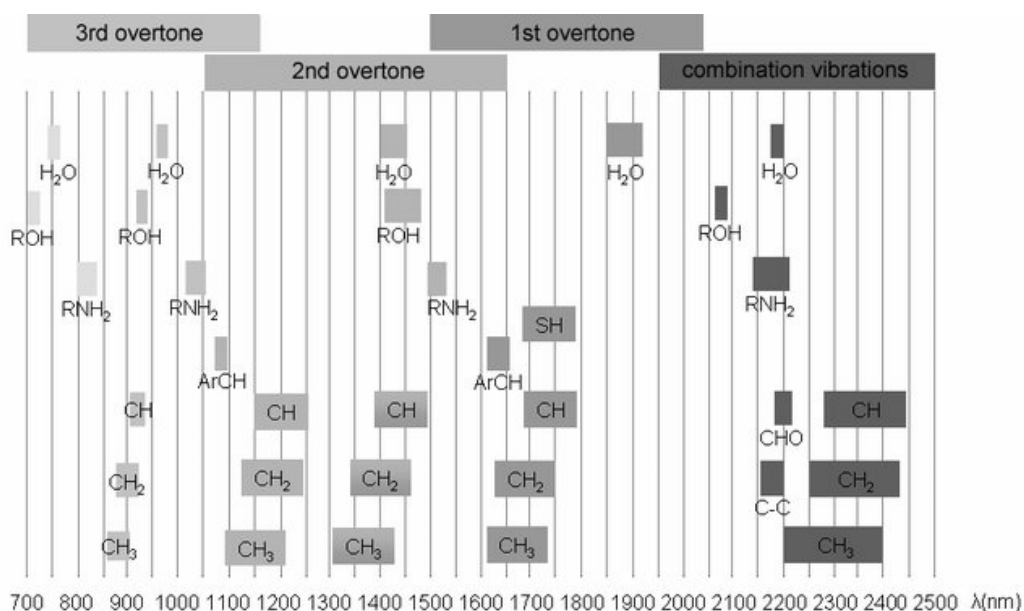


Fig. 1.19 NIR bands [144]

The bands in the NIR region are weaker in intensity and more difficult to interpret than the fundamental vibrations. Therefore chemometrics and multivariate analysis is often used to obtain useful information from the spectra.

Samples can be analysed in different modes, including transmission and diffuse reflectance. The diffuse reflectance mode is a widely accepted method for quantitative analysis and was used in this study.

#### 1.6.2.2.1 Diffuse reflectance mode

The diffuse reflectance measurement is based on the principle that not all reflected light comes from the surface (specular reflection), but some are reflected internally (diffuse reflection) Fig. 1.20 [146]. Diffusely reflected photons interact with the interior of the



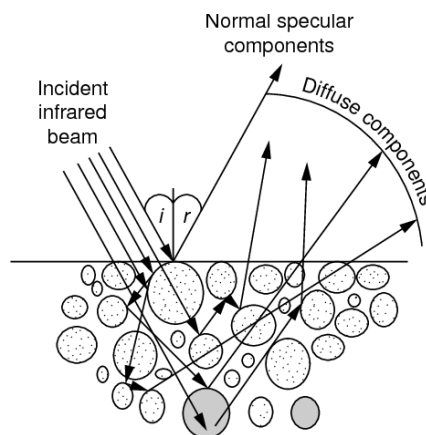
sample by penetrating into the material before reemerging at the surface after multiple scattering events. The diffusely reflected light is then detected by the detector [136,147]. The diffuse reflectance of a sample is influenced by the sample properties such as refractive index, particle size, packing density, homogeneity, concentration and absorption coefficient [146].

The reflectance of the sample is defined as the ratio of the intensities of the diffusely reflected light from the sample and from a non-absorbent reference material such as a ceramic disc [146]. This reflectance is usually expressed in absorbance units as  $\log(1/R)$  based on the Lambert-Beer's law which was initially strictly valid for systems with no scatter and is redefined as follows for reflectance measurements [142]:

$$A_{\lambda} = -\log_{10}(R) \cong \varepsilon_{\lambda} \cdot l \cdot c \quad (1.1)$$

Where:  $A$  is the absorbance,  $\varepsilon$  is the molar absorptivity or extinction coefficient [ $M^{-1} \text{cm}^{-1}$ ],  $c$  is the concentration of the analyte [ $M$ ], and  $l$  is the light path length [ $\text{cm}^{-1}$ ]

NIR spectroscopy has become a preferred method for industrial process monitoring due to its ability to measure turbid samples quickly, inexpensively and non-invasively. Diffuse reflectance measurements can penetrate within a few millimetres of the front surface of samples [136].



**Fig. 1.20** Schematic diagram of diffuse reflectance [146]

### 1.6.2.3 Pre-processing and multivariate analysis of spectral data

Direct interpretation of spectra in IR spectroscopy, especially in the NIR region, is limited. Therefore, multivariate mathematical methods are used to obtain useful information. These methods help to create mathematical models that establish a

correlation between spectral characteristics and properties of interest. For quantitative analysis, calibration models are required that relate the spectral data to the concentration of the sample analyte.

The first step in building a calibration model is pre-processing the collected spectral data to reduce or remove variability within the spectra unrelated to the investigated property. Many factors can cause spectral artefacts, including changes in temperature, path length, sample surface roughness, particle size, and more. These factors contribute to additive (causing baseline shift), multiplicative (scaling of spectra) and frequency-dependent scattering effects, resulting in baseline shifts, spectral tilts and unwanted peaks at certain wavelengths [148]. To overcome these problems, appropriate pre-processing techniques should be applied.

Commonly used pre-processing data treatment methods include multiplicative scatter correction, extended multiplicative signal correction, standard normal variate (SNV) and spectral derivatives. The techniques used in this study, i.e. SNV and second derivatives (Savitzky-Golay and Gap-Segment), are described in the following sections, followed by an introduction to multivariate analysis with emphasis on the methods used in this study.

#### **1.6.2.3.1 Standard normal variate**

The standard normal variate is a pre-processing method commonly used in chemometrics due to its simplicity. SNV normalises the spectrum by subtracting its mean value from each variable and dividing the resulting variables by the spectrum standard deviation [148,149].

Assuming a data matrix of  $X$ , comprising  $m$  samples and  $n$  spectral wavelengths, the SNV-corrected spectrum is given as follows [148]:

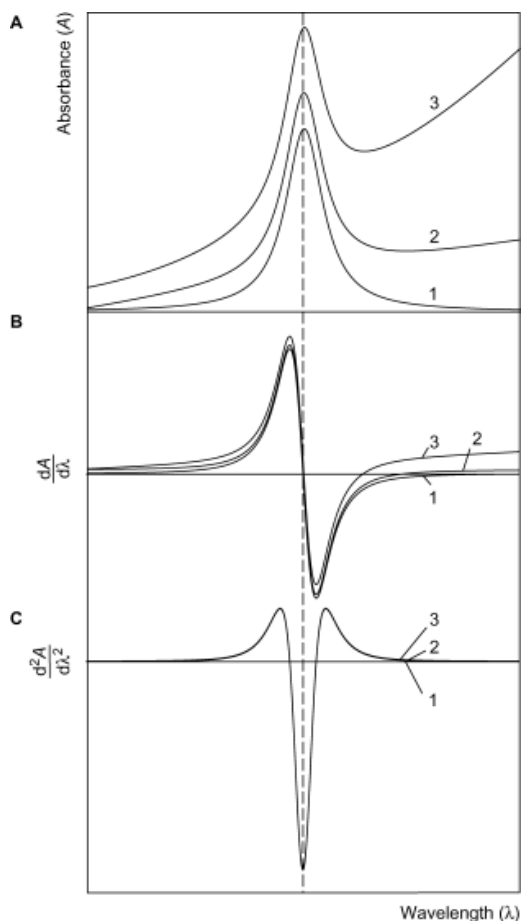
$$X_{mn} = \frac{X_{mn} - \bar{X}_n}{\sqrt{\frac{\sum (X_{mn} - \bar{X}_n)^2}{n-1}}} \quad (1.2)$$

SNV is useful for correcting spectra for varying path length, light scattering and surface roughness [148].

#### **1.6.2.3.2 Derivatives**

Derivatives are used to correct scattering effects and distinguish overlapping peaks. However, they can also amplify spectral noise along with the signal. The most commonly used methods are the first and second derivatives, which can be calculated using the

Savitzky-Golay algorithm or the gap-segment derivative. The first derivative is the slope of the spectrum, and the second derivative is a measure of change in the slope of the spectrum [149]. The first derivative removes only the baseline offset, while the second derivative removes both the baseline offset and the linear tilting of the spectra [149]. Second derivative spectra have a negative peak that matches precisely the position of the positive peak in the original spectrum **Fig. 1.21** p[150]. This study used the second derivative method to pre-process the spectral data.



**Fig. 1.21** Effect of first and second derivative on the spectra: (A) original spectra, (B) first-derivative spectra, and (C) second-derivative spectra. 1, zero baseline; 2, linear sloping baseline; 3, curved (quadratic) baseline with offset [150].

#### 1.6.2.3.2.1 Savitzky-Golay derivative

In the Savitzky-Golay (SG) derivative method, a polynomial is fitted to the raw data in a symmetric window in order to find the derivative at the centre point of the window

[151]. The user defines the number of points used to calculate the polynomial, i.e. the window size, and the degree of the fitted polynomial [149]. Once the polynomial parameters have been calculated, it is easy to analytically obtain the derivative of any order of this function for the centre point. This operation is applied sequentially to all points in the spectra.

#### **1.6.2.3.2 Gap-Segment derivative method**

The Gap-Segment (G-S) derivative, also called the Norris derivative, involves two steps (1) the moving average smoothing and (2) differential derivation [149,152]. It uses three parameters: the derivative order, the number of smoothing points (segment size), and the distance between the segments (gap size).

In the first step of the second derivative calculation, three segments are defined at one end of the spectrum, each separated by a gap [153]. The average absorbance values for the first, second and third segments, labelled *A*, *B* and *C* respectively, are then calculated. The second derivative value is then determined by subtracting twice the value of segment *B* from the sum of segments *A* and *C* ( $A + C - 2B$ ), and this value is assigned to the centre of the second segment. The entire sequence of three segments and the gaps between them is then shifted by one data point, and the calculation is repeated until a second derivative value has been calculated for all data points in the spectrum.

#### **1.6.2.3.3 Principle component analysis**

Principal Component Analysis (PCA) is an unsupervised multivariate statistical technique used to reduce the dimensionality of data, i.e. extract a smaller set of new variables from a large number of original variables that represent higher sample variability [154–156]. It creates latent variables, so-called principal components (PCs), which are linear combinations of the original spectral data and contain information about the entire spectrum. The maximum variability determines the direction of the new variables. The principal components are chosen to explain most of the remaining variability in the data and are orthogonal to each other. The matrix is decomposed into loadings and scores. The loadings of the variables on the principal components can be interpreted as the correlation between the variables and the principal components. The scores represent the value of each component for each observation and can be used to identify patterns or relationships in the data.

PCA is useful for exploring and visualising high-dimensional data, identifying patterns and trends, and reducing the dimensionality of data sets for subsequent analysis [154–156].

#### 1.6.2.3.4 Partial Least Squares Regression

Multivariate calibration models are built by obtaining representative calibration samples, collecting a spectrum for each, and determining the properties (Y) of interest by a reference method. The aim is to describe the sample property (Y) as a function of the measured spectral signals (X). The Partial Least Squares Regression (PLSR) is a popular choice of algorithm for developing multivariate regression models as it can efficiently capture the covariance between Y and X [154–156]. It does this by performing a simultaneous decomposition of X and Y with the constraint that these components explain as much of the covariance between X and Y as possible.

The present research aimed to develop a PLSR model for the prediction of lignin content in fungally treated wood. This requires obtaining a set of representative calibration samples, i.e. fungally pretreated samples, and recording the spectrum of each sample together with the determination of lignin content using a reference method such as Klason lignin determination.

##### 1.6.2.3.4.1 Evaluation of the PLSR model

To ensure that the PLSR model captures the underlying relationship between the spectral data and the chemical property (e.g. lignin content), cross-validation (CV) is typically performed on the calibration (C) set [157]. The resulting calibration model is then evaluated using independent samples in a validation set to ensure it is neither over- nor under-fitted. However, if independent samples are unavailable, researchers can divide their data set into a calibration and a validation set. In order to assess the predictive ability of the model for future samples, different partitioning techniques can be used during cross-validation. In this study, leave-one-out cross-validation was used, which excludes one sample at each iteration.

To evaluate the performance of IR calibration models, the root mean square errors of calibration ( $RMSE_C$ ) and cross-validation ( $RMSE_{CV}$ ), and the determination coefficients of calibration ( $R_C^2$ ) and cross-validation ( $R_{CV}^2$ ) can be used as performance metrics [157,158].

$$RMSE = \sqrt{\frac{\sum_{i=1}^n (\hat{y}_i - y_i)^2}{n}} \quad (1.3)$$

$$R^2 = \frac{SSR}{SST} = \frac{\sum_{i=1}^n (\hat{y}_i - \bar{y})^2}{\sum_{i=1}^n (y_i - \bar{y})^2} \quad (1.4)$$

Where  $\hat{y}_i$  is the predicted variable,  $y_i$  is the value of the property of interest,  $\bar{y}$  is the mean value of the property of interest,  $n$  is the number of samples, SSR (Sum of Squared Regression) is the sum of squared differences between predicted data points ( $\hat{y}_i$ ) and the mean of the response variable ( $\bar{y}$ ). SST (Sum of Squares Total) is the sum of squared differences between the observed data points ( $y_i$ ) and the mean of the response variable ( $\bar{y}$ ).

#### **1.6.2.4 Application for lignin quantification in fungus-treated wood**

The potential of NIR spectroscopy to quantify the amount of lignin in wood has been recognised by many researchers [19–21]. Fackler et al. used both FT-MIR spectroscopy in transmission mode and FT-NIR reflectance spectroscopy to determine lignin content in beech wood before and after fungal decay of wood was performed in Petri dishes [159]. ATR-FTIR with PLSR modelling could be applied for the quantitative determination of the lignin in lignocellulose [22,23]. In the field of wood decay, ATR-FTIR has been recognised for its potential to qualitatively assess the fungal deconstruction of lignocellulose [160,161]. However, ATR-FTIR has not been applied to the quantitative determination of lignin in wood pretreated with white-rot fungi.

### **1.7 Techno-economic feasibility of fungal pretreatment**

Techno-economic analysis (TEA) is used to assess both the technical and economic feasibility of a process or system. A comprehensive TEA considers all upstream and downstream unit operations of a process, considering their capital and operating costs, with particular emphasis on the production phase. However, it is important to note that TEA does not take into account the potential environmental impacts of the technology under consideration [162,163].

TEA serves as an essential bridge between small-scale laboratory research and industrial production, helping to assess the feasibility of the technology and also highlighting areas of the process where further improvements are needed. Although a particular technology may appear viable on a small scale, assessing its viability on a larger scale becomes more complex and challenging. Several models are currently available to assist in estimating the costs of project scale-up. Process simulation software tools, such as Aspen Plus and SuperPro, are widely used to simulate processes and determine economic parameters, including the capital required to build and operate an industrial-scale plant.

Fungal pretreatment offers several advantages over traditional chemical and physical pretreatment methods, including mild reaction conditions, reduced energy

consumption, and the absence of inhibitory by-products. As a result, the need for post-treatment detoxification is eliminated. However, this method has some limitations, such as long pretreatment times, lower sugar yields and the need for sterilisation of the feedstock. **Table 1.5** compares physical, thermochemical and biological pretreatment methods from a techno-economic and environmental point of view [164].

**Table 1.5** Comparison of different pretreatment methods on the basis of techno-economic and environmental parameters (Adapted from Ref. [164])

Parameters	Pretreatment methods		
	Physical	Thermochemical	Biological
Energy requirement	+++	+++	+
Operational cost	\$\$	\$\$\$	\$\$
Capital cost	\$\$\$	\$\$\$	\$\$\$*
Process efficiency	++	+++	+
Environmental impact	+	+++	+
Odour generation	+	+++	+++
Biomass solubilization	NA	+++	+++
Inhibitor generation	NA	+++	–
Applications in lignocellulosic biomass	++	+++	++

NA not applicable; – negligible; +/\$ low; ++/\$\$ medium; +++/\$\$\$ high

\*Adapted from \$\$ to \$\$\$ based on literature evidence [10,24]

Several authors have claimed that fungal pretreatment is a low-cost technology due to the advantages described above [87,164], but the techno-economic feasibility of the process at a commercial scale has only recently been evaluated. Vasco-Correa and Shah evaluated the economic and technical feasibility of producing fermentable sugars for a biorefinery producing 75,700 m<sup>3</sup> of ethanol per year using a fungal pretreatment starting from various lignocellulosic feedstocks such as corn stover, herbaceous energy crops, agricultural residues and woody feedstocks [10]. The estimated cost of sugar production was relatively high, ranging from \$1.7 to \$2.8/kg sugars for different feedstocks, which was 4-15 times higher than that achieved by conventional pretreatments. The cost associated with the facility was found to be the largest

contributor (46-51%) to the sugar price due to the high number and large size of the equipment required due to the long pretreatment times, low sugar yields, low feedstock bulk density and sterilisation requirements of the fungal pretreatment process.

Therefore, to improve the techno-economic performance of fungal pretreatment of lignocellulosic biomass, it is essential to improve key parameters such as sugar yield, pretreatment time and sterilisation requirements.



## **Chapter 2. Enhanced fungal delignification and enzymatic digestibility of poplar wood by combined CuSO<sub>4</sub> and MnSO<sub>4</sub> supplementation**

---

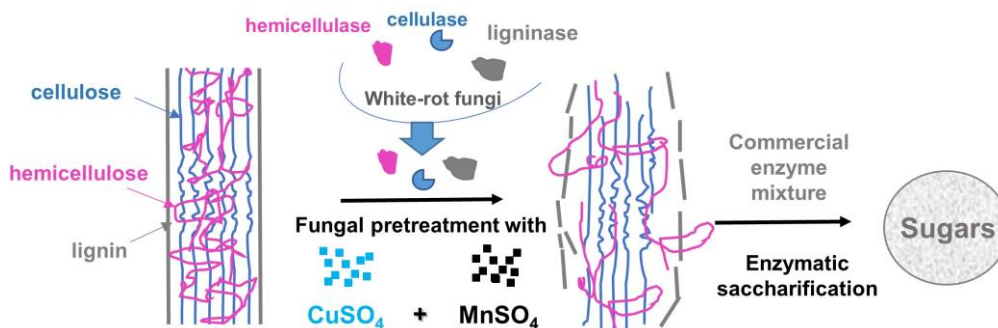
This chapter was redrafted from the manuscript published in *Process Biochemistry*.

N. Wittner, W. Broos, J. Bauwelinck, J. Slezsák, S.E. Vlaeminck, I. Cornet, Enhanced fungal delignification and enzymatic digestibility of poplar wood by combined CuSO<sub>4</sub> and MnSO<sub>4</sub> supplementation, *Process Biochem.* 108 (2021) 129–137.

<https://doi.org/10.1016/J.PROCBIO.2021.06.002>.

**Abstract**

Fungal pretreatment of lignocellulose by white-rot fungi is a biotechnological alternative to chemical and physical approaches to enhance enzymatic saccharification. However, inefficient lignin degradation and substantial cellulose consumption during fungal pretreatment can cause low sugar yields. In this study, the combined action of  $\text{CuSO}_4$  and  $\text{MnSO}_4$  effectively improved the degree and selectivity of delignification during solid-state fungal pretreatment of poplar wood by *Phanerochaete chrysosporium*. Compared to pretreatment without this supplementation, a 1.9-fold higher lignin degradation and 2.4 times higher delignification selectivity value were obtained due to the increased and prolonged manganese peroxidase activity. Enzymatic saccharification of supplemented pretreated wood resulted in a 2.9 times higher glucose yield compared to the non-supplemented system. This study has demonstrated that the combined application of  $\text{Mn}^{2+}$  and  $\text{Cu}^{2+}$  can significantly improve the fungal pretreatment process and that the beneficial effect of  $\text{Cu}^{2+}$  on delignification is not restricted to laccase-producing fungi.



**Fig. 2.1** Graphical abstract

## 2.1 Introduction

Lignocellulose from the plant cell wall is a potential raw material for the production of biofuels and biochemicals due to its sustainable production, high abundance and low cost. However, utilization of its carbohydrate content requires a pretreatment process to reduce biomass recalcitrance and subsequently improve carbohydrate accessibility to hydrolytic enzymes.

Currently, physical/chemical pretreatment methods are considered the leading pretreatment technologies. However, they usually require high energy, corrosion-resistant and high-pressure reactors, and detoxification of inhibitory by-products, and they produce a large volume of waste streams [165,166].

Biological pretreatment as a sustainable alternative has gained great interest due to its low energy requirements and mild reaction conditions. In general, white-rot fungi (WRF) are considered the most efficient lignin-degrading microorganisms due to their unique ligninolytic enzyme systems [167]. Four major extracellularly produced lignin-degrading enzymes, namely lignin peroxidase (LiP), manganese peroxidase (MnP), versatile peroxidase and laccase, are responsible for this [68]. Despite its advantages, fungal pretreatment suffers from the main drawbacks of long pretreatment time, non-selective lignin degradation and substantial cellulose consumption. The latter is due to the cellulolytic enzyme production by the fungi resulting in a low delignification selectivity (indicated by the selectivity value, SV, that is, the ratio of lignin degradation [%] and cellulose consumption [%]) and low glucose yield after enzymatic saccharification of the pretreated biomass [77].

*Phanerochaete chrysosporium* is widely studied due to its fast growth. This white-rot fungus is known to secrete manganese-peroxidase (MnP) and lignin peroxidase (LiP) but not laccase nor versatile peroxidase [9,65,66]. Depending on the fungal pretreatment system, delignification selectivity values between 0.59 and 1.2 were reported in the literature for *P. chrysosporium* [77,86–88]. Indeed, the SV during pretreatment not only depends on the ligninolytic ability of the fungal strains but also on the substrate applied and, even more important, on the culture conditions [79,80]. Therefore several studies have focused on the use of supplements such as metal ions to enhance the production and activity of ligninolytic enzymes in liquid cultures [11]. Wang et al. reported that the addition of  $Mn^{2+}$  not only increases the production of MnP by *P. chrysosporium* but, to a lesser extent, of LiP as well [12]. In contrast, the study of Mester et al. indicated that the exogenous addition of  $Mn^{2+}$  enhanced the production of MnP and, at the same time, decreased the secretion of LiP and the secondary metabolite veratryl alcohol (VA), suggesting that  $Mn^{2+}$  plays a regulatory role in the ligninolytic enzyme production [118].

The study of Singhal and Rathore revealed that the addition of a low amount (1.2  $\mu\text{M}$ ) of  $\text{Cu}^{2+}$  improves both LiP and MnP enzyme production of *P. chrysosporium* in liquid culture [13].

Furthermore, in a different field, i.e. the field of enzymatic saccharification of glucan substrate, inhibition of cellulolytic enzyme activities by  $\text{Cu}^{2+}$  and  $\text{Mn}^{2+}$  has been reported [124,125]. Moreover, the study of Xu et al. showed that  $\text{Cu}^{2+}$  ions oxidise the reducing ends of cellulose, resulting in a structurally modified cellulose with decreased enzymatic digestibility [126].

Copper is a well-known inducer of laccase enzyme production in white-rot fungi and was successfully applied as a supplement for improved delignification of lignocellulose by laccase-producing fungi [121,168,169]. However, the effect of  $\text{Cu}^{2+}$  ions on the degree and selectivity of lignin degradation during solid-state fungal pretreatment of lignocellulose by the non-laccase-producing *P. chrysosporium* has not been studied yet. Moreover, the combined addition of the abovementioned heavy metal ions to alter the ligninolytic and cellulolytic enzyme activities of *P. chrysosporium* and, in this way, improve the degree and selectivity of delignification has not been investigated to the best of our knowledge.

In the present study on solid-state fungal pretreatment of poplar wood by *P. chrysosporium*, the individual and combined effect of  $\text{Mn}^{2+}$  and  $\text{Cu}^{2+}$  supplements on the effectivity and selectivity of delignification and the enzymatic digestibility of pretreated biomass has been reported for the first time.

## **2.2 Materials and Methods**

### **2.2.1 Fungal strain and spore suspension preparation**

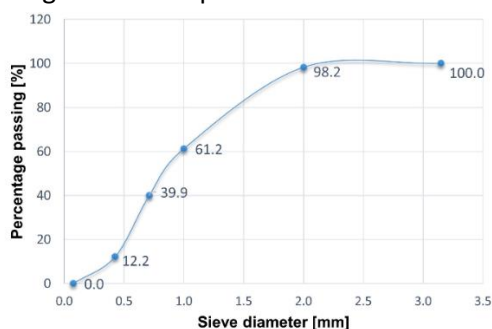
The white-rot fungus *Phanerochaete chrysosporium* MUCL 19343 was purchased from the Mycothèque of the Catholic University of Louvain (Belgium) and used for solid-state fermentation experiments. A spore suspension was freshly prepared from 5 days old cultures grown on potato dextrose agar at 39°C according to the study of Tien and Kirk [170]. Spore concentration was adjusted to  $5 \cdot 10^6$  spores/mL with sterile water, counted in a hemocytometer, which corresponds to 0.49 OD at 650 nm (Genesys 10S UV-Vis Spectrophotometer).

### **2.2.2 Lignocellulose substrate**

Poplar wood sawdust (Sawmill Caluwaerts Willy, Holsbeek, BE) was used as a substrate for solid-state fermentation. Sieving was used to obtain the particle size distribution. 86.1% w/w of the pellets were collected between the 2 mm and 0.075 mm screens (**Fig. 2.2**). The dry weight (DW) content of the wood was measured by freeze-drying (Alpha 1-2 LD plus) and found to be  $91.75 \pm 0.31\%$ .

### 2.2.3 Medium

For the standard fermentation medium, a modified composition of the one applied by Keller et al. was used, with the addition of veratryl alcohol and Tween 80 to enhance ligninolytic enzyme production [12,171]. 3 g of NaNO<sub>3</sub>, 0.5 g of KCl, 0.5 g of MgSO<sub>4</sub>·7H<sub>2</sub>O, 0.5 g of FeSO<sub>4</sub>·7H<sub>2</sub>O, 1 g of KH<sub>2</sub>PO<sub>4</sub>, 0.34 g of veratryl alcohol, 1 mL of Tween 80 and 20 g of glucose were dissolved per litre of demineralised water. The added glucose in the media (10.9 mg glucose/g DW wood) supports spore germination and mycelial growth at the start of the SSF. This general medium was supplemented with CuSO<sub>4</sub> and MnSO<sub>4</sub> according to the design of each experiment and was autoclaved at 121°C for 20 min.



**Fig. 2.2** Cumulative percentage of wood passing through the sieves

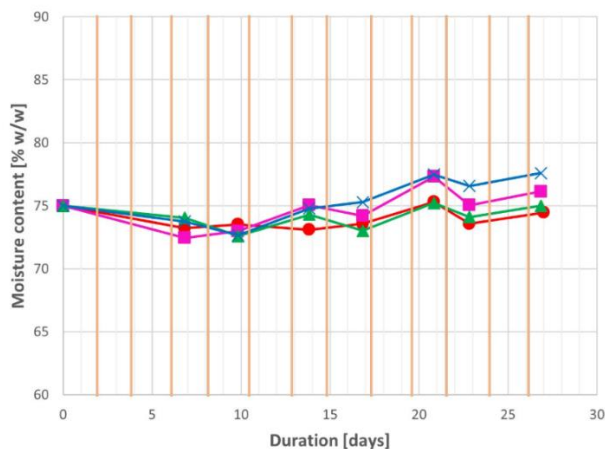
### 2.2.4 Fungal pretreatment

Fungal pretreatment experiments were conducted in 100 mL Schott bottles closed with sterile-venting screw caps with welded-in 0.2 µm PTFE membrane (DURAN®). These membrane screw caps allow sterile gas exchange and due to the naturally hydrophobic character of PTFE, they limit water evaporation during fermentation. Bottles containing 4 g of wood (3.67 g DW) and 5 mL distilled water were autoclaved at 121°C for 60 min, cooled and mixed with sterile water (the amount which evaporated during autoclaving), 2 mL sterile media and 3.7 mL spore suspension ( $5 \cdot 10^6$  spores/g DW wood [87]) creating a wet basis moisture content of 75% w/w for the final fermentation mixture. Each bottle was rolled at 4 rpm on a bottle roller (Thermo Scientific™ 88881004) and incubated (Lovibond® Tintometer GmbH) at 37°C (optimal temperature for MnP production [172]) for 4 weeks (**Fig. 2.3**). At the end of the fermentation, the dry solid loss was measured

[% w/w]. Water trays filled with deionised water were placed at the bottom of the incubator to increase the humidity inside and hereby decrease water loss by evaporation in the fermentation mixture. Furthermore, every 2 to 3 days sterile water was added to the bottles by replacing the measured weight loss with sterile water and hereby ensuring a moisture content (on a wet basis) above 72% w/w (empirically tested) during the entire fermentation (**Fig. 2.4**).



**Fig. 2.3** Fermentation bottles placed on a bottle roller



**Fig. 2.4** Moisture content of poplar wood during SSF under different metal supplementation, i.e. (—●—) without supplement, (—▲—) with  $2.18 \mu\text{mol CuSO}_4 \text{g}^{-1}$  DW wood, (—■—)  $1.09 \mu\text{mol MnSO}_4 \text{g}^{-1}$  DW wood, and (—×—)  $2.18 \mu\text{mol CuSO}_4$  and  $1.09 \mu\text{mol MnSO}_4 \text{g}^{-1}$  DW substrate. The orange-coloured vertical lines show the time of the water addition.

### 2.2.5 Experimental design and statistical analysis

Due to the heterogeneity of the solid-state cultivation and the sensitivity of the fungal mycelium to shear stress [113], as would be induced during mixing at a periodical sampling of the fermentation system, it was chosen to harvest the whole content of the fermentation bottle after pretreatment conducted for predefined time intervals. The general influence of the metal ions  $\text{Cu}^{2+}$  and  $\text{Mn}^{2+}$  on the SSF was measured in bottles after 4 weeks of fermentation (Section 2.2.5.1), while for the analysis of the ligninolytic enzyme activity (which often evolves to an optimum and then shows a decrease [88,173,174] several bottles were prepared and harvested after increasing pretreatment time to follow-up the evolution of SSF (Section 2.2.5.2)

#### 2.2.5.1 Influence of metal supplementation by Response Surface Methodology

The effect of metal supplementation by  $\text{CuSO}_4$  and  $\text{MnSO}_4$  addition on the performance of SSF was determined using a Central Composite Design (CCD) and Response Surface Methodology (RSM). The design (referred to as CCD1 in the text) consisted of 13 experimental runs with both factors at three levels ( $0 \mu\text{mol}$ ,  $1.09 \mu\text{mol}$ ,  $2.18 \mu\text{mol}$   $\text{Cu}^{2+}$ ;  $0 \mu\text{mol}$ ,  $0.545 \mu\text{mol}$ ,  $1.09 \mu\text{mol}$   $\text{Mn}^{2+}$   $\text{g}^{-1}$  DW substrate) with four replications of the centre point, as listed in **Table 2.1**. These metal dosages were based on preliminary experiments conducted in our laboratory (data not shown). Along with each of the 13 experimental runs, a control run (untreated wood), containing the same metal dosage as the experimental run but without fungal inoculum, was set up. The purpose of these control experiments was to exclude that metal ions themselves, at their investigated concentrations, can affect enzymatic saccharification of the pretreated wood, either by the inhibition of cellulase enzymes or by  $\text{Cu}^{2+}$ -induced oxidation of lignocellulose [124–126]. Design-Expert software (Version 12.0, Stat-Ease, USA) was used to build and evaluate the experimental design. Analysis of variance (ANOVA) was used to estimate the F-values, p-values, lack of fits and determination coefficients ( $R^2$ ) of the obtained experimental models.

**Table 2.1** Central Composite Design 1 (CCD1)

Run	Metal supplement ( $\mu\text{mol g}^{-1}$ DW substrate)	
	A: $\text{CuSO}_4$	B: $\text{MnSO}_4$
1	1.09	0.54
2	2.18	1.09
3	1.09	0.00
4	2.18	0.00
5	0.00	0.54
6	1.09	0.54
7	1.09	0.54
8	0.00	1.09
9	1.09	1.09
10	2.18	0.54
11	1.09	0.54
12	0.00	0.00
13	1.09	0.54

### 2.2.5.2 Effect of metal supplementation on ligninolytic enzyme production

Four sets of experiments were run, i.e. non-supplemented,  $\text{Mn}^{2+}$  supplemented ( $1.09 \mu\text{mol g}^{-1}$  DW substrate),  $\text{Cu}^{2+}$  supplemented ( $2.18 \mu\text{mol g}^{-1}$  DW substrate) pretreatment systems and experiments with the combined addition of these metal ions. In this experimental set-up, every measurement point in the function of time represents an individual fermentation. The evolution of SSF is followed up with each experimental value confirming the previous ones.

## 2.2.6 Analytical methods

### 2.2.6.1 Enzyme extraction

When harvesting, a portion of the pretreated wood was immediately used for the extraction of ligninolytic enzymes. Extraction was performed with acetate buffer (pH 4.5, 50 mM) for 1 h at 400 rpm and  $4^\circ\text{C}$  applying a solid-to-liquid ratio of 1:12 on a dry weight basis, followed by centrifugation (Sigma 3-16KL) for 10 min at 4500 rpm and  $4^\circ\text{C}$ . Extracts were stored at  $4^\circ\text{C}$  and used for ligninolytic enzyme activity assays within 24 h after extraction. After the removal of the extraction liquid, the solid fraction was freeze-dried (CHRIST ALPHA 1-2 Ldplus) and used for composition analysis and characterization by Fourier transform-infrared spectroscopy (FTIR).



The remaining portion of the pretreated wood was freeze-dried without extraction and used for the determination of dry weight content, fungal growth measurement and enzymatic saccharification. The dry weight content [% w/w] was used to calculate the dry solid loss after fungal pretreatment.

#### **2.2.6.2 Ligninolytic enzyme assays**

MnP activity was determined by monitoring the formation of Mn<sup>3+</sup>-malonate complexes [175]. The malonate assay mixture contained 0.4 mL of 5 mM MnSO<sub>4</sub> (pH 4.5), 1 mL of 100 mmol/L malonate buffer (pH 4.5), 0.2 mL enzyme extract diluted with acetate buffer (pH 4.5, 50 mM) and 0.4 mL of 0.5 mM H<sub>2</sub>O<sub>2</sub>. The reaction was started by the addition of H<sub>2</sub>O<sub>2</sub> at 30°C, and the increase of absorbance was monitored for 5 min at 270 nm ( $\epsilon_{270\text{ nm}} = 11.59\text{ L}/(\text{mmol}\cdot\text{cm})$ ) against distilled water. Dilution of the enzyme extract was necessary to reduce the interference of UV-absorbing degradation products released during the fungal pretreatment. Control assays were performed by replacing the active enzyme solution with an inactivated enzyme (enzyme extract boiled for 15 min at 100°C before centrifugation at 21,500 x g for 1 min).

Lignin peroxidase activity was measured by monitoring the oxidation of the dye Azure B [176,177]. 1.25 mL of reaction mixture consisted of 0.5 mL of 125 mM sodium tartrate buffer (pH 4.5), 0.25 mL of 160  $\mu\text{M}$  Azure B, 0.25 mL enzyme filtrate and 0.25 mL of 2 mM H<sub>2</sub>O<sub>2</sub>. The reaction was initiated by the addition of H<sub>2</sub>O<sub>2</sub>. The absorbance decrease was measured against distilled water at 651 nm ( $\epsilon_{651\text{ nm}} = 48.8\text{ L}/(\text{mmol}\cdot\text{cm})$ ) for 5 min at 25°C. Enzyme preparation, inactivated by boiling, served as a control. All measurements were done in duplicate. One unit (U) of enzyme activity was expressed as the amount of enzyme that catalyses the oxidation of 1  $\mu\text{mol}$  of substrate per min. Specific activity was defined as the number of units per gram (g) of protein measured in the crude extract.

#### **2.2.6.3 Total protein determination**

The protein concentration of enzyme extracts was determined by the bicinchoninic acid (BCA) method using Pierce™ BCA Protein Assay Kit (Thermo Scientific).

#### **2.2.6.4 Composition analysis of lignocellulose**

Compositions of pretreated and control poplar wood samples were determined before and after the pretreatment according to the standard NREL protocol (NREL/TP-510-42618) [135]. In short, acid-soluble (ASL) and acid-insoluble lignin (AIL), glucan, and xylan content of the samples were measured by two-stage acid hydrolysis with sulfuric acid. ASL was calculated using the absorbance of the hydrolysate measured at 240 nm ( $\epsilon_{240\text{ nm}} = 25\text{ L}/(\text{g}\cdot\text{cm})$ ). The glucan and xylan contents in the samples were calculated from

released glucose and xylose, respectively. For sugar analysis, HPLC (1260 Infinity II LC system, Agilent Technologies) equipped with a refractive index detector maintained at 55°C, and a Coregel ORH 801 6.5 ID x 300 mm column (Concise separations) were used. 8 mM H<sub>2</sub>SO<sub>4</sub> was applied as a mobile phase at a flow rate of 0.6 mL/min at 75°C. Samples were filtered through 0.2 µm PES filters before analysis. The glucan and xylan contents were calculated with anhydro correction using Equation (3.1) and (3.2), respectively:

$$\% \text{Glucan} = (G \cdot 0.9) / w \cdot 100 \quad (2.1)$$

$$\% \text{Xylan} = (X \cdot 0.88) / w \cdot 100 \quad (2.2)$$

Where G is the glucose released (g) and w is the sample dry weight (g). The X value included the xylose released and the co-eluting minor sugars mannose and galactose (owning a comparable response factor to xylose). However, poplar wood comprises a relatively low portion of galactan (1.7–3.9%) and mannan (0.6–1.5%), compared to xylan 13.0–18.7% [1,178–180].

Lignin degradation discussed in this paper refers to the total lignin degradation, i.e. ASL and AIL. The degradation of lignocellulose biomass components after fungal treatment was calculated using Equation (3.3):

$$\% \text{ degradation of biomass component} = (1 - (w \cdot \alpha) / (w_0 \cdot \alpha_0)) \cdot 100 \quad (2.3)$$

Where  $w_0$  is the initial dry weight of poplar wood,  $w$  is the dry weight of pretreated poplar wood (g),  $\alpha_0$  and  $\alpha$  are the percentages of lignocellulose components in untreated wood (control) and pretreated wood, respectively. Since the substrate sterilisation slightly altered the original wood composition (**Table 2.2**), biomass degradation was calculated against control samples in the case of the CCD experiments (Section 2.2.5.1), or against samples immediately harvested after inoculation when SSF was followed up in the function of time (Section 2.2.5.2).

**Table 2.2** Composition of raw feedstock, autoclaved (control) poplar wood from CCD1, and autoclaved (initial) wood from experiments described in 2.5.2.

	Raw feedstock	Autoclaved (control)	Autoclaved (initial)
<b>Composition</b>			
Total lignin [%]	30.80 ± 0.76	31.04 ± 0.20	30.03 ± 0.26
AIL [%]	26.32 ± 0.70	26.48 ± 0.26	25.58 ± 0.40
ASL [%]	4.48 ± 0.14	4.56 ± 0.08	4.45 ± 0.08
Glucan [%]	45.10 ± 1.04	44.40 ± 0.74	45.01 ± 1.54
Xylan (mannan, galactan) <sup>a</sup> [%]	17.10 ± 0.83	17.01 ± 0.30	17.24 ± 0.78
Arabinan [%]	0.25 ± 0.02	0.31 ± 0.08	0.25 ± 0.04
Acetate [%]	2.46 ± 0.21	2.77 ± 0.25	3.14 ± 0.28
Extractives [%]	3.46	n.d.	n.d.
Total [%]	98.99		

<sup>a</sup>Xylan value also included mannan and galactan due to the coelution of the minor sugars mannose and galactose with xylose, <sup>b</sup> Determined by two-steps extraction with water and ethanol (NREL/TP-510-42619 [181]); 'n.d.' not determined. The results are based on the analysis of six raw feedstock, 13 autoclaved (control) and 4 autoclaved (initial) samples.

### 2.2.6.5 Fungal growth measurement

Indirect measurement of fungal biomass was carried out by quantification of ergosterol content in the non-washed, freeze-dried samples. Before analysis, the lyophilised samples were ground with a ball mill. Hereto, 500 mg of sample was measured into a stainless steel grinding jar (25 mL) together with four 10 mm and one 15 mm stainless steel grinding balls. The jar was immersed in liquid nitrogen for 30 seconds to embrittle the sample and avoid its thermal damage. Milling was carried out for 4 min at a frequency of 25 Hz in a mixer mill (Retsch MM200). Ergosterol determination was carried out according to the protocol described in the study of Niemenmaa et al. [182]. In summary, 250 mg of the pretreated wood sample was saponified in 3 ml 10% w/w KOH in methanol for 1 h at 80°C. After cooling, hexane and distilled water were added for extraction, which was repeated once. The hexane phases were pooled and

evaporated under vacuum. The extracted ergosterol was dissolved in 0.75 mL methanol, filtered through a 0.2  $\mu\text{m}$  PTFE filter and analysed by HPLC equipped with a UV-VIS diode array detector (282 nm) using a reversed-phase C18 column (Phenomenex Aqua<sup>®</sup> 5  $\mu\text{m}$ , 125  $\text{\AA}$ , 250  $\times$  4.6 mm) at 25°C. A mixture of 90% methanol and 10% (1:1) 2-propanol/hexane was used as eluent with a flow rate of 0.4 mL/min. Areas under the peak were corrected for the extraction efficiency based on the internal standard 7-dehydrocholesterol (9.6  $\mu\text{g}$  added to each sample). The ergosterol content of the fungi, for ergosterol-to-fungal biomass conversion, was determined in *P. chrysosporium* scraped from a PDA agar plate (5 days of cultivation at 39 °C) and was measured to be  $7.24 \pm 0.26 \mu\text{g}$  ergosterol/mg fungal biomass.

Fungal growth measurements were performed without replicates due to the lack of an efficient sample size. The average standard deviation (STD) of the analysis, tested on 32 fungus-treated samples of other fermentations, was determined to be  $\pm 0.251 \text{ mg}$  fungal biomass/g wood.

### **2.2.6.6 Enzymatic saccharification of pretreated biomass**

Enzymatic saccharification of untreated and pretreated wood was carried out by Optimase CX 15L commercial enzyme mixture (DuPont) under the conditions optimised in our laboratory for the current substrate. Before its use, the enzyme mixture was sterile-filtered (PES, 0.45  $\mu\text{m}$ ) to remove insoluble solid particles. Total cellulase activity was measured in filter paper units (FPU) based on the NREL/TP-510-42628 protocol [183]. Enzymatic saccharification was carried out with 0.6 g of dry biomass, 0.6 mL of 0.5 M citrate buffer (pH 4.6), 0.396 mL of cellulase enzyme mixture (Optimase CX 15L, 38 FPU /g dry biomass) and 24  $\mu\text{l}$  of tetracycline stock solution (10 mg/mL in 70% ethanol). Distilled water was added to bring the solid-to-liquid ratio up to 1:10, and the mixture was incubated at 50°C, 240 rpm for 72 hours. Hydrolysates were boiled for 10 min in a water bath to precipitate the protein content and centrifuged at 21,500 g for 3 min. The supernatant was filtered through a syringe filter (0.2  $\mu\text{m}$ , PES) and was analysed for its glucose and xylose content by HPLC (as described in 2.6.4) and its reducing sugar content by 3,5-dinitrosalicylic acid (DNS) method [184]. The glucose, xylose and reducing sugar yields are defined relative to the theoretical yield from the raw feedstock [18,185].

### **2.2.6.7 Characterization of pretreated biomass by FTIR**

Pretreated wood samples after the removal of water-soluble substances (as described in 2.6.1) were characterised by FTIR [160]. Before FTIR analysis, the samples were thoroughly rinsed with distilled water, lyophilised and ground with a ball mill (as

described in 2.6.5). FTIR analysis was carried out in attenuated total reflectance (ATR) mode using a Bruker ALPHA II spectrometer. Spectra were recorded from 600  $\text{cm}^{-1}$  to 4000  $\text{cm}^{-1}$  at a spectral resolution of 4  $\text{cm}^{-1}$  with 64 scans. The spectral data were pre-processed by vector normalisation using the spectral region of 1800-600  $\text{cm}^{-1}$  followed by baseline correction by the rubber band correction with 64 points.

## 2.3 Results and discussion

### 2.3.1 Effect of metal supplements based on RSM

#### 2.3.1.1 Degradation of biomass

In this investigation, response surface methodology was applied to study the interactions between variable  $\text{Mn}^{2+}$  and  $\text{Cu}^{2+}$  concentrations during fungal pretreatment of poplar wood by *P. chrysosporium*. The main components of the raw feedstock were measured to be  $30.80 \pm 0.76\%$  w/w total lignin,  $26.32 \pm 0.70\%$  w/w AIL,  $4.48 \pm 0.14\%$  w/w ASL,  $45.10 \pm 1.04\%$  w/w glucan and  $17.10 \pm 0.83\%$  w/w xylan (**Table 2.2**). The initial manganese (Mn) and copper (Cu) contents of the sawdust were 0.12  $\mu\text{mol/g}$  and 0.03  $\mu\text{mol/g}$ , respectively (**Table 2.3**). Analysis of the control runs (untreated, metal-supplemented wood) revealed that the 1 hour of autoclaving did not alter significantly ( $p < 0.05$ ) the composition of wood (**Table 2.2**).

**Table 2.3** Heavy metal content of poplar wood

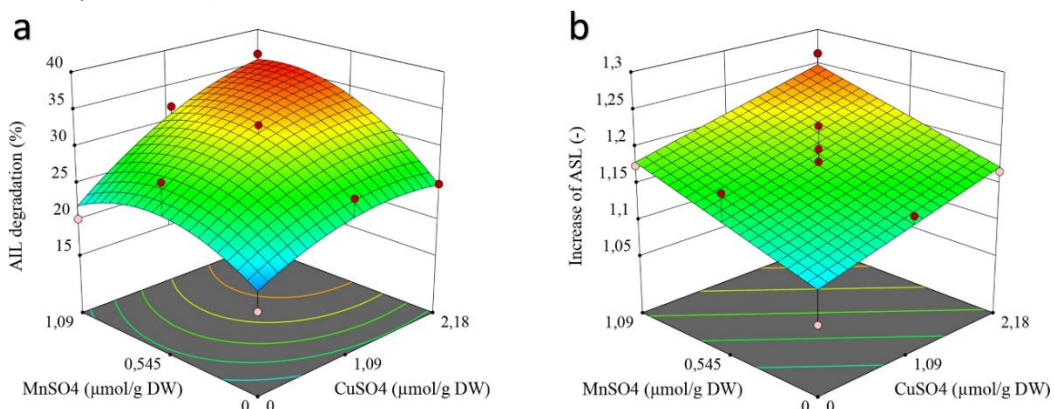
		Cd	Pb	Cr	Mn	Fe	Ni	Cu	Zn
Metal	[ $\mu\text{g/g}$ ]	0.54	0.12	5.69	6.50	33.46	2.23	2.04	26.75
content <sup>a</sup>	[ $\mu\text{mol/g}$ ]	0.005	0.002	0.11	0.12	0.60	0.04	0.03	0.41

<sup>a</sup>Determined by high-resolution inductively coupled plasma mass spectrometry in the SPHERE research group (Department of Biology) at University of Antwerp

**Acid-insoluble lignin.** The AIL degradation response surface could be described by a quadratic model of the  $\text{Mn}^{2+}$  and  $\text{Cu}^{2+}$  dosages (**Fig. 2.5a**). The model was significant ( $p = 0.0061$ ) despite a significant lack of fit ( $p = 0.0240$ ). The model equation had an  $R^2$  of 0.8639. In the conditions with the maximum supplementation of 2.18  $\mu\text{mol Cu}^{2+}$  and 1.09  $\mu\text{mol Mn}^{2+} \text{ g}^{-1}$  DW substrate, a maximum acid-insoluble lignin degradation of 36.43% was measured which was two times higher compared to non-supplemented pretreatment system. Both copper and manganese contributed to this increase.

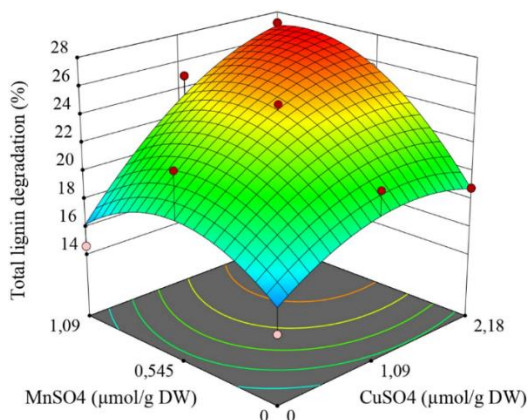
**Acid-soluble lignin.** After fungal pretreatment, the applied supplementations resulted in a small increase of 1.1 to 1.3 fold in ASL content of wood compared to the untreated wood (**Fig. 2.5b**), which is in agreement with the study of Isroi et al. [186]. The experimental data of the increase in AIL content could be fitted by a linear model with

high significance ( $p = 0.0105$ ) along with an  $R^2$  of 0.5982 and without a significant lack of fit ( $p = 0.2613$ ).



**Fig. 2.5** Response surface plot of interactions between  $\text{Cu}^{2+}$  and  $\text{Mn}^{2+}$  dosages for (a) acid-insoluble lignin degradation and (b) increase of acid-soluble lignin content after pretreatment of poplar wood

**Total lignin.** The untreated poplar wood comprises a relatively low portion of ASL (4.48%) compared to AIL (26.32%) (**Table 2.2**). Despite the only slight increase in ASL content after fungal pretreatment, the total lignin degradation was greatly improved by metal supplementation due to the enhanced AIL lignin degradation (discussed above). The increase in total lignin degradation could be described by a statistically significant quadratic model ( $p = 0.0063$ ) with an  $R^2$  of 0.8628 despite the significant lack of fit ( $p = 0.0122$ ) (**Fig. 2.6**).

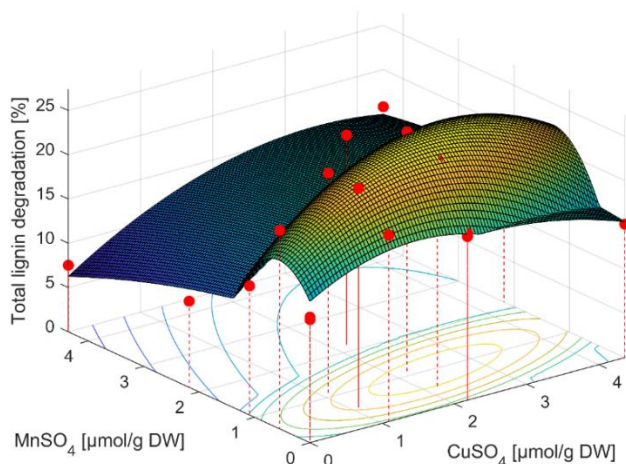


**Fig. 2.6** Response surface plot of interactions of  $\text{Cu}^{2+}$  and  $\text{Mn}^{2+}$  variables and total lignin degradation after pretreatment of poplar wood

The obtained optimal metal dosage, i.e. 2.18  $\mu\text{mol Cu}^{2+}$  and 0.90  $\mu\text{mol Mn}^{2+} \text{ g}^{-1} \text{ DW}$ , for maximum total lignin degradation of 27.25% (1.9 times higher compared to the non-supplemented system) was equal to the maximum  $\text{Cu}^{2+}$  amount and close to the maximum  $\text{Mn}^{2+}$  amount of 1.09  $\mu\text{mol g}^{-1} \text{ DW}$ . Therefore, a central composite design (CCD2) applying higher supplement dosages, i.e. 2.18  $\mu\text{mol}$  (centre point) and 4.36  $\mu\text{mol}$  metal ion  $\text{g}^{-1} \text{ DW}$  wood, was also investigated for the possible further improvement of the delignification efficiency (**Table 2.4**). A combined response surface plot from the two experimental designs was constructed using Matlab R2018b by plotting the highest response based on the equations obtained in the Design-Expert software. This combined surface plot of total lignin degradation indicates that the further increase of metal supplementation negatively influences the fungal pretreatment process (**Fig. 2.7**). It remains to be *investigated* whether it is caused by fungal growth inhibition and/or by a decrease in ligninolytic enzyme activities since  $\text{Cu}^{2+}$  and  $\text{Mn}^{2+}$  in excess can inhibit the growth of *P. chrysosporium* [187]. Additionally,  $\text{Cu}^{2+}$  can cause oxidative damage to proteins [188] and decrease the activity of MnP [189].

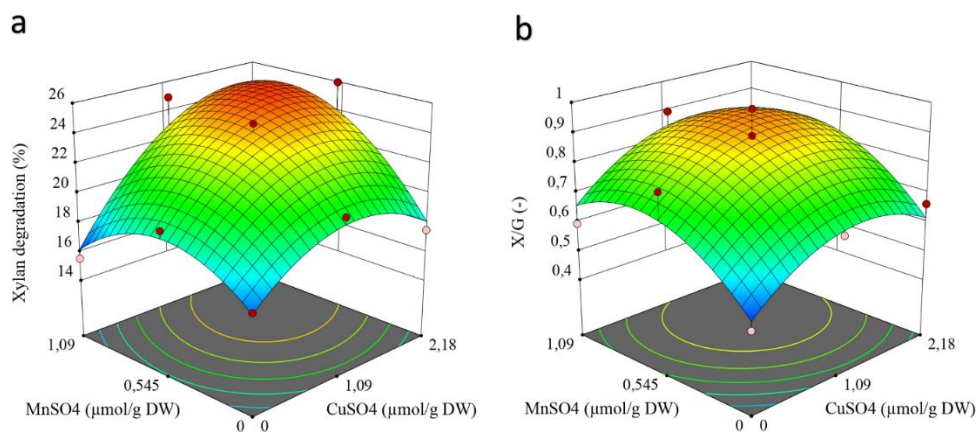
**Table 2.4** Central Composite Design 2 (CCD2)

Run	Metal supplement ( $\mu\text{mol g}^{-1} \text{ DW}$ substrate)	
	A: $\text{CuSO}_4$	B: $\text{MnSO}_4$
1	2.18	2.18
2	0	4.36
3	4.36	0
4	2.18	4.36
5	0	2.18
6	4.36	4.36
7	2.18	0
8	2.18	2.18
9	4.36	2.18
10	2.18	2.18
11	2.18	2.18
12	0	0
13	2.18	2.18



**Fig. 2.7** Response surface plot of interactions of  $\text{Cu}^{2+}$  and  $\text{Mn}^{2+}$  variables and total lignin degradation under 0–4.36  $\mu\text{mol}$  metal ion  $\text{g}^{-1}$  DW wood supplement dosages

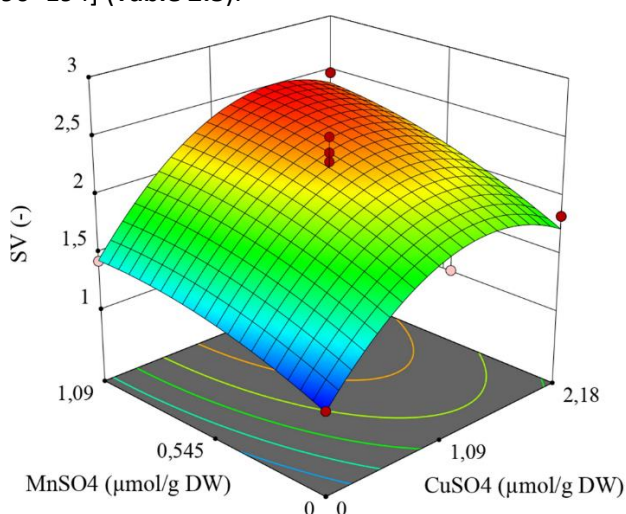
**Structural carbohydrates.** In this study, metal supplementation significantly ( $p = 0.0022$ ) increased the xylan degradation, described by a quadratic model with an  $R^2$  of 0.8991 (**Fig. 2.8**). However, it had no significant influence ( $p > 0.05$ ) on the glucan degradation which varied between 9.28% and 13.52% at the investigated  $\text{Cu}^{2+}$  and  $\text{Mn}^{2+}$  dosages (data not shown).



**Fig. 2.8** (a) Xylan consumption and (b) xylan/glucan consumption ratio after pretreatment of poplar wood as a function of  $\text{MnSO}_4$  and  $\text{CuSO}_4$  supplements



**Delignification selectivity.** For the selectivity value, a quadratic model could be fitted to the experimental data ( $p = 0.0057$ ) with an  $R^2$  of 0.9009 (**Fig. 2.9**). A maximum SV of 2.52 (2.4 fold higher compared to the non-supplemented system) was determined for the pretreatment system containing  $1.59 \mu\text{mol Cu}^{2+}$  and  $1.09 \mu\text{mol Mn}^{2+} \text{ g}^{-1}$  DW substrate. This obtained SV is exceptionally high for *P. chrysosporium* since selectivity values between only 0.59 and 1.2 were reported before [77,86–88]. Selectivity values between 1.6 and 7.2 were reported in the literature during fungal pretreatment of hardwood by other fungal species such as *Ceriporiopsis subvermispora*, *Trametes orientalis*, *Trametes velutina*, and 28.9, an exceptionally high value, by *Echinodontium taxodii* [18,185,190–194] (**Table 2.5**).



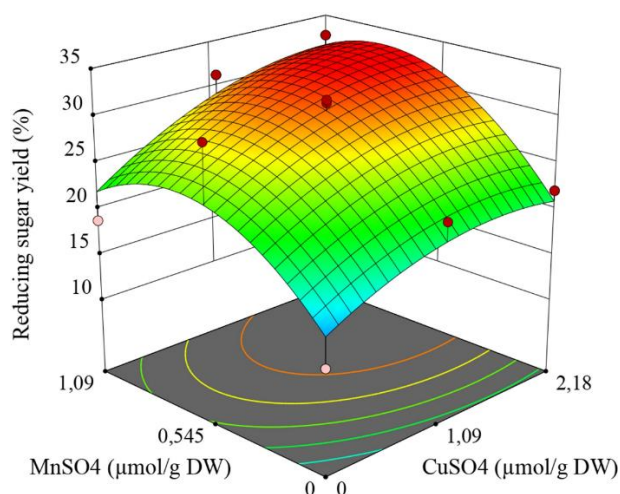
**Fig. 2.9** Selectivity value in the function of  $\text{MnSO}_4$  and  $\text{CuSO}_4$  pretreatment variables after pretreatment of poplar wood

### 2.3.1.2 Enzymatic saccharification by a commercial enzyme complex

The pretreated biomass was directly subjected to enzymatic saccharification to demonstrate that this pretreatment technique does not require an additional washing step, unlike alkali or acid pretreatment technologies where removal of inhibitory by-products is necessary [165].

The combined addition of  $\text{Cu}^{2+}$  and  $\text{Mn}^{2+}$  supplements during pretreatment significantly improved glucose, xylose, and reducing sugar yield. Similar to lignin degradation, quadratic models could be obtained (respectively,  $p = 0.0075$ ,  $p = 0.0304$ ,  $p = 0.0286$ ). The maximum glucose yield of 26.48% (2.9 and 5.4 times higher than in non-supplemented pretreated and untreated wood, respectively) and reducing sugar yield of 33.20% (2.6 and 4.4 times higher, respectively) were measured for the SSF system

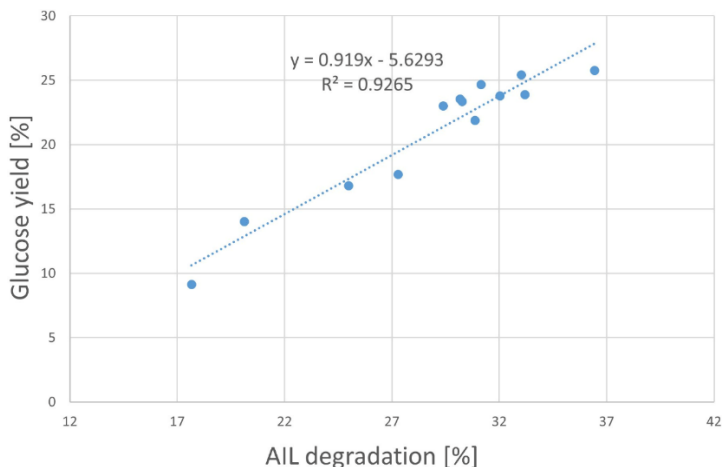
where  $2.01 \mu\text{mol Cu}^{2+}$  and  $0.77 \mu\text{mol Mn}^{2+} \text{ g}^{-1}$  DW wood supplement dosages were applied (**Fig. 2.10**).



**Fig. 2.10** Response surface plot of interactions between  $\text{Cu}^{2+}$  and  $\text{Mn}^{2+}$  supplements and reducing sugar yield

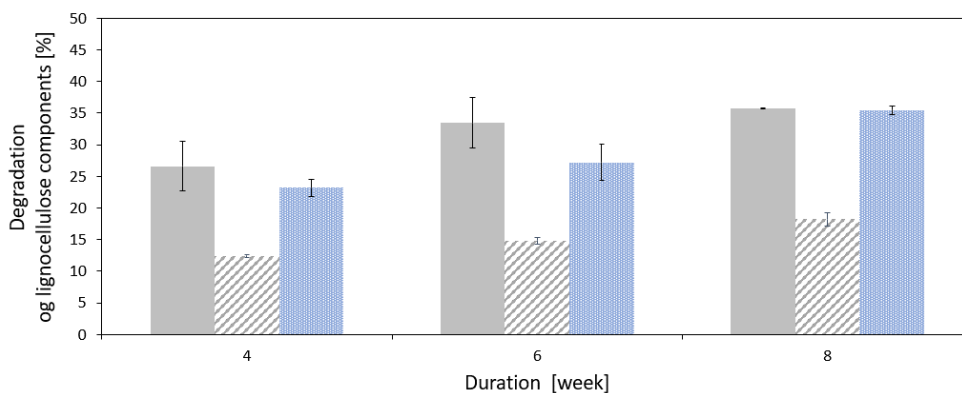
The lignocellulose degrading properties of this fungal pretreatment system are shown in **Table 2.5**. While in literature,  $\text{Cu}^{2+}$  ions negatively influence the enzymatic cellulolysis both on the enzyme ( $50\%$  loss in the initial hydrolysis rate at  $8.7 \mu\text{mol CuSO}_4 \text{ g}^{-1}$  Avicel [125]) and on the substrate level (decreased enzymatic digestibility by reducing end oxidation in cellulose at  $140 \mu\text{mol Cu}^{2+} \text{ g}^{-1}$  Avicel [126]) they did not have a significant effect on the enzymatic digestibility ( $4.85\% \pm 0.23\%$  glucose yield) of poplar wood at the applied lower concentrations.

The increase in the digestibility of poplar wood in the presence of metal ions can be assigned to the improved degradation of lignin by ligninolytic enzymes. It is known that the presence of lignin decreases the accessibility of cellulase enzymes to cellulose [88,195]. This is well confirmed by the linear correlation ( $R^2 = 0.9265$ ) found in this study between ALL lignin degradation and the glucose yield (**Fig. 2.11**). This finding is in agreement with the study of Nazarpour et al., where a linear correlation between reducing sugar yield and lignin degradation was reported [18].

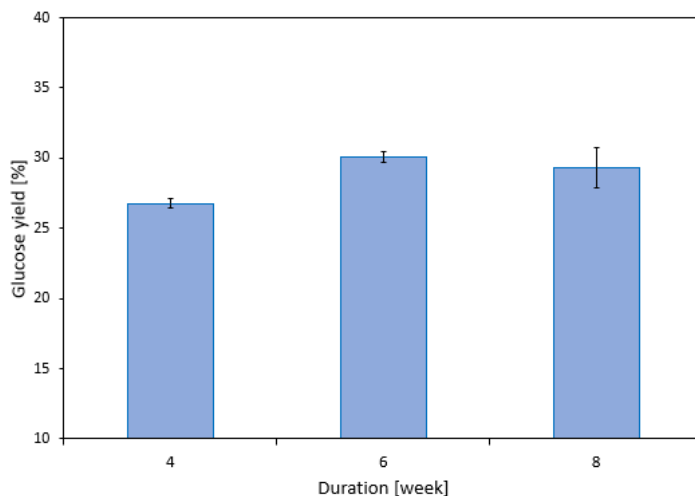


**Fig. 2.11** Positive linear correlation between glucose yield and acid-insoluble lignin degradation

However, it should be noted that the achievable sugar yield depends on both the degree and selectivity of delignification. This is well confirmed by our research on SSF using combined metal supplementation ( $2.01 \mu\text{mol Cu}^{2+}$  and  $0.77 \mu\text{mol Mn}^{2+} \text{ g}^{-1}$  DW wood) and longer pretreatment times, including 6 and 8 weeks. Compared to 4 weeks, 6 weeks of SSF further increased both the degree ( $26.59 \pm 3.89\% \rightarrow 33.45 \pm 4.01\%$ ) and the selectivity ( $\text{SV}=2.13 \rightarrow 2.26$ ) of lignin degradation and thus the glucose yield ( $26.77 \pm 0.33\% \rightarrow 30.06 \pm 0.38\%$ ) (**Fig. 2.12-2.13**). However, 8 weeks of pretreatment resulted in increased lignin degradation ( $35.74 \pm 0.08\%$ ) but reduced delignification selectivity ( $\text{SV}=1.96$ ) and, therefore, no improvement in glucose yield ( $29.33 \pm 1.43\%$ ) compared to 6 weeks (**Fig. 2.12-2.13**).



**Fig. 2.12** Degradation of (■) lignin; (▨) glucan and (▤) xylan using different pretreatment time



**Fig. 2.13** Glucose yield obtained for SSFs performed for different time

It is well known in the literature that hardwood, such as poplar, willow, Albizia or rubberwood, is more recalcitrant than herbaceous feedstock and consequently yields a lower amount of sugars after enzymatic saccharification [10]. Lignin degradation of 18-45% and sugar yield of 15-54% were reported for hardwood using strains such as *C. subvermispota*, *T. orientalis*, *T. velutina* or *E. taxodii* and a pretreatment time of up to 120 days [18,185,190–194] (**Table 2.5**). When the results after 28-30 days of fermentation are compared to our results, we attain a higher or comparable yield of reducing sugars. It can also be noticed that the achievable sugar yield is highly dependent on the enzymatic digestibility of the raw feedstock, i.e. reducing sugar yields of 2.9% to 18.7% were reported for untreated hardwood. The highest reported increase in reducing sugar yield found in the literature for poplar wood and 4 weeks of pretreatment, as in our research, was 1.9 fold (18.7 % → 36%) [193], while 4.4 fold increase (7.5% → 33.2%) was obtained in this study.

**Table 2.5** Biomass degradation and sugar yields after fungal pretreatment of hardwood by white-rot fungi

Substrate	Species	Fungal pretreatment				Enzymatic hydrolysis conditions				Saccharification yield [% w/w] untreated/pretreated; ↑ <sup>b</sup>			Ref.
		Time [days]	Component degradation [% w/w]			SV [-]	Enzyme loading <sup>a</sup>	Substrate loading [% w/v]	Time [h]	Glucose	Xylose	Reducing sugar	
			Lignin	Cellulose	Hemicellulose								
<b>Albizia</b>	<i>Ceriporiopsis subvermispora</i>	48	24	10.5	15	1.6	15 / 60	2	72	8 / 38; (↑4.8)	7 / 29; (↑4.1)	- / -	[185]
<b>Chinese willow</b>	<i>Echinodontium taxodii</i>	30	26.0 ± 1.5	0.9 ± 0.9	31.0 ± 1.5	28.9	20 / -	2.5	120	- / -	- / -	5 / 15; (↑3.0)	[191]
		120	45.6 ± 2.0	26.7 ± 0.2	50.8 ± 1.8	1.7	20 / -	2.5	120	- / -	- / -	5 / 32.5 (↑6.5)	
<b>Hardwood chips (forest residue)</b>	<i>Ceriporiopsis subvermispora</i>	18	18	2.5	18	7.2	10 / -	2.5	72	10 / 24.1; (↑2.4)	2 / 11; (↑5.5)	- / -	[190]
		35	-	-	-	-	10 / -	2.5	72	10 / 54.2; (↑5.4)	2 / 27; (↑13.5)	- / -	
<b>Rubberwood</b>	<i>Ceriporiopsis subvermispora</i>	30	18.8 ± 0.6	5.2 ± 0.5	25.1 ± 0.7	3.65 ± 0.3	47 / 113	1.9	168	- / -	- / -	2.9 / 17.3; (↑6.0)	[18]
		90	45.1 ± 0.8	9.5 ± 0.5	42.1 ± 1.2	4.8 ± 0.3	47 / 113	1.9	168	- / -	- / -	2.9 / 27.7; (↑9.6)	
<b>Poplar</b>	<i>Trametes orientalis</i>	28	26.4	1	13	2.2	30 / 37.5	2	96	- / -	- / -	18 / 30.0; (↑1.7)	[192]
		84	45.3	13	22.5	3.5	30 / 37.5	2	96	- / -	- / -	18 / 41.3; (↑2.3)	

<b>Poplar</b>	<i>Trametes velutina</i>	28	-	-	-	-	35 / 37.5	2	96	- / -	- / -	18.7 / 37; (↑2.0)	[193]
		56	-	-	-	-	35 / 37.5	2	96	- / -	- / -	18.7/43.6 (↑2.3)	
<b>Poplar</b>	<i>Trametes velutina</i>	56	-	-	-	-	35 / 37.5	2	72	- / -	- / -	18 / 37.5; (↑2.1)	[194]
<b>Poplar</b>	<i>Phanerochaete chrysosporium</i>	28	26.9	11.2	25.2	2.4	38 / n.d.	9	72	4.9 / 26.5; (↑5.4)	3.9 / 10.4; (↑2.7)	7.5 / 33.2; (↑4.4)	This study

'-' not available, 'n.d.' not determined, <sup>a</sup>Cellulase loading (FPU/g substrate) /  $\beta$ -glucosidase loading (IU/g substrate), <sup>b</sup>Increase in sugar yield compared to untreated wood

### 2.3.2 The concerted actions of $Mn^{2+}$ and $Cu^{2+}$ on improved delignification

To reveal the mechanism behind the combined actions of  $Cu^{2+}$  and  $Mn^{2+}$  on improved delignification, the ligninolytic enzyme production in relation to fungal growth during the biomass degradation was measured and compared in non-supplemented,  $Cu^{2+}$  (2.18  $\mu\text{mol g}^{-1}$  DW),  $Mn^{2+}$  (1.09  $\mu\text{mol g}^{-1}$  DW substrate) and combined supplemented SSF systems (2.18  $\mu\text{mol Cu}^{2+}$  and 1.09  $\mu\text{mol Mn}^{2+}$   $\text{g}^{-1}$  DW, i.e. dosages where maximum acid-soluble lignin degradation was measured).

Using the Azure B assay, lignin peroxidase activity could not be detected in any of the fermentations, which might be due to the low enzyme concentrations. Therefore, lignin degradation was related only to the MnP activities measured in every culture.

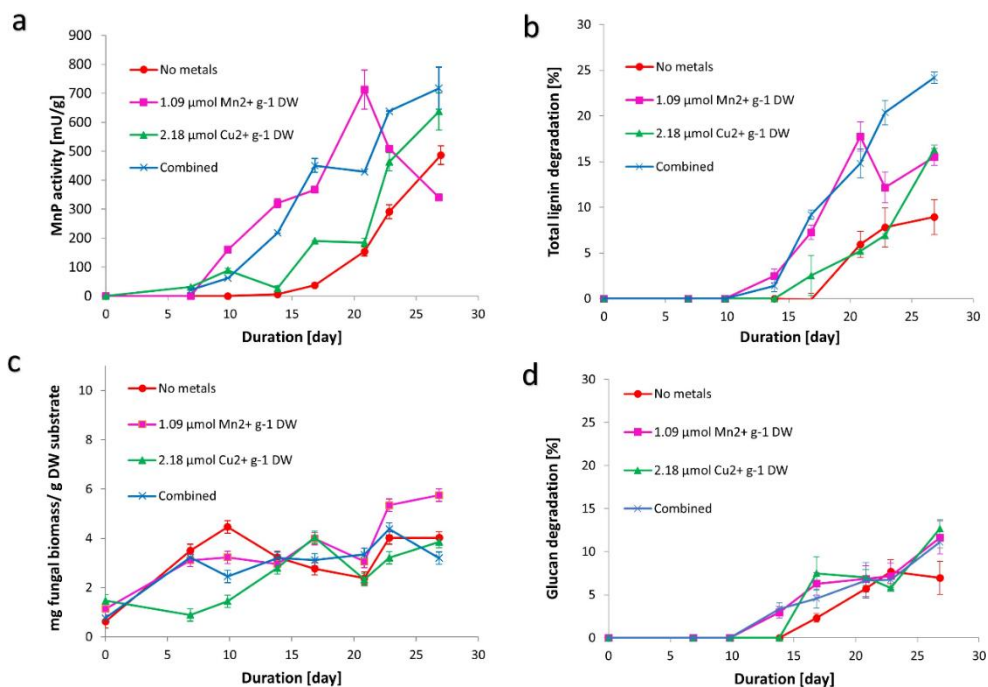
The presence of  $Cu^{2+}$  and  $Mn^{2+}$  is known to increase the MnP activities in cultivations of *P. chrysosporium* [12,13,118]. In this study, the addition of  $Cu^{2+}$  and  $Mn^{2+}$ , separately or combined, also resulted in enhanced MnP activity compared to the non-supplemented SSF system and consequently improved the delignification, but  $Mn^{2+}$  had a greater effect than  $Cu^{2+}$  (**Fig. 2.14a-b**).

The lowest lignin degradation was found in non-supplemented, and  $Cu^{2+}$  supplemented fermentations with no significant difference except for day 27 when 1.9 fold higher lignin degradation (16.3%) was determined in the  $Cu^{2+}$  supplemented system (**Fig. 2.14b**). In cultures containing only  $Mn^{2+}$  ions, the maximum delignification (17.1%) was reached after 21 days of fermentation and did not improve any further with prolonged pretreatment in agreement with the measured rapid decrease of MnP activity presented in **Fig. 2.14a**. However, in the combined supplemented system, both the MnP activities and the lignin degradation progressively increased until 27 days, reaching a maximum lignin degradation of 24.2% (**Fig. 2.14a-b**).

The sudden drop in MnP activity in the  $Mn^{2+}$  supplemented SSF can be associated with the high lignin decomposition (**Fig. 2.14b**), which makes cellulose more accessible for the fungus, which in turn produces more cellulase enzymes to degrade glucan over lignin (**Fig. 2.14d**) [87]. Consequently, glucose is released in the fermentation system, leading to the restart of the growth on day 21 (**Fig. 2.14c**) and, hereby to a decreased production of the secondary metabolites, i.e., MnP enzymes [83]. However, in the combined supplemented system ( $Cu^{2+} + Mn^{2+}$ ), **Fig. 2.14c** shows that the stationary growth phase is maintained and thus, the MnP production results in an increased specific MnP activity (20.07 U/g protein) on day 27 (**Table 2.6**). In this system, the explanation for this difference by supplementation can be that the  $Cu^{2+}$  ions inhibit the growth either directly (via physiological changes caused by metal bioaccumulation) or

indirectly by preventing cellulase-based glucan degradation since  $\text{Cu}^{2+}$  ions are known inhibitors of cellulolytic enzymes [124,125].

However, no significant difference in glucan degradation was found between the  $\text{Cu}^{2+}$ ,  $\text{Mn}^{2+}$  and combined supplemented systems (**Fig. 2.14d**), suggesting direct growth inhibition.



**Fig. 2.14** Time course of the important responses for the SSF mechanism, with (a) MnP activities, (b) total lignin degradation, (c) fungal growth, and (d) glucan degradation (—●—) without supplement, (—▲—) with 2.18  $\mu\text{mol CuSO}_4$  g<sup>-1</sup> DW wood, (—■—) 1.09  $\mu\text{mol MnSO}_4$  g<sup>-1</sup> DW wood, and (—×—) 2.18  $\mu\text{mol CuSO}_4$  and 1.09  $\mu\text{mol MnSO}_4$  g<sup>-1</sup> DW substrate. STD values are obtained for analytical replicates (duplicate-MnP activity, triplicate-biomass degradation, fixed standard deviation of fungal growth determination (as described in 2.2.6.5)



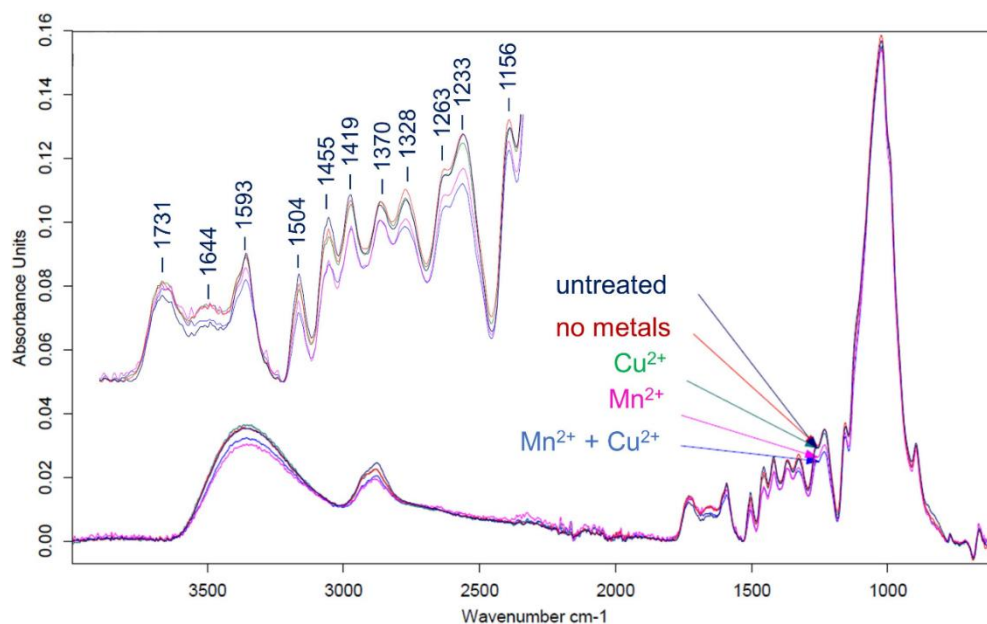
**Table 2.6** Degradation of lignin in relation to fungal growth, MnP activity and specific MnP activity measured after 27 days of fermentation with and without Cu<sup>2+</sup> and Mn<sup>2+</sup> supplementation

Supplement	Lignin degradation [% w/w]	Fungal growth [mg fungal biomass/g wood]	MnP activity [mU/g wood]	Specific MnP activity [U/g protein]
None	8.91 ± 1.91	4.01 ± 0.25	486.32 ± 32.75	12.00 ± 1.00
Mn <sup>2+</sup>	15.50 ± 0.93	5.75 ± 0.25	337.81 ± 3.44	12.07 ± 0.12
Cu <sup>2+</sup>	16.23 ± 0.55	3.86 ± 0.25	637.18 ± 64.37	22.87 ± 2.31
Combined	24.18 ± 0.62	3.2 ± 0.25	717.10 ± 72.44	20.60 ± 2.08

STD values are obtained for analytical replicates (duplicate-MnP activity, triplicate-biomass degradation, fixed standard deviation of fungal growth determination (as described in 2.6.5))

### 2.3.3 Characterization of biomass by FTIR spectroscopy

FTIR in ATR mode was used to determine the influence of Mn<sup>2+</sup> and Cu<sup>2+</sup> ions on the functional groups in the pretreated poplar wood samples. The SSF samples with different supplementation were analysed after 27 days of pretreatment. Significant spectral changes compared to untreated wood were observed for samples supplemented with only Mn<sup>2+</sup> or Mn<sup>2+</sup> and Cu<sup>2+</sup> together (**Fig. 2.15**). The lignin removal in these samples was confirmed by the decreased peak intensities at 1593 cm<sup>-1</sup> (aromatic skeletal vibration and C=O stretch), 1504 cm<sup>-1</sup> (the diagnostic band for C=C stretching in aromatic rings) and 1455 cm<sup>-1</sup> (aromatic C-H deformation) [159]. The decrease in peak intensity at 1263 cm<sup>-1</sup> (guaiacyl unit, C-O stretch in lignin), 1233 cm<sup>-1</sup> (syringyl unit, C-O stretch in lignin and xylan) and 1156 cm<sup>-1</sup> (aromatic skeletal vibration and C-O stretch) was greater for SSF supplemented with both Cu<sup>2+</sup> and Mn<sup>2+</sup> compared to when only Mn<sup>2+</sup> was used [159,161].



**Fig. 2.15** FTIR characterization of (—) untreated and pretreated poplar wood (—) without supplements; (—) with  $2.18 \mu\text{mol CuSO}_4 \text{ g}^{-1} \text{ DW}$  wood; (—)  $1.09 \mu\text{mol MnSO}_4 \text{ g}^{-1} \text{ DW}$  wood and (—)  $2.18 \mu\text{mol CuSO}_4$  and  $1.09 \mu\text{mol MnSO}_4 \text{ g}^{-1} \text{ DW}$  substrate

## 2.4 Conclusions

The degree and selectivity of delignification during fungal pretreatment of poplar wood by *P. chrysosporium* were effectively improved by the combined application of  $\text{MnSO}_4$  and  $\text{CuSO}_4$  supplements.  $\text{Mn}^{2+}$  and  $\text{Cu}^{2+}$  ions showed a concerted action on improved delignification.  $\text{Mn}^{2+}$  ions induced MnP production, while  $\text{Cu}^{2+}$  ions prolonged it by maintaining the stationary growth phase responsible for MnP production. Enzymatic saccharification of metal supplemented ( $2.01 \mu\text{mol Cu}^{2+}$  and  $0.77 \mu\text{mol Mn}^{2+} \text{ g}^{-1} \text{ DW}$  substrate) pretreated wood resulted in 2.6 times higher reducing sugar yield (i.e. 33.20%) compared to non-supplemented pretreated wood. This measured increase could significantly reduce the sugar production cost in large-scale processes at the low additional cost of the applied supplements.

**Chapter 3. To sterilise or not to sterilise?  
Comparable saccharification yields obtained  
after fungal pretreatment of non-sterilised  
poplar wood**

---

This chapter was redrafted from the manuscript that is under review.

N. Wittner, K. Vasilakou, W. Broos, S.E. Vlaeminck, P. Nimmegeers, I. Cornet,  
Investigating the technical and economic potential of solid-state fungal pretreatment at  
non-sterile conditions for sugar production from poplar wood

## Abstract

Fungal pretreatment is a biotechnological process that uses rotting fungi to reduce the recalcitrance of lignocellulose and subsequently improve the accessibility of polysaccharides to hydrolytic enzymes resulting in an increased saccharification yield. Compared to traditional chemical/physical pretreatments, fungal pretreatment operates at low temperatures, with low wastewater generation and without added chemicals. However, its substrate sterilisation requirement contributes to lower techno-economic performance.

In this study, solid-state fungal pretreatment of non-sterilised poplar wood was carried out using an uncommon inoculum type, namely wood pre-colonised with the white-rot fungus *Phanerochaete chrysosporium*, and spores for comparison. In addition, different fermentation supplements (metal ions, glucose and sodium nitrate) and cultivation methods (rolling bottle and tray) were investigated to optimise the process.

The fungal pretreatment, performed in trays with a 1:3 ratio of pre-colonised and untreated wood, using only  $\text{Cu}^{2+}$ ,  $\text{Mn}^{2+}$  and sodium nitrate as supplements, resulted in a high lignin degradation of  $34.45 \pm 3.43\%$  and a delignification selectivity value of  $1.67 \pm 0.26$ . This led to a comparably high glucose yield ( $28.51 \pm 0.28\%$ ) compared to the traditional method, using sterilised wood, spores as inoculum and sterile ventilation. This process reduces the amount of feedstock to be sterilised by 71.2% in fungal pretreatment-based biorefineries.

## Graphical abstract

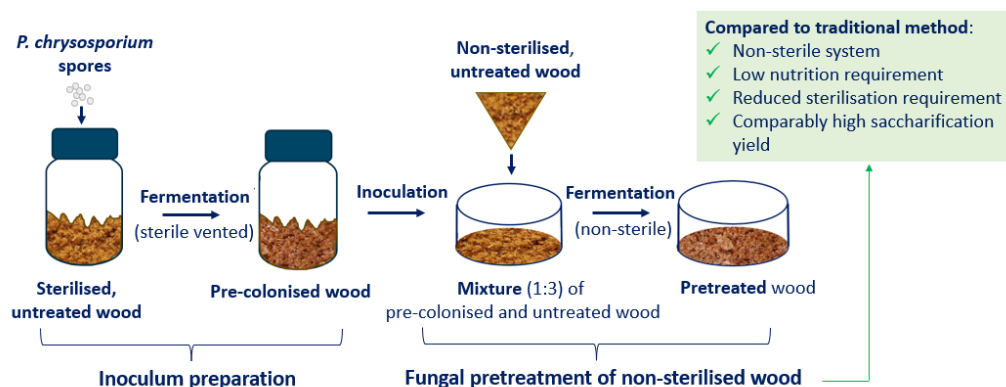


Fig. 3.1 Graphical abstract

### 3.1 Introduction

Lignocellulose is the most abundantly available source of carbohydrates for the sustainable fermentative production of biochemicals and biofuels. However, it is highly recalcitrant to enzymatic saccharification and therefore requires a pretreatment step to enhance the accessibility of cellulose to hydrolytic enzymes. The commonly used chemical/physical pretreatment technologies need harmful chemicals and/or high energy input and often generate by-products that inhibit fermentative microorganisms [165,166]. Fungal pretreatment is a biotechnological alternative that uses white-rot fungi in a solid-state fermentation system to break down lignin and reduce biomass recalcitrance effectively [49]. Compared to the conventional pretreatment methods, solid-state fungal pretreatment is operated under mild reaction conditions, with low wastewater generation and no or limited addition of chemicals. However, it also suffers from potential weaknesses, including feedstock sterilisation requirement, long pretreatment time and relatively low saccharification yield due to the inefficient and non-selective lignin degradation. The latter is caused by the cellulase enzyme production of the white-rot fungi resulting in the undesired degradation of cellulose with a lower glucose yield after the enzymatic hydrolysis process step. The low delignification selectivity is indicated by the selectivity value (SV), which is defined as the ratio of lignin degradation [%] and cellulose consumption [%] [77–79]. These disadvantages lead to low techno-economic performance [10]. Therefore, optimising the operating parameters has a crucial role in improving the economic feasibility of fungal pretreatment. One of these parameters is the elimination of the sterilisation process, which can reduce both the capital and operating costs of the fungal pretreatment.

Most fungal pretreatment studies were performed on sterilised feedstock to prevent indigenous microbial communities from competing with the white-rot fungi. Steam sterilisation is the routinely used sterilisation method with a sterilisation time typically ranging from 15 to 60 minutes [76,169,171].

In research, only a few attempts have been made on the fungal delignification of non-sterilised feedstock. The direct inoculation of the feedstock with the fungal mycelium, which was proven to be effective on sterilised feedstock, often led to low pretreatment efficiency when used on non-sterilised feedstock [15,16]. However, a few studies have reported effective fungal pretreatment using an inoculation strategy that is uncommon in the field of fungal pretreatment, i.e. first growing the white-rot fungi on sterilised feedstock and then using the pre-colonised substrate as inoculum during fungal pretreatment.

In the study of Zhao et al., the fungal pretreatment of non-sterilised yard trimmings using yard trimmings pre-colonised with *Ceriporiopsis subvermispora* as inoculum provided a comparable degradation of the lignocellulose components as those obtained in the sterilised system inoculated with fungal mycelium [15]. In the work of Vasco-Correa et al., the use of pre-colonised feedstock as inoculum resulted in an effective fungal pretreatment of non-sterilised miscanthus, softwood (*Pinus sp.*) and hardwood (*Fraxinus Americana*) but was unsuccessful for corn stover [17]. Indeed, it is well known from the literature that the effectiveness of fungal pretreatment is highly dependent on the applied substrate and microorganism [109,190]. The inoculation technique of applying pre-colonised feedstock has not yet been studied for the fungal pretreatment of non-sterilised poplar wood by *Phanerochaete chrysosporium*.

In a previous study, the fungal delignification of poplar wood was optimised using sterilised poplar wood as substrate, spore suspension of *P. chrysosporium* as inoculum and a standard, complex fermentation medium supplemented with  $Mn^{2+}$  and  $Cu^{2+}$  at their optimal concentrations to enhance the delignification [196]. In the present research, we aimed to reduce the energy requirement of this process by using non-sterilised poplar wood as a substrate. This main research goal included the comparison of two inoculation techniques, i.e. inoculation with spores and with pre-colonised wood, and the evaluation of different fermentation supplements (metal ions with or without glucose and sodium nitrate) and cultivation methods (sterile vented bottles and open trays) to optimise the non-sterile fungal pretreatment process. The degradation of lignocellulose in non-sterilised wood and the resulting enzymatic saccharification yield were compared with those obtained from sterilised wood.

### **3.2 Materials and Methods**

#### **3.2.1 Lignocellulose substrate**

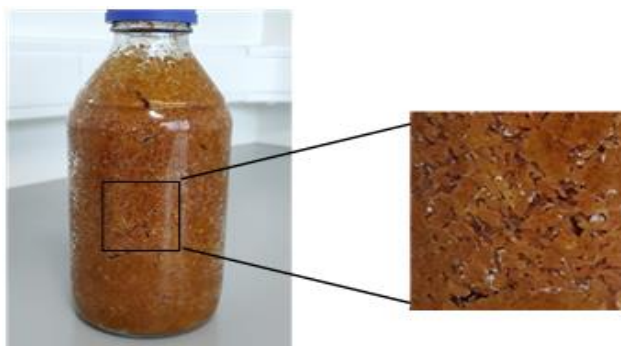
Poplar wood sawdust was obtained from Sawmill Caluwaerts Willy (Holsbeek, BE) and used as a substrate for solid-state fungal pretreatment. The particle size distribution was determined by sieve analysis. 86.1% w/w of the wood particles were collected between the 2 mm and 0.075 mm screens. The composition of the raw feedstock was  $30.80 \pm 0.76\%$  w/w lignin,  $45.10 \pm 1.04\%$  w/w glucan and  $17.10 \pm 0.83\%$  w/w xylan [196]. The sawdust was used with or without sterilisation, depending on the solid-state fermentation set-up. Sterilisation was performed by autoclaving at 121 °C for 20 min.

### 3.2.2 Fermentation media

Five fermentation media, including metal salts alone (M), with glucose (M+G), with NaNO<sub>3</sub> (M+N), with glucose and NaNO<sub>3</sub> (M+G+N) and with a complex medium (M+CM), were examined in this study. The metals salts were used in 3.69 mM CuSO<sub>4</sub> and 1.41 mM MnSO<sub>4</sub> concentrations, creating the optimal metal ion dosages of 2.01 μmol Cu<sup>2+</sup> and 0.77 μmol Mn<sup>2+</sup> g<sup>-1</sup> dry weight (DW) wood for enhanced delignification [196]. The glucose and NaNO<sub>3</sub> were added at concentrations of 20 g/L and 3 g/L, respectively. The complex medium, i.e. the standard medium used in the optimisation study of Wittner et al., contained 20 g/L glucose, 3 g/L NaNO<sub>3</sub>, 0.5 g/L KCl, 0.5 g/L of MgSO<sub>4</sub>·7H<sub>2</sub>O, 0.5 g/L FeSO<sub>4</sub>·7H<sub>2</sub>O, 1 g/L KH<sub>2</sub>PO<sub>4</sub>, 0.34 g/L veratryl alcohol, 0.1% v/v of Tween 80, 3.69 mM CuSO<sub>4</sub>·5H<sub>2</sub>O and 1.41 mM MnSO<sub>4</sub>·H<sub>2</sub>O [196]. All media were sterilised by autoclaving at 121 °C for 20 min.

### 3.2.3 Inoculum preparation

*Phanerochaete chrysosporium* (MUCL 19343) was purchased from the Mycothèque of the Catholic University of Louvain (Belgium). Two different inoculation strategies, i.e. inoculation with spore suspension and with pre-colonised poplar wood, were tested for the SSF studies. Spore suspension of 5·10<sup>6</sup> spores/mL was prepared in distilled water from 5 days old *P. chrysosporium* cultures grown on potato dextrose agar plates at 39°C. Pre-colonised poplar wood was obtained by performing SSF in sterile vented Schott bottles, as described in the study of Wittner et al. [196]. In brief, the bottle (1 L volume) contained 36.7 g dry-weight sterilised poplar wood, 20 mL sterile M+G+N media, 37 mL spore suspension (5·10<sup>6</sup> spores/g DW wood) and sterile distilled water creating a moisture content of 75% w/w on a wet basis (Fig. 3.2). The SSF bottles were rolled on a bottle roller (88881004 Bottle/Tube Roller, Thermo Scientific™) at 4 rpm and incubated (TC 255 S, Tintometer Inc.) at 37°C for 4 weeks.



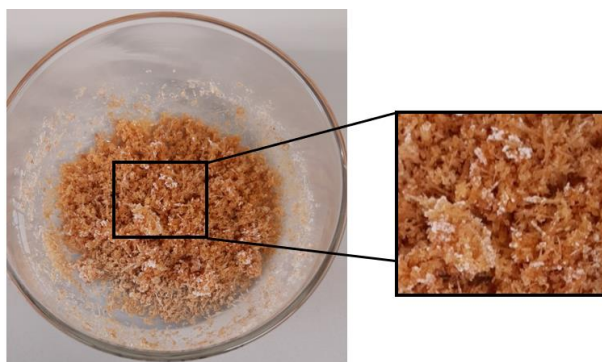
**Fig. 3.2** Pre-colonised wood prepared in the 1 L Schott bottle. The white spots indicate the growth of *P. chrysosporium*

### 3.2.4 Solid-state fungal pretreatment

Solid-state fermentations were carried out at varying fermentation conditions. The pretreatments differed in the applied substrate sterilisation (none or autoclaving at 121 °C for 20 min), medium composition (Section 2.2), inoculation strategies (Section 2.3) and fermentation set-up (rolling bottles or trays).

Bottle fermentation (B) was carried out in 100 mL Scott bottles closed with sterile vented screw caps with a welded-in 0.2 µm PTFE membrane (DURAN®) as described in the study of Wittner et al. [196]. The spore-inoculated bottle SSFs contained 3.67 g DW poplar wood, 2 mL sterile medium, 3.7 mL spore suspension ( $5 \cdot 10^6$  spores/g DW wood) and sterile distilled water creating a moisture content of 75% w/w on a wet basis. The bottle SSFs inoculated with pre-colonised wood contained 0.9 g DW of freshly harvested pre-colonised wood and 2.8 g DW untreated wood (mixing ratio of 1:3), 2 mL sterile medium and sterile distilled water to obtain the 75% moisture content. The bottles were rolled at 4 rpm on a bottle roller (88881004 Bottle/Tube Roller, Thermo Scientific™) and incubated (TC 255 S, Tintometer Inc.) at 37°C for 4 weeks.

Tray fermentations (T) of non-sterilised poplar wood were carried out in 500 mL glass dishes containing 0.9 g freshly harvested pre-colonised wood as inoculum, 2.8 g DW untreated non-sterilised wood in a layer of approximately 1 cm, 2 mL sterile medium and sterile distilled water were added to obtain a final moisture content of 75% (**Fig. 3.3**). Tray fermentations were carried out for up to 4 weeks at 37°C in a humidified chamber placed in a Heratherm IMH 100 incubator (Thermo Scientific™). The humidified chamber was built by bubbling compressed air through an aeration stone at an aeration rate of 3 L per minute into the water bath placed at the bottom of the chamber.



**Fig. 3.3** Poplar wood pretreated in a tray. The white spots indicate the growth of *P. chrysosporium*.



The bottle and tray fermentations were performed in triplicate and duplicate, respectively. Negative controls consisted of untreated non-sterilised wood without fungal inoculation under the same conditions as the pretreatment. After harvesting the entire content of the bottle and tray, the compositional analysis and enzymatic saccharification of the pretreated biomass were performed.

### **3.2.5 Analytical methods**

#### **3.2.5.1 Compositional analysis**

Before compositional analysis, the pretreated biomass samples were thoroughly washed to remove the produced lignocellulolytic enzymes and other water-soluble substances. One washing cycle included the shaking of the pretreated biomass (400 rpm, 20 min) with 50 mM acetate buffer (pH 4.5) using a solid-to-liquid ratio of 1:80, followed by centrifugation (Sigma 3-16KL) for 15 min at 4500 rpm and 4°C. After removing the supernatant, the rinsing cycle was repeated once with acetate buffer and twice with distilled water to remove the traces of acetic acid. The rinsed solid was freeze-dried (ALPHA 1-2 Ldplus, Martin Christ Gefriertrocknungsanlagen GmbH) and used for compositional analysis.

The compositions of the wood samples were determined by the standard NREL protocol (NREL/TP-510-42618) [135]. Briefly, glucan, xylan, acid-soluble (ASL) and acid-insoluble lignin (AIL) content of the samples were measured by two-stage acid hydrolysis with sulfuric acid. ASL was determined at 240 nm ( $\epsilon_{240\text{ nm}}=25\text{ L}/(\text{g}\cdot\text{cm})$ ). The lignin content discussed in this paper refers to the sum of AIL and ASL. The glucan and xylan contents in the samples were calculated from the monomeric sugars glucose and xylose, respectively, using the anhydro coefficient of 0.88 for xylose and 0.9 for glucose. The sugar analysis was carried out with an HPLC system (1260 Infinity II LC system, Agilent Technologies) with the detailed procedure described in the study of Wittner et al. [196]. In brief, a Coregel ORH 801 6.5 ID x 300 mm column (Concise separations) equipped with a refractive index detector (55°C) was used. As a mobile phase, 8 mM H<sub>2</sub>SO<sub>4</sub> was applied at a flow rate of 0.6 mL/min at 75°C.

After fungal treatment, the degradation of the different lignocellulose components (lignin, glucan and xylan) was calculated as a percentage of the initial content of these components in the bottle/tray [196].

### 3.2.5.2 Enzymatic saccharification

Enzymatic saccharification of the biomass was performed using the commercial enzyme mixture of Cellic® Ctec3 (Novozymes) with a total cellulase activity of 474 FPU/mL determined by the NREL/TP-510-42628 protocol [183]. Hydrolysis reaction contained 0.5 g dry biomass (10% w/w solid loading), 0.5 mL of 0.5 M citrate buffer (pH 4.6), 40 µL of cellulase enzyme mixture (38 FPU /g dry biomass), 20 µL of tetracycline solution (10 mg/mL in 70% ethanol), 15 µL of cycloheximide solution (10 mg/mL in distilled water) and 4.425 mL distilled water. Enzymatic saccharification was carried out at 50°C, 240 rpm for 72 hours. The obtained hydrolysates were boiled for 15 min in a water bath to precipitate the protein content and centrifuged at 21,500 g for 3 min. The supernatant was filtered through a syringe filter (0.2 µm, PES) and was analysed for its glucose and xylose content by HPLC as described in the study of Wittner et al. [196]. The glucose and xylose yields were calculated relative to the theoretical yield from the raw feedstock [18,185]. Additionally, when it was applied, the added glucose in the media was subtracted from the glucose yield.

### 3.2.6 Statistical analysis

Statistical comparisons were made to assess lignocellulose degradation and saccharification yields. The normality of data distribution was confirmed using the Shapiro-Wilk test, while the homogeneity of variances was assessed using Levene's test. Analysis of variance (ANOVA) followed by Tukey's post hoc test was used. Specifically, one-way ANOVA was applied to evaluate the effect of medium composition or pretreatment time within a given fermentation set-up. In addition, two-way ANOVA was used to examine the effects of the medium composition along with factors such as the ratio of pre-colonised to untreated wood, cultivation environment or sterile/non-sterile conditions. Jamovi 2.3.26 software was used for all statistical analyses. Statistical significance was set at a level of  $p < 0.05$ .

## 3.3 Results and discussion

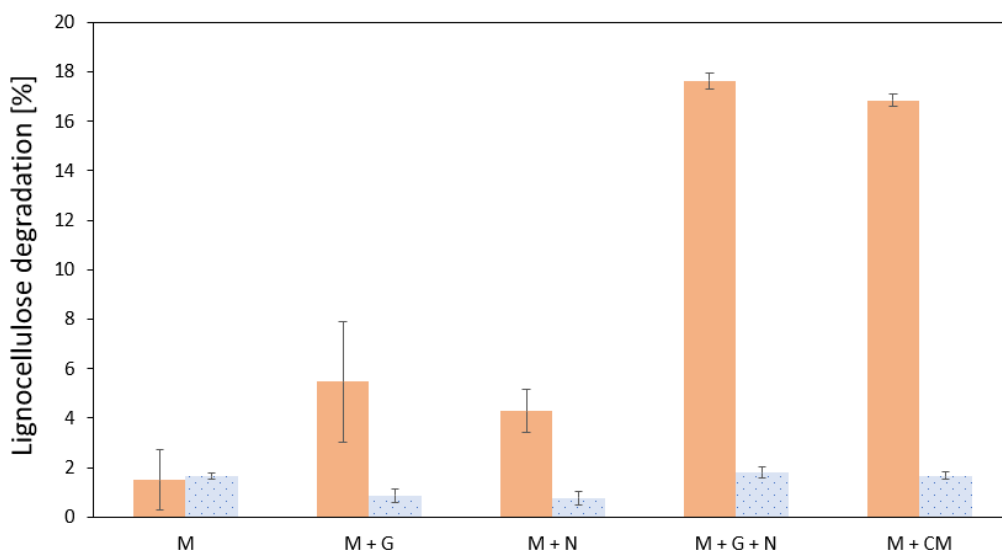
### 3.3.1 Spore-inoculated solid-state fermentation

A comparison was made between the fungal pretreatment efficiency of sterilised and non-sterilised poplar wood using spore suspension as inoculum, five different fermentation media and sterile vented fermentation bottles as cultivation environment. The five media included the metal salts  $\text{CuSO}_4$  and  $\text{MnSO}_4$  alone (M), with glucose (M+G), with  $\text{NaNO}_3$  (M+N), with both of these compounds (M+G+N) and with a complex

medium (M+CM) containing glucose,  $\text{NaNO}_3$ ,  $\text{KH}_2\text{PO}_4$ , KCl,  $\text{MgSO}_4$ ,  $\text{FeSO}_4$ , veratryl alcohol and Tween 80 as described in 3.2.2.

In the case of non-sterilised poplar wood, less than 2% of the total solids were degraded for each fermentation medium used (<0.5% in negative controls), see **Fig. 3.4**. These results indicate unsuccessful fungal pretreatment, probably caused by the presence of indigenous microorganisms outcompeting the applied *P. chrysosporium*.

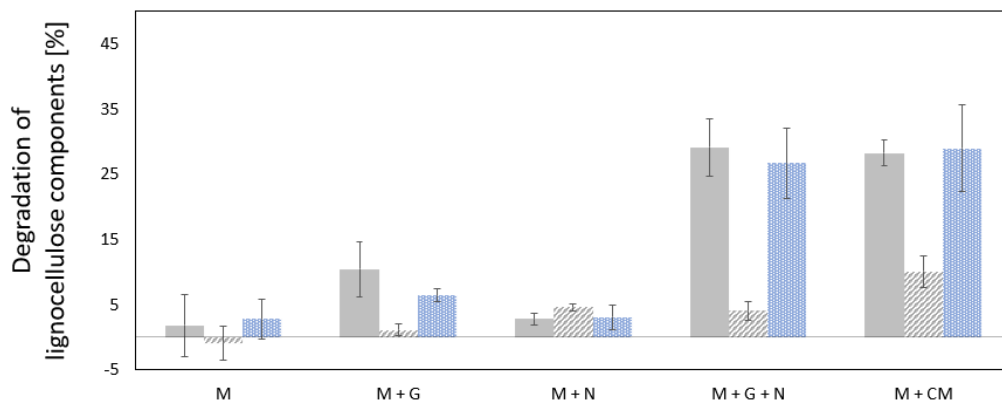
In contrast, solid-state fermentation of sterilised wood showed degradation values ranging from 1.49% to 17.64%. The highest degradation values of  $17.64 \pm 0.33\%$  and  $16.86 \pm 0.23\%$  were achieved in the M+G+N and M+CM supplemented fermentations, respectively (**Fig. 3.4**).



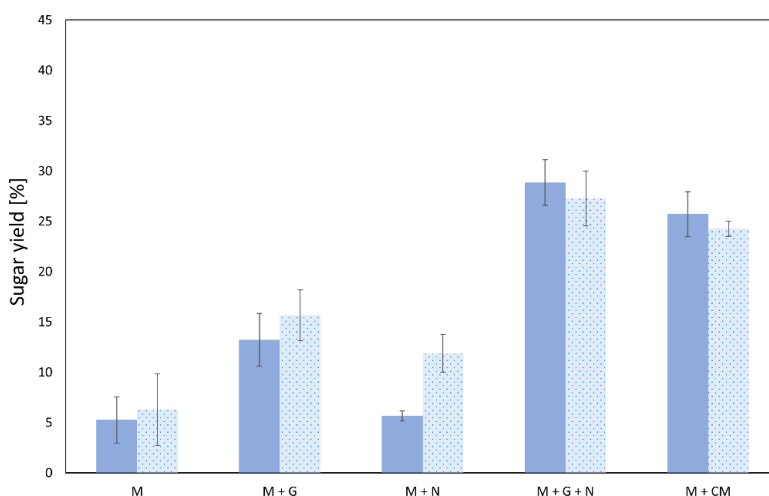
**Fig. 3.4** Lignocellulose degradation after spore-inoculated pretreatment of ( ■ ) sterilised and ( ■ ) non-sterilised wood in the presence of metal salts (M), metal salts with glucose (M+G), metal salts with  $\text{NaNO}_3$  (M+N), metal salts with glucose and  $\text{NaNO}_3$  (M+G+N) or metals salts with a complex medium (M+CM)

The medium composition significantly influenced the degradation of the individual lignocellulose components, i.e. lignin ( $p < 0.001$ ), glucan ( $p < 0.001$ ) and xylan ( $p = 0.021$ ) (**Fig. 3.5**), and consequently the glucose ( $p < 0.001$ ) and xylose ( $p < 0.001$ ) yields (**Fig. 3.6**). The fermentation using a complex medium (M+CM) resulted in the degradation of  $28.29 \pm 1.92\%$  lignin,  $10.09 \pm 2.41\%$  glucan and  $28.99 \pm 6.63\%$  xylan, giving a delignification selectivity value (SV) of  $2.91 \pm 0.88$ . In comparison, in the simplified M+G+N medium, a comparably high lignin and xylan degradation ( $29.16 \pm$

4.41% and  $26.76 \pm 5.41\%$ , respectively) but a significantly reduced ( $p = 0.024$ ) glucan consumption ( $4.10 \pm 1.44$ ) was obtained, resulting in a 2.2 times higher delignification selectivity value ( $SV = 8.84 \pm 3.02$ ) and the highest glucose and xylose yields ( $28.84 \pm 2.26\%$  and  $27.28 \pm 2.72\%$ , respectively) after enzymatic saccharification of the pretreated biomass (see Fig. 3.6).



**Fig. 3.5** Degradation of (■) lignin; (▨) glucan and (▤) xylan after spore-inoculated pretreatment of sterilised wood in the presence of metal salts (M), metal salts with glucose (M+G), metal salts with glucose and  $\text{NaNO}_3$  (M+G+N) and metals salts with a complex medium (M+CM)



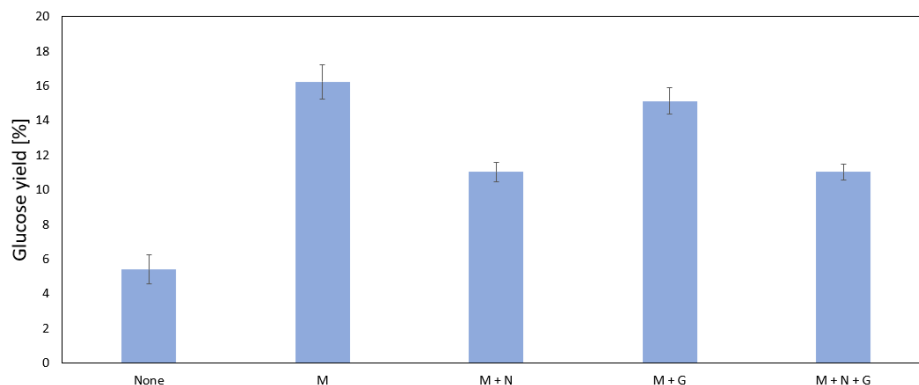
**Fig. 3.6** The obtained (■) glucose and (▤) xylose yield after the enzymatic saccharification of previously sterilised wood pretreated in the presence of metal salts alone (M), with glucose (M+G), with  $\text{NaNO}_3$  (M+N), with glucose and  $\text{NaNO}_3$  (M+G+N) and with a complex medium (M+CM)

These results indicate that the addition of both glucose and sodium nitrate is crucial for the SSF process when spores are used for inoculation and that one or more components present exclusively in the complex medium, enhance the degradation of cellulose over lignin. The presence of glucose supports spore germination and mycelial growth [197]. A nitrogen source, i.e. sodium nitrate in this study, plays a complex role in the fungal pretreatment system. Nitrogen is used for fungal growth and enzyme production but must be present in an optimal concentration since nitrogen limitation is important for the production of lignin-degrading enzymes by *P. chrysosporium* [83]. Further investigation aiming to reveal which component(s) in the complex fermentation medium (i.e.  $\text{KH}_2\text{PO}_4$ ,  $\text{KCl}$ ,  $\text{MgSO}_4$ ,  $\text{FeSO}_4$ , veratryl alcohol and Tween 80) are responsible for the increased cellulose degradation is out of the scope of this research.

In conclusion, the sterilisation of poplar wood prior to fungal pretreatment is essential when spores are used as inoculum. In addition, the use of a simplified medium containing only glucose,  $\text{NaNO}_3$ ,  $\text{Cu}^{2+}$  and  $\text{Mn}^{2+}$  provides the most selective delignification and highest sugar yields after the enzymatic saccharification of the pretreated and previously sterilised wood.

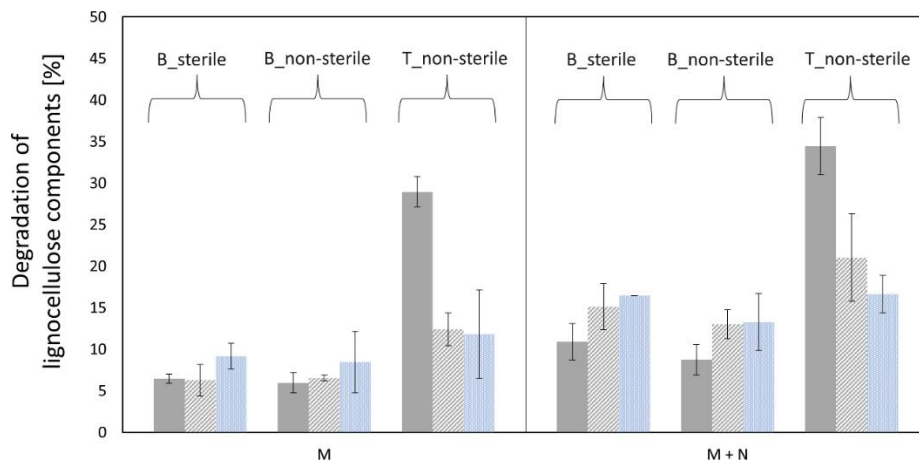
### 3.3.2 Pre-colonised wood as inoculum

The possibility of eliminating substrate sterilisation was also tested with the use of pre-colonised wood as inoculum instead of fungal spores. This inoculation technique has several important advantages. Firstly, the fungus is already adapted to the wood substrate. Secondly, the pre-inoculated wood contains fully developed white-rot fungi, eliminating the need for spore germination. In addition, the lignin-degrading enzymes are also already present. These combined effects effectively promote faster fungal growth and lignocellulose utilisation. An additional benefit of using pre-colonised wood as inoculum is that it eliminates the need for glucose supplementation, which is critical for spore germination when spores are used as inoculum. This hypothesis was also confirmed in our preliminary experiments, where the addition of glucose to the fermentation medium did not improve the pretreatment efficiency and, consequently, the achievable glucose yield after the enzymatic saccharification of the pretreated biomass (**Fig. 3.7**). Therefore, in further experiments, only metal ions with or without  $\text{NaNO}_3$  were investigated as fermentation supplements. In addition to sterile aerated Schott bottles, open trays were also investigated as a cultivation environment for the SSF of the non-sterilised wood, as the omission of the sterilisation step eliminated the need for sterile aeration. The SSF of sterilised wood was tested in Schott bottles for comparison.

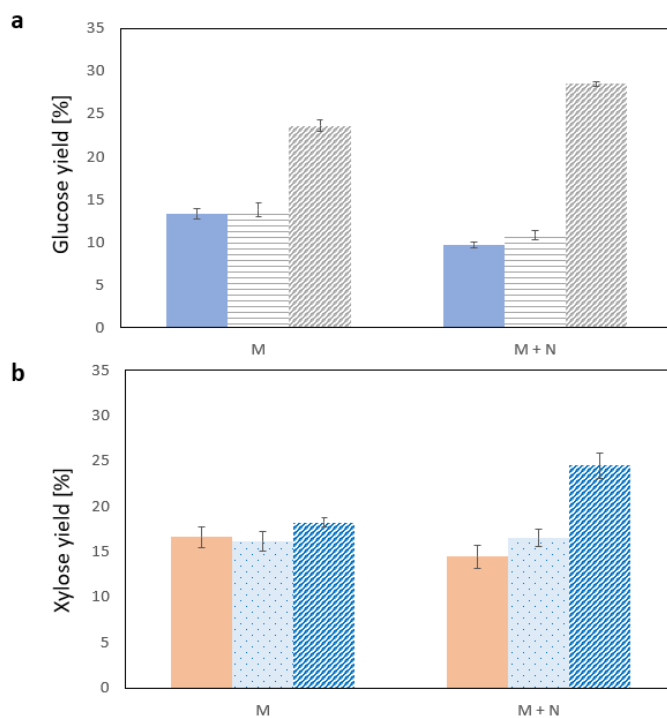


**Fig. 3.7** Glucose yield after pretreatment of non-sterilised wood inoculated with pre-colonised wood in bottles, without any supplements (None) and in the presence of metal salts alone (M), with  $\text{NaNO}_3$  (M+N), with glucose or with glucose and  $\text{NaNO}_3$  (M+G+N). Supplements were used with the dosages of 10.9 mg glucose, 1.6 mg  $\text{NaNO}_3$ , 0.10 mg  $\text{MnSO}_4 \cdot \text{H}_2\text{O}$  and 0.38 mg  $\text{CuSO}_4 \cdot 5\text{H}_2\text{O}$  per g wood.

The degradation of the individual lignocellulose components, i.e. lignin, glucan and xylan, in the sterilised and non-sterilised wood, is shown in **Fig. 3.8**. In the Schott bottles, the SSF of sterilised and non-sterilised wood resulted in a comparable lignocellulose degradation profile. Compared to the M medium, the supplementation with sodium nitrate (M+N medium) significantly increased the lignin degradation ( $p = 0.008$ ), with a 1.7-fold increase ( $6.45 \pm 0.55\% \rightarrow 10.91 \pm 2.20\%$ ) in the sterilised wood, and 1.5-fold increase ( $5.97 \pm 1.22\% \rightarrow 8.76 \pm 1.86\%$ ) in the non-sterilised wood. However, the consumption of carbohydrates, especially the one of cellulose, increased to a greater extent ( $p < 0.001$ ), i.e. 4.6-fold ( $6.28 \pm 1.88\% \rightarrow 15.13 \pm 2.78\%$ ) in the sterilised poplar and 2.0-fold ( $6.55 \pm 0.36\% \rightarrow 13.00 \pm 1.73\%$ ) in the non-sterilised wood. This resulted in a significant reduction ( $p = 0.005$ ) in glucose yield and no significant effect on xylose yield (**Fig. 3.9**).



**Fig. 3.8** Degradation of (■) lignin; (▨) glucan and (▤) xylan after pretreatment of sterilised wood in bottles (B\_sterile), non-sterilised wood in bottles (B\_non-sterile) and in trays (T\_non-sterile) in the presence of metal salts (M) or metal salts with  $\text{NaNO}_3$  (M+N)



**Fig. 3.9** (a) Glucose and (b) xylose yield after the enzymatic saccharification of (■) sterilised wood pretreated for 4 weeks in bottles and non-sterilised wood pretreated for 4 weeks (▤) in bottles or (▨) in trays in the presence of metal salts (M) and metal salts with  $\text{NaNO}_3$  (M+N).

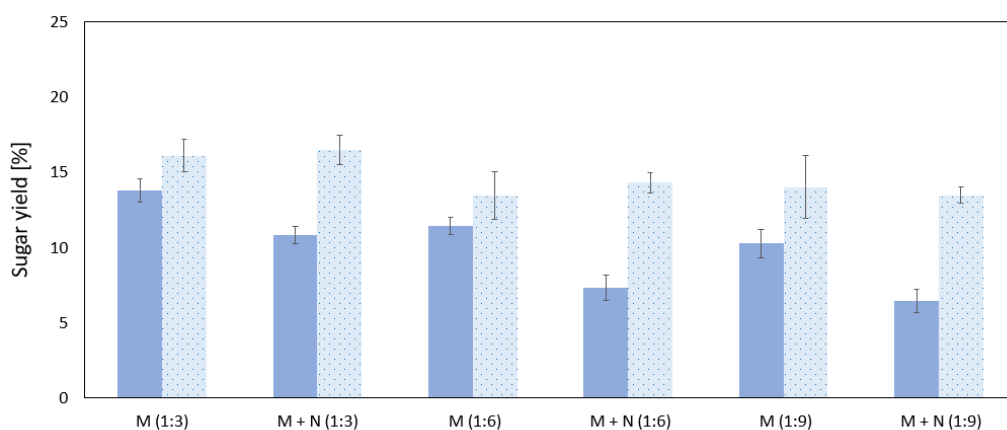
When the results were compared with the use of spores (see Section 3.3.1), inoculation with pre-colonised wood improved the fungal pretreatment of non-sterilised wood. However, it provided lower lignin degradations and saccharification yields in the sterilised wood. This might be caused by an easier distribution of spores in the heterogeneous SSF, leading to better fungal colonisation or by a different inoculum size. However, it is difficult to make a quantitative comparison for the latter due to the different types of inoculum used. The applied fungal inoculum size was  $5 \cdot 10^6$  spores/g DW wood in the case of the spore-inoculated SSF, and 1.12 mg fungal biomass/g DW wood in the SSF inoculated with pre-colonised wood, using a mixing ratio of 1:3, as determined by ergosterol measurement [198]. Based on our earlier research, increasing the spore concentration to  $10^7$  spores/g DW did not improve the pretreatment efficiency and saccharification yield (data not shown). However, the effect of reducing the spore concentration on the process was not investigated in this study.

Adding spores along with the pre-colonised wood or increasing the amount of fungal biomass on the pre-colonised wood could potentially further improve the pretreatment of both sterilised and non-sterilised wood. Higher fungal biomass can be achieved by optimising conditions favourable to fungal growth. The use of a packed bed reactor for the preparation of pre-colonised wood allows for forced aeration, which promotes fungal growth and can improve biomass yield. This approach not only increases biomass but also reduces the preparation time for pre-colonised wood.

Increasing the proportion of pre-colonised wood could be another approach, but it should be noted that this will increase the sterilisation requirements of the inoculum preparation. Conversely, the energy requirement for sterilisation could be further reduced by using a lower ratio of pre-colonised to untreated wood for inoculation. However, in this study, the use of a lower mixing ratio (1:6 or 1:9) had a statistically significant negative effect on glucose yields ( $p < 0.001$ ), but no significant effect on xylose yields (**Fig. 3.10**). Another approach could be to use a sequential fungal pretreatment process where pretreated feedstock from one pretreatment step is used to inoculate the subsequent fungal pretreatment cycle. This sequential process was investigated in the study of Vasco-Correa et al. on four different non-sterilised feedstocks, including miscanthus, corn stover, hardwood (white ash) and softwood (pine). However, the sequential fungal pretreatment was ineffective in the case of all feedstock for the second and third pretreatment cycles [17]. Nevertheless, it should be emphasised that the efficiency of fungal pretreatment is highly dependent on the applied microorganism and substrate. Therefore, further research is needed to evaluate



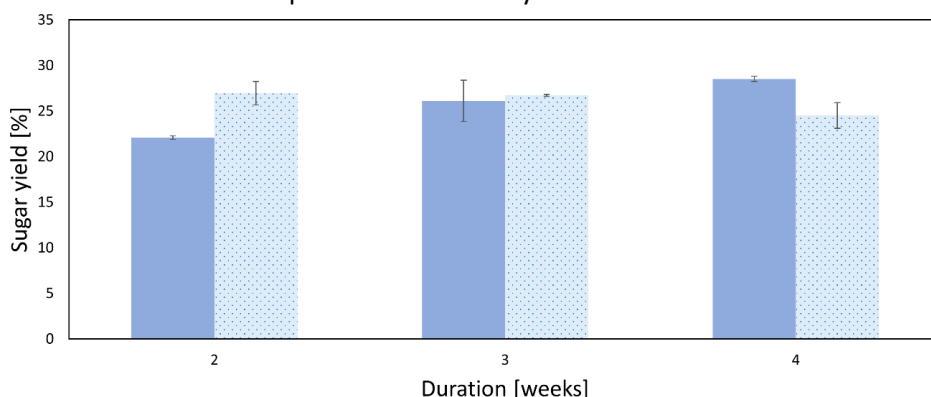
the feasibility of a sequential process for the fungal pretreatment of poplar wood with *P. chrysosporium*.



**Fig. 3.10** The obtained (■) glucose and (▨) xylose yield after the enzymatic saccharification of wood pretreated in bottles applying different mixing ratios of pre-colonised and untreated wood (mixing ratios are indicated in brackets) in the presence of metal salts (M) and metal salts with NaNO<sub>3</sub> (M+N)

Compared to the bottle experiments with a 1:3 mixing ratio, SSF in trays resulted in significantly higher lignin degradation ( $p < 0.001$ ), i.e.  $28.97 \pm 1.82\%$  and  $34.45 \pm 3.43\%$  in the M and M+N systems, respectively (**Fig. 3.8**). This can be attributed to the higher oxygen availability in the open trays which is markedly important for the ligninase activity of the white-rot fungi [76]. There was no statistically significant difference in lignocellulose degradation between the M and M+N systems. However, the nitrogen supplementation had a significant positive effect on both the glucose ( $p = 0.002$ ) and xylose ( $p = 0.006$ ) yields, probably due to the higher reproducibility of sugar yield determination compared to the compositional analysis which uses a smaller sample size than the enzymatic saccharification (300 mg vs 500 mg) and is very laborious. The increased glucose ( $28.51 \pm 0.28\%$ ) and xylose ( $24.49 \pm 1.41\%$ ) yields obtained in the M+N-supplemented trays (**Fig. 3.9**) indicate that nitrogen supplementation has a positive effect on the pretreatment efficiency when the fermentation conditions are favourable (e.g. adequate colonisation and oxygen availability), and substantial lignin degradation (>20%) can occur, requiring a higher nitrogen availability for ligninase production. Pretreatment durations of less than 4 weeks were also investigated for the M+N-supplemented tray SSFs. Although the glucose yield increased steadily with prolonged pretreatment compared to 3 weeks of SSF, 4 weeks of pretreatment did not

significantly increase the saccharification yields (**Fig. 3.11**). These results indicate that the fungal pretreatment went fast and that the gain in saccharification yield was limited after more than 3 weeks of pretreatment in trays.



**Fig. 3.11** The obtained (■) glucose and (▨) xylose yield after the enzymatic saccharification of wood pretreated in trays for different pretreatment times

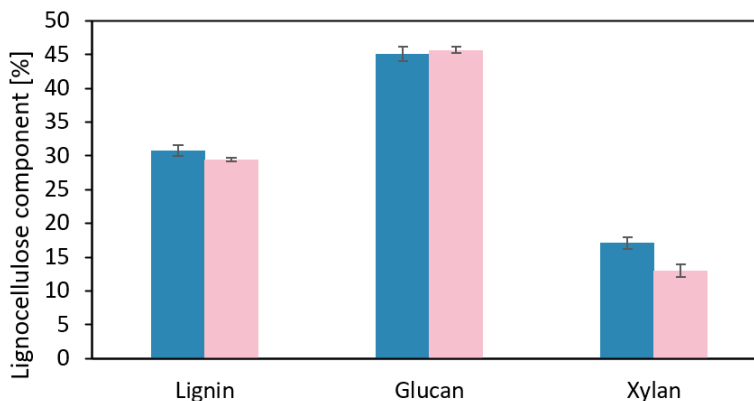
In conclusion,  $28.51 \pm 0.28\%$  glucose yield was obtained for the 4 weeks of tray fermentation of non-sterilised wood, i.e. a similar value to the one measured in the sterile, spore-inoculated system ( $28.84 \pm 2.26\%$ ). However, tray fermentation using only  $\text{NaNO}_3$  and a small amount of metal ions, but no glucose supplementation, eliminated the need for sterile aeration and required sterilisation of only 28.83% of the feedstock. The latter was necessary to produce pre-colonised wood given the 1:3 mixing ratio and the loss of dry matter ( $17.70 \pm 0.26\%$ ) during inoculum preparation.

Although the glucose yield obtained in this optimisation study ( $28.51 \pm 0.28\%$ ) is significantly lower than that already achieved by chemical pretreatment ( $>90\%$ ), it is comparable to the average glucose yield ( $\sim 30\%$ ) obtained from fungal pretreatment of sterilised hardwood [10], but with the advantage of reduced sterilisation requirements.

### 3.3.3 Application on new sawdust feedstock

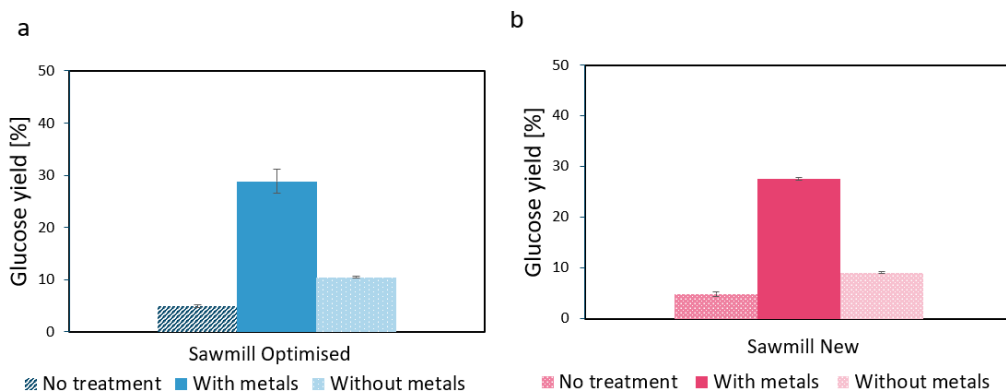
The optimised sterilised wood bottle SSF (Section 3.3.1) and non-sterilised wood tray SSF (Section 3.3.2) were applied to a new batch of sawdust feedstock obtained from the Caluwaerts Willy sawmill to assess the feasibility of the optimised fermentations on new feedstock batches. The exact species/hybrid of poplar trees processed by the sawmill is not known, and a particular batch of sawdust may be a mixture of different species/hybrids. The difference in glucan and lignin content between the previously studied feedstock (referred to as Sawdust Optimised) and the new feedstock (Sawdust

New) was insignificant ( $p > 0.05$ ). However, a 24% lower xylan content ( $17.10 \pm 0.83\% \rightarrow 13.01 \pm 0.92\%$ ) was measured in Sawdust New ( $p = 0.015$ ) (**Fig. 3.12**).

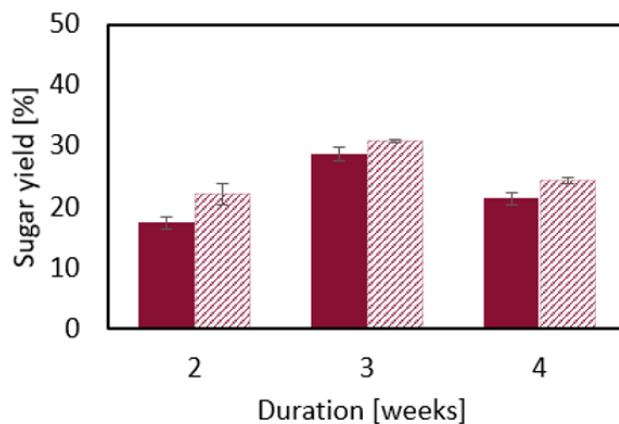


**Fig. 3.12** Composition of Sawdust Optimised (■) and Sawdust New (■)

Bottle SSF of the sterilised Sawdust New feedstock provided similar pretreatment efficiencies and sugar yields to those obtained with Sawdust Optimised, with metal supplementation remaining critical for efficient SSF and increased sugar yields (**Fig. 3.13**). The non-sterilised wood tray SSF was also successfully applied to the new feedstock with an optimum glucose yield of  $28.63 \pm 1.17\%$  obtained at 3 weeks pretreatment time (**Fig. 3.14**), due to the decreased delignification selectivity occurring with longer pretreatment time. This finding is different from the SSF Sawdust Optimised where the glucose yield still showed a slight increase from 3 to 4 weeks reaching its maximum of  $28.51 \pm 0.28\%$  at week 4 (**Fig. 3.11**). This may be due to the different indigenous microbial communities present in the new feedstock, which may affect substrate colonisation and thus lignocellulose degradation rates.



**Fig. 3.13** Comparison of glucose yields obtained after the enzymatic saccharification of two different sawdust batches with and without pretreatment and metal supplementation



**Fig. 3.14** The obtained (■) glucose and (▨) xylose yield after the enzymatic saccharification of Sawdust New pretreated in trays for different pretreatment times

In conclusion, the optimised solid-state fermentation strategies were effectively implemented on the fresh batch of feedstock, suggesting effective applicability on new feedstocks as long as the sawdust particle size and composition are comparable to those of Sawdust Optimised.

### **3.4 Conclusion**

Although fungal pretreatment is a biotechnological process with mild reaction conditions, further process development can improve its economics. This paper introduces a simple solid-state fermentation set-up using pre-colonised wood to inoculate non-sterilised wood, solely  $\text{NaNO}_3$  and a minor amount of metal ions as supplements in a tray without sterile ventilation as a cultivation environment. This technology provides a comparable glucose yield ( $28.51 \pm 0.28\%$ ) after the enzymatic saccharification of the pretreated biomass as the traditional method using spore-inoculated sterilised wood and sterile vented bottles. The proposed process, which was also successfully applied to a new batch of sawdust, could significantly reduce the energy required for sterilisation in fungal pretreatment-based biorefineries.



## **Chapter 4. Rapid lignin quantification for fungal wood pretreatment by ATR-FTIR spectroscopy**

---

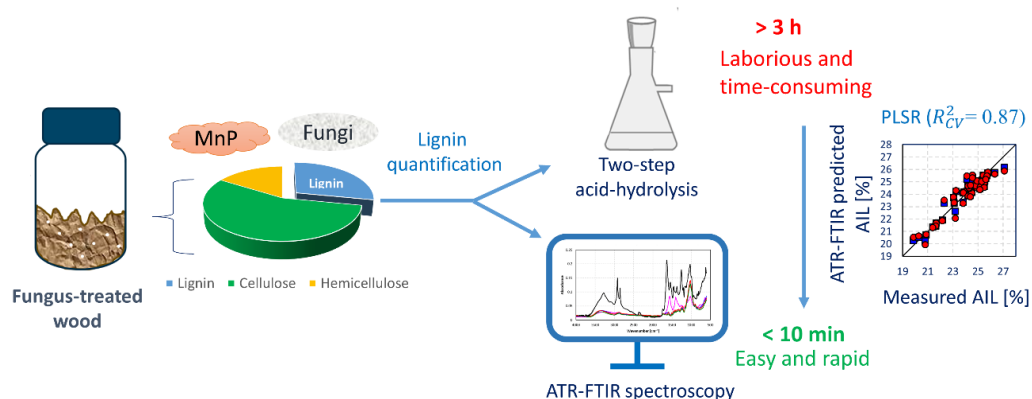
The research work was performed in collaboration with professor dr. ir. Szilveszter Gergely and ir. János Slezsák from Budapest University of Technology and Economics and was redrafted from the manuscript published in *Spectrochimica Acta, Part A: Molecular and Biomolecular Spectroscopy*.

N. Wittner, J. Slezsák, W. Broos, J. Geerts, S. Gergely, S.E. Vlaeminck, I. Cornet, Rapid lignin quantification for fungal wood pretreatment by ATR-FTIR spectroscopy, *Spectrochim. Acta Part A Mol. Biomol. Spectrosc.* 285 (2023) 121912. <https://doi.org/10.1016/J.SAA.2022.121912>

**Abstract**

Lignin determination in lignocellulose with the conventional two-step acid hydrolysis method is highly laborious and time-consuming. However, its quantification is crucial to monitor the fungal pretreatment of wood, as the increase of acid-insoluble lignin degradation linearly correlates with the achievable enzymatic saccharification yield. Therefore, in this study, a new attenuated total reflectance Fourier transform infrared (ATR-FTIR) spectroscopy method was developed to track fungal delignification in an easy and rapid manner.

Partial least square regression (PLSR) with cross-validation (CV) was applied to correlate the ATR-FTIR spectra with the AIL content (19.9%–27.1%). After variable selection and normalisation, a PLSR model with a high coefficient of determination ( $R_{CV}^2 = 0.87$ ) and a low root mean square ( $RMSE_{CV} = 0.60\%$ ) were obtained despite the heterogeneous nature of the fungal solid-state fermentation. These results show that ATR-FTIR can reliably predict the AIL content in fungus-treated wood while being a high-throughput method. This novel method can facilitate the transition to a wood-based bioeconomy.

**Fig. 4.1** Graphical abstract



## 4.1 Introduction

The depletion of fossil resources resulted in increased interest in the search for an alternative source of energy and chemicals. Lignocellulosic biomass from plant cell walls is one of the most promising feedstocks for the production of biofuels and value-added biochemicals due to its broad availability, renewable production and low cost [199]. Lignocellulose consists of three main compounds, i.e. the polysaccharides cellulose and hemicellulose and the polyaromatic compound lignin. In a sugar platform biorefinery, the degradation of this lignin has crucial importance in obtaining fermentable sugars from the polysaccharides [200]. Various pretreatment techniques, including physical, chemical, fungal, and physicochemical methods, have been employed to reduce the amount of lignin in lignocellulose. Fungal pretreatment, which mainly uses white-rot fungi for the degradation of lignin, is a pretreatment method that does not use hazardous chemicals and conditions and does not produce fermentation-inhibiting by-products [49]. *Phanerochaete chrysosporium* is one of the most widely studied white-rot fungi, which produces manganese-peroxidase (MnP) and lignin peroxidase (LiP) for the degradation of lignin. In our previous study on the solid-state fermentation of poplar wood by *P. chrysosporium*, a positive linear correlation was found between the acid-insoluble lignin degradation and the obtained enzymatic saccharification yield which is in agreement with the findings of other studies [18,196]. Therefore, the monitoring of lignin has great importance in the optimization of the fungal pretreatment process.

The oldest and most popular method for lignin quantitation is the Klason method which has been outlined by the National Renewable Energy Laboratory (NREL) [135].

In this procedure, a two-step acid hydrolysis is performed on lignocellulose. First, the biomass is treated with concentrated sulphuric acid (72% w/w) at 30°C for 1 h; then the mixture is diluted with water to 4% w/w sulphuric acid and autoclaved at 121°C for 1 h to hydrolyse the polysaccharides into monomeric sugars. The acid-insoluble lignin (so-called Klason lignin) is gravimetrically quantified, while the acid-soluble lignin is spectrophotometrically determined. Although this conventional wet chemistry method has been markedly useful for lignin quantification in lignocellulose, it is highly laborious, time-consuming (> 3 h) and requires the use of hazardous concentrated sulphuric acid and a relatively high amount of biomass (300 mg). Hence, the need is reinforced to develop an alternative method that allows rapid and easy lignin quantification with minimal sample preparation.

Fourier transform infrared (FTIR) analytical spectroscopy in the mid-infrared region (4000–400 cm<sup>-1</sup>) has received increased interest in wood characterization due to the advances in the development of the attenuated total reflectance (ATR) technique

[201,202]. In the traditional KBr pellet-based FTIR analysis in transmission geometry, the additional preparation of pellets from infrared inactive KBr and the sample is required. In contrast, the ATR technique uses only minimal sample preparation, i.e., drying and homogenization (e.g. milling), after which the sample is directly pressed onto the ATR crystal, and the spectral acquisition is performed within minutes allowing a very convenient analysis.

In the field of wood decay, ATR-FTIR has been recognised for its potential to assess the fungal deconstruction of lignocellulose [160,161]. Although it was demonstrated that ATR-FTIR with multivariate data analysis, such as partial least squares regression modelling, can be applied for the quantitative determination of lignin in lignocellulose [22,23], its use for lignin estimation has not been evaluated yet in wood which was pretreated by white-rot fungi.

In this work, an ATR-FTIR method combined with PLSR was developed to determine the acid-insoluble lignin content in fungus-treated poplar wood hereby providing a simple and fast alternative (< 10 min) to the conventional labour- and time-intensive (> 3 h) two-step acid hydrolysis. This included the research subgoals of (1) obtaining a set of fungus-treated poplar wood samples with a wide range of AIL, (2) correlating the quantification of lignin in wood that is pretreated with white-rot fungi by ATR-FTIR coupled with PLSR to the traditional Klason lignin determination, (3) uncover and overcome possible interferences (4) optimise the PLSR model by variable selection and spectral pre-processing.

## **4.2 Materials and Methods**

### **4.2.1 Lignocellulose substrate and white-rot fungi**

Poplar wood sawdust was obtained from Sawmill Caluwaerts Willy (Holsbeek, BE). The particle size distribution of the sawdust was determined by sieve analysis. 86.1% w/w of the pellets were collected between the 2 mm and 0.075 mm screens. The white-rot fungus *Phanerochaete chrysosporium* MUCL 19343 was used for the solid-state fungal pretreatment studies. A spore suspension of  $5 \cdot 10^6$  spores/mL (corresponds to 0.49 OD at 650 nm) was freshly prepared in distilled water from 5 days old cultures grown on potato dextrose agar at 39°C.

### **4.3 Fermentation media**

Based on our previous study, the complex medium contained 3 g/L NaNO<sub>3</sub>, 20 g/L glucose, 0.5 g/L KCl, 0.5 g/L MgSO<sub>4</sub>·7H<sub>2</sub>O, 0.5 g/L FeSO<sub>4</sub>·7H<sub>2</sub>O, 1 g/L KH<sub>2</sub>PO<sub>4</sub>, 0.34 g/L veratryl alcohol, 0.1% v/v Tween 80, 20 g/L of glucose, 3.69 mM CuSO<sub>4</sub> and 1.41 mM MnSO<sub>4</sub> creating the optimal metal ion dosage of 2.01 μmol Cu<sup>2+</sup>, 0.77 μmol Mn<sup>2+</sup> g<sup>-1</sup> dry

weight (DW) wood for enhanced delignification [171,196]. The simplified media were composed of 3.69 mM CuSO<sub>4</sub>, 1.41 mM MnSO<sub>4</sub> with or without 20 g/L glucose and/or 3 g/L NaNO<sub>3</sub>.

#### 4.4 Solid-state fungal pretreatment

Solid-state fermentation of poplar wood was performed at different fermentation conditions to obtain pretreated poplar wood with varying lignin content for lignin calibration. These SSFs differed in the applied substrate sterilisation, fermentation duration, medium composition and fermentation set-up (rolling bottles or trays).

SSF of sterilised wood in rolling bottles was performed in Schott bottles as described in Section 2.2.4. Briefly, these fermentations were conducted in 100 mL Schott bottles closed with sterile-venting screw caps. The fermentation bottles contained 3.67 g dry-weight poplar wood, 2 mL sterile media, 3.7 mL spore suspension ( $5 \cdot 10^6$  spores/g DW wood) and distilled water, creating a moisture content of 75% w/w on a wet basis. The media and the poplar wood were sterilised separately by autoclaving each at 121°C for 20 min. The SSF bottles were rolled at 4 rpm on a bottle roller (88881004 Bottle/Tube Roller, Thermo Scientific™) and incubated (TC 255 S, Tintometer Inc.) at 37°C for up to 4 weeks. Tray fermentations of non-sterilised poplar wood were carried out in 500 mL crystallizing dishes containing 2 mL medium, 2.8 g DW untreated non-sterilised wood and 0.9 g DW pretreated wood as inoculum. Pretreated wood for inoculation was obtained after 4 weeks of SSF performed in Schott bottles as described in Section 2.2.4 applying a medium composition of 3.69 mM CuSO<sub>4</sub>, 1.41 mM MnSO<sub>4</sub> with or without 20 g/L glucose and/or 3 g/L NaNO<sub>3</sub>.

In the inoculation step of the tray fermentation, the freshly harvested pretreated wood (0.9 g dry weight (DW)) was mixed with non-sterilised untreated wood (2.8 g DW) in 500 mL crystallizing dishes. 2 mL sterile medium containing 3.69 mM CuSO<sub>4</sub>, 1.41 mM MnSO<sub>4</sub> and 3 g/L NaNO<sub>3</sub> was added, and the moisture content was brought to 75% w/w with sterile demineralised water. Fermentations were carried out for up to 4 weeks at 37°C in a humidified chamber placed in a *Heratherm IMH 100 incubator* (Thermo Scientific). The humidified chamber was built by bubbling compressed air through an aeration stone at an aeration rate of 3 L per minute into the water bath placed at the bottom of the chamber. This inoculation technique was necessary to avoid the outcompetition of indigenous microbial communities with the white-rot fungi during the SSF of non-sterilised wood [15]. At the end of the fermentation, the entire content of the SSF bottle/tray was harvested, and the pretreated wood was analysed for its acid-insoluble lignin content by the conventional two-step acid hydrolysis [135] as a reference method and by Fourier transform infrared spectroscopy. **Table 4.1** shows the

applied medium composition, fermentation set-up and fermentation duration with the corresponding AIL content for each pretreated wood sample.

**Table 4.1** Fermentation conditions and the corresponding acid-insoluble lignin content

#Sample	Set-up <sup>a</sup>	Medium <sup>b</sup>	Feedstock sterilisation <sup>c</sup> [min]	SSF time [day]	AIL content <sup>e</sup> [% w/w]
raw wood	B	-	-	-	26.32 ± 0.69
SSF1	B	Cu <sup>2+</sup> , Mn <sup>2+</sup>	20	28	24.54
SSF2	B	Cu <sup>2+</sup> , Mn <sup>2+</sup>	20	28	24.11
SSF3	B	Cu <sup>2+</sup> , Mn <sup>2+</sup>	20	28	24.55 ± 2.17
SSF4	B	Glucose, Cu <sup>2+</sup> , Mn <sup>2+</sup>	20	28	23.80 ± 0.26
SSF5	B	Glucose, Cu <sup>2+</sup> , Mn <sup>2+</sup>	20	28	24.37
SSF6	B	Glucose, Cu <sup>2+</sup> , Mn <sup>2+</sup>	20	28	23.08 ± 0.49
SSF7	B	Nitrogen, glucose, Cu <sup>2+</sup> , Mn <sup>2+</sup>	20	28	19.85 ± 0.01
SSF8	B	Nitrogen, glucose, Cu <sup>2+</sup> , Mn <sup>2+</sup>	20	28	20.80 ± 0.33
SSF9	B	Complex, Cu <sup>2+</sup> , Mn <sup>2+</sup>	20	28	20.27
SSF10	B	Complex, Cu <sup>2+</sup> , Mn <sup>2+</sup>	20	28	25.61 ± 0.58
SSF11	B	Complex, -	60	0 <sup>d</sup>	25.79 ± 0.14
SSF12	B	Complex, -	60	26.8	24.20 ± 0.61
SSF13	B	Complex, Mn <sup>2+</sup>	60	0 <sup>d</sup>	25.60 ± 0.41
SSF14	B	Complex, Mn <sup>2+</sup>	60	26.8	23.20 ± 0.28
SSF15	B	Complex, Cu <sup>2+</sup>	60	0 <sup>d</sup>	25.70 ± 0.25
SSF16	B	Complex, Cu <sup>2+</sup>	60	26.8	22.29 ± 0.02
SSF17	B	Complex, Cu <sup>2+</sup> , Mn <sup>2+</sup>	60	0 <sup>d</sup>	25.29 ± 0.53
SSF18	B	Complex, Cu <sup>2+</sup> , Mn <sup>2+</sup>	60	26.8	21.39 ± 0.27
SSF19	T	Nitrogen, Cu <sup>2+</sup> , Mn <sup>2+</sup>	-	28	21.67
SSF20	T	Nitrogen, Cu <sup>2+</sup> , Mn <sup>2+</sup>	-	28	22.16
SSF21	T	Nitrogen, Cu <sup>2+</sup> , Mn <sup>2+</sup>	-	28	21.63
SSF22	T	Nitrogen, Cu <sup>2+</sup> , Mn <sup>2+</sup>	-	28	20.87
SSF23	B	Nitrogen, glucose, Cu <sup>2+</sup> , Mn <sup>2+</sup>	20	0 <sup>d</sup>	27.08

SSF24	B	Nitrogen, glucose, Cu <sup>2+</sup> , Mn <sup>2+</sup>	20	14	24.84 ± 0.55
SSF25	B	Nitrogen, glucose, Cu <sup>2+</sup> , Mn <sup>2+</sup>	20	14	23.87 ± 0.55
SSF26	B	Nitrogen, glucose, Cu <sup>2+</sup> , Mn <sup>2+</sup>	20	14	23.03 ± 0.13
SSF27	B	Nitrogen, glucose, Cu <sup>2+</sup> , Mn <sup>2+</sup>	20	17	23.84 ± 0.10
SSF28	B	Nitrogen, glucose, Cu <sup>2+</sup> , Mn <sup>2+</sup>	20	17	24.33 ± 0.84
SSF29	B	Nitrogen, glucose, Cu <sup>2+</sup> , Mn <sup>2+</sup>	20	17	24.27 ± 0.82
SSF30	B	Nitrogen, glucose, Cu <sup>2+</sup> , Mn <sup>2+</sup>	20	19	24.2
SSF31	B	Nitrogen, glucose, Cu <sup>2+</sup> , Mn <sup>2+</sup>	20	19	24.17 ± 0.20
SSF32	B	Nitrogen, glucose, Cu <sup>2+</sup> , Mn <sup>2+</sup>	20	19	24.81 ± 0.85
SSF33	B	Nitrogen, glucose, Cu <sup>2+</sup> , Mn <sup>2+</sup>	20	21	24.19 ± 0.61
SSF34	B	Nitrogen, glucose, Cu <sup>2+</sup> , Mn <sup>2+</sup>	20	21	24.93 ± 0.01
SSF35	B	Nitrogen, glucose, Cu <sup>2+</sup> , Mn <sup>2+</sup>	20	21	25.35
SSF36	B	Nitrogen, glucose, Cu <sup>2+</sup> , Mn <sup>2+</sup>	20	24	25.41 ± 0.20
SSF37	B	Nitrogen, glucose, Cu <sup>2+</sup> , Mn <sup>2+</sup>	20	24	23.23 ± 1.27
SSF38	B	Nitrogen, glucose, Cu <sup>2+</sup> , Mn <sup>2+</sup>	20	24	24.40 ± 0.22
SSF39	B	Nitrogen, glucose, Cu <sup>2+</sup> , Mn <sup>2+</sup>	20	26.7	25.16 ± 0.20
SSF40	B	Nitrogen, glucose, Cu <sup>2+</sup> , Mn <sup>2+</sup>	20	26.7	25.48 ± 0.08

SSF41	B	Nitrogen, glucose, Cu <sup>2+</sup> , Mn <sup>2+</sup>	20	26.7	25.54 ± 0.18
SSF42	B	Nitrogen, glucose, Cu <sup>2+</sup> , Mn <sup>2+</sup>	20	28	25.15
SSF43	B	Nitrogen, glucose, Cu <sup>2+</sup> , Mn <sup>2+</sup>	20	28	24.49 ± 1.05
SSF44	B	Nitrogen, glucose, Cu <sup>2+</sup> , Mn <sup>2+</sup>	20	28	24.83

<sup>-</sup>: not applicable

<sup>a</sup> B: bottle, T: tray fermentation; <sup>b</sup> The complex medium consists of 3 g/L NaNO<sub>3</sub>, 20 g/L glucose, 0.5 g/L KCl, 0.5 g/L MgSO<sub>4</sub>·7H<sub>2</sub>O, 0.5 g/L FeSO<sub>4</sub>·7H<sub>2</sub>O, 1 g/L KH<sub>2</sub>PO<sub>4</sub>, 0.34 g/L veratryl alcohol, 0.1 %v/v Tween 80, 3.69 mM CuSO<sub>4</sub> and 1.41 mM MnSO<sub>4</sub>. The simplified medium is composed of 3.69 mM CuSO<sub>4</sub>, 1.41 mM MnSO<sub>4</sub> with or without 20 g/L glucose and/or 3 g/L NaNO<sub>3</sub>. <sup>c</sup> Autoclaving at 121°C; <sup>d</sup> Fermentations immediately harvested after inoculation <sup>e</sup> Acid-insoluble lignin content measured once or in duplicate by the standard NREL protocol (NREL/TP-510-42618)

## 4.5 Analytical methods

### 4.5.1 Removal of water-soluble substances

Before AIL quantification, the biomass samples were thoroughly washed to remove the lignocellulolytic enzymes and other water-soluble compounds. One rinsing cycle included the shaking of the biomass with 50 mM acetate buffer (pH 4.5), applying a solid-to-liquid ratio of 1:80 at 400 rpm for 20 min. The shaking was followed by centrifugation (Sigma 3-16KL) for 15 min at 4500 rpm and 4°C. After the removal of the supernatant, this rinsing cycle was repeated once with acetate buffer and twice with distilled water to remove the traces of acetic acid. The rinsed solid was freeze-dried (ALPHA 1-2 Ldplus, Martin Christ Gefriertrocknungsanlagen GmbH) until a constant weight was achieved and used for lignin and infrared analysis.

### 4.5.2 Total protein determination

Protein concentration in the rinsing liquids (4.5.1) was determined by Bradford Assay Kit (TCI Europe N.V).

### 4.5.3 Analysis of phenolic compounds

In the washing liquid, the detection and quantification of seven phenolic compounds, i.e. 3,4-dihydroxybenzaldehyde, 4-hydroxybenzoic acid, 4-hydroxybenzaldehyde, vanillic acid, syringic acid, vanillin, and syringaldehyde were carried out by HPLC-UV

analysis (1290 Infinity II LC system equipped with a UV-Vis diode array detector, Agilent Technologies, Inc.). The identification of each compound was based on a combination of retention time and spectral matching with external standards. The chromatographic separation was obtained on a C18 column (Aqua® 5 µm, 125 Å, 250 × 4.6 mm, Phenomenex Inc.) at 25°C. UV detection was performed at 250, 280 and 310 nm at a flow rate of 0.4 mL per minute. Combined gradient-isocratic elution was used with a mobile phase of methanol (solvent A) and 2% acetic acid in water (solvent B): 0–3 min 10% solvent A; 3–8 min a gradient to 19.3% solvent A; 8–23 min a gradient to 33.6% solvent A; 23–35 min gradient to 55% solvent A; 35–45 min a gradient to 100% solvent A; 45–60 min 100% solvent A. Prior to the HPLC analysis, all samples were filtered through a 0.2 µm polyethersulfone syringe filter.

#### 4.5.4 Fungal biomass estimation

The ergosterol content of the fungal cell membrane was used to determine the fungal biomass in the pretreated wood before and after the rinsing cycles (Section 4.5.1). Ergosterol determination was carried out based on the study of Niemenmaa et al., 2006. For the conversion of the mass of ergosterol measured to the fungal mass, the ergosterol content of *P. chrysosporium* was determined through plate cultivation and was measured to be  $7.24 \pm 0.26$  µg ergosterol/mg fungal biomass [4].

#### 4.5.5 Acid-insoluble lignin determination

The acid-insoluble lignin (AIL) content of poplar wood was determined before and after pretreatment by the standard NREL protocol (NREL/TP-510-42618) [135]. Briefly, the AIL content of the samples was measured gravimetrically after two-step acid hydrolysis with sulfuric acid. Measurements were carried out once or in duplicate (**Table 4.1**). The average standard laboratory error, determined from the duplicate measurements, was calculated to be 0.32%.

#### 4.5.6 Milling

Before FTIR analysis, the washed and non-washed wood samples were freeze-dried (Alpha 1-2 Ldplus, Martin Christ Gefriertrocknungsanlagen GmbH) and ground with a ball mill. Hereto, 200 mg of lyophilised sample was measured into a stainless-steel grinding jar (25 mL) together with four 10 mm and one 15 mm stainless steel grinding balls. The jar was immersed in liquid nitrogen for 30 seconds to embrittle the sample and avoid its thermal damage. Milling was carried out for 4 min at a frequency of 25 Hz in a mixer mill (MM 200, Retsch GmbH).

#### 4.5.7 ATR-FTIR analysis

FTIR analysis was carried out on both washed (Section 4.5.1) and non-washed freeze-dried pretreated wood samples, as well as on freeze-dried *P. chrysosporium* (scraped from potato dextrose agar (PDA) plate) and on freeze-dried MnP enzymes (extract was obtained according to the study of Wittner et al., 2021). FTIR in attenuated total reflectance (ATR) mode was carried out using a Spectrum 400 spectrometer (PerkinElmer, Inc.) equipped with a Universal ATR (UATR) accessory (PerkinElmer, Inc.). Spectra were recorded from  $4000\text{ cm}^{-1}$  to  $650\text{ cm}^{-1}$  (i.e., the wavelength range of 2500–15385 nm) at a spectral resolution of  $4\text{ cm}^{-1}$  with 32 co-added scans applying a contact pressure of 100 N. Samples were measured in triplicate with Spectrum 6.3.2 software (Perkin Elmer, Inc.). Triplicate measurements were performed by placing separate subsamples on the internal reflection element (IRE) to cover the inhomogeneity of the solid sample of biological origin.

#### 4.5.8 Spectral data processing and multivariate analysis

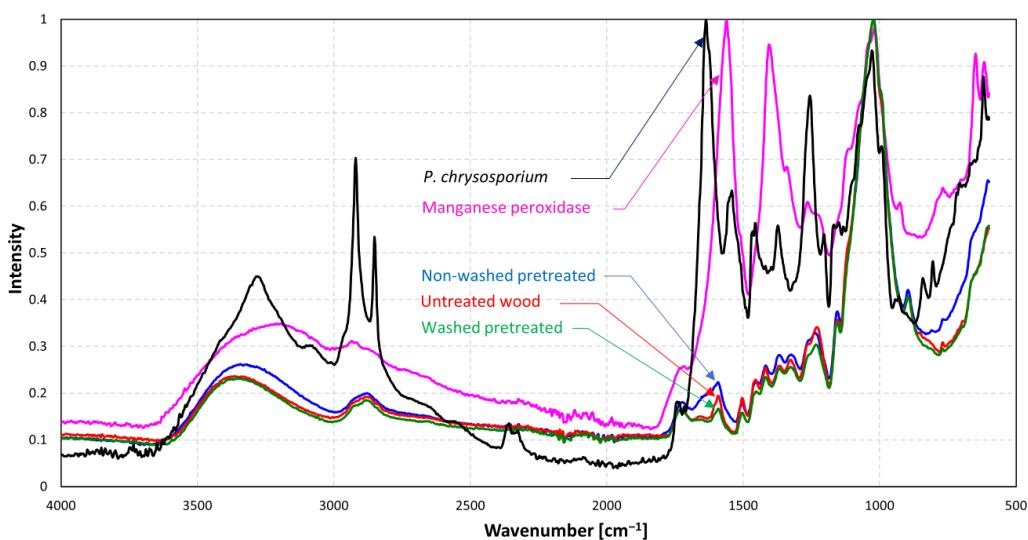
All IR spectra were processed using The Unscrambler<sup>®</sup> X 10.4 (CAMO Software, Oslo, Norway) and Microsoft<sup>®</sup> Excel<sup>®</sup> 2019 (Microsoft Corp., Redmond, WA, USA) software. Standard normal variate (SNV) pre-processing was applied to reduce baseline shift caused by light scattering and by variable spectral path length [203]. After SNV normalisation, principal component analysis (PCA) was performed on the washed and non-washed wood samples for dimensionality reduction and to identify outlier samples [204]. For lignin calibration, partial least squares regression was used, which is a well-researched quantitative approach extensively referenced in the literature [205]. Prior to PLSR, the average spectra of the FTIR measurement of subsamples were calculated and were subsequently pre-processed by SNV analysis. During PLSR, the infrared spectral data are regressed against the measured acid-insoluble lignin content to find a prediction model with a high coefficient of determination ( $R^2$ ) and a low root means square error ( $RMSE$ ). The quality of the prediction models was estimated by leave-one-out cross-validation. Therefore, during the PLSR, the performance indicators ( $R^2$  and  $RMSE$ ) of the models were calculated for both the calibration I and validation (CV) data sets.



## 4.6 Results and Discussion

### 4.6.1 Interpretation of ATR-FTIR spectra and PCA

The FTIR spectra of *P. chrysosporium*, its manganese peroxidase enzyme, and the untreated and fungus-treated poplar wood (with or without washing) are presented in **Fig. 4.2**. The wavenumber assignments of cellulose, hemicellulose, lignin and the most significant bands assigned to the solid-state fermentation are shown in **Table 4.2**.



**Fig. 4.2** FTIR characterization of (—) manganese peroxidase (MnP), (—) *P. chrysosporium*, (—) untreated poplar wood, and pretreated poplar wood (—) with and (—) without washing

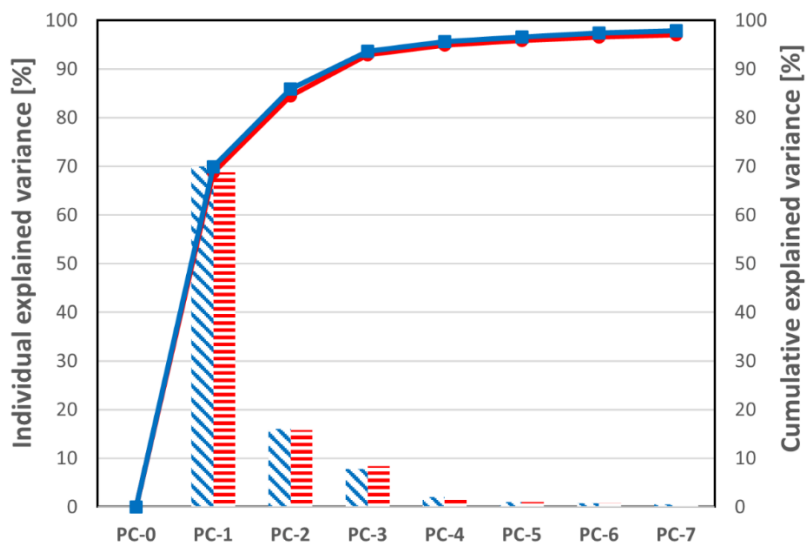
Since all samples were freeze-dried prior to FTIR analysis, the assumption was made that the effect of the minor amount of moisture, possibly still present after freeze-drying, is constant in all samples and neglectable. Due to the complexity of woody biomass, most absorbance bands cannot be exclusively assigned to lignin but to all three wood components. The spectral region of 1700–1145  $\text{cm}^{-1}$  provides the most information about the aromatic structure and functional groups occurring in lignin while containing the least carbohydrate-dominated bands and therefore is suitable for ATR-FTIR-based lignin estimation. However, this region is also affected by the presence of extracellular enzymes such as manganese peroxidase (MnP), i.e. the main enzyme responsible for lignin degradation by *P. chrysosporium*, and by the fungus itself both absorbing at 1644  $\text{cm}^{-1}$  (C=O stretching in the amide I peptide [206,207]) (**Fig. 4.2**).

**Table 4.2** ATR-FTIR peak assignment in poplar wood with and without fungal pretreatment

	Wavenumber [cm <sup>-1</sup> ]	Functional group	Lignocellulose/ SSF related compound	Reference
<b>Untreated poplar</b>	895	C–H deformation	Cellulose	[161,208]
	1023	C–O stretch	Cellulose, hemicellulose	[161,208]
	1118	Aromatic skeletal vibration and C–O stretch	Lignin	[161,208]
	1156	C–O–C vibrations	Cellulose, hemicellulose	[161,208]
	1230	Syringyl ring vibrations and C–O stretch of lignin and xylan	Lignin, xylan	[161]
	1263	C–O stretch in lignin and C–O linkage in guaiacyl aromatic methoxyl groups	Lignin	[161,208]
	1327	C <sub>1</sub> –O vibration in syringyl derivatives and C–H vibration in cellulose	Lignin, cellulose	[161,208]
	1368	C–H deformation	Cellulose, hemicellulose	[161,208]
	1418	C–H deformation	Lignin, cellulose, hemicellulose	[161,208]
	1456	C–H deformation	Lignin, cellulose, hemicellulose	[161,208]
	1504	Aromatic skeletal vibration	Lignin	[161,208]

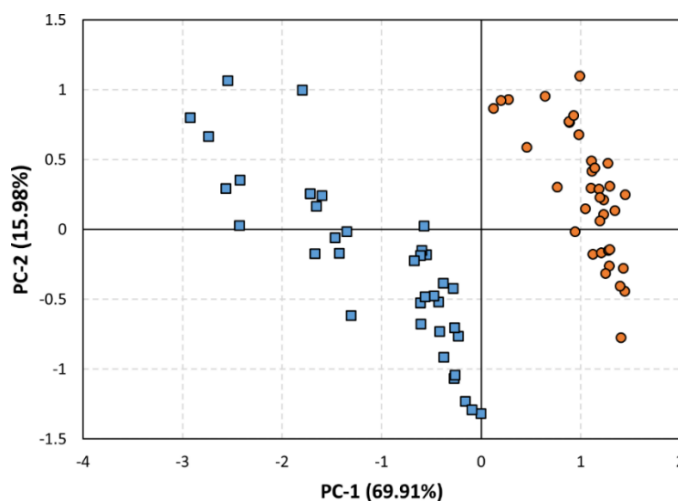
	1591	Aromatic skeletal vibration and C=O stretch	Lignin	[161,209]
	1654	Absorbed O–H and conjugated C=O in carbonyl groups	Lignin	[161]
	1731	Unconjugated C=O stretch	Xylan (hemicellulose)	[161,209]
	2883	C–H stretching	Lignin, cellulose, hemicellulose	[161,209]
	3364	O–H stretching	Cellulose, hemicellulose	[161,208]
<b>Pretreated poplar wood</b>	1644	C=O stretching in the amide I peptide	Enzymes produced by <i>P. chrysosporium</i> and the fungus itself	[206,207]
	1730	C=O stretching in the amide I peptide	Enzymes produced by <i>P. chrysosporium</i> and the fungus itself	[210]

The spectral interference of these compounds with lignin quantification was also confirmed by the principal component analysis carried out in the region of 1700–1180  $\text{cm}^{-1}$  on the SNV-pretreated ATR-FTIR spectra of both washed and non-washed pretreated. Since the fungal delignification starts progressively increasing after 2 weeks of pretreatment [196], the SSFs with a pretreatment time longer than 20 days (SSF23–SSF44 in **Table 4.1**), were used for the PCA analysis to obtain a good differentiation between the two sample groups (i.e., washed and non-washed). The first three principal components of the PCA analysis explained 93.64% of the variance (**Fig. 4.3**).

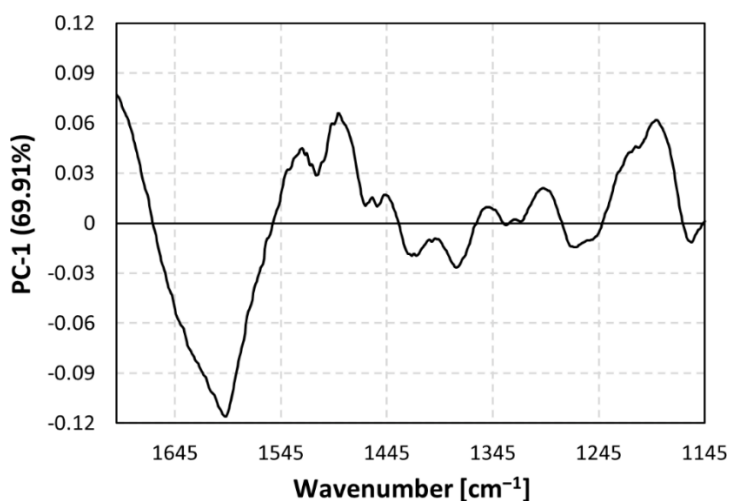


**Fig. 4.3** The individual variance ((▨) calibration; (▨) validation) and cumulative variance ((■) calibration; (●) validation) explained by principal component analysis

The first principal component (PC-1), which is responsible for 69.91% of the variance, clearly differentiates the washed and non-washed sample groups (**Fig. 4.4**). The washed samples have positive scores, while the non-washed SSFs own negative ones. In the loadings of PC-1, the most intense contribution is negative and found between 1700  $\text{cm}^{-1}$  and 1500  $\text{cm}^{-1}$  meaning that the non-washed samples own higher band intensities in this region compared to the washed samples (**Fig. 4.5**). The contribution at the spectral range of 1600–1700  $\text{cm}^{-1}$  (Amide I vibration, arises mainly from the C=O stretching) and at 1500–1600  $\text{cm}^{-1}$  (Amide II vibration, originates from C=N and C–N–H stretching) most probably appeared due to the enzymes secreted by *P. chrysosporium* as well as the microorganism itself both present in the non-washed [160,210–212]. This interpretation is supported by the ATR-FTIR spectra of the freeze-dried *P. chrysosporium* and its secreted manganese peroxidase enzyme, both absorbing at the 1500–1700  $\text{cm}^{-1}$  region (**Fig. 4.2**).



**Fig. 4.4** PCA scores of the first two principal components for (●) washed and (■) non-washed fungus-treated poplar wood samples



**Fig. 4.5** PCA loading plot of the first principal component

Furthermore, the removal of these compounds by washing was also confirmed by determining the protein content in the rinsing liquids and quantifying the amount of fungal biomass in the pretreated wood before and after the rinsing procedure of the 28-day fermentations (SSF42–SSF44). The protein concentration in the washing liquids of the four consecutive washing steps showed a decreasing trend, i.e. concentrations of  $9.23 \pm 0.14 \mu\text{g/mL}$ ,  $4.31 \pm 0.55 \mu\text{g/mL}$ ,  $1.28 \pm 0.13 \mu\text{g/mL}$  and  $1.02 \pm 0.11 \mu\text{g/mL}$  were obtained hereby confirming the removal of lignocellulolytic enzymes produced by *P. chrysosporium*. The rinsing procedure also sufficiently decreased the amount of fungal

biomass present in the pretreated wood. The initial  $4.49 \pm 0.09$  mg fungal biomass/g dry wood was reduced to  $1.10 \pm 0.01$  mg fungal biomass/g dry wood by the four-step rinsing procedure. However, one should consider that during solid-state fer[213], thereby making a complete fungal biomass removal unfeasible. Additionally, the washing liquids were also tested for lignin-derived phenolics. However, none of the seven common phenolic compounds, i.e., 3,4-dihydroxybenzaldehyde, 4-hydroxybenzoic acid, 4-hydroxybenzaldehyde, vanillic acid, syringic acid, vanillin, and syringaldehyde, was detected in the rinsing liquids by HPLC-UV analysis indicating the complete mineralization of lignin.

Considering that in the above-discussed spectral range of  $1500\text{--}1700\text{ cm}^{-1}$  also the important bands assigned to lignin can be found, including the aromatic skeletal vibration and C=O stretch at  $1596\text{ cm}^{-1}$ , and the C=C stretching in the aromatic structure at  $1505\text{ cm}^{-1}$  [159], the removal of the extracellular enzymes and the white-rot fungus by washing is essential for adequate lignin quantification.

#### **4.6.2 Estimation of lignin content from ATR-FTIR**

Until now, ATR-FTIR has been used only for the qualitative assessment of fungal lignin degradation [159,209] but not for the quantitative measurement of lignin in wood pretreated with fungi. Reliable lignin quantification with ATR-FTIR requires a sufficient set of samples with great variability in lignin content and the removal of interfering proteins, as discussed in Section 4.6.1.

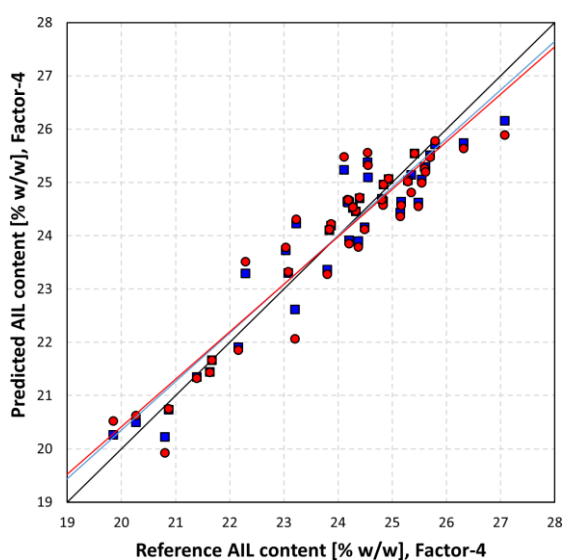
In this study, a set of 45 poplar wood samples with an acid-insoluble lignin content varying from 19.9% to 27.1% were used to build the partial least squares regression model for lignin calibration. These samples included the raw feedstock and 44 pretreated wood samples, each obtained in an individual fermentation (**Table 4.1**). PLSR models were constructed using leave-one-out cross-validation.

Most often, only certain wavenumbers of the FTIR spectra are strongly correlated to the target compound, i.e. to lignin in this study. Therefore the exclusion of the non-relevant wavenumbers can greatly improve the predictive ability of the model [214]. Therefore, first, the PLSR model was developed using the spectral range of  $1800\text{--}650\text{ cm}^{-1}$  since absorption bands at  $3364\text{ cm}^{-1}$  (O–H stretching) and  $2883\text{ cm}^{-1}$  (C–H stretching) have strong contributions from cellulose and hemicellulose [215]. By constructing our PLSR model in this range, an  $R_{CV}^2$  of 0.80 and an  $RMSE_{CV} = 0.75\%$  were obtained for cross-validation with 5 PLSR factors.

The model was further improved by selecting the spectral range of  $1700\text{--}1145\text{ cm}^{-1}$ , i.e., the wavenumbers which provide the most information about lignin and contain the least carbohydrate-dominating bands (**Table 4.2**). Using this spectral range, the

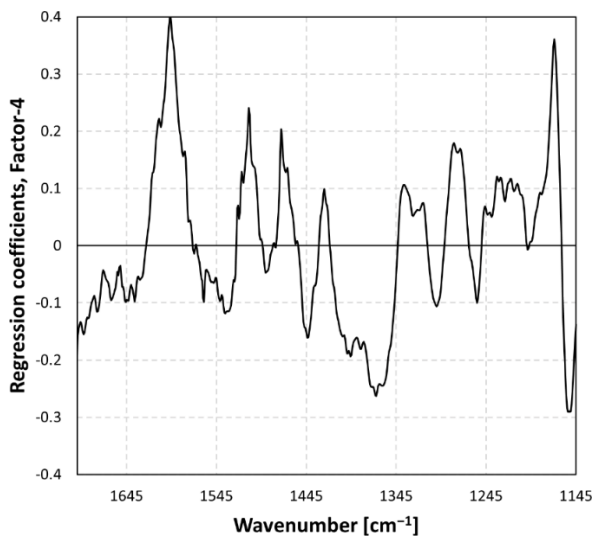
obtained PLSR model required a lower number of PLSR factors (4) while it had a slightly higher  $R_{CV}^2$  value (0.81) and a decreased error ( $RMSE_{CV} = 0.73\%$ ). To further improve the predictive ability of the PLSR model, standard normal variate normalisation was applied at this spectral range before PLSR modelling.

The SNV normalisation improved the PLSR model in comparison with the utilization of raw spectra, which was shown by a higher  $R_{CV}^2$  of 0.87 ( $R_C^2 = 0.91$  for calibration) and a lower  $RMSE_{CV}$  of 0.60% ( $RMSE_C = 0.49\%$ ) with the same number of PLSR factors (4) (Fig. 4.6). These high  $R^2$  values and low root mean square errors indicate a good prediction of lignin content considering the high variability of the heterogeneous solid-state fermentation, the varying fermentation conditions and the complexity of the reference NREL method directly affecting the prediction results.



**Fig. 4.6** The predicted vs. reference acid-insoluble lignin (AIL) values of (■) calibration and (●) validation

The interpretation of the weighted regression coefficients of PLS factor-4 revealed that the prediction of acid-insoluble lignin content is positively correlated with the peak intensities at  $1591\text{ cm}^{-1}$  (aromatic skeletal vibration and C=O stretch),  $1504\text{ cm}^{-1}$  (aromatic skeletal vibration),  $1456\text{ cm}^{-1}$  (aromatic C–H deformation),  $1418\text{ cm}^{-1}$  (C–H deformation),  $1327\text{ cm}^{-1}$  (C<sub>1</sub>–O vibration in syringyl derivatives and C–H vibration in cellulose),  $1263\text{ cm}^{-1}$  (C–O stretch in lignin and C–O linkage in guaiacyl aromatic methoxyl groups),  $1230\text{ cm}^{-1}$  (syringyl ring vibration, C–O stretch in lignin) [159,161,208] (Fig. 4.7).



**Fig. 4.7** Regression coefficients of PLSR factor-4 for acid-insoluble lignin determination

In this study, ATR-FTIR spectroscopy was proven to be suitable for predicting AIL content in wood pretreated with white-rot fungi. A previous study using FTIR-KBr in transmission mode obtained a comparably strong correlation ( $R_{CV}^2$  of 0.91), and low error ( $RMSE_{CV} = 0.71\%$ ) while applying a higher number of PLSR factors [159]. In comparison, our proposed ATR-FTIR method does not require the preparation of a KBr pellet and therefore is an easy and high-throughput alternative to the time-consuming and exhaustive two-step hydrolysis-based AIL determination in fungus-treated wood.

#### 4.7 Conclusions

In this study, ATR-FTIR combined with PLSR allowed the reliable prediction of acid-insoluble lignin content in poplar wood pretreated by *P. chrysosporium* under different fermentation conditions (medium, cultivation environment and pretreatment time). The PLSR model was established using the spectral range of 1700–1145  $\text{cm}^{-1}$  and had an  $R_{CV}^2$  of 0.87 and an error ( $RMSE_{CV}$ ) of less than 1%. Compared to the conventional acid-insoluble lignin determination (> 3 h), the required sample size, sample preparation and time of lignin analysis were substantially reduced since only milling was additionally required before the spectrum acquisition with ATR-FTIR (< 10 min). However, it is important to note that when applying this method to a novel lignocellulosic substrate with a different composition, it is necessary to obtain specific reference values for the PLSR modelling that are tailored to that particular substrate. The present work contributes to the faster development of the wood-based bioeconomy.



## **Chapter 5. Follow-up of solid-state fungal wood pretreatment by a novel near-infrared spectroscopy-based lignin calibration model**

---

The research work was performed in collaboration with professor dr. ir. Szilveszter Gergely and ir. János Slezsák from Budapest University of Technology and Economics and was redrafted from the manuscript, which is published in the Journal of Microbiological Methods.

N. Wittner, S. Gergely, J. Slezsák, W. Broos, S.E. Vlaeminck, I. Cornet, Follow-up of solid-state fungal wood pretreatment by a novel near-infrared spectroscopy-based lignin calibration model, *J Microbiol Methods*. 208 (2023) 106725.

<https://doi.org/10.1016/J.MIMET.2023.106725>

**Abstract**

Lignin removal plays a crucial role in the efficient bioconversion of lignocellulose to fermentable sugars. As a delignification process, fungal pretreatment has gained great interest due to its environmental friendliness and low energy consumption. In our previous study, a positive linear correlation between acid-insoluble lignin degradation and the achievable enzymatic saccharification yield has been found, hereby highlighting the importance of the close follow-up of lignin degradation during the solid-state fungal pretreatment process.

However, the standard quantification of lignin, which relies on the two-step acid hydrolysis of the biomass, is highly laborious and time-consuming. Vibrational spectroscopy has been proven as a fast and easy alternative; however, it has not been extensively researched on lignocellulose subjected to solid-state fungal pretreatment. Therefore, the present study examined the suitability of near-infrared (NIR) spectroscopy for the rapid and easy assessment of lignin content in poplar wood pretreated with *Phanerochaete chrysosporium*. Furthermore, the predictive power of the obtained calibration model and the recently published Attenuated Total Reflection Fourier Transform Infrared spectroscopy-based model were compared for the first time using the same fungus-treated wood data set.

Partial least squares regression was used to correlate the NIR spectra to the acid-insoluble lignin contents (19.9%–27.1%) of pretreated wood. After normalisation and second derivation, a PLSR model with a good coefficient of determination ( $R_{CV}^2 = 0.89$ ) and a low root mean square error ( $RMSE_{CV} = 0.55\%$ ) were obtained despite the heterogeneous nature of the fungal solid-state fermentation. The performance of this PLSR model was comparably good to the one obtained by ATR-FTIR ( $R_{CV}^2 = 0.87$ ) while it required more extensive spectral pre-processing. In conclusion, both methods will be highly useful for the high-throughput and user-friendly monitoring of lignin degradation in a solid-state fungal pretreatment-based biorefinery concept.

## 5.1 Introduction

Lignocellulosic biomass derived from plant cell walls is one of the most promising renewable feedstocks for the production of biofuels and biochemicals. However, the genuine recalcitrance of lignocellulose and, consequently, the need to disrupt the cell wall structure to facilitate access to cellulose and hemicellulose leads to an expensive and challenging conversion process. The presence of lignin in the biomass largely hinders the conversion of carbohydrates to fermentable sugars, both by acting as a physical barrier and binding non-productively to cellulase enzymes during enzymatic saccharification [216,217]. Pretreatment is a crucial step in improving the efficiency of enzymatic saccharification by removing lignin and reducing the recalcitrance of lignocellulose. Many pretreatment techniques, including alkali, sulfite, organosolv, ionic liquids, deep eutectic solvents, and fungal pretreatment have been evaluated to decrease the lignin content of the biomass prior to enzymatic saccharification. Fungal pretreatment, which mainly uses white-rot fungi for the degradation of lignin, has been widely investigated due to its advantages, such as environmental friendliness, low chemical addition, and lack of the production of inhibiting by-products [49]. Sufficient delignification during fungal pretreatment was proven to greatly improve the conversion of carbohydrates into fermentable sugars. Moreover, studies reported a positive linear correlation between lignin degradation and the obtained enzymatic saccharification yield, highlighting the significance of delignification and its monitoring during the fungal pretreatment process [18,196].

The most widely used method for quantifying lignin in lignocellulose is based on the two-step acid hydrolysis of the biomass (NREL) [135]. However, this method suffers from the disadvantages of the highly laborious, time-consuming (> 3 h) and destructive procedure and the relatively large sample size (300 mg). These disadvantages can be effectively circumvented by techniques based on infrared spectroscopy. Recently, the study of Wittner et al. demonstrated that Attenuated Total Reflection Fourier Transform Infrared (ATR-FTIR) spectroscopy in the mid-infrared (MIR) region, coupled with partial least squares regression (PLSR) has a high potential to be a fast and accurate analytical tool for predicting lignin content in fungus-treated poplar wood [198]. Fackler et al. used both Fourier Transform MIR spectroscopy in transmission mode and Fourier Transform near-infrared (FT-NIR) reflectance spectroscopy to determine lignin content in beech wood before and after fungal decay [159]. In their study, the fungal decay of wood was performed in Petri dishes by placing the inoculated beech veneers in water agar and incubating them for up to 10 weeks. However, their application was not aimed at fungal pretreatment and delignification, as in our study. On the contrary, mainly an increase in

lignin content was observed, showing that cellulose and hemicellulose compounds were consumed instead. Moreover, NIR spectroscopy has not yet been used for lignin calibration using fungus-treated wood samples obtained by solid-state fermentation, i.e. in an industry-relevant fungal pretreatment environment [76,218].

Additionally, the predictive performances of the above-mentioned NIR and ATR-FTIR spectroscopy-based calibration models have not yet been compared based on the same fungus-treated sample set.

Therefore, this study has aimed to achieve the following main research goals. (1) Developing a fast and easy NIR spectroscopy-based lignin determination method using fungus-treated wood samples obtained at optimised solid-state fermentation conditions, hereby opening a new door to the practical implementation of the NIR spectroscopy-based lignin quantification. (2) Investigating the effect of the presence of lignin-degrading enzymes and the fungus itself on the NIR spectra by comparing washed and non-washed pretreated wood samples. (3) Evaluating the use of different spectral pre-processing methods to obtain a PLSR model with a high coefficient of determination and low error for reliable lignin prediction. (4) Comparing the predictive power of the NIR and ATR-FTIR spectroscopy-based calibration models using the same fungus-treated samples to provide important information regarding the right choice of IR instrumentation, spectral data processing and modelling.

## **5.2 Materials and Methods**

### **5.2.1 Poplar wood substrate and white-rot fungi**

Poplar wood sawdust was obtained from Sawmill Caluwaerts Willy (Holsbeek, BE). Sieve analysis was used to determine the particle size distribution of the wood particles. 86.1% w/w of the poplar wood pellets were collected between the 2 mm and 0.075 mm screens. The white-rot fungus *Phanerochaete chrysosporium* MUCL 19343 was used for the solid-state fungal pretreatment studies. A spore suspension of  $5 \cdot 10^6$  spores/mL was freshly prepared in distilled water from 5 days old cultures grown on potato dextrose agar plates at 39°C.

### **5.2.2 Solid-state fungal pretreatment**

In order to obtain fungus-treated wood samples with a sufficient range of variability in AIL content for lignin calibration, the solid-state fermentation experiments were carried out at different fermentation conditions as described in the study of Wittner et al. [198]. In brief, the fermentations were different in the applied substrate sterilisation (none or autoclaving at 121°C for 20 min), duration of fermentation (up to 28 days), medium composition (complex or simple) and fermentation set-up (rolling bottles or trays).

The complex medium was composed of 3 g/L NaNO<sub>3</sub>, 20 g/L glucose, 0.5 g/L KCl, 0.5 g/L MgSO<sub>4</sub>·7H<sub>2</sub>O, 0.5 g/L FeSO<sub>4</sub>·7H<sub>2</sub>O, 1 g/L KH<sub>2</sub>PO<sub>4</sub>, 0.34 g/L veratryl alcohol, 0.1% v/v Tween 80, 3.69 mM CuSO<sub>4</sub> and 1.41 mM MnSO<sub>4</sub> [171,196]. The simplified media consisted of 3.69 mM CuSO<sub>4</sub>, 1.41 mM MnSO<sub>4</sub> with or without 20 g/L glucose and/or 3 g/L NaNO<sub>3</sub>. The Schott bottles (100 mL) contained 3.67 g dry weight (DW) poplar wood, 2 mL sterile media, 3.7 mL spore suspension (5·10<sup>6</sup> spores/g DW wood) and distilled water, creating a moisture content of 75% w/w on a wet basis. The media and the poplar wood were sterilised separately by autoclavation at 121°C for 20 min. The SSF bottles were rolled on a bottle roller (88881004 Bottle/Tube Roller, Thermo Scientific™) at 4 rpm and incubated (TC 255 S, Tintometer Inc.) at 37°C for up to 4 weeks. Tray fermentations of non-sterilised poplar wood were carried out at 37°C for 4 weeks in 500 mL glass dishes containing 2 mL medium, 2.8 g DW untreated non-sterilised wood, 0.9 g DW pretreated wood as inoculum and distilled water resulting in the moisture content of 75% [198]. At the end of the fermentation, the pretreated wood was analysed for its acid-insoluble lignin (AIL) content by the conventional two-step acid hydrolysis [181] as a reference method and by near-infrared spectroscopy. **Table 4.1** shows the applied medium conditions with the corresponding AIL content for each pretreated wood sample (SSF1–SSF44). SSF37 was not included in the NIR spectroscopy-based PLSR model due to the lack of sufficient sample size for NIR analysis.

### 5.2.3 Analytical methods

#### 5.2.3.1 Removal of water-soluble substances

Prior to the lignin determination, the pretreated wood samples were thoroughly washed to remove the lignocellulolytic enzymes and partially the fungus itself. The washing was carried out as described in the study by Wittner et al. [198]. Briefly, the biomass was shaken with 50 mM acetate buffer (pH 4.5) at 400 rpm for 20 min, applying a solid-to-liquid ratio of 1:80, followed by centrifugation (Sigma 3-16KL) for 15 min at 4500 rpm and 4°C. After removing the supernatant, the washing was repeated once with acetate buffer and twice with distilled water to remove the traces of acetic acid. The rinsed solid was freeze-dried (ALPHA 1-2 Ldplus, Martin Christ Gefriertrocknungsanlagen GmbH) to a constant weight and used for lignin and infrared analysis.

#### 5.2.3.2 Lignin quantification

The poplar wood samples, before and after fungal pretreatments, were analysed for their acid-insoluble content by the standard NREL protocol (NREL/TP-510-42618) [181]. Briefly, the AIL content of the samples was measured gravimetrically after a two-step

acid hydrolysis with sulfuric acid. Measurements were carried out either once or in duplicate, as shown in **Table 4.1**. The average standard laboratory error, determined from the duplicate measurements, was calculated to be 0.32%.

### **5.2.3.3 Milling**

Prior to near-infrared (NIR) analysis, the washed and freeze-dried (Alpha 1-2 Ldplus, Martin Christ Gefriertrocknungsanlagen GmbH) wood samples were ground using the method of Cornet et al., with slight modifications [160]. The wood samples (200 mg) were placed in a grinding jar (25 mL) containing four 10 mm and one 15 mm stainless steel grinding balls. The jar was cooled down by immersion in liquid nitrogen for 30 seconds, and ball milling was carried out in a mixer mill (MM 200, Retsch GmbH) for 4 min at 25 Hz.

### **5.2.3.4 NIR analysis**

The milled, freeze-dried wood samples were placed in a powder mini sample holder having a quartz window and an inner ring with a diameter of 6 mm (Foss NIRSystems Inc.) and closed with a disposable sample cup lid (Foss NIRSystems Inc.). The samples were measured in diffuse reflectance mode using a NIR Systems 6500 spectrophotometer (Foss NIRSystems Inc.) equipped with an internal ceramic reference and four PbS detectors. Spectral data were collected between 1100 and 2498 nm at a data interval of 2 nm with 32 scans. Spectra were recorded using Vision 3.20 software (Foss NIRSystems, Inc.).

### **5.2.3.5 Spectral data processing and multivariate analysis**

All NIR spectra were processed using The Unscrambler<sup>®</sup> X 10.4 (CAMO Software AS.) and Microsoft<sup>®</sup> Excel<sup>®</sup> 2019 (Microsoft Corp.) software. Standard normal variate (SNV) pre-processing was applied to reduce baseline shift [203]. After SNV, principal component analysis (PCA) was carried out on the washed and non-washed wood samples for dimensionality reduction and to identify outlier samples [204]. Since the fungal delignification starts progressively increasing after 14 days of SSF [196], the fermentations carried out longer than 20 days (SSF23–SSF44 in **Table 4.1**), were used for the PCA analysis to obtain a good differentiation between the two sample groups (i.e., washed and non-washed). Partial least squares regression models were developed using the acid-insoluble lignin content of the washed SSF samples as reference data (**Table 4.1**). PLSR models were built using different spectral pretreatment methods, including the SNV and the second derivative methods of gap-segment (G-S) (also known as Norris-Williams derivative) and Savitzky-Golay (SG) derivative [151]. The gap-segment algorithm generally performs first a smoothing under a given segment size,

followed by a derivative of a given order under a given gap size [219]. In this study, the use of different segment sizes (1–15 points) at the constant gap size of 1 point was evaluated. The SG algorithm fits polynomials to the spectrum within windows around each point in the spectrum, and these polynomials are then used to smooth the obtained data and subsequently differentiate them [220]. A quadratic polynomial and smoothing windows varying from 3 to 15 points were evaluated in this study. Polynomial smoothing involves fitting an odd number of sequential spectral data points to a polynomial and calculating the centre point of the resulting polynomial [221]. When using a window that is too wide, peaks and troughs become rounded off, while a narrow window amplifies the noise present in the original spectrum through the derivative calculation [222]. However, Shenk and Westerhaus suggest that the best mathematical treatment can only be attained by trial and error [223].

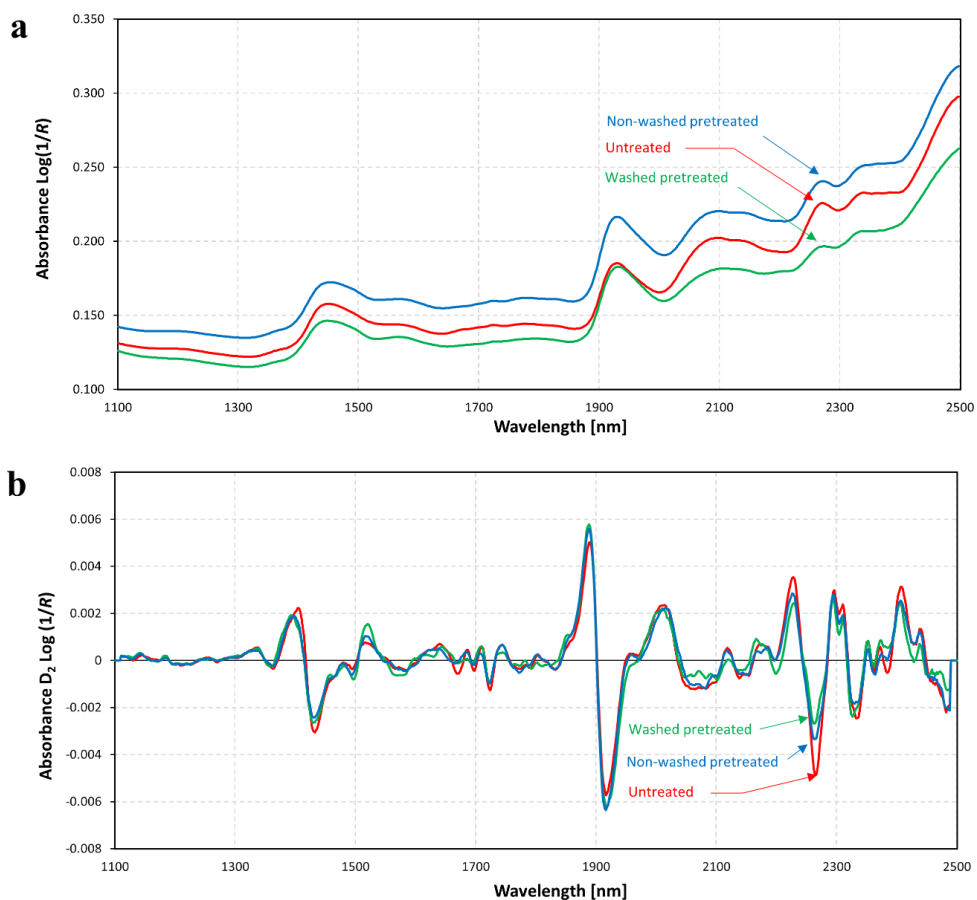
PLSR models were validated using a leave-one-out (i.e. full) cross-validation (CV) to find the best-fitting model that has an optimal combination of the highest coefficient of determination ( $R_{CV}^2$ ) and the lowest root mean square error of cross-validation ( $RMSE_{CV}$ ) with the lowest number of PLSR terms used.

### 5.3 Results and Discussion

#### 5.3.1 NIR spectra of fungus-treated wood

The NIR spectra of the untreated and pretreated wood with or without washing were compared. The corresponding raw and standard normal variate (SNV) treated second derivative NIR spectra are presented in **Fig. 5.1**. SNV is applied to reduce baseline shift caused by light scattering and variable spectral path [203]. Second derivative spectra have a negative peak that matches exactly the absorption maximum (positive peak) of an absorbance band in  $\log 1/R$ , and these negative peaks are used to detect chemical changes among samples. Second derivative spectra provide more resolved absorption bands and hereby easier band assignments [224] and, therefore, were used in this study for the detailed investigation of spectral changes.

In the second derivative of SNV-treated spectra, the main changes in the peak intensities after fungal treatment were observed at the lignin-related spectral regions of 1440 nm (1<sup>st</sup> overtone of C–H stretch and C–H deformation), 1670 nm (1<sup>st</sup> overtone of aromatic C–H stretch) and 2267 nm (O–H and C–O stretch in lignin), and also at the carbohydrate-dominated regions of 2080 nm (O–H stretch and C–H deformation of semi-crystalline or crystalline regions in cellulose) and 2332 nm (C–H stretch and C–H deformation) [225,226].



**Fig. 5.1** Raw (a) and Savitzky-Golay second derivative ( $D_2$ , 11 smoothing points) of SNV-treated NIR spectra (b) of (—) untreated poplar wood and pretreated poplar wood (—) with and (—) without washing

The intensity of the lignin-associated peaks decreased after fungal pretreatment, confirming the degradation of lignin moieties. However, the non-washed SSF samples showed a smaller decrease in the lignin-related band intensities than the washed pretreated samples, indicating a spectral interference probably caused by the ligninolytic enzymes and the white-rot fungus, both present in the non-washed sample. The removal of these interfering compounds through washing was confirmed by Bradford protein assay and fungal biomass measurement in the work of Wittner et al. [198]. In that study, the same sample set as the one used in this research was measured by ATR-FTIR and principal component analysis was applied to the SNV-treated spectral data [198]. The PCA analysis provided a distinct sample group for the washed and non-washed samples. This good differentiation was obtained due to the increased band intensities measured in the non-washed samples in the spectral range of 1700–1500



$\text{cm}^{-1}$ , assigned to Amide I and Amide II vibrations originating from the lignin-degrading enzymes and the fungus itself. In comparison, in the NIR spectra, the main influence of the washing was observed at 2267 nm, i.e. at the spectral region, which can also be assigned to proteins besides lignin [227,228]. However, unlike in the work of Wittner et al., in this study, no good differentiation could be seen between these sample groups (data not shown). This can be explained by the increased surface sensitivity and lower optical penetration depth (up to a few micrometres) of ATR-FTIR spectroscopy compared to NIR reflectance spectroscopy (up to a few millimetres) [143,226,229]. Therefore, ATR-FTIR might be more sensitive to the presence of the ligninolytic enzymes, which cannot penetrate the wood cell wall due to their large size and therefore are deposited on the cell wall surface [68].

### 5.3.2 Development of PLSR models for lignin quantification

PLSR was performed to correlate the near-infrared spectra to the acid-insoluble lignin content of 44 wood samples, including the raw feedstock and 43 pretreated wood samples, each obtained via an individual solid-state fermentation (**Table 4.1**). The acid-insoluble lignin contents of these samples ranged from 19.9% to 27.1%. The PLSR models were constructed using leave-one-out cross-validation. In comparison with the utilization of the raw spectra ( $R_{CV}^2 = 0.79$ ,  $RMSE_{CV} = 0.79\%$ ), SNV improved the PLSR model, which was shown by a higher  $R_{CV}^2$  of 0.82 and a lower  $RMSE_{CV}$  of 0.73% with the same number of PLSR factors (7) (**Table 5.1**). In comparison, a higher coefficient of determination ( $R_{CV}^2 = 0.87$ ) and a lower error ( $RMSE_{CV} = 0.60\%$ ) were obtained with ATR-FTIR using only 4 PLSR factors and SNV as a pre-processing technique [198].

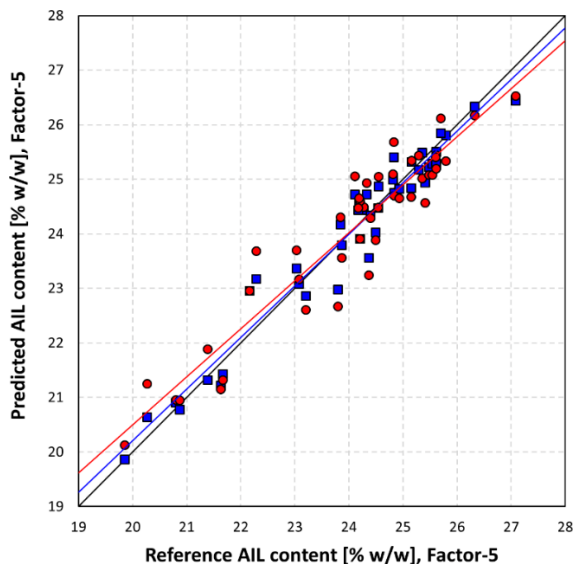
In order to further improve the NIR spectroscopy-based method, the two most common second derivative methods, i.e. the gap-segment (G-S) derivative and Savitzky-Golay (SG) derivative, were tested with or without combining with SNV [151]. Each method (i.e. G-S and SG derivative) requires some trade-off between the amount of sharpening and the creation of artefacts and usually involves some smoothing of the spectra [230]. The second derivative helps resolve the broad, overlapping bands and peak shoulders and accentuates low-intensity peaks in the NIR region. By using a second derivation, the predictive ability of the PLSR model was efficiently improved. Furthermore, the subsequent use of SNV and second derivation resulted in the best-performing models (**Table 5.1**). In the case of the G-S method, the segment size influenced the predictive performance of the model. The optimum segment size was 3 points (PLSR19 in **Table 5.1**), corresponding to a high determination coefficient of 0.89 and a low  $RMSE_{CV}$  value of 0.56% using 5 PLSR factors.

**Table 5.1** Results of NIR spectroscopy-based PLSR models for lignin quantification

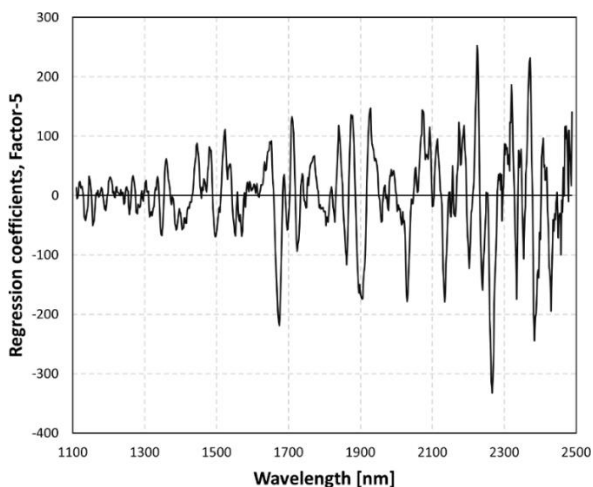
#PLSR model	Treatment	NF <sup>a</sup>	$R_C^2$ <sup>b</sup>	$RMSE_C$ <sup>c</sup> [%]	$R_{CV}^2$ <sup>d</sup>	$RMSE_{CV}$ <sup>e</sup> [%]
PLSR1	raw spectra	7	0.88	0.58	0.79	0.79
PLSR2	SNV	7	0.91	0.51	0.82	0.73
PLSR3	G1-S1	7	1.00	0.08	0.52	1.18
PLSR4	G1-S3	6	0.96	0.33	0.88	0.60
PLSR5	G1-S5	6	0.94	0.40	0.88	0.60
PLSR6	G1-S7	6	0.93	0.43	0.86	0.63
PLSR7	G1-S9	6	0.93	0.45	0.86	0.64
PLSR8	G1-S11	6	0.92	0.48	0.85	0.67
PLSR9	G1-S13	6	0.91	0.51	0.84	0.68
PLSR10	G1-S15	6	0.90	0.52	0.84	0.68
PLSR11	SG3	4	0.96	0.34	0.19	1.53
PLSR12	SG5	7	1.00	0.08	0.63	1.03
PLSR13	SG7	6	0.98	0.26	0.82	0.72
PLSR14	SG9	6	0.97	0.31	0.87	0.61
PLSR15	SG11	6	0.96	0.34	0.88	0.59
PLSR16	SG13	7	0.88	0.58	0.79	0.79
PLSR17	SG15	6	0.94	0.40	0.87	0.60
PLSR18	SNV + G1-S1	4	0.97	0.29	0.50	1.21
PLSR19	SNV + G1-S3	5	0.96	0.35	0.89	0.56
PLSR20	SNV + G1-S5	5	0.93	0.43	0.89	0.58
PLSR21	SNV + G1-S7	5	0.92	0.47	0.87	0.61
PLSR22	SNV + GS-S9	5	0.91	0.50	0.86	0.63
PLSR23	SNV + GS-S11	5	0.90	0.53	0.85	0.66
PLSR24	SNV + GS-S13	6	0.91	0.49	0.85	0.65
PLSR25	SNV + GS-S15	6	0.91	0.50	0.85	0.66
PLSR26	SNV + SG3	3	0.90	0.54	0.19	1.53
PLSR27	SNV + SG5	4	0.98	0.26	0.60	1.07
PLSR28	SNV + SG7	5	0.98	0.24	0.85	0.66
PLSR29	SNV + SG9	5	0.96	0.32	0.89	0.56
PLSR30*	SNV + SG11	5	0.95	0.37	0.89	0.55
PLSR31	SNV + SG13	5	0.94	0.41	0.89	0.56
PLSR32	SNV + SG15	5	0.93	0.43	0.88	0.58

\* Spectral pretreatment for which the standardised regression coefficients are shown (Fig. 5.3). <sup>a</sup> NF: Number of factors; <sup>b</sup>  $R_C^2$ : Coefficient of determination of calibration; <sup>c</sup>  $RMSE_C$ : Root mean square error of calibration; <sup>d</sup>  $R_{CV}^2$ : Coefficient of determination of cross-validation; <sup>e</sup>  $RMSE_{CV}$ : Root mean square error of cross-validation.

The utilization of SG second derivative provided similarly good results, i.e. an  $R_{CV}^2$  of 0.89 and an  $RMSE_{CV}$  of 0.55% using 5 factors and the optimal smoothing window of 11 points (PLSR30) (Fig. 5.2). The weighted regression coefficients corresponding to this PLSR model (PLSR30), with the highest coefficient obtained at the lignin-specific wavelength of 2267 nm (O–H and C–O stretching [226]), are presented in Fig. 5.3.



**Fig. 5.2** The predicted vs. reference acid-insoluble lignin (AIL) values of (■) calibration and (●) validation based PLSR30 model **Table 5.1**

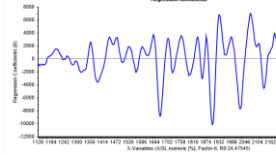
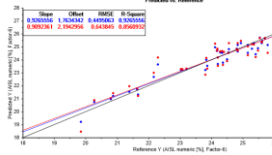
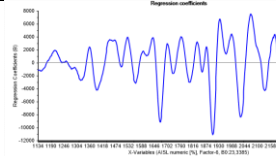
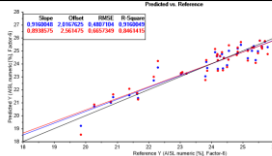
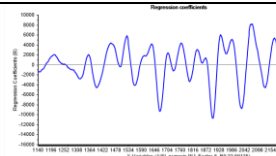
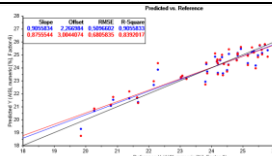
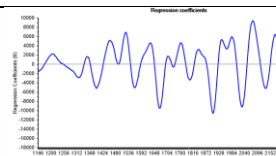
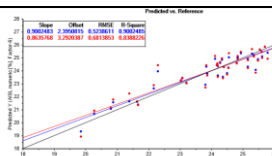
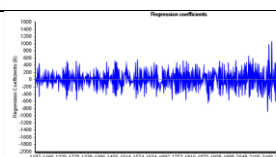
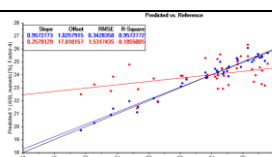
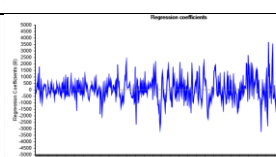
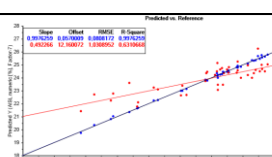
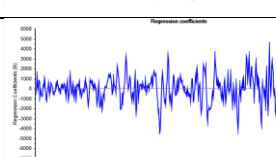
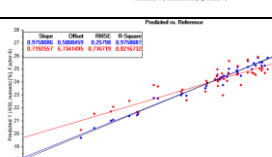
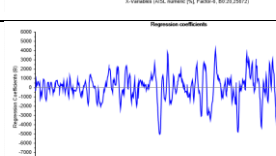
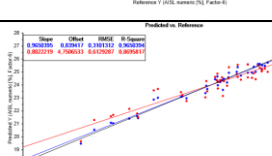

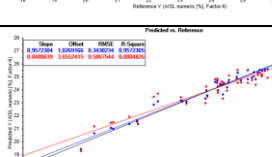


**Fig. 5.3** Regression coefficients of the PLSR30 model (**Table 5.1**) for acid-insoluble lignin determination

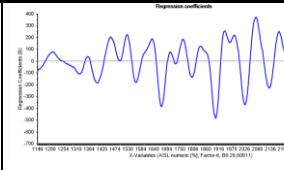
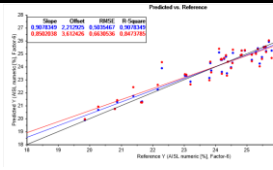
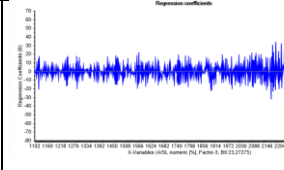
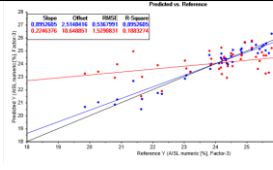
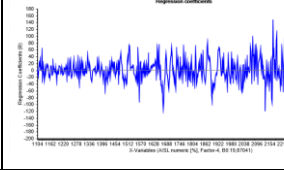
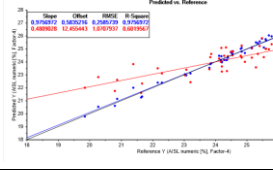
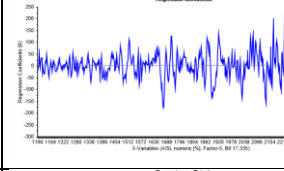
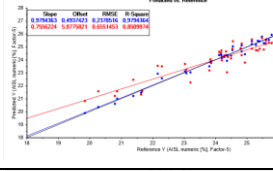
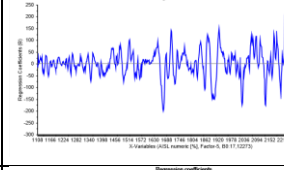
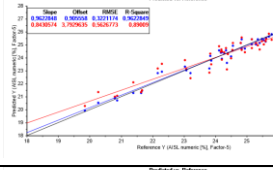
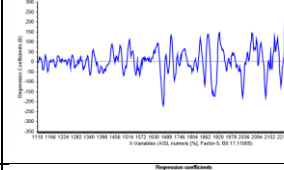
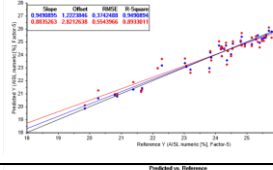
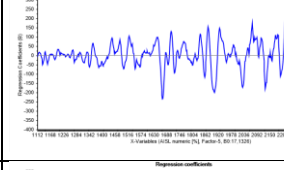
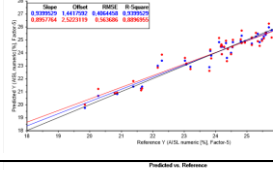
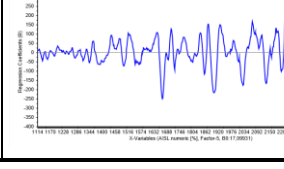
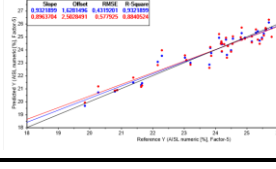
Changing the size of the smoothing window had no effect on the location (2267 nm) of the maximum regression coefficient except when using small smoothing windows, i.e. 1 point segment size with G-S method and less than 7 points smoothing window with SG method (**Table 5.2**).

**Table 5.2** Regression coefficients (line plots) and predicted vs reference data (scatter plots) of NIR spectroscopy-based PLSR models for lignin quantification

#PLSR model	Treatment	NF <sup>a</sup>	Regression coefficients	Predicted vs reference data
PLSR1	raw spectra	7		
PLSR2	SNV	7		
PLSR3	G1-S1	7		
PLSR4	G1-S3	6		
PLSR5	G1-S5	6		
PLSR6	G1-S7	6		

PLSR7	G1-S9	6		
PLSR8	G1-S11	6		
PLSR9	G1-S13	6		
PLSR10	G1-S15	6		
PLSR11	SG3	4		
PLSR12	SG5	7		
PLSR13	SG7	6		
PLSR14	SG9	6		
PLSR15	SG11	6		

PLSR16	SG13	7	<p>Regression coefficients (B)</p>	<p>Predicted vs Reference</p> <table border="1"> <thead> <tr> <th>Stat</th> <th>Value</th> </tr> </thead> <tbody> <tr> <td>Slope</td> <td>0.942883</td> </tr> <tr> <td>Offset</td> <td>1.267726</td> </tr> <tr> <td>RMSD</td> <td>0.310810</td> </tr> <tr> <td>R-Square</td> <td>0.942883</td> </tr> <tr> <td>RMSECV</td> <td>2.140723</td> </tr> <tr> <td>RMSEP</td> <td>0.301434</td> </tr> <tr> <td>RMSE</td> <td>0.310810</td> </tr> </tbody> </table>	Stat	Value	Slope	0.942883	Offset	1.267726	RMSD	0.310810	R-Square	0.942883	RMSECV	2.140723	RMSEP	0.301434	RMSE	0.310810
Stat	Value																			
Slope	0.942883																			
Offset	1.267726																			
RMSD	0.310810																			
R-Square	0.942883																			
RMSECV	2.140723																			
RMSEP	0.301434																			
RMSE	0.310810																			
PLSR17	SG15	6	<p>Regression coefficients (B)</p>	<p>Predicted vs Reference</p> <table border="1"> <thead> <tr> <th>Stat</th> <th>Value</th> </tr> </thead> <tbody> <tr> <td>Slope</td> <td>0.942883</td> </tr> <tr> <td>Offset</td> <td>1.267726</td> </tr> <tr> <td>RMSD</td> <td>0.310810</td> </tr> <tr> <td>R-Square</td> <td>0.942883</td> </tr> <tr> <td>RMSECV</td> <td>2.140723</td> </tr> <tr> <td>RMSEP</td> <td>0.301434</td> </tr> <tr> <td>RMSE</td> <td>0.310810</td> </tr> </tbody> </table>	Stat	Value	Slope	0.942883	Offset	1.267726	RMSD	0.310810	R-Square	0.942883	RMSECV	2.140723	RMSEP	0.301434	RMSE	0.310810
Stat	Value																			
Slope	0.942883																			
Offset	1.267726																			
RMSD	0.310810																			
R-Square	0.942883																			
RMSECV	2.140723																			
RMSEP	0.301434																			
RMSE	0.310810																			
PLSR18	SNV + G1-S1	4	<p>Regression coefficients (B)</p>	<p>Predicted vs Reference</p> <table border="1"> <thead> <tr> <th>Stat</th> <th>Value</th> </tr> </thead> <tbody> <tr> <td>Slope</td> <td>0.942883</td> </tr> <tr> <td>Offset</td> <td>1.267726</td> </tr> <tr> <td>RMSD</td> <td>0.310810</td> </tr> <tr> <td>R-Square</td> <td>0.942883</td> </tr> <tr> <td>RMSECV</td> <td>2.140723</td> </tr> <tr> <td>RMSEP</td> <td>0.301434</td> </tr> <tr> <td>RMSE</td> <td>0.310810</td> </tr> </tbody> </table>	Stat	Value	Slope	0.942883	Offset	1.267726	RMSD	0.310810	R-Square	0.942883	RMSECV	2.140723	RMSEP	0.301434	RMSE	0.310810
Stat	Value																			
Slope	0.942883																			
Offset	1.267726																			
RMSD	0.310810																			
R-Square	0.942883																			
RMSECV	2.140723																			
RMSEP	0.301434																			
RMSE	0.310810																			
PLSR19	SNV + G1-S3	5	<p>Regression coefficients (B)</p>	<p>Predicted vs Reference</p> <table border="1"> <thead> <tr> <th>Stat</th> <th>Value</th> </tr> </thead> <tbody> <tr> <td>Slope</td> <td>0.942883</td> </tr> <tr> <td>Offset</td> <td>1.267726</td> </tr> <tr> <td>RMSD</td> <td>0.310810</td> </tr> <tr> <td>R-Square</td> <td>0.942883</td> </tr> <tr> <td>RMSECV</td> <td>2.140723</td> </tr> <tr> <td>RMSEP</td> <td>0.301434</td> </tr> <tr> <td>RMSE</td> <td>0.310810</td> </tr> </tbody> </table>	Stat	Value	Slope	0.942883	Offset	1.267726	RMSD	0.310810	R-Square	0.942883	RMSECV	2.140723	RMSEP	0.301434	RMSE	0.310810
Stat	Value																			
Slope	0.942883																			
Offset	1.267726																			
RMSD	0.310810																			
R-Square	0.942883																			
RMSECV	2.140723																			
RMSEP	0.301434																			
RMSE	0.310810																			
PLSR20	SNV + G1-S5	5	<p>Regression coefficients (B)</p>	<p>Predicted vs Reference</p> <table border="1"> <thead> <tr> <th>Stat</th> <th>Value</th> </tr> </thead> <tbody> <tr> <td>Slope</td> <td>0.942883</td> </tr> <tr> <td>Offset</td> <td>1.267726</td> </tr> <tr> <td>RMSD</td> <td>0.310810</td> </tr> <tr> <td>R-Square</td> <td>0.942883</td> </tr> <tr> <td>RMSECV</td> <td>2.140723</td> </tr> <tr> <td>RMSEP</td> <td>0.301434</td> </tr> <tr> <td>RMSE</td> <td>0.310810</td> </tr> </tbody> </table>	Stat	Value	Slope	0.942883	Offset	1.267726	RMSD	0.310810	R-Square	0.942883	RMSECV	2.140723	RMSEP	0.301434	RMSE	0.310810
Stat	Value																			
Slope	0.942883																			
Offset	1.267726																			
RMSD	0.310810																			
R-Square	0.942883																			
RMSECV	2.140723																			
RMSEP	0.301434																			
RMSE	0.310810																			
PLSR21	SNV + G1-S7	5	<p>Regression coefficients (B)</p>	<p>Predicted vs Reference</p> <table border="1"> <thead> <tr> <th>Stat</th> <th>Value</th> </tr> </thead> <tbody> <tr> <td>Slope</td> <td>0.942883</td> </tr> <tr> <td>Offset</td> <td>1.267726</td> </tr> <tr> <td>RMSD</td> <td>0.310810</td> </tr> <tr> <td>R-Square</td> <td>0.942883</td> </tr> <tr> <td>RMSECV</td> <td>2.140723</td> </tr> <tr> <td>RMSEP</td> <td>0.301434</td> </tr> <tr> <td>RMSE</td> <td>0.310810</td> </tr> </tbody> </table>	Stat	Value	Slope	0.942883	Offset	1.267726	RMSD	0.310810	R-Square	0.942883	RMSECV	2.140723	RMSEP	0.301434	RMSE	0.310810
Stat	Value																			
Slope	0.942883																			
Offset	1.267726																			
RMSD	0.310810																			
R-Square	0.942883																			
RMSECV	2.140723																			
RMSEP	0.301434																			
RMSE	0.310810																			
PLSR22	SNV + GS-S9	5	<p>Regression coefficients (B)</p>	<p>Predicted vs Reference</p> <table border="1"> <thead> <tr> <th>Stat</th> <th>Value</th> </tr> </thead> <tbody> <tr> <td>Slope</td> <td>0.942883</td> </tr> <tr> <td>Offset</td> <td>1.267726</td> </tr> <tr> <td>RMSD</td> <td>0.310810</td> </tr> <tr> <td>R-Square</td> <td>0.942883</td> </tr> <tr> <td>RMSECV</td> <td>2.140723</td> </tr> <tr> <td>RMSEP</td> <td>0.301434</td> </tr> <tr> <td>RMSE</td> <td>0.310810</td> </tr> </tbody> </table>	Stat	Value	Slope	0.942883	Offset	1.267726	RMSD	0.310810	R-Square	0.942883	RMSECV	2.140723	RMSEP	0.301434	RMSE	0.310810
Stat	Value																			
Slope	0.942883																			
Offset	1.267726																			
RMSD	0.310810																			
R-Square	0.942883																			
RMSECV	2.140723																			
RMSEP	0.301434																			
RMSE	0.310810																			
PLSR23	SNV + GS-S11	5	<p>Regression coefficients (B)</p>	<p>Predicted vs Reference</p> <table border="1"> <thead> <tr> <th>Stat</th> <th>Value</th> </tr> </thead> <tbody> <tr> <td>Slope</td> <td>0.942883</td> </tr> <tr> <td>Offset</td> <td>1.267726</td> </tr> <tr> <td>RMSD</td> <td>0.310810</td> </tr> <tr> <td>R-Square</td> <td>0.942883</td> </tr> <tr> <td>RMSECV</td> <td>2.140723</td> </tr> <tr> <td>RMSEP</td> <td>0.301434</td> </tr> <tr> <td>RMSE</td> <td>0.310810</td> </tr> </tbody> </table>	Stat	Value	Slope	0.942883	Offset	1.267726	RMSD	0.310810	R-Square	0.942883	RMSECV	2.140723	RMSEP	0.301434	RMSE	0.310810
Stat	Value																			
Slope	0.942883																			
Offset	1.267726																			
RMSD	0.310810																			
R-Square	0.942883																			
RMSECV	2.140723																			
RMSEP	0.301434																			
RMSE	0.310810																			
PLSR24	SNV + GS-S13	6	<p>Regression coefficients (B)</p>	<p>Predicted vs Reference</p> <table border="1"> <thead> <tr> <th>Stat</th> <th>Value</th> </tr> </thead> <tbody> <tr> <td>Slope</td> <td>0.942883</td> </tr> <tr> <td>Offset</td> <td>1.267726</td> </tr> <tr> <td>RMSD</td> <td>0.310810</td> </tr> <tr> <td>R-Square</td> <td>0.942883</td> </tr> <tr> <td>RMSECV</td> <td>2.140723</td> </tr> <tr> <td>RMSEP</td> <td>0.301434</td> </tr> <tr> <td>RMSE</td> <td>0.310810</td> </tr> </tbody> </table>	Stat	Value	Slope	0.942883	Offset	1.267726	RMSD	0.310810	R-Square	0.942883	RMSECV	2.140723	RMSEP	0.301434	RMSE	0.310810
Stat	Value																			
Slope	0.942883																			
Offset	1.267726																			
RMSD	0.310810																			
R-Square	0.942883																			
RMSECV	2.140723																			
RMSEP	0.301434																			
RMSE	0.310810																			

PLSR25	SNV + GS-S15	6		
PLSR26	SNV + SG3	3		
PLSR27	SNV + SG5	4		
PLSR28	SNV + SG7	5		
PLSR29	SNV + SG9	5		
PLSR30*	SNV + SG11	5		
PLSR31	SNV + SG13	5		
PLSR32	SNV + SG15	5		

<sup>a</sup> NF: Number of factors

When the model performance of PLSR30 is compared to the ATR-FTIR spectroscopy-based method ( $R_{CV}^2 = 0.87$ ,  $RMSE_{CV} = 0.60\%$ , 4 PLSR factors [198]), PLSR30 provided a higher coefficient of determination ( $R_{CV}^2 = 0.89$ ) and a lower error ( $RMSE_{CV} = 0.55\%$ ), using 5 PLSR factors. However, NIR spectroscopy required more complex spectral pretreatment, i.e. the combination of SNV and second derivation instead of SNV alone, in order to achieve a coefficient of determination similar high to the ATR-FTIR method. In conclusion, both NIR spectroscopy and ATR-FTIR spectroscopy showed really good predictive abilities considering the heterogeneous nature of the fungal solid-state fermentation, the different fermentation conditions and the complication of the reference acid-hydrolysis-based method while both are fast, easy and non-destructive methods.

#### **5.4 Conclusions**

In this study, measuring samples with NIR combined with PLSR succeeded in providing a reliable prediction of acid-insoluble lignin content in poplar wood pretreated by *P. chrysosporium* during solid-state fermentation. High correlations ( $R_{CV}^2 = 0.89$ ) between predicted and measured values were obtained with a low error ( $RMSE_{CV} = 0.55\%$ ) using 5 PLSR components. The performance of this PLSR model was comparable to the one obtained by ATR-FTIR ( $R_{CV}^2 = 0.87$ ,  $RMSE_{CV} = 0.60\%$ , 4 PLSR factors), while it required the combined application of SNV and second derivation instead of SNV alone. In conclusion, both methods are highly suitable for the use as fast and easy lignin quantification in fungus-treated biomass in a wood-based biorefinery concept.



## **Chapter 6. Techno-economic evaluation of fungal pretreatment for sugar production from sterilised and non-sterilised wood**

---

This chapter was redrafted from the manuscript that is under review.

N. Wittner, K. Vasilakou, W. Broos, S.E. Vlaeminck, P. Nimmegeers, I. Cornet, Investigating the technical and economic potential of solid-state fungal pretreatment at non-sterile conditions for sugar production from poplar wood

### **Contribution by the authors**

This chapter is based on a collaboration with PhD student Konstantina Vasilakou from the Environmental Economics team (University of Antwerp) and her supervisor, Prof. dr. Philippe Nimmegeers (University of Antwerp).

Prof. dr. Philippe Nimmegeers conceived the project and the main conceptual ideas and supervised the work together with the project supervisors Prof. dr. Iris Cornet and Prof. dr. Siegfried Vlaeminck. I calculated the mass balances for the different processes based on my experimental data. PhD student Konstantina Vasilakou processed these data, performed the model simulations, and conducted the economic analysis. After interpreting these results together with Konstantina, I wrote this chapter, which will form the basis of a future publication with the above-mentioned research collaborators.

### **Abstract**

The production of sugar from lignocellulosic biomass is a critical process that serves as an intermediate for producing biofuels and high-value chemicals. It is, therefore important to understand and minimise the costs associated with the production of sugar from lignocellulosic biomass. This research investigates the economic feasibility of a biorefinery producing sugars at a commercial scale from poplar wood in a fungal pretreatment-based biorefinery. Two process scenarios were compared that differed in substrate sterilisation and inoculation strategy. Scenario I included feedstock sterilisation and inoculation with fungal mycelium, while Scenario II used a non-sterilised substrate inoculated with the pre-colonised feedstock.

Scenario II showed a 14.5% reduction in sugar production cost (€2.15/kg) compared to Scenario I. This cost reduction was mainly due to the 2.7 times lower utility costs in Scenario II as a result of the reduced sterilisation requirement leading to lower steam and cooling water consumption.

While the evaluation of non-sterilised wood pretreatment showed promising cost reductions, it is important to note that fungal pretreatment remained more expensive than conventional chemical and physicochemical methods due to the significant capital investment required as a result of long pretreatment time and low sugar yields.

## 6.1 Introduction

Lignocellulosic biomass is a promising feedstock for the production of biochemicals and biofuels. Among the various biomasses, poplar wood, a type of hardwood, is a promising feedstock due to its year-round availability for harvesting, rapid growth rate, and higher bulk density compared to herbaceous feedstocks, which makes transportation and storage more manageable [1,231]. Although lignocellulose-based biorefineries have several advantages and made significant technological advances over the past decade, their commercial success has remained limited due to high production costs and large capital investments [232]. The production of fermentable sugars from lignocellulosic biomass involves pretreatment and enzymatic hydrolysis. The pretreatment process is required to break down the recalcitrant structure of the cell wall and make the carbohydrate polymers cellulose and hemicellulose accessible to (hemi)cellulolytic enzymes. Various types of pretreatment, including chemical, physicochemical and biological pretreatment, have been used to enhance enzymatic hydrolysis. However, each pretreatment method has its own advantages and disadvantages, such as the high cost of chemicals, low efficiency, strict operating parameters and production of fermentation-inhibiting by-products. These factors contribute to the high cost of the pretreatment process and are barriers to commercialisation.

Fungal pretreatment is a biotechnological pretreatment technology that can be used as an alternative to conventional chemical/physicochemical pretreatment [40]. White-rot fungi are typically used for fungal pretreatment due to their ability to effectively mineralise lignin in lignocellulosic biomass under aerobic conditions. Fungal pretreatment is typically carried out in a solid-state fermentation with low water consumption, at atmospheric pressure, low temperature (25-37°C), without the use of chemicals that may require disposal or recovery, and without the production of inhibitors that reduce the need for washing and/or detoxification prior to enzymatic hydrolysis [5,76]. However, fungal pretreatment has some potential drawbacks compared to conventional pretreatment, including long reaction times (several weeks compared to hours), the need for feedstock sterilisation, non-selective delignification and lower sugar yields [10,77]. Fungal pretreatment is often considered a low-cost technology [87,164,232]. However, only a few studies investigated the techno-economic performance of a fungal pretreatment-based facility. The study by Baral and Shah on a corn stover to butanol biorefinery reported significantly higher capital investment and sugar production costs than for conventional methods [24]. This was partly due to the larger amount of feedstock required to produce the same amount of fermentable sugars and the need for larger pretreatment reactors in high quantity, to

which the long pretreatment time also contributes [24]. The work of Vasco-Correa and Shah on the production of fermentable sugars from various feedstocks in a fungal pretreatment-based facility reported 4-15 times higher sugar production costs than previously obtained with conventional chemical/physicochemical pretreatment. They identified the long pretreatment time, low sugar yields, low feedstock bulk density, and feedstock sterilisation requirements as the main bottlenecks of the fungal pretreatment process [10].

This research aimed to assess the economic and technological feasibility of producing fermentable sugars from poplar wood on a commercial scale in a fungal pretreatment-based biorefinery based on experimental data. Two different process scenarios aimed to be investigated. In Scenario I, sterilised poplar wood inoculated with fungal mycelium is used. Substrate sterilisation before fungal pretreatment is a common practice to prevent indigenous microbial communities from competing with the white-rot fungi [76,169,171] and is considered one of the major bottlenecks of the fungal pretreatment process [10]. Scenario II uses non-sterile feedstock requiring a different inoculation approach to achieve efficient fungal pretreatment. Instead of direct inoculation with mycelium, the non-sterilised wood is inoculated with a pre-colonised substrate. This inoculation strategy involves growing white-rot fungi on sterilised feedstock and using it as inoculum during the fungal pretreatment of non-sterilised lignocellulose [15,17]. Thus, the non-sterile scenario still requires sterilising a part of the feedstock for inoculum preparation but can greatly reduce the sterilisation requirement depending on the inoculum ratio used [15]. The impact of these two scenarios on the cost of sugar production in the fungal pretreatment plant is investigated in terms of capital and operating expenditure to support the transition to a wood-based bioeconomy.

## **6.2 Materials and Methods**

### **6.3 Techno-economic assessment**

#### **6.3.1 Process design and modelling**

The production of fermentable sugars from poplar wood was simulated in Aspen Plus® v.12.1 (Aspen Technology Inc.), based on the National Renewable Energy Laboratory (NREL) report on the biochemical conversion of lignocellulosic biomass to bioethanol [233]. Scenario I included feedstock sterilisation, inoculation with fungal mycelium and supplementation with M+G+N medium. Scenario II used non-sterilised wood as substrate, pre-colonised wood as inoculum and M+N supplemented medium. The ASPEN models for Scenarios I and II are shown in **Fig. S1-S2**. Both scenarios produce

135,000 tonnes of fermentable sugar per year to be comparable to the techno-economic study of Vasco-Correa and Shah [10].

### 6.3.2 Data sources

Feedstock properties, fungal pretreatment and enzymatic hydrolysis conditions, degradation of lignocellulosic components during pretreatment and enzymatic saccharification yields were based on the small-scale bottle and tray experiments described in this study (Chapter 3). Where additional data were required, recently published studies on the fungal pretreatment of lignocellulose were consulted, and the data sources were indicated in the text.

### 6.3.3 Process description

Poplar sawdust is assumed to be delivered ready for pretreatment with  $51.9 \pm 3.2\%$  dry matter content [234] and no storage is required. Details on the feedstock properties can be found in **Table 6.1**. When applied, the raw feedstock was transferred to the horizontal batch autoclaves for 20 min sterilisation with saturated steam at  $121^\circ\text{C}$  using a screw conveyor. No dry matter loss was observed during autoclavation, and the alteration in composition was insignificant (Section 2.3.1) [196].

**Table 6.1** Feedstock properties

	Parameter	Value	Unit	Data source
<b>Feedstock properties</b>	Bulk density (wet)	333	kg/m <sup>3</sup>	Sawmill Caluwaerts Willy
	Dry matter	51.9	w/w %	[234]
	Lignin	30.8	w/w %	
	Glucan	45.1	w/w %	
	Xylan <sup>a</sup>	17.1	w/w %	
	Arabinan	0.3	w/w %	Laboratory analysis
	Acetate	2.5	w/w %	(Chapter 2)
	Extractives <sup>b</sup>	3.5	w/w %	
	Ash	0.3	w/w %	
	Other	0.4	w/w %	

Feedstock composition is presented on a dry basis. <sup>a</sup>Xylan value also included mannan and galactan due to the coelution of the minor sugars mannose and galactose with xylose [196], <sup>b</sup> Determined by two-steps extraction with water and ethanol (NREL/TP-510-42619 [181])

After sterilisation, the feedstock was transferred from the autoclave to the solid-state fungal pretreatment unit, composed of packed bed reactors operating at 37°C for 28 days. This reactor type is recommended for solid-state fungal pretreatment because its static operation is advantageous for microorganisms sensitive to shear stress [76,129] and because it provides sterile conditions during the fungal pretreatment [10]. Similar to the study by Vasco and Shah [10], inoculation with mycelium suspension grown in yeast mould (YM) broth in an air-lift fermenter was assumed for the SSF of sterilised wood due to insufficient literature data on the large-scale production of white-rot fungi spores. Pre-colonised wood was prepared under the same conditions as SSF of sterilised wood and used to inoculate non-sterilised poplar wood. [ was used to manage the heat generated by the metabolism of the white-rot fungi and maintain the operating temperature during inoculum preparation and fungal pretreatment.

After fungal pretreatment, the pretreated feedstock is transferred to the stirred tank reactor, where the enzymatic hydrolysis takes place, based on the applied laboratory-scale conditions (Section 3.2.5.2) but without antibiotics. The sugar yields and enzymatic digestibility values were assumed to be identical to those obtained in laboratory-scale conditions (**Table 6.2**). The glucose and xylose yields are calculated relative to the theoretical yield from the raw feedstock [18,185]. In contrast, the enzymatic digestibility is calculated based on the amount of glucose and xylose released relative to the theoretical yield from the pretreated feedstock entering the enzymatic hydrolysis unit; thus, it does not take into account the carbohydrate consumption occurring during the pretreatment process. Detailed process conditions can be found in **Table 6.2** for both Scenarios.

**Table 6.2** Fungal pretreatment conditions, lignocellulose degradation and enzymatic digestibility in Scenario I and II

Parameter	Scenario I	Scenario II	Reference
<b>Mycelia preparation</b>			
Temperature [°C]		37	
Duration [days]		5	[235]
Yeast mould broth [g/L]		21	
Aeration rate [vvm]		0.40	[10]
Fungal biomass yield [g/L]		12	[236]
<b>Fungal pretreatment<sup>b</sup></b>			
Inoculum ratio			
Scenario I: [g fungal biomass/kg	1.5	1:3	[237] & Present study <sup>a</sup>
Scenario II: [untreated wood: pre-colonised wood]			
Aeriation rate [L/min]		3.2	[237]
Temperature [°C]		37	Present study <sup>a</sup>
Duration [days]		28	
Heat production [MJ/kg fungal biomass]		8.366	[238]
Medium/substrate [L/kg dry wood]		0.54	
Moisture content [kg/kg wet wood]		0.75	
CuSO <sub>4</sub> · 5H <sub>2</sub> O [g /kg dry wood]		0.50	Present study <sup>a</sup>
MnSO <sub>4</sub> · H <sub>2</sub> O [g /kg dry wood]		0.13	
NaNO <sub>3</sub> [g /kg dry wood]		1.63	
Glucose [g /kg dry wood]	10.90	-	
<b>Lignocellulose degradation<sup>c</sup></b>			
Glucan [kg /kg dry wood]	0.04	0.17	
Xylan [kg /kg dry wood]	0.27	0.21	Present study <sup>a</sup>
Lignin [kg /kg dry wood]	0.29	0.34	
Total solid [kg /kg dry wood]	0.18	0.26	
<b>Enzymatic digestibility</b>			
Glucose [%]	35.49	38.44	Present study <sup>a</sup>
Xylose [%]	33.14	33.00	
<b>Sugar yield</b>			
Glucose [%]	28.84	28.51	Present study <sup>a</sup>
Xylose [%]	27.28	24.49	

<sup>a</sup>Experimental conditions and results are based on the laboratory-scale bottle and tray SSF of this study (Section 3.2). <sup>b</sup>Pre-colonised wood was prepared according to the pretreatment conditions of Scenario I. <sup>c</sup>The degradation of lignocellulosic components is expressed as the ratio of the component degraded [kg] to the initial amount of that component [kg] present in the raw feedstock entering the fungal pretreatment unit.

### 6.3.4 Economic analysis

The main economic assumptions are shown in **Table 6.3**. Capital Expenditure (CAPEX) was determined based on the NREL report of Humbird et al. [233] and ASPEN Capital Cost Estimator. All costs were adjusted to the scale of the process. The values provided by the NREL report were used as the base case, while the new case was based on mass balances and energy requirements obtained from the modelling software (Aspen Plus®) using the following equation:

$$New\ cost = (Base\ cost) \cdot \left(\frac{New\ size}{Base\ size}\right)^n \quad (6.1)$$

The scaling exponent "n" was used to adjust the costs for each equipment type, ranging from 0.5 to 0.8, depending on the specific equipment used. The costs are adjusted to the analysis year of 2022 using the Chemical Engineering Plant Cost Indices [239], while installation factors for each equipment type are used to calculate the final equipment cost [233]. The Total Capital Investment (TCI or CAPEX) was calculated as the sum of three cost components: Fixed Capital Investment (FCI), working capital and land costs. The Fixed Capital Investment (FCI) is calculated as the sum of the Total Direct Cost (TDC) and Total Indirect Cost (TIC) based on the assumptions of the NREL report [233]. The TDC includes the total installed equipment cost and additional costs for warehouse, site development, piping and instrumentation. The TIC accounts for fringe benefits, burdens, construction insurance, field expenses, construction fees, project contingency, and other costs. The working capital cost was calculated as 5% of the fixed capital cost, while the land cost was set at 2% of FCI [233,240].

The OPEX is composed of the variable and the fixed operating costs. The variable operating cost includes the costs for raw materials and utilities. Biomass price is assumed to include all feed-handling costs until the biorefinery gate. When required, prices were updated to 2022 using the Producer Price Index [241]. The fixed operating cost is calculated as the sum of supervision, direct salary overhead, maintenance, property taxes and insurance, as summarized in **Table 6.3**. Annual EU wages were estimated at €32,511 in 2021 [242]. The total operating labour is estimated according to Sinnott and Towler's operator shift positions analysis [243]. The biorefinery is assumed to be located in Europe.

The levelized cost of sugars is calculated for both scenarios as follows:

$$C = \frac{CAPEX \cdot \delta + OPEX}{Q} \quad (6.2)$$

Where Q is the annual sugar (sum of glucose and xylose) production [kg/year] and  $\delta$  is the annuity factor.



The annuity factor is calculated as follows [244]:

$$\delta = \frac{d \cdot (1+d)^n}{(1+d)^n - 1} \quad (6.3)$$

Where  $d$  is the discount rate and  $n$  is the plant lifetime.

**Table 6.3** Main techno-economic assessment assumptions. (FCI: Fixed Capital Investment; ISBL: Inside the Battery Limits)

Parameter	Value	Reference
<b>Economic parameters</b>		
Plant lifetime (years)	30	Assumption
Year of analysis	2022	Assumption
Discount rate (%)	15	[245]
Annual operating hours (h)	8000	Assumption
Working capital	5% of FCI	[233]
Land cost	2% of FCI	[240]
Operator wages (EUR/y)	33511	[242]
Biomass cost (EUR/t)	98.27	Sawmill Caluwaerts Willy (Holsbeek, BE)
Enzyme cost (EUR/kg)	9.64	[246]
<b>Fixed operating costs</b>		
Supervision	25% of operating labour	[243]
Direct salary overhead	50% of operating labour and supervision	[243]
Maintenance	3% of ISBL	[233]
Property taxes and insurance	0.7% of FCI	[233]

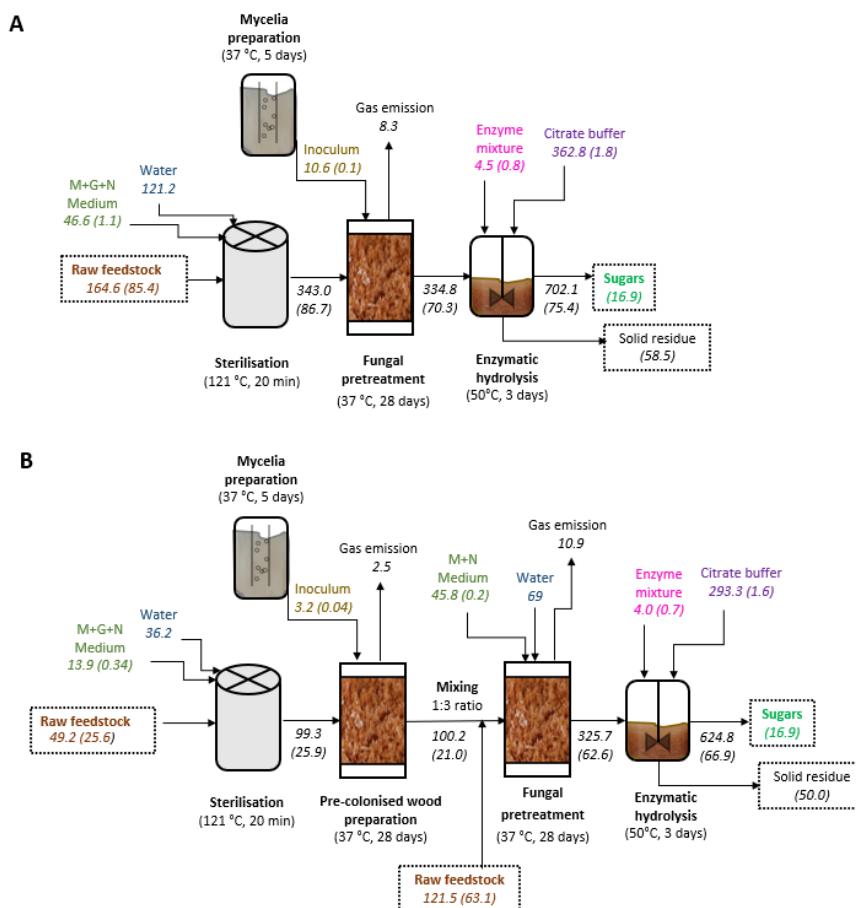
### 6.3.5 Economic global sensitivity analysis

The combined influence of various economic parameters (i.e. fixed capital investment (FCI), discount rate and costs for biomass, enzyme, utilities and chemicals) on the sugar production cost is evaluated by conducting a global sensitivity analysis for both scenarios. This consists of Monte Carlo simulations with 5000 model evaluations by sampling economic parameters simultaneously from a triangular distribution with  $\pm 15\%$  deviation from the base case values.

## 6.4 Results and discussion

### 6.4.1 Economic performance of process scenarios

The techno-economic analysis compared two process scenarios differing primarily in substrate sterilisation and subsequently in inoculation strategy and nutrient input. **Fig. 6.1** gives an overview of the two process scenarios and overall material balances and **Table 6.4** shows the energy requirements of the main units.



**Fig. 6.1** Process flow diagrams and mass balances are presented for a fungal pretreatment-based wood biorefinery producing 135,000 tonnes of sugar per year (16.9 tonnes per hour) in two scenarios: (A) Scenario I and (B) Scenario II. The feedstock is sterilised by autoclaving. Fungal mycelium is prepared in an air-lift fermenter. Solid-state fungal pretreatment and pre-colonised wood preparation are performed in a packed bed bioreactor. Wet mass flows are shown in italics, with the equivalent dry mass values in brackets. Please note that values may not add up exactly due to rounding. Aeration flows are not included in the graphs.

**Table 6.4** Energy requirements of the main units for Scenario I and II

	Duty [GJ/h]	
	Scenario I	Scenario II
<b>Steam</b>	<b>669</b>	<b>252.1</b>
Sterilization	609	182
Heaters	61	70
<b>Cooling water</b>	<b>-587.703</b>	<b>-179.3</b>
Mycelia preparation	-0.334	-0.100
Pre-colonised wood preparation		-0.639
Fungal pretreatment	-2.15	-1.87
Saccharification	-0.891	-0.865
Coolers	-584.33	-175.79
<b>Electricity (Pumps, Agitators, etc.)</b>	<b>7.27</b>	<b>7.12</b>

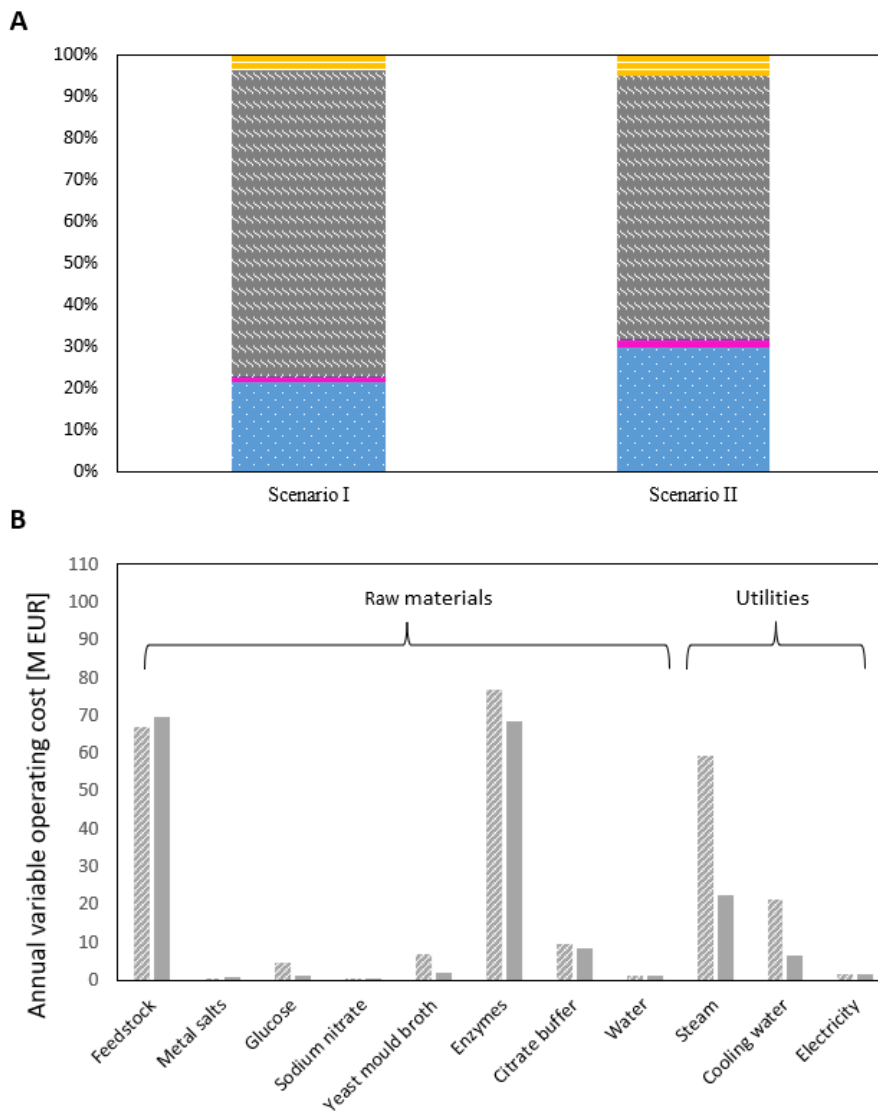
The analysis was carried out considering a sugar production scale of 135,000 tonnes per year (16.9 tonnes per hour). This production scale is capable of feeding a biorefinery producing approximately 76,500 m<sup>3</sup> of ethanol per year, assuming 90% and 80% of the theoretical conversion of glucose and xylose to ethanol, respectively [233]. The economic analysis resulted in a levelised sugar production cost of €2.51/kg in Scenario I, which was reduced by 14.5% (€2.15/kg) in Scenario II. The latter was approximately 17% lower than previously reported for the fungal pretreatment-based biorefinery of hardwood at the same sugar production scale [10]. However, it was still 7-13 times higher than estimated in wood biorefineries using conventional chemical and physicochemical pretreatment [247].

The annual sugar production costs were further broken down into capital expenditure (fixed capital, working capital and land costs) and operating expenditure (fixed and variable) in order to identify the main cost drivers and to explain the reduced production costs in Scenario II (**Fig. 6.2A**). The two scenarios showed a similar trend in terms of cost drivers, with some notable findings. In both scenarios, the largest cost contributor was the annual variable operating costs (**Fig. 6.2A**), with utilities, raw materials and enzymes being the main drivers of these costs (**Fig. 6.2B**). However, a 26.8% lower annual operating cost (€183 M) was obtained in Scenario II, compared to Scenario I. This is mainly due to the 2.7 times lower (€30 M) annual utility costs as a result of the reduced sterilisation requirements in Scenario II, leading to lower steam and cooling water consumption (**Fig. 6.2B**). In addition, the enzyme and nutrient inputs required (YM broth and glucose) were also lower in Scenario II. The lower nutrient input is due to the use

of pre-colonised wood as inoculum instead of mycelia grown in YM broth, which allows fungal pretreatment with  $\text{NaNO}_3$  and metal ions as the only supplements without the need for glucose. The decreased enzyme cost can be explained by the increased enzymatic digestibility (38.44% vs 35.49% for glucose) measured in Scenario II compared to Scenario I (**Table 6.2**). In Scenario I, raw material and enzyme costs accounted for 26.9% and 30.9% of the variable operating costs, respectively, while in Scenario II, they represented 27.9% and 27.5%, respectively. Despite advances in technology, the cost of feedstock and enzymes remains a significant challenge for lignocellulose-based biorefineries as it represents a large proportion of the product cost [248]. As commercial hydrolytic enzymes continue to advance, enzyme dosages and costs may decrease, thereby reducing the overall enzyme cost as a proportion of the sugar production cost in fungal pretreatment plants. In addition, on-site enzyme production can play a key role in leveraging low-cost sugar production [249].

The cost of metal salts was exceptionally low in both scenarios (**Fig. 6.2B**), representing only 0.3% of the variable operating costs. However, their importance cannot be overemphasised as these metal salts play a vital role in achieving improved delignification [196].

The second largest cost contributor was the fixed capital investment (**Fig. 6.2A**) which was €476 M and €569 M in Scenario I and II, respectively. These FCIs were approximately 2-3 times lower than estimated in other studies evaluating fungal pretreatment-based facilities [10,24] but 4-6 times higher than those found for chemical and physicochemical pretreatment technologies at a comparable sugar production scale [24]. The higher capital investment required for biological pretreatment can be attributed to the need for large equipment in high quantities (**Table 6.5**) to produce the same amount of fermentable sugars as conventional pretreatment methods, which are generally faster and offer higher saccharification yields [24]. The 1.2 times higher FCI in Scenario II compared to Scenario I can be explained by the additional equipment used to prepare pre-colonised wood (**Table 6.5**).



**Fig. 6.2** (A) The contribution of (■) fixed capital investment, (■) working capital, (■) land cost, (■) variable operating and (■) fixed operating cost to the levelised sugar production cost. (B) Annual variable operating costs in (■) Scenario I and (■) Scenario II.

**Table 6.5** Size, quantity and installation cost of major equipment used in Scenario I and II

Process	Major equipment	Equipment size [m <sup>3</sup> ]	Number of vessels [-]		Installation cost in 2022 [M EUR]	
			Scenario I	Scenario II	Scenario I	Scenario II
<b>Mycelia preparation</b>	Airlift fermenter	303	5	2	4.51	1.80
<b>Sterilisation</b>	Autoclave	34	6	2	4.67	1.35
<b>Pre-colonised wood</b>	Packed bed reactor	3000		21		61.26
<b>Fungal pretreatment</b>	Packed bed reactor	3000	69	67	204.86	201.44
<b>Enzymatic hydrolysis</b>	Stirred tank reactor	3785	14	13	26.62	24.72

The cost of these additional units offsets the reduction in installation costs achieved by the less equipment required for autoclaving, mycelial preparation and enzymatic saccharification in Scenario II. A cost-saving approach could be to use a tray reactor or a pretreatment hall similar to a composting facility since fungal pretreatment of non-sterilised wood does not require a packed bed reactor with sterile conditions. However, due to the lack of relevant reference studies on scale-up and reactor design, the evaluation of these configurations was outside the scope of this study. Further methods of cost reduction include the evaluation of shorter inoculum preparation times and the implementation of a sequential fungal pretreatment process where the pretreated feedstock from one pretreatment step is used to inoculate the subsequent fungal pretreatment cycle. This sequential process was investigated in the study of Vasco-Correa et al. on four different non-sterilised feedstocks, including miscanthus, corn stover, hardwood (white ash) and softwood (pine) [17]. However, the sequential fungal pretreatment was ineffective in the case of all feedstock for the second and third pretreatment cycles. Nevertheless, it should be emphasised that the efficiency of fungal pretreatment is highly dependent on the applied microorganism and substrate. Therefore, further research is needed to evaluate the feasibility of a sequential process for the fungal pretreatment of poplar wood with *P. chrysosporium*.

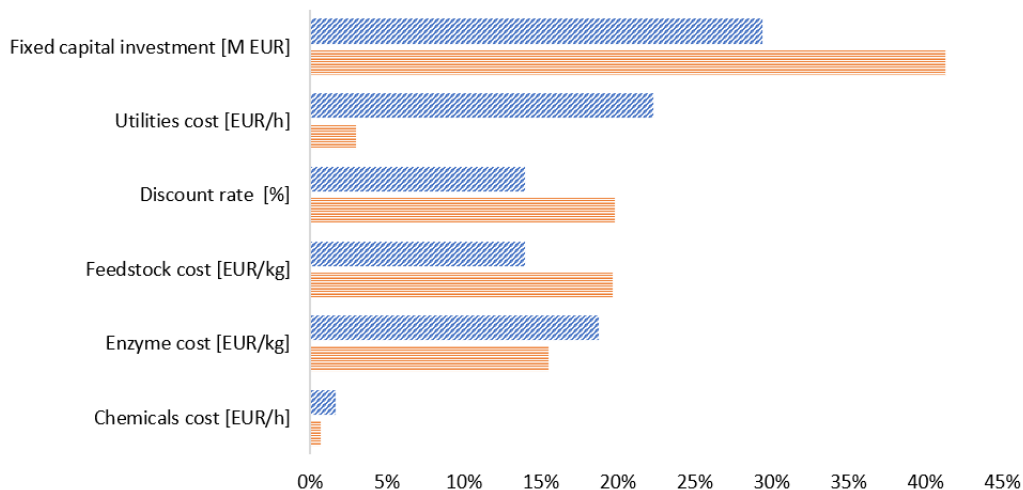
Since the experimental results of tray SSF of non-sterilised wood suggested that the improvement in saccharification yield is limited beyond 3 weeks of pretreatment (see the Supplementary materials), the economic feasibility of Scenario II using 3 weeks of

pretreatment was also evaluated and compared to 4 weeks of pretreatment. By using the shortened pretreatment time, there was a 14% reduction in capital expenditure (€609 M→€526 M) due to the reduced number of parallel reactors required to produce the same amount of sugar per year. However, more feedstock and enzymes were required to achieve the desired sugar production scale resulting in slightly higher annual operating expenditure (€197 M→€203 M). As a result, the final cost of sugar production was at €2.1/kg, only 2.3% lower than in Scenario II.

This study did not include the utilisation of the lignin-rich solid residue after enzymatic hydrolysis, which typically means incineration for heat and power generation [233,250] However, given that lignin is the most abundant renewable source of aromatics in nature, its valorisation represents an attractive opportunity. Pyrolysis and hydrothermal liquefaction have proven to be successful in the valorisation of lignin-rich residues [251–253].

#### **6.4.2 Global sensitivity analysis**

The sensitivity of sugar production cost to several economic parameters was investigated by performing a global sensitivity analysis for both scenarios (**Fig. 6.3**). The FCI was found to have the highest impact for both scenarios. However, a contribution of 29% was calculated for Scenario I, while a significantly higher contribution of 41% was obtained for Scenario II, due to its higher equipment costs. The most significant difference between the two scenarios is observed for the cost of utilities, with a contribution of 22% and 3% for Scenarios I and II respectively. This is attributed to the remarkable difference in energy consumption between the two scenarios, mainly related to the need for sterilisation. Discount rate, feedstock and enzyme costs also have a considerable influence on both scenarios, although Scenario II is more sensitive to the discount rate due to its high CAPEX. On the other hand, the sugar production cost is the least sensitive to the cost of chemicals, as the variable operating cost is mainly dominated by the cost of feedstock, enzymes and utilities (for Scenario II).



**Fig. 6.3** Global sensitivity analysis results for (▨) Scenario I and (▨) Scenario II

## 6.5 Conclusion

In this study, the techno-economic performance of a fungal pretreatment-based biorefinery for commercial-scale sugar production from poplar wood was investigated by comparing two scenarios which differed in substrate sterilisation and inoculation strategy. The techno-economic study showed that using non-sterilised wood as substrate and pre-colonised wood as inoculum resulted in a 14.5% reduction in sugar production costs (€2.15/kg) compared to using sterilised wood. This cost reduction can be attributed to the lower utility costs associated with the reduced need for sterilisation.

Although the evaluation of non-sterilised wood pretreatment showed promising cost reductions, fungal pretreatment remained more expensive than conventional chemical and physicochemical methods due to the high capital investment required, as the low sugar yields and long pretreatment times of the fungal pretreatment led to the need for large amounts of equipment to produce sugars on a commercial scale.



**Chapter 7.      General conclusions and outlook for  
future work**

---

## 7.1 General conclusions

Efficient pretreatment is essential for a sustainable biorefinery that uses lignocellulosic biomass to produce valuable biofuels and biochemicals. Poplar wood, with its rapid growth, year-round harvestability and higher bulk density, is emerging as a preferred feedstock in this regard compared to herbaceous feedstocks. Although chemical and physicochemical methods are currently the leading pretreatment technologies, they have drawbacks such as high energy consumption, use of chemicals and formation of inhibitory by-products. Fungal pretreatment, on the other hand, is a biotechnological alternative that uses white-rot fungi in a solid-state fermentation process with milder reaction conditions and without the formation of microbial inhibitors. However, it has limitations such as long pretreatment times, low delignification efficiency and selectivity, low saccharification yield and the need for feedstock sterilisation, which make it difficult to commercialise compared to conventional methods.

This study aimed to increase the efficiency of fungal pretreatment of poplar wood by *Phanerochaete chrysosporium* by improving key factors such as delignification efficiency and selectivity, sugar yield and sterilisation requirements to facilitate its implementation in wood-based biorefineries. *P. chrysosporium* was chosen as a white-rot fungus due to its rapid growth rate, relatively high optimum temperature and spore production.

In the first phase of this research, the fungal delignification of sterilised poplar wood by *P. chrysosporium* was improved using a combined metal supplementation of  $\text{MnSO}_4$  and  $\text{CuSO}_4$  in sterile venting SSF bottles as a cultivation environment. Using response surface methodology, the optimal doses of metal ions were determined to be  $2.01 \mu\text{mol Cu}^{2+}$  and  $0.77 \mu\text{mol Mn}^{2+}$  per g substrate.  $\text{Mn}^{2+}$  and  $\text{Cu}^{2+}$  ions showed a concerted effect on improved delignification, with  $\text{Mn}^{2+}$  ions inducing MnP production and  $\text{Cu}^{2+}$  ions prolonging it by maintaining the stationary growth phase responsible for MnP production. A 1.9-fold increase in lignin degradation (26.9%) and a 2.3-fold increase in delignification selectivity ( $\text{SV}=2.4$ ) were obtained compared to the pretreatment without metal addition. This selectivity value of 2.4 is significantly higher than that reported in the literature for the fungal species of *P. chrysosporium*, where selectivity values between 0.59 and 1.2 have been documented [77,86–88]. This finding greatly emphasises the crucial effect of culture conditions on the ligninolytic ability of a given white-rot fungus.

While higher selectivity values have been achieved with certain white-rot fungal species such as *Ceriporiopsis subvermispota*, *Trametes orientalis*, *Trametes velutina* and *Echinodontium taxodii* for fungal pretreatment of hardwood [18,185,190–194], it is important to note that selectivity value alone does not determine the overall efficiency of fungal pretreatment. It should be interpreted in conjunction with pretreatment time, lignin degradation and saccharification yields. The study of Yu et al. reported an exceptionally high selectivity value of 28.9 for the 30-day fungal pretreatment of hardwood (Chinese willow) using *E. taxodii* [191]. However, it is noteworthy that only a 15% yield of reducing sugar was obtained after enzymatic saccharification of the pretreated biomass which is relatively low for hardwood pretreatment. It is well known in the literature that hardwood, such as poplar, willow, or rubberwood, is more recalcitrant than herbaceous feedstock and consequently yields a lower amount of sugars after enzymatic saccharification [10]. Reducing sugar yields of 15-37% were reported for hardwood using strains such as *C. subvermispota*, *T. orientalis*, *T. velutina* and *E. taxodii* and 28-30 days pretreatment [18,185,190–194] (**Table 2.5**). In the present study, a reducing sugar yield of 33.2% was obtained after 28 days of SSF using a combined metal supplementation of 2.01  $\mu\text{mol Cu}^{2+}$  and 0.77  $\mu\text{mol Mn}^{2+}$  per g substrate. This value represents a remarkable 2.6-fold increase compared to the yield obtained without metal supplementation.

In the subsequent phase of the study, the optimised metal supplementation method was applied to the solid-state fermentation of non-sterilised wood using an inoculum type not commonly used in the field of fungal pretreatment, i.e. wood pre-colonised with the white-rot fungus. This inoculation method has not yet been applied for the fungal pretreatment of poplar wood by *P.chrysosporium*. Different fermentation additives (glucose,  $\text{NaNO}_3$  and metal ions) and cultivation methods (sterile aerated bottles and open trays) were investigated to optimise the process. The results showed that fungal pretreatment in open trays with a 1:3 inoculum ratio of pre-colonised and untreated wood, using  $\text{Cu}^{2+}$ ,  $\text{Mn}^{2+}$  and sodium nitrate as only additives, provides comparable fungal delignification efficiency and glucose yield ( $28.51 \pm 0.28\%$ ) to the traditional method using spore-inoculated sterilised wood and sterile aerated bottles ( $28.84 \pm 2.26\%$ ). Furthermore, the proposed method was successfully applied to a new batch of sawdust, demonstrating the robustness and good applicability of the process to new batches.

These above-described optimisation studies provided a large amount of experimental data, which were successfully used (1) to develop infrared-spectroscopy-based lignin quantification methods and (2) to evaluate and compare the techno-economic feasibility of fungal pretreatment of sterilised and non-sterilised wood.

For the first time, ATR-FTIR spectroscopy combined with partial least square regression (PLSR) and cross-validation (CV) has been effectively applied to establish a correlation between ATR-FTIR spectra and acid-insoluble lignin (AIL) content of fungus-treated wood. Despite the heterogeneity of the fungal solid-state fermentation, a PLSR model with a high coefficient of determination ( $R_{CV}^2 = 0.87$ ) and a low root mean square error ( $RMSE_{CV} = 0.60\%$ ) was obtained after variable selection and normalisation. The  $RMSE_{CV}$  value of 0.60% is only slightly higher than the standard laboratory error of 0.32% obtained using the conventional two-step acid hydrolysis as a reference method. This approximation is notable considering that a predictive model should yield an error no smaller than the standard laboratory error of the reference measurement. These results demonstrate that ATR-FTIR is a reliable and high-throughput method for predicting AIL content in fungus-treated wood and, thus, is an excellent alternative to laborious and time-consuming wet-chemistry-based methods.

In the subsequent research phase of the study, NIR spectroscopy was used to determine the lignin content of the pretreated wood using the same set of fungus-treated samples, providing insight into the most appropriate choice of IR instrumentation, spectral data processing and modelling strategies. This study is the first to compare ATR-FTIR and NIR spectroscopy-based methods for the quantification of lignin in fungus-treated wood using the same fungus-treated samples. After normalisation and second derivation, a PLSR model was developed with a good coefficient of determination ( $R_{CV}^2 = 0.89$ ) and a low root mean square error ( $RMSE_{CV} = 0.55\%$ ). Although this method required more extensive spectral pre-processing, its performance was comparable to that of ATR-FTIR ( $R_{CV}^2 = 0.87$ ). A previous study using FTIR-KBr in transmission mode obtained a comparably strong correlation ( $R_{CV}^2$  of 0.91), and low error ( $RMSE_{CV} = 0.71\%$ ) while applying a higher number of PLSR factors [159]. In comparison, our proposed ATR-FTIR method does not require the preparation of a KBr pellet and therefore is an easy and high-throughput alternative to the time-consuming and exhaustive two-step hydrolysis-based AIL determination in fungus-treated wood. In conclusion, both the ATR-FTIR and NIR spectroscopy-based methods are valuable for high-throughput and user-friendly monitoring of lignin degradation in a fungal pretreatment-based facility.

In the last phase of the research, the economic feasibility of a fungal pretreatment-based biorefinery for commercial-scale sugar production from poplar wood was investigated by comparing two scenarios that differed in substrate sterilisation and inoculation strategy. Scenario I used feedstock sterilisation and inoculation with fungal mycelium, while Scenario II used unsterilised substrate inoculated with pre-colonised feedstock. Scenario II showed a 14.5% reduction in sugar production costs (€2.15/kg) compared to Scenario I. This cost reduction was primarily due to the 2.7 times lower utility costs in Scenario II, which was attributed to reduced sterilisation requirements resulting in lower steam and cooling water consumption. The reduced sugar production cost in Scenario II was approximately 17% lower than previously reported for the fungal pretreatment-based biorefinery of hardwood at the same sugar production scale [10].

Although non-sterilised wood pretreatment showed promising cost reductions, it is important to acknowledge that fungal pretreatment remained 7-13 times more expensive than conventional chemical and physicochemical methods. This higher cost is primarily due to the significant capital investment required due to long pretreatment times and low sugar yields.

In conclusion, further research and process optimisation are required to improve sugar yield and reduce pretreatment time to make large-scale fungal pretreatment commercially viable.

## **7.2 Outlook for future work**

Although fungal pretreatment is a biotechnological method with great potential, its commercial use is still hindered by techno-economic challenges that require further fundamental and applied research to overcome. These challenges include the long pretreatment time, sterilisation requirement, non-selective and/or low degree of delignification leading to low sugar yields compared to conventional pretreatment methods.

### **7.2.1 Fundamental research**

Screening for potent strains with fast growth, high optimum growth temperature and selective lignin-degrading ability is recommended.

Most white-rot basidiomycetes grow best at relatively low temperatures (25-30°C [51]). However, a higher cultivation temperature may accelerate the delignification reaction. The selection of thermophilic fungi with a wide temperature tolerance or genetic modification of fungi to grow and efficiently degrade lignin at elevated temperatures

could reduce pretreatment time. In addition, higher temperature tolerance is particularly important in solid-state fermentation processes, as it enables the fungi to withstand the temperature gradient more effectively. Furthermore, fungal growth generates a significant amount of heat that must be removed in large-scale reactors. The use of thermophilic fungi could help to reduce the costs associated with cooling consumption. Investigating the growth performance and lignin degradation efficiency of white-rot fungal strains grown at different temperatures can be a promising approach to identifying potential candidates for fungal lignocellulose pretreatment. However, this specific approach has not yet been applied in the context of fungal lignocellulose pretreatment. In a study by Chairattanananokorn et al, thermotolerant white-rot fungi were screened to identify potential candidates for dye wastewater decolourisation under thermophilic culture conditions (43°C). Among the 38 fungal strains evaluated, *P. coccineus* FPF 97091303 showed remarkable decolourisation efficiencies [254]. This fungal species has been shown to grow well on hardwood [255] but has not yet been evaluated for wood pretreatment purposes at elevated temperatures (>30°C).

Strains with high selectivity for lignin degradation are crucial for obtaining high sugar yields during enzymatic saccharification of the pretreated lignocellulose. Performing ligninase (peroxidases [121,176,177] and laccase [256]) and cellulase activity assays [257] to measure the activity of ligninolytic and cellulolytic enzymes can help identify strains with high ligninolytic and low cellulolytic activity.

Genetic screening techniques, such as polymerase chain reaction (PCR)-based methods or genomic sequencing, can also be used to identify specific genes or gene variants associated with fast growth, high temperature tolerance or lignin degradation. This can help in the targeted selection of strains with desired traits.

Once an ideal fungal strain has been identified, metabolic engineering tools can be used to improve its growth rate, temperature tolerance and ability to produce ligninolytic enzymes. The clustered regularly interspaced short palindromic repeats (CRISPR) with associated nucleases (Cas) is a highly efficient tool for modifying fungal genomes [258]. This technique involves the expression of short RNA sequences to guide the Cas proteins to target and cut specific DNA sequences. CRISPR-Cas9 has been successfully used for gene knockout and metabolic pathway engineering in filamentous fungi such as *Aspergillus* [259]. However, CRISPR-Cas systems have not yet been used to enhance the expression of ligninolytic enzymes in fungi due to the lack of sequenced genomes and the challenges of precise DNA targeting [258]. Heterologous expression of ligninolytic enzymes has been achieved in hosts including fungi and yeast. Yeasts offer advantages

such as rapid growth, simple morphology, biomass production and safety. They can be engineered using homologous recombination and strong synthetic promoters to optimise enzyme expression [258].

In this study, non-sterilised feedstock was successfully used for fungal pretreatment. However, conducting further research to identify the indigenous fungi competing with the white-rot fungi would be beneficial. This knowledge could help develop fermentation conditions that support the growth of white-rot fungi while suppressing the growth of their competitors. The possible application of sequential fungal pretreatment of non-sterilised poplar wood with *P. chrysosporium* is also recommended to be investigated. Identifying the reasons that limit the number of cycles that can be used is also essential.

Combining fungal pretreatment with other pretreatment methods may be a solution to the problems of long pretreatment times and insufficient sugar yield. While physical, chemical and biological pretreatment methods have been extensively studied, combined pretreatment strategies have recently been developed for their synergistic effects [260,261]. The combination of microbial and chemical/physicochemical pretreatment can reduce pretreatment times, the strength of chemicals, the severity of operating conditions used, as well as the associated inhibitor production. From the perspective of fungal pretreatment, the pretreatment time and carbohydrate losses can be reduced.

### **7.2.2 Applied research**

The journey from laboratory research to industrial implementation often presents a significant challenge known as the 'valley of death'. This metaphorical valley represents the gap between promising laboratory results and the successful translation of these results into large-scale industrial processes. This challenge is particularly relevant in the context of solid-state fungal pretreatment.

One of the main obstacles to scaling up solid-state fermentation is ensuring sufficient mass and heat transfer within the SSF bioreactors [53]. In laboratory-scale setups, the limited volume and surface area facilitate efficient diffusion of nutrients, gases and heat. However, when scaling up to an industrial scale, achieving uniform distribution becomes increasingly challenging. Variations in temperature, moisture content and nutrient availability can lead to uneven growth, inefficient enzymatic activity and suboptimal lignocellulosic degradation. In addition, solid-state fermentation processes often exhibit temperature gradients within the bioreactor due to heat generated during

microbial activity. These temperature gradients can affect the growth rate and metabolism of the fungi, resulting in uneven performance across the substrate. It is critical to manage these temperature gradients to maintain consistent fungal activity and ensure reproducible results during scale-up.

Another consideration is the difficulty of monitoring and controlling process variables in industrial-scale solid-state fermentation. Unlike submerged fermentation, where parameters such as pH, dissolved oxygen and agitation can be easily measured and controlled, solid-state fermentation presents challenges in accurately assessing key process variables such as moisture content, oxygen availability and microbial growth kinetics [53]. The lack of accurate monitoring and control can lead to inconsistent performance and reduced predictability when scaling up fungal pretreatment.

To facilitate the large-scale implementation of fungal pretreatment, it is essential to prioritise comprehensive scale-up studies that include optimisation of process parameters, modelling, simulation and economic analysis. These studies should focus on key issues such as selecting an appropriate reactor design, including a simple pretreatment hall based on the composting hall concept and analysing the impact of scaling up on factors such as mass, oxygen and heat transfer, moisture control and substrate compaction. A life cycle assessment will also be required to assess the environmental impact of fungal pretreatment compared to conventional pretreatment technologies.

In conclusion, this PhD study encourages the global research community to address the open questions presented here to utilise the full potential of white-rot fungi.



## Appendix

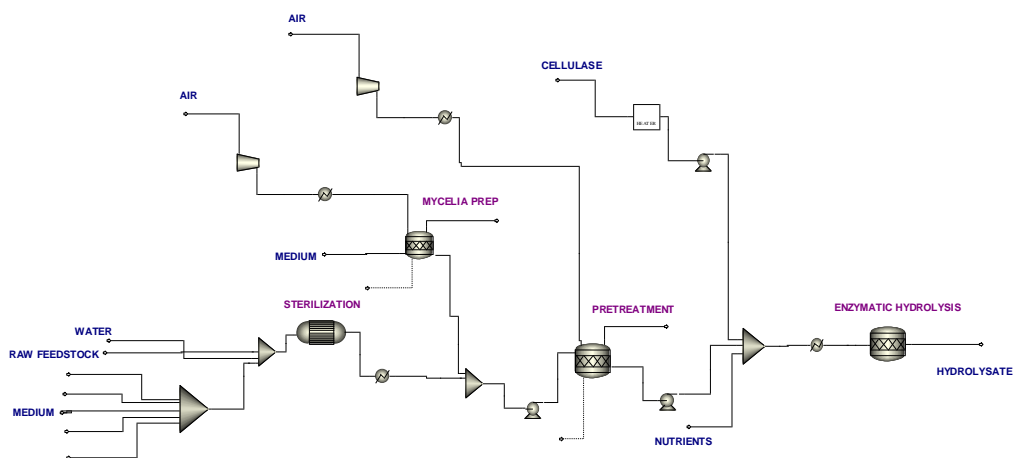


Fig. S1 ASPEN model of Scenario I

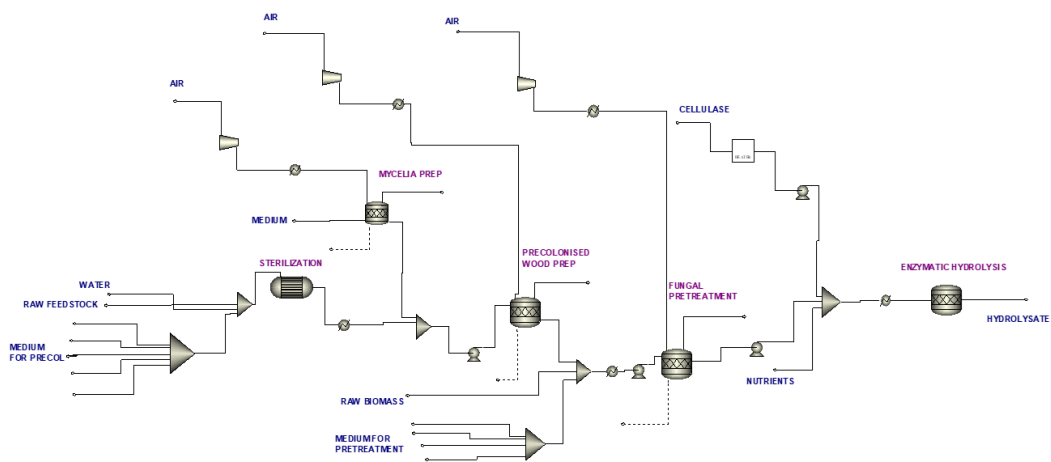


Fig. S2 ASPEN model of Scenario II



## References

- [1] P. Sannigrahi, A.J. Ragauskas, G.A. Tuskan, Poplar as a feedstock for biofuels: A review of compositional characteristics, *Biofuels, Bioproducts and Biorefining*. 4 (2010) 209–226. <https://doi.org/10.1002/bbb.206>.
- [2] E.O. Ajala, Y.O. Olonade, M.A. Ajala, G.S. Akinpelu, Lactic Acid Production from Lignocellulose – A Review of Major Challenges and Selected Solutions, *ChemBioEng Reviews*. 7 (2020) 38–49. <https://doi.org/10.1002/CBEN.201900018>.
- [3] L. Venkateswar Rao, J.K. Goli, J. Gentela, S. Koti, Bioconversion of lignocellulosic biomass to xylitol: An overview, *Bioresour Technol*. 213 (2016) 299–310. <https://doi.org/10.1016/J.BIORTECH.2016.04.092>.
- [4] C.R. Soccol, V. Faraco, S.G. Karp, L.P.S. Vandenberghe, V. Thomaz-Soccol, A.L. Woiciechowski, A. Pandey, Lignocellulosic Bioethanol: Current Status and Future Perspectives, *Biomass, Biofuels, Biochemicals: Biofuels: Alternative Feedstocks and Conversion Processes for the Production of Liquid and Gaseous Biofuels*. (2019) 331–354. <https://doi.org/10.1016/B978-0-12-816856-1.00014-2>.
- [5] N. Nadir, N.L. Ismail, A.S. Hussain, N. Nadir, N.L. Ismail, A.S. Hussain, Fungal Pretreatment of Lignocellulosic Materials, *Biomass for Bioenergy - Recent Trends and Future Challenges*. (2019). <https://doi.org/10.5772/INTECHOPEN.84239>.
- [6] A.K.S. Kameshwar, W. Qin, Metadata Analysis of *Phanerochaete chrysosporium* Gene Expression Data Identified Common CAZymes Encoding Gene Expression Profiles Involved in Cellulose and Hemicellulose Degradation, *Int J Biol Sci*. 13 (2017) 85. <https://doi.org/10.7150/IJBS.17390>.
- [7] H. Suzuki, J. MacDonald, K. Syed, A. Salamov, C. Hori, A. Aerts, B. Henrissat, A. Wiebenga, P.A. VanKuyk, K. Barry, E. Lindquist, K. LaButti, A. Lapidus, S. Lucas, P. Coutinho, Y. Gong, M. Samejima, R. Mahadevan, M. Abou-Zaid, R.P. de Vries, K. Igarashi, J.S. Yadav, I. V. Grigoriev, E.R. Master, Comparative genomics of the white-rot fungi, *Phanerochaete carnososa* and *P. chrysosporium*, to elucidate the genetic basis of the distinct wood types they colonize, *BMC Genomics*. 13 (2012) 1–17. <https://doi.org/10.1186/1471-2164-13-444>.

- [8] P. Kersten, D. Cullen, Extracellular oxidative systems of the lignin-degrading Basidiomycete *Phanerochaete chrysosporium*, *Fungal Genetics and Biology*. 44 (2007) 77–87. <https://doi.org/10.1016/j.fgb.2006.07.007>.
- [9] D. Martinez, L.F. Larrondo, N. Putnam, M.D. Sollewijn Gelpke, K. Huang, J. Chapman, K.G. Helfenbein, P. Ramaiya, J.C. Detter, F. Larimer, P.M. Coutinho, B. Henrissat, R. Berka, D. Cullen, D. Rokhsar, Genome sequence of the lignocellulose degrading fungus *Phanerochaete chrysosporium* strain RP78, 22 (2004) 695–700. <https://doi.org/10.1038/nbt967>.
- [10] J. Vasco-Correa, A. Shah, Techno-economic bottlenecks of the fungal pretreatment of lignocellulosic biomass, *Fermentation*. 5 (2019) 30. <https://doi.org/10.3390/fermentation5020030>.
- [11] R.Ö. Ürek, N.K. Pazarlioğlu, Production and stimulation of manganese peroxidase by immobilized *Phanerochaete chrysosporium*, *Process Biochemistry*. 40 (2005) 83–87. <https://doi.org/10.1016/j.procbio.2003.11.040>.
- [12] P. Wang, X. Hu, S. Cook, M. Begonia, K.S. Lee, H.M. Hwang, Effect of culture conditions on the production of ligninolytic enzymes by white rot fungi *Phanerochaete chrysosporium* (ATCC 20696) and separation of its lignin peroxidase, *World J Microbiol Biotechnol*. 24 (2008) 2205–2212. <https://doi.org/10.1007/s11274-008-9731-5>.
- [13] V. Singhal, V.S. Rathore, Effects of Zn<sup>2+</sup> and Cu<sup>2+</sup> on growth, lignin degradation and ligninolytic enzymes in *Phanerochaete chrysosporium*, *World J Microbiol Biotechnol*. 17 (2001) 235–240. <https://doi.org/10.1023/A:1016617025769>.
- [14] P. Baldrian, Interactions of heavy metals with white-rot fungi, *Enzyme Microb Technol*. 32 (2003) 78–91. [https://doi.org/10.1016/S0141-0229\(02\)00245-4](https://doi.org/10.1016/S0141-0229(02)00245-4).
- [15] J. Zhao, X. Ge, J. Vasco-Correa, Y. Li, Fungal pretreatment of unsterilized yard trimmings for enhanced methane production by solid-state anaerobic digestion, *Bioresour Technol*. 158 (2014) 248–252. <https://doi.org/10.1016/J.BIORTECH.2014.02.029>.
- [16] I.D. Reid, Optimization of solid-state fermentation for selective delignification of aspen wood with *Phlebia tremellosa*, *Enzyme Microb Technol*. 11 (1989) 804–809. [https://doi.org/10.1016/0141-0229\(89\)90053-7](https://doi.org/10.1016/0141-0229(89)90053-7).
- [17] J. Vasco-Correa, X. Luo, Y. Li, A. Shah, Comparative study of changes in composition and structure during sequential fungal pretreatment of non-sterile lignocellulosic feedstocks, *Ind Crops Prod*. 133 (2019) 383–394. <https://doi.org/10.1016/J.INDCROP.2019.03.043>.

- [18] F. Nazarpour, D.K. Abdullah, N. Abdullah, R. Zamiri, Evaluation of biological pretreatment of rubberwood with white rot fungi for enzymatic hydrolysis, *Materials*. 6 (2013) 2059–2073. <https://doi.org/10.3390/ma6052059>.
- [19] T.-F. Yeh, H. Chang, J.F. Kadla, Rapid Prediction of Solid Wood Lignin Content Using Transmittance Near-Infrared Spectroscopy, *J Agric Food Chem*. 52 (2004) 1435–1439. <https://doi.org/10.1021/jf034874r>.
- [20] L.M. Fahey, M.K. Nieuwoudt, P.J. Harris, Using near infrared spectroscopy to predict the lignin content and monosaccharide compositions of *Pinus radiata* wood cell walls, *Int J Biol Macromol*. 113 (2018) 507–514. <https://doi.org/10.1016/J.IJBIOMAC.2018.02.105>.
- [21] M. Schwanninger, J.C. Rodrigues, N. Gierlinger, B. Hinterstoisser, Determination of Lignin Content in Norway Spruce Wood by Fourier Transformed near Infrared Spectroscopy and Partial Least Squares Regression Analysis. Part 2: Development and Evaluation of the Final Model, <Http://Dx.Doi.Org/10.1255/Jnirs.945>. 19 (2011) 331–341. <https://doi.org/10.1255/JNIRS.945>.
- [22] C. Zhou, W. Jiang, B.K. Via, O. Fasina, G. Han, Prediction of mixed hardwood lignin and carbohydrate content using ATR-FTIR and FT-NIR, *Carbohydr Polym*. 121 (2015) 336–341. <https://doi.org/10.1016/j.carbpol.2014.11.062>.
- [23] G. Zhou, G. Taylor, A. Polle, FTIR-ATR-based prediction and modelling of lignin and energy contents reveals independent intra-specific variation of these traits in bioenergy poplars, *Plant Methods*. 7 (2011) 1–10. <https://doi.org/10.1186/1746-4811-7-9>.
- [24] N.R. Baral, A. Shah, Comparative techno-economic analysis of steam explosion, dilute sulfuric acid, ammonia fiber explosion and biological pretreatments of corn stover, *Bioresour Technol*. 232 (2017) 331–343. <https://doi.org/10.1016/J.BIORTECH.2017.02.068>.
- [25] H. Chen, J. Liu, X. Chang, D. Chen, Y. Xue, P. Liu, H. Lin, S. Han, A review on the pretreatment of lignocellulose for high-value chemicals, *Fuel Processing Technology*. 160 (2017) 196–206. <https://doi.org/10.1016/J.FUPROC.2016.12.007>.
- [26] H. Zhang, L. Han, H. Dong, An insight to pretreatment, enzyme adsorption and enzymatic hydrolysis of lignocellulosic biomass: Experimental and modeling studies, *Renewable and Sustainable Energy Reviews*. 140 (2021) 110758. <https://doi.org/10.1016/J.RSER.2021.110758>.

- [27] K. Rajendran, E. Drielak, V. Sudarshan Varma, S. Muthusamy, G. Kumar, Updates on the pretreatment of lignocellulosic feedstocks for bioenergy production—a review, *Biomass Convers Biorefin.* 8 (2018) 471–483. <https://doi.org/10.1007/S13399-017-0269-3>.
- [28] X. Zhao, L. Zhang, D. Liu, Biomass recalcitrance. Part I: the chemical compositions and physical structures affecting the enzymatic hydrolysis of lignocellulose, *Biofuels, Bioproducts and Biorefining.* 6 (2012) 465–482.
- [29] M.T. Holtzapple, HEMICELLULOSES, *Encyclopedia of Food Sciences and Nutrition.* (2003) 3060–3071. <https://doi.org/10.1016/B0-12-227055-X/00589-7>.
- [30] S. Brethauer, R.L. Shahab, M.H. Studer, Impacts of biofilms on the conversion of cellulose, *Appl Microbiol Biotechnol.* 104 (2020) 5201–5212. <https://doi.org/10.1007/s00253-020-10595-y>.
- [31] Y. Zhang, M. Naebe, Lignin: A Review on Structure, Properties, and Applications as a Light-Colored UV Absorber, *ACS Sustain Chem Eng.* 9 (2021) 1427–1442. <https://doi.org/10.1021/acssuschemeng.0c06998>.
- [32] J. Ralph, K. Lundquist, G. Brunow, F. Lu, H. Kim, P.F. Schatz, J.M. Marita, R.D. Hatfield, S.A. Ralph, J.H. Christensen, W. Boerjan, Lignins: Natural polymers from oxidative coupling of 4-hydroxyphenyl- propanoids, *Phytochemistry Reviews.* 3 (2004) 29–60. <https://doi.org/10.1023/B:PHYT.0000047809.65444.a4>.
- [33] M.J. Suota, T.A. da Silva, S.F. Zawadzki, G.L. Sasaki, F.A. Hansel, M. Paleologou, L.P. Ramos, Chemical and structural characterization of hardwood and softwood LignoForce™ lignins, *Ind Crops Prod.* 173 (2021) 114138. <https://doi.org/10.1016/J.INDCROP.2021.114138>.
- [34] S. Guadix-Montero, M. Sankar, Review on Catalytic Cleavage of C–C Inter-unit Linkages in Lignin Model Compounds: Towards Lignin Depolymerisation, *Top Catal.* 61 (2018) 183–198. <https://doi.org/10.1007/s11244-018-0909-2>.
- [35] D. Tarasov, M. Leitch, P. Fatehi, Lignin–carbohydrate complexes: properties, applications, analyses, and methods of extraction: a review, *Biotechnol Biofuels.* 11 (2018) 269. <https://doi.org/10.1186/S13068-018-1262-1>.

- [36] H. Nishimura, A. Kamiya, T. Nagata, M. Katahira, T. Watanabe, Direct evidence for  $\alpha$  ether linkage between lignin and carbohydrates in wood cell walls, *Scientific Reports* 2018 8:1. 8 (2018) 1–11. <https://doi.org/10.1038/s41598-018-24328-9>.
- [37] X. Zhang, L. Li, F. Xu, Chemical Characteristics of Wood Cell Wall with an Emphasis on Ultrastructure: A Mini-Review, *Forests* 2022, Vol. 13, Page 439. 13 (2022) 439. <https://doi.org/10.3390/F13030439>.
- [38] J. Littlewood, R.J. Murphy, L. Wang, Importance of policy support and feedstock prices on economic feasibility of bioethanol production from wheat straw in the UK, *Renewable and Sustainable Energy Reviews*. 17 (2013) 291–300. <https://doi.org/10.1016/J.RSER.2012.10.002>.
- [39] A. Mazzoli, O. Favoni, Particle size, size distribution and morphological evaluation of airborne dust particles of diverse woods by Scanning Electron Microscopy and image processing program, *Powder Technol.* 225 (2012) 65–71. <https://doi.org/10.1016/J.POWTEC.2012.03.033>.
- [40] D. Krutul, A. Antczak, A. Radomski, M. Drożdżek, T. Kłosińska, J. Zawadzki, The chemical composition of poplar wood in relation to the species and age of trees, *Forestry and Wood Technology*. 105 (2019) 125–132. <https://doi.org/10.5604/01.3001.0013.7728>.
- [41] V. Safdari, H. Khodadadi, S.K. Hosseinihashemi, E. Ganjian, The effects of poplar bark and wood content on the mechanical properties of wood-polypropylene composites, *Bioresources*. 6 (2011) 5180–5192. <https://doi.org/10.15376/BIORES.6.4.5180-5192>.
- [42] S. Mallakpour, F. Sirous, C.M. Hussain, Sawdust, a versatile, inexpensive, readily available bio-waste: From mother earth to valuable materials for sustainable remediation technologies, *Adv Colloid Interface Sci.* 295 (2021) 102492. <https://doi.org/10.1016/J.CIS.2021.102492>.
- [43] B. Shen, S. Hou, Y. Jia, C. Yang, Y. Su, Z. Ling, C. Huang, C. Lai, Q. Yong, Synergistic effects of hydrothermal and deep eutectic solvent pretreatment on co-production of xylo-oligosaccharides and enzymatic hydrolysis of poplar, *Bioresour Technol.* 341 (2021) 125787. <https://doi.org/10.1016/J.BIORTECH.2021.125787>.
- [44] D. Dai, M. Fan, Preparation of bio-composite from wood sawdust and gypsum, *Ind Crops Prod.* 74 (2015) 417–424. <https://doi.org/10.1016/J.INDCROP.2015.05.036>.

- [45] A.R. Mankar, A. Pandey, A. Modak, K.K. Pant, Pretreatment of lignocellulosic biomass: A review on recent advances, *Bioresour Technol.* 334 (2021) 125235. <https://doi.org/10.1016/J.BIORTECH.2021.125235>.
- [46] S. Soltanian, M. Aghbashlo, F. Almasi, H. Hosseinzadeh-Bandbafha, A.S. Nizami, Y.S. Ok, S.S. Lam, M. Tabatabaei, A critical review of the effects of pretreatment methods on the exergetic aspects of lignocellulosic biofuels, *Energy Convers Manag.* 212 (2020) 112792. <https://doi.org/10.1016/J.ENCONMAN.2020.112792>.
- [47] P. Kumar, D.M. Barrett, M.J. Delwiche, P. Stroeve, Methods for Pretreatment of Lignocellulosic Biomass for Efficient Hydrolysis and Biofuel Production, *Ind. Eng. Chem. Res.* (2009). <https://doi.org/10.1021/ie801542g>.
- [48] M. V. Galkin, J.S.M. Samec, Lignin Valorization through Catalytic Lignocellulose Fractionation: A Fundamental Platform for the Future Biorefinery, *ChemSusChem.* 9 (2016) 1544–1558. <https://doi.org/10.1002/CSSC.201600237>.
- [49] R. Sindhu, P. Binod, A. Pandey, Biological pretreatment of lignocellulosic biomass – An overview, *Bioresour Technol.* 199 (2016) 76–82. <https://doi.org/10.1016/J.BIORTECH.2015.08.030>.
- [50] S.S. Hassan, G.A. Williams, A.K. Jaiswal, Emerging technologies for the pretreatment of lignocellulosic biomass, *Bioresour Technol.* 262 (2018) 310–318. <https://doi.org/10.1016/J.BIORTECH.2018.04.099>.
- [51] M. Madadi, A. Abbas, Lignin Degradation by Fungal Pretreatment: A Review, *J Plant Pathol Microbiol.* 08 (2017). <https://doi.org/10.4172/2157-7471.1000398>.
- [52] D. Araújo, M. Vilarinho, A. Machado, Effect of combined dilute-alkaline and green pretreatments on corncob fractionation: Pretreated biomass characterization and regenerated cellulose film production, *Ind Crops Prod.* 141 (2019) 111785. <https://doi.org/10.1016/J.INDCROP.2019.111785>.
- [53] A.K. Kumar, S. Sharma, Recent updates on different methods of pretreatment of lignocellulosic feedstocks: a review, *Bioresour Bioprocess.* 4 (2017) 7. <https://doi.org/10.1186/s40643-017-0137-9>.
- [54] J.K. Saini, Himanshu, Hemansi, A. Kaur, A. Mathur, Strategies to enhance enzymatic hydrolysis of lignocellulosic biomass for biorefinery applications: A review, *Bioresour Technol.* 360 (2022) 127517. <https://doi.org/10.1016/J.BIORTECH.2022.127517>.



- [55] R. Kumar, S. Singh, O. V. Singh, Bioconversion of lignocellulosic biomass: biochemical and molecular perspectives, *J Ind Microbiol Biotechnol.* 35 (2008) 377–391. <https://doi.org/10.1007/s10295-008-0327-8>.
- [56] J.K. Saini, R. Saini, L. Tewari, Lignocellulosic agriculture wastes as biomass feedstocks for second-generation bioethanol production: concepts and recent developments, *3 Biotech.* 5 (2015) 337–353. <https://doi.org/10.1007/S13205-014-0246-5>.
- [57] N. Akhtar, D. Goyal, A. Goyal, BIODIVERSITY OF CELLULASE PRODUCING BACTERIA AND THEIR APPLICATIONS, *Cellulose Chemistry and Technology.* 50 (2016) 9–10.
- [58] S. Sun, S. Sun, X. Cao, R. Sun, The role of pretreatment in improving the enzymatic hydrolysis of lignocellulosic materials, *Bioresour Technol.* 199 (2016) 49–58. <https://doi.org/10.1016/J.BIORTECH.2015.08.061>.
- [59] P. Singh, O. Sulaiman, R. Hashim, L.C. Peng, R.P. Singh, Evaluating biopulping as an alternative application on oil palm trunk using the white-rot fungus *Trametes versicolor*, *Int Biodeterior Biodegradation.* 82 (2013) 96–103. <https://doi.org/10.1016/J.IBIOD.2012.12.016>.
- [60] M.M. Rahman, M. Lourenço, H.A. Hassim, J.J.P. Baars, A.S.M. Sonnenberg, J.W. Cone, J. De Boever, V. Fievez, Improving ruminal degradability of oil palm fronds using white rot fungi, *Anim Feed Sci Technol.* 169 (2011) 157–166. <https://doi.org/10.1016/J.ANIFEEDSCI.2011.06.014>.
- [61] T. Stella, S. Covino, M. Čvančarová, A. Filipová, M. Petruccioli, A. D’Annibale, T. Cajthaml, Bioremediation of long-term PCB-contaminated soil by white-rot fungi, *J Hazard Mater.* 324 (2017) 701–710. <https://doi.org/10.1016/J.JHAZMAT.2016.11.044>.
- [62] X. fei Tian, Z. Fang, F. Guo, Impact and prospective of fungal pre-treatment of lignocellulosic biomass for enzymatic hydrolysis, *Biofuels, Bioproducts and Biorefining.* 6 (2012) 335–350. <https://doi.org/10.1002/bbb.346>.
- [63] M. Dashtban, H. Schraft, T.A. Syed, W. Qin, Fungal biodegradation and enzymatic modification of lignin., *Int J Biochem Mol Biol.* 1 (2010) 36–50.
- [64] G. Atiwesh, C.C. Parrish, J. Banoub, T.A.T. Le, Lignin degradation by microorganisms: A review, *Biotechnol Prog.* 38 (2022) e3226. <https://doi.org/10.1002/BTPR.3226>.

- [65] A. Vanden Wymelenberg, P. Minges, G. Sabat, D. Martinez, A. Aerts, A. Salamov, I. Grigoriev, H. Shapiro, N. Putnam, P. Belinky, C. Dosoretz, J. Gaskell, P. Kersten, D. Cullen, Computational analysis of the *Phanerochaete chrysosporium* v2.0 genome database and mass spectrometry identification of peptides in ligninolytic cultures reveal complex mixtures of secreted proteins, *Fungal Genetics and Biology*. 43 (2006) 343–356. <https://doi.org/10.1016/j.fgb.2006.01.003>.
- [66] L.F. Larrondo, L. Salas, F. Melo, R. Vicuña, D. Cullen, A Novel Extracellular Multicopper Oxidase from *Phanerochaete chrysosporium* with Ferroxidase Activity, *Appl Environ Microbiol*. 69 (2003) 6257–6263. <https://doi.org/10.1128/AEM.69.10.6257-6263.2003>.
- [67] E. Srebotnik, K. Messner, R. Foisner, Penetrability of White Rot-Degraded Pine Wood by the Lignin Peroxidase of *Phanerochaete chrysosporium*, *Appl Environ Microbiol*. 54 (1988) 2608–2614. <https://doi.org/10.1128/AEM.54.11.2608-2614.1988>.
- [68] A. Kumar, R. Chandra, Ligninolytic enzymes and its mechanisms for degradation of lignocellulosic waste in environment, 2020. <https://doi.org/10.1016/j.heliyon.2020.e03170>.
- [69] A.O. Falade, U.U. Nwodo, B.C. Iweriebor, E. Green, L. V. Mabinya, A.I. Okoh, Lignin peroxidase functionalities and prospective applications, *Microbiologyopen*. 6 (2017). <https://doi.org/10.1002/mbo3.394>.
- [70] D.W.S. Wong, Structure and action mechanism of ligninolytic enzymes, *Appl Biochem Biotechnol*. 157 (2009) 174–209. <https://doi.org/10.1007/S12010-008-8279-Z>.
- [71] A.O. Falade, U.U. Nwodo, B.C. Iweriebor, E. Green, L. V. Mabinya, A.I. Okoh, Lignin peroxidase functionalities and prospective applications, *Microbiologyopen*. 6 (2017). <https://doi.org/10.1002/mbo3.394>.
- [72] M. Hofrichter, Review: Lignin conversion by manganese peroxidase (MnP), *Enzyme Microb Technol*. 30 (2002) 454–466. [https://doi.org/10.1016/S0141-0229\(01\)00528-2](https://doi.org/10.1016/S0141-0229(01)00528-2).
- [73] M. Hofrichter, Review: Lignin conversion by manganese peroxidase (MnP), *Enzyme Microb Technol*. 30 (2002) 454–466. [https://doi.org/10.1016/S0141-0229\(01\)00528-2](https://doi.org/10.1016/S0141-0229(01)00528-2).

- [74] E. Bari, G. Daniel, N. Yilgor, J.S. Kim, M.A. Tajick-Ghanbary, A.P. Singh, J. Ribera, Comparison of the Decay Behavior of Two White-Rot Fungi in Relation to Wood Type and Exposure Conditions, *Microorganisms*. 8 (2020) 1–20. <https://doi.org/10.3390/MICROORGANISMS8121931>.
- [75] G.J. Langer, J. Bußkamp, E. Terhonen, K. Blumenstein, Fungi inhabiting woody tree tissues, *Forest Microbiology: Volume 1: Tree Microbiome: Phyllosphere, Endosphere and Rhizosphere*. (2021) 175–205. <https://doi.org/10.1016/B978-0-12-822542-4.00012-7>.
- [76] C. Wan, Y. Li, Fungal pretreatment of lignocellulosic biomass, *Biotechnol Adv*. 30 (2012) 1447–1457. <https://doi.org/10.1016/j.biotechadv.2012.03.003>.
- [77] J. Shi, R.R. Sharma-Shivappa, M. Chinn, N. Howell, Effect of microbial pretreatment on enzymatic hydrolysis and fermentation of cotton stalks for ethanol production, *Biomass Bioenergy*. 33 (2009) 88–96. <https://doi.org/10.1016/j.biombioe.2008.04.016>.
- [78] H.M. Zabed, S. Akter, J. Yun, G. Zhang, F.N. Awad, X. Qi, J.N. Sahu, Recent advances in biological pretreatment of microalgae and lignocellulosic biomass for biofuel production, *Renewable and Sustainable Energy Reviews*. 105 (2019) 105–128. <https://doi.org/10.1016/J.RSER.2019.01.048>.
- [79] V. Mishra, A.K. Jana, M.M. Jana, A. Gupta, Synergistic effect of syringic acid and gallic acid supplements in fungal pretreatment of sweet sorghum bagasse for improved lignin degradation and enzymatic saccharification, *Process Biochemistry*. 55 (2017) 116–125. <https://doi.org/10.1016/j.procbio.2017.02.011>.
- [80] E. Rouches, S. Zhou, J.P. Steyer, H. Carrere, White-Rot Fungi pretreatment of lignocellulosic biomass for anaerobic digestion: Impact of glucose supplementation, *Process Biochemistry*. 51 (2016) 1784–1792. <https://doi.org/10.1016/j.procbio.2016.02.003>.
- [81] A. Justo, O. Miettinen, D. Floudas, B. Ortiz-Santana, E. Sjökvist, D. Lindner, K. Nakasone, T. Niemelä, K.H. Larsson, L. Ryvarden, D.S. Hibbett, A revised family-level classification of the Polyporales (Basidiomycota), *Fungal Biol*. 121 (2017) 798–824. <https://doi.org/10.1016/J.FUNBIO.2017.05.010>.
- [82] C.L. Schoch, S. Ciufu, M. Domrachev, C.L. Hotton, S. Kannan, R. Khovanskaya, D. Leipe, R. McVeigh, K. O’Neill, B. Robbertse, S. Sharma, V. Soussov, J.P. Sullivan, L. Sun, S. Turner, I. Karsch-Mizrachi, NCBI Taxonomy: A comprehensive update on curation, resources and tools, *Database*. 2020 (2020). <https://doi.org/10.1093/DATABASE/BAAA062>.

- [83] D. Singh, S. Chen, The white-rot fungus *Phanerochaete chrysosporium*: Conditions for the production of lignin-degrading enzymes, *Appl Microbiol Biotechnol.* 81 (2008) 399–417. <https://doi.org/10.1007/s00253-008-1706-9>.
- [84] M.H. Fulekar, B. Pathak, J. Fulekar, T. Godambe, Bioremediation of Organic Pollutants Using *Phanerochaete chrysosporium*, (2013) 135–157. [https://doi.org/10.1007/978-3-642-33811-3\\_6](https://doi.org/10.1007/978-3-642-33811-3_6).
- [85] A. Sośnicka, B. Kózka, K. Makarova, J. Giebułtowicz, M. Klimaszewska, J. Turło, Optimization of White-Rot Fungi Mycelial Culture Components for Bioremediation of Pharmaceutical-Derived Pollutants, *Water (Switzerland)*. 14 (2022) 1374. <https://doi.org/10.3390/W14091374/S1>.
- [86] A. Kamcharoen, V. Champreda, L. Eurwilaichitr, P. Boonsawang, Screening and optimization of parameters affecting fungal pretreatment of oil palm empty fruit bunch (EFB) by experimental design, *International Journal of Energy and Environmental Engineering*. 5 (2014) 303–312. <https://doi.org/10.1007/s40095-014-0136-y>.
- [87] J. Shi, M.S. Chinn, R.R. Sharma-Shivappa, Microbial pretreatment of cotton stalks by solid state cultivation of *Phanerochaete chrysosporium*, *Bioresour Technol.* 99 (2008) 6556–6564. <https://doi.org/10.1016/j.biortech.2007.11.069>.
- [88] J.S. Bak, J.K. Ko, I.G. Choi, Y.C. Park, J.H. Seo, K.H. Kim, Fungal pretreatment of lignocellulose by *Phanerochaete chrysosporium* to produce ethanol from rice straw, *Biotechnol Bioeng.* 104 (2009) 471–482. <https://doi.org/10.1002/bit.22423>.
- [89] T.Y. James, M. Lee, L.T.A. van Diepen, A Single Mating-Type Locus Composed of Homeodomain Genes Promotes Nuclear Migration and Heterokaryosis in the White-Rot Fungus *Phanerochaete chrysosporium*, *Eukaryot Cell.* 10 (2011) 249. <https://doi.org/10.1128/EC.00212-10>.
- [90] J.W. Taylor, J. Spatafora, K. O’Donnell, F. Lutzoni, T. James, D. Hibbett, D. Geiser, T. Bruns, M. Blackwell, *The Fungi*, in: *Assembling the Tree of Life*, 2018.
- [91] H.S. Park, J.H. Yu, Genetic control of asexual sporulation in filamentous fungi, *Curr Opin Microbiol.* 15 (2012) 669–677. <https://doi.org/10.1016/J.MIB.2012.09.006>.
- [92] C. Namhyun, I.S. Lee, H.S. Song, W.G. Bang, Mechanisms used by white-rot fungus to degrade lignin and toxic chemicals, *J Microbiol Biotechnol.* 10 (2000) 737–752.

- [93] A. Pandey, Recent process developments in solid-state fermentation, *Process Biochemistry*. 27 (1992) 109–117. [https://doi.org/10.1016/0032-9592\(92\)80017-W](https://doi.org/10.1016/0032-9592(92)80017-W).
- [94] E.B.N. Graminha, A.Z.L. Gonçalves, R.D.P.B. Pirota, M.A.A. Balsalobre, R. Da Silva, E. Gomes, Enzyme production by solid-state fermentation: Application to animal nutrition, *Anim Feed Sci Technol*. 144 (2008) 1–22. <https://doi.org/10.1016/J.ANIFEEDSCI.2007.09.029>.
- [95] Isroi, R. Millati, S. Syamsiah, C. Niklasson, M.N. Cahyanto, K. Lundquist, M.J. Taherzadeh, Biological pretreatment of lignocelluloses with white-rot fungi and its applications: A review, *Bioresources*. 6 (2011) 5224–5259. <https://doi.org/10.15376/BIORES.6.4.ISROI>.
- [96] S. Sahuand, K. Pramanik, Evaluating Fungal Mixed Culture for Pretreatment of Cotton Gin Waste to Bioethanol by Enzymatic Hydrolysis and Fermentation Using Co-Culture, *Pol J Environ Stud*. 26 (2017) 1215–1223. <https://doi.org/10.15244/PJOES/64641>.
- [97] V. Elisashvili, H. Parlar, E. Kachlishvili, D. Chichua, M. Bakradze, N. Kokhreidze, G. Kvesitadze, Ligninolytic activity of basidiomycetes grown under submerged and solid-state fermentation on plant raw material (sawdust of grapevine cuttings), *Advances in Food Sciences*. (2001).
- [98] L. Wang, S.T. Yang, Solid State Fermentation and Its Applications, *Bioprocessing for Value-Added Products from Renewable Resources: New Technologies and Applications*. (2007) 465–489. <https://doi.org/10.1016/B978-044452114-9/50019-0>.
- [99] U. Hölker, M. Höfer, J. Lenz, Biotechnological advantages of laboratory-scale solid-state fermentation with fungi, *Appl Microbiol Biotechnol*. 64 (2004) 175–186. <https://doi.org/10.1007/S00253-003-1504-3>.
- [100] V. Kumar, V. Ahluwalia, S. Saran, J. Kumar, A.K. Patel, R.R. Singhanian, Recent developments on solid-state fermentation for production of microbial secondary metabolites: Challenges and solutions, *Bioresour Technol*. 323 (2021) 124566. <https://doi.org/10.1016/J.BIORTECH.2020.124566>.
- [101] I.D. Reid, Solid-state fermentations for biological delignification, *Enzyme Microb Technol*. 11 (1989) 786–803. [https://doi.org/10.1016/0141-0229\(89\)90052-5](https://doi.org/10.1016/0141-0229(89)90052-5).

- [102] C. Wan, Y. Li, Microbial pretreatment of corn stover with *Ceriporiopsis subvermispora* for enzymatic hydrolysis and ethanol production, *Bioresour Technol.* 101 (2010) 6398–6403. <https://doi.org/10.1016/J.BIORTECH.2010.03.070>.
- [103] H. Itoh, M. Wada, Y. Honda, M. Kuwahara, T. Watanabe, Bioorganosolve pretreatments for simultaneous saccharification and fermentation of beech wood by ethanolysis and white rot fungi, *J Biotechnol.* 103 (2003) 273–280. [https://doi.org/10.1016/S0168-1656\(03\)00123-8](https://doi.org/10.1016/S0168-1656(03)00123-8).
- [104] E. Shirkavand, S. Baroutian, D.J. Gapes, B.R. Young, Pretreatment of radiata pine using two white rot fungal strains *Stereum hirsutum* and *Trametes versicolor*, *Energy Convers Manag.* 142 (2017) 13–19. <https://doi.org/10.1016/J.ENCONMAN.2017.03.021>.
- [105] A. Ferraz, C. Parra, J. Freer, J. Baeza, J. Rodríguez, Characterization of white zones produced on *Pinus radiata* wood chips by *Ganoderma australe* and *Ceriporiopsis subvermispora*, *World J Microbiol Biotechnol.* 16 (2000) 641–645. <https://doi.org/10.1023/A:1008981521479>.
- [106] L. Axelsson, M. Franzén, M. Ostwald, G. Berndes, G. Lakshmi, N.H. Ravindranath, Perspective: *Jatropha* cultivation in southern India: Assessing farmers' experiences, *Biofuels, Bioproducts and Biorefining.* 6 (2012) 246–256. <https://doi.org/10.1002/bbb>.
- [107] L. Hou, D. Ji, W. Dong, L. Yuan, F. Zhang, Y. Li, L. Zang, The Synergistic Action of Electro-Fenton and White-Rot Fungi in the Degradation of Lignin, *Front Bioeng Biotechnol.* 8 (2020). <https://doi.org/10.3389/FBIOE.2020.00099>.
- [108] P.D. Patil, G.D. Yadav, Comparative Studies of White-Rot Fungal Strains (*Trametes hirsuta* MTCC-1171 and *Phanerochaete chrysosporium* NCIM-1106) for Effective Degradation and Bioconversion of Ferulic Acid, *ACS Omega.* 3 (2018) 14858–14868. <https://doi.org/10.1021/ACSOMEGA.8B01614>.
- [109] C. Ding, X. Wang, M. Li, Evaluation of six white-rot fungal pretreatments on corn stover for the production of cellulolytic and ligninolytic enzymes, reducing sugars, and ethanol, *Appl Microbiol Biotechnol.* 103 (2019) 5641–5652. <https://doi.org/10.1007/S00253-019-09884-y>.
- [110] G.M. Scott, M. Akhtar, M.J. Lentz, R.E. Swaney, Engineering, Scale-Up, and Economic Aspects of Fungal Pretreatment of Wood Chips, *Biology (Basel)*. (1998).

- [111] S.J.A. van Kuijk, A.S.M. Sonnenberg, J.J.P. Baars, W.H. Hendriks, J.W. Cone, Fungal treated lignocellulosic biomass as ruminant feed ingredient: A review, *Biotechnol Adv.* 33 (2015) 191–202. <https://doi.org/10.1016/J.BIOTECHADV.2014.10.014>.
- [112] S.J.A. van Kuijk, A.S.M. Sonnenberg, J.J.P. Baars, W.H. Hendriks, J.W. Cone, The effect of particle size and amount of inoculum on fungal treatment of wheat straw and wood chips, *J Anim Sci Biotechnol.* 7 (2016) 1–9. <https://doi.org/10.1186/S40104-016-0098-4>.
- [113] T.K. Kirk, E. Schultz, W.J. Connors, L.F. Lorenz, J.G. Zeikus, Influence of culture parameters on lignin metabolism by *Phanerochaete chrysosporium*, *Arch Microbiol.* 117 (1978) 277–285. <https://doi.org/10.1007/BF00738547>.
- [114] R. Hilgers, J.-P. Vincken, H. Gruppen, M.A. Kabel, Laccase/Mediator Systems: Their Reactivity toward Phenolic Lignin Structures, *ACS Sustain Chem Eng.* 6 (2018) 2037–2046. <https://doi.org/10.1021/acssuschemeng.7b03451>.
- [115] Y. Liu, J. Sun, Z. Luo, S. Rao, Y. Su, Y. Yang, Effect of Supplements Mn<sup>2+</sup>, Cu<sup>2+</sup>, and Aromatic Compounds and *Penicillium decumbens* on Lignocellulosic Enzyme Activity and Productivity of *Catathelasma ventricosum*, *J. Microbiol. Biotechnol.* 23 (2013) 565–571. <https://doi.org/10.4014/JMB.1211.11007>.
- [116] P. Nousiainen, J. Kontro, H. Manner, A. Hatakka, J. Sipilä, Phenolic mediators enhance the manganese peroxidase catalyzed oxidation of recalcitrant lignin model compounds and synthetic lignin, *Fungal Genetics and Biology.* 72 (2014) 137–149. <https://doi.org/10.1016/J.FGB.2014.07.008>.
- [117] A.M. Falih, Influence of heavy-metals toxicity on the growth of *Phanerochaete chrysosporium*, *Bioresour Technol.* 60 (1997) 87–90. [https://doi.org/10.1016/S0960-8524\(96\)00177-0](https://doi.org/10.1016/S0960-8524(96)00177-0).
- [118] T. Mester, E. de Jong, J.A. Field, Manganese regulation of veratryl alcohol in white rot fungi and its indirect effect on lignin peroxidase, *Appl Environ Microbiol.* 61 (1995) 1881–1887. <https://doi.org/10.1128/aem.61.5.1881-1887.1995>.
- [119] A. Kumar, P.K. Arora, Biotechnological Applications of Manganese Peroxidases for Sustainable Management, *Front Environ Sci.* 10 (2022) 365. <https://doi.org/10.3389/fenvs.2022.875157>.
- [120] O.M. Gomaa, O.A. Momtaz, Copper induction and differential expression of laccase in *Aspergillus flavus*, *Brazilian Journal of Microbiology.* 46 (2015) 285. <https://doi.org/10.1590/S1517-838246120120118>.

- [121] V. Mishra, A.K. Jana, Fungal Pretreatment of Sweet Sorghum Bagasse with Combined CuSO<sub>4</sub>-Gallic Acid Supplement for Improvement in Lignin Degradation, Selectivity, and Enzymatic Saccharification, *Appl Biochem Biotechnol.* 183 (2017) 200–217. <https://doi.org/10.1007/s12010-017-2439-y>.
- [122] G.M. Zeng, M.H. Zhao, D.L. Huang, C. Lai, C. Huang, Z. Wei, P. Xu, N.J. Li, C. Zhang, F.L. Li, M. Cheng, Purification and biochemical characterization of two extracellular peroxidases from *Phanerochaete chrysosporium* responsible for lignin biodegradation, *Int Biodeterior Biodegradation.* 85 (2013) 166–172. <https://doi.org/10.1016/J.IBIOD.2013.07.005>.
- [123] J.M. Álvarez, P. Canessa, R.A. Mancilla, R. Polanco, P.A. Santibáñez, R. Vicuña, Expression of genes encoding laccase and manganese-dependent peroxidase in the fungus *Ceriporiopsis subvermispora* is mediated by an ACE1-like copper-fist transcription factor, *Fungal Genetics and Biology.* 46 (2009) 104–111. <https://doi.org/10.1016/j.fgb.2008.10.002>.
- [124] G. Geiger, H. Brandl, G. Furrer, R. Schulin, The effect of copper on the activity of cellulase and  $\beta$ -glucosidase in the presence of montmorillonite or Al-montmorillonite, *Soil Biol Biochem.* 30 (1998) 1537–1544. [https://doi.org/10.1016/S0038-0717\(97\)00231-9](https://doi.org/10.1016/S0038-0717(97)00231-9).
- [125] A. Tejirian, F. Xu, Inhibition of cellulase-catalyzed lignocellulosic hydrolysis by iron and oxidative metal ions and complexes, *Appl Environ Microbiol.* 76 (2010) 7673–7682. <https://doi.org/10.1128/AEM.01376-10>.
- [126] F. Xu, H. Ding, A. Tejirian, Detrimental effect of cellulose oxidation on cellulose hydrolysis by cellulase, *Enzyme Microb Technol.* 45 (2009) 203–209. <https://doi.org/10.1016/j.enzmictec.2009.06.002>.
- [127] S. Arora, R. Rani, S. Ghosh, Bioreactors in solid state fermentation technology: Design, applications and engineering aspects, *J Biotechnol.* 269 (2018) 16–34. <https://doi.org/10.1016/J.JBIOTECH.2018.01.010>.
- [128] F. Gassara, C.M. Ajila, S.K. Brar, R.D. Tyagi, M. Verma, J. Valero, Influence of aeration and agitation modes on solid-state fermentation of apple pomace waste by *Phanerochaete chrysosporium* to produce ligninolytic enzymes and co-extract polyphenols, *Int J Food Sci Technol.* 48 (2013) 2119–2126. <https://doi.org/10.1111/ijfs.12194>.
- [129] M.A. Fanaei, B.M. Vaziri, Modeling of temperature gradients in packed-bed solid-state bioreactors, *Chemical Engineering and Processing: Process Intensification.* 48 (2009) 446–451. <https://doi.org/10.1016/J.CEP.2008.06.001>.



- [130] X. Ge, J. Vasco-Correa, Y. Li, *Solid-State Fermentation Bioreactors and Fundamentals, Current Developments in Biotechnology and Bioengineering: Bioprocesses, Bioreactors and Controls*. (2017) 381–402.  
<https://doi.org/10.1016/B978-0-444-63663-8.00013-6>.
- [131] H.Kh.Q. Ali, M.M.D. Zulkali, *Design Aspects of Bioreactors for Solid-state Fermentation: A Review*, *Chem Biochem Eng Q*. 25 (2011) 255–266.
- [132] M. Krishania, R. Sindhu, P. Binod, V. Ahluwalia, V. Kumar, R.S. Sangwan, A. Pandey, *Design of Bioreactors in Solid-State Fermentation, Current Developments in Biotechnology and Bioengineering*. (2018) 83–96.  
<https://doi.org/10.1016/B978-0-444-63990-5.00005-0>.
- [133] M.K. Gowthaman, C. Krishna, M. Moo-Young, *Fungal solid state fermentation — an overview*, *Applied Mycology and Biotechnology*. 1 (2001) 305–352.  
[https://doi.org/10.1016/S1874-5334\(01\)80014-9](https://doi.org/10.1016/S1874-5334(01)80014-9).
- [134] F.C. Moreira-Vilar, R.D.C. Siqueira-Soares, A. Finger-Teixeira, D.M. De Oliveira, A.P. Ferro, G.J. Da Rocha, M.D.L.L. Ferrarese, W.D. Dos Santos, O. Ferrarese-Filho, *The Acetyl Bromide Method Is Faster, Simpler and Presents Best Recovery of Lignin in Different Herbaceous Tissues than Klason and Thioglycolic Acid Methods*, *PLoS One*. 9 (2014) e110000.  
<https://doi.org/10.1371/JOURNAL.PONE.0110000>.
- [135] A. Sluiter, B. Hames, R. Ruiz, C. Scarlata, J. Sluiter, D. Templeton, D. Crocker, *Determination of Structural Carbohydrates and Lignin in Biomass: Laboratory Analytical Procedure (LAP) (Revised August 2012)*, (2008).
- [136] U.P. Agarwal, R.H. Atalla, *A Vibrational Spectroscopy, Lignin and Lignans*. (2010) 103–136. <https://doi.org/10.1201/EBK1574444865-c4>.
- [137] E. Mendes, N. Duarte, *Mid-Infrared Spectroscopy as a Valuable Tool to Tackle Food Analysis: A Literature Review on Coffee, Dairies, Honey, Olive Oil and Wine*, *Foods* 2021, Vol. 10, Page 477. 10 (2021) 477.  
<https://doi.org/10.3390/FOODS10020477>.
- [138] P.R. Armstrong, E.B. Maghirang, F. Xie, F.E. Dowell, *Comparison of Dispersive and Fourier-transform NIR Instruments for Measuring Grain and Flour Attributes*, *Appl Eng Agric*. 22 (n.d.) 453–457.  
<https://doi.org/10.13031/2013.20448>.
- [139] J.J. Ojeda, M. Dittrich, *Fourier transform infrared spectroscopy for molecular analysis of microbial cells*, *Methods in Molecular Biology*. 881 (2012) 187–211.  
[https://doi.org/10.1007/978-1-61779-827-6\\_8](https://doi.org/10.1007/978-1-61779-827-6_8).

- [140] H. Kaur, B. Rana, D. Tomar, S. Kaur, K.C. Jena, Fundamentals of ATR-FTIR Spectroscopy and Its Role for Probing In-Situ Molecular-Level Interactions, (2021) 3–37. [https://doi.org/10.1007/978-981-33-6084-6\\_1](https://doi.org/10.1007/978-981-33-6084-6_1).
- [141] A. Ausili, M. Sánchez, J.C. Gómez-Fernández, Attenuated total reflectance infrared spectroscopy: A powerful method for the simultaneous study of structure and spatial orientation of lipids and membrane proteins, *Biomed Spectrosc Imaging*. 4 (2015) 159–170. <https://doi.org/10.3233/BSI-150104>.
- [142] S.E. Glassford, B. Byrne, S.G. Kazarian, Recent applications of ATR FTIR spectroscopy and imaging to proteins, *Biochimica et Biophysica Acta (BBA) - Proteins and Proteomics*. 1834 (2013) 2849–2858. <https://doi.org/10.1016/J.BBAPAP.2013.07.015>.
- [143] Z. Lu, S.A. DeJong, B.M. Cassidy, R.G. Belliveau, M.L. Myrick, S.L. Morgan, Detection Limits for Blood on Fabrics Using Attenuated Total Reflection Fourier Transform Infrared (ATR FT-IR) Spectroscopy and Derivative Processing, *Appl Spectrosc*. 71 (2017) 839–846. [https://doi.org/10.1177/000370281665415\\_4](https://doi.org/10.1177/000370281665415_4).
- [144] T. Otto, R. Saupe, A. Weiss, V. Stock, K. Wiesner, U. Lampe, M. Fleischer, T. Gessner, Dual-detector optical MEMS spectrum analyzer: advances, applications, and prospects, *MOEMS and Miniaturized Systems VII*. 6887 (2008) 68870D. <https://doi.org/10.1117/12.768356>.
- [145] C. Sandorfy, R. Buchet, G. Lachenal, Principles of Molecular Vibrations for Near-Infrared Spectroscopy, *Near-Infrared Spectroscopy in Food Science and Technology*. (2006) 11–46. <https://doi.org/10.1002/9780470047705.CH2>.
- [146] J.M. Olinger, P.R. Griffiths, Quantitative Effects of an Absorbing Matrix on Near-Infrared Diffuse Reflectance Spectra, *Anal Chem*. 60 (1988) 2427–2435. [https://doi.org/10.1021/AC00172A022/ASSET/AC00172A022.FP.PNG\\_V03](https://doi.org/10.1021/AC00172A022/ASSET/AC00172A022.FP.PNG_V03).
- [147] O. Faix, *Fourier Transform Infrared Spectroscopy*, in: Springer, Berlin, Heidelberg, 1992: pp. 83–109. [https://doi.org/10.1007/978-3-642-74065-7\\_7](https://doi.org/10.1007/978-3-642-74065-7_7).
- [148] J. Sandak, A. Sandak, R. Meder, Assessing Trees, Wood and Derived Products with near Infrared Spectroscopy: Hints and Tips, *J Near Infrared Spectrosc*. 24 (2016) 485–505. <https://doi.org/10.1255/jnirs.1255>.
- [149] N. Kumar, P.C. Panchariya, S.S. Patel, A.H. Kiranmayee, R. Ranjan, Application of Various Pre-Processing Techniques on Infrared (IR) Spectroscopy Data for Classification of Different Ghee Samples, in: 2018 Fourth International Conference on Computing Communication Control and Automation (ICCUBEA), 2018: pp. 1–6. <https://doi.org/10.1109/ICCUBEA.2018.8697787>.

- [150] Near-infrared (NIR) Spectroscopy » Analytical Toxicology, (n.d.).  
<https://www.analyticaltoxicology.com/en/near-infrared-nir-spectroscopy/>.
- [151] Å. Rinnan, F. van den Berg, S.B. Engelsen, Review of the most common pre-processing techniques for near-infrared spectra, *TrAC Trends in Analytical Chemistry*. 28 (2009) 1201–1222. <https://doi.org/10.1016/J.TRAC.2009.07.007>.
- [152] Y. Yang, T. Pan, J. Zhang, Y. Yang, T. Pan, J. Zhang, Global Optimization of Norris Derivative Filtering with Application for Near-Infrared Analysis of Serum Urea Nitrogen, *Am J Analyt Chem*. 10 (2019) 143–152.  
<https://doi.org/10.4236/AJAC.2019.105013>.
- [153] Calculation of the second derivative | Metrohm Vision – Theory User Manual | Page 13, n.d.
- [154] T. Hasegawa, Principal Component Regression and Partial Least Squares Modeling, *Handbook of Vibrational Spectroscopy*. (2001).  
<https://doi.org/10.1002/0470027320.S4604>.
- [155] D. Cozzolino, W.U. Cynkar, N. Shah, P. Smith, Multivariate data analysis applied to spectroscopy: Potential application to juice and fruit quality, *Food Research International*. 44 (2011) 1888–1896.  
<https://doi.org/10.1016/J.FOODRES.2011.01.041>.
- [156] B. Lavine, A user-friendly guide to multivariate calibration and classification, Tomas Naes, Tomas Isakson, Tom Fearn and Tony Davies, NIR Publications, Chichester, 2002, ISBN 0-9528666-2-5, £45.00., John Wiley & Sons, Ltd, 2003.  
<https://doi.org/10.1002/CEM.815>.
- [157] S. Takahama, A.M. Dillner, Model selection for partial least squares calibration and implications for analysis of atmospheric organic aerosol samples with mid-infrared spectroscopy, *J Chemom*. 29 (2015) 659–668.  
<https://doi.org/10.1002/CEM.2761>.
- [158] N. Zhao, Z.S. Wu, Q. Zhang, X.Y. Shi, Q. Ma, Y.J. Qiao, Optimization of Parameter Selection for Partial Least Squares Model Development, *Scientific Reports* 2015 5:1. 5 (2015) 1–10. <https://doi.org/10.1038/srep11647>.
- [159] K. Fackler, M. Schwanninger, C. Gradinger, B. Hinterstoisser, K. Messner, Qualitative and quantitative changes of beech wood degraded by wood-rotting basidiomycetes monitored by Fourier transform infrared spectroscopic methods and multivariate data analysis, *FEMS Microbiol Lett*. 271 (2007) 162–169. <https://doi.org/10.1111/j.1574-6968.2007.00712.x>.

- [160] I. Cornet, N. Wittner, G. Tofani, S. Tavernier, FTIR as an easy and fast analytical approach to follow up microbial growth during fungal pretreatment of poplar wood with *Phanerochaete chrysosporium*, *J Microbiol Methods*. 145 (2018) 82–86. <https://doi.org/10.1016/j.mimet.2018.01.004>.
- [161] K.K. Pandey, A.J. Pitman, FTIR studies of the changes in wood chemistry following decay by brown-rot and white-rot fungi, *Int Biodeterior Biodegradation*. 52 (2003) 151–160. [https://doi.org/10.1016/S0964-8305\(03\)00052-0](https://doi.org/10.1016/S0964-8305(03)00052-0).
- [162] R. Mahmud, S.M. Moni, K. High, M. Carbajales-Dale, Integration of techno-economic analysis and life cycle assessment for sustainable process design – A review, *J Clean Prod*. 317 (2021) 128247. <https://doi.org/10.1016/J.JCLEPRO.2021.128247>.
- [163] P.K. Gandam, M.L. Chinta, N.P.P. Pabbathi, R.R. Baadhe, M. Sharma, V.K. Thakur, G.D. Sharma, J. Ranjitha, V.K. Gupta, Second-generation bioethanol production from corncob – A comprehensive review on pretreatment and bioconversion strategies, including techno-economic and lifecycle perspective, *Ind Crops Prod*. 186 (2022) 115245. <https://doi.org/10.1016/J.INDCROP.2022.115245>.
- [164] R. Saini, C.S. Osorio-Gonzalez, K. Hegde, S.K. Brar, S. Magdoui, P. Vezina, A. Avalos-Ramirez, Lignocellulosic Biomass-Based Biorefinery: an Insight into Commercialization and Economic Standout, *Current Sustainable/Renewable Energy Reports*. 7 (2020) 122–136. <https://doi.org/10.1007/S40518-020-00157-1>.
- [165] L.J. Jönsson, C. Martín, Pretreatment of lignocellulose: Formation of inhibitory by-products and strategies for minimizing their effects, *Bioresour Technol*. 199 (2016) 103–112. <https://doi.org/10.1016/j.biortech.2015.10.009>.
- [166] D. Haldar, M.K. Purkait, Lignocellulosic conversion into value-added products: A review, *Process Biochemistry*. 89 (2020) 110–133. <https://doi.org/10.1016/j.procbio.2019.10.001>.
- [167] R. Sindhu, P. Binod, A. Pandey, Biological pretreatment of lignocellulosic biomass - An overview, *Bioresour Technol*. 199 (2016) 76–82. <https://doi.org/10.1016/j.biortech.2015.08.030>.
- [168] R. Tinoco, A. Acevedo, E. Galindo, L. Serrano-Carreón, Increasing *Pleurotus ostreatus* laccase production by culture medium optimization and copper/lignin synergistic induction, *J Ind Microbiol Biotechnol*. 38 (2011) 531–540. <https://doi.org/10.1007/s10295-010-0797-3>.

- [169] V. Mishra, A.K. Jana, M.M. Jana, A. Gupta, Improvement of selective lignin degradation in fungal pretreatment of sweet sorghum bagasse using synergistic CuSO<sub>4</sub>-syringic acid supplements, *J Environ Manage.* 193 (2017) 558–566. <https://doi.org/10.1016/j.jenvman.2017.02.057>.
- [170] M. Tien, T.K. Kirk, Lignin peroxidase of *Phanerochaete chrysosporium*, *Methods Enzymol.* 161 (1988) 238–249. [https://doi.org/10.1016/0076-6879\(88\)61025-1](https://doi.org/10.1016/0076-6879(88)61025-1).
- [171] F.A. Keller, J.E. Hamilton, Q.A. Nguyen, Microbial Pretreatment of Biomass, *Biotechnology for Fuels and Chemicals.* 105 (2003) 27–41. [https://doi.org/10.1007/978-1-4612-0057-4\\_3](https://doi.org/10.1007/978-1-4612-0057-4_3).
- [172] R.O. Urek, N.K. Pazarlioglu, Enhanced production of manganese peroxidase by *Phanerochaete chrysosporium*, *Brazilian Archives of Biology and Technology.* 50 (2007) 913–920. <https://doi.org/10.1590/S1516-89132007000700001>.
- [173] D.S. Arora, M. Chander, P.K. Gill, Involvement of lignin peroxidase, manganese peroxidase and laccase in degradation and selective ligninolysis of wheat straw, *Int Biodeterior Biodegradation.* 50 (2002) 115–120. [https://doi.org/10.1016/S0964-8305\(02\)00064-1](https://doi.org/10.1016/S0964-8305(02)00064-1).
- [174] D.R. Cabaleiro, S. Rodríguez-Couto, A. Sanromán, M.A. Longo, Comparison between the protease production ability of ligninolytic fungi cultivated in solid state media, *Process Biochemistry.* 37 (2002) 1017–1023. [https://doi.org/10.1016/S0032-9592\(01\)00307-7](https://doi.org/10.1016/S0032-9592(01)00307-7).
- [175] H. Wariishi, K. Valli, M.H. Gold, Manganese(II) oxidation by manganese peroxidase from the basidiomycete *Phanerochaete chrysosporium*. Kinetic mechanism and role of chelators, *Journal of Biological Chemistry.* 267 (1992) 23688–23695.
- [176] F.S. Archibald, A new assay for lignin-type peroxidases employing the dye Azure B, *Appl Environ Microbiol.* 58 (1992) 3110–3116. <https://doi.org/10.1128/aem.58.9.3110-3116.1992>.
- [177] D.S. Arora, P.K. Gill, Comparison of two assay procedures for lignin peroxidase, *Enzyme Microb Technol.* 28 (2001) 602–605. [https://doi.org/10.1016/S0141-0229\(01\)00302-7](https://doi.org/10.1016/S0141-0229(01)00302-7).
- [178] C.E. Wyman, B.E. Dale, R.T. Elander, M. Holtzapple, M.R. Ladisch, Y.Y. Lee, C. Mitchinson, J.N. Saddler, Comparative sugar recovery and fermentation data following pretreatment of poplar wood by leading technologies, *Biotechnol Prog.* 25 (2009) 333–339. <https://doi.org/10.1002/btpr.142>.

- [179] X. Pan, N. Gilkes, J. Kadla, K. Pye, S. Saka, D. Gregg, K. Ehara, D. Xie, D. Lam, J. Saddler, Bioconversion of hybrid poplar to ethanol and co-products using an organosolv fractionation process: Optimization of process yields, *Biotechnol Bioeng.* 94 (2006) 851–861. <https://doi.org/10.1002/bit.20905>.
- [180] A. Carroll, C. Somerville, Cellulosic Biofuels, *Annu Rev Plant Biol.* 60 (2009) 165–182. <https://doi.org/10.1146/annurev.arplant.043008.092125>.
- [181] A. Sluiter, R. Ruiz, C. Scarlata, J. Sluiter, D. Templeton, Determination of Extractives in Biomass: Laboratory Analytical Procedure (LAP), 2008.
- [182] O. Niemenmaa, A. Uusi-Rauva, A. Hatakka, Wood stimulates the demethoxylation of [O14CH3]-labeled lignin model compounds by the white-rot fungi *Phanerochaete chrysosporium* and *Phlebia radiata*, *Arch Microbiol.* 185 (2006) 307–315. <https://doi.org/10.1007/s00203-006-0097-5>.
- [183] B. Adney, J. Baker, Measurement of Cellulase Activities: Laboratory Analytical Procedure (LAP). Technical Report NREL/TP-510-42628., 1996.
- [184] G.L. Miller, Use of Dinitrosalicylic Acid Reagent for Determination of Reducing Sugar, *Anal Chem.* 31 (1959) 426–428. <https://doi.org/10.1021/ac60147a030>.
- [185] X. Ge, T. Matsumoto, L. Keith, Y. Li, Fungal pretreatment of albizia chips for enhanced biogas production by solid-state anaerobic digestion, *Energy and Fuels.* 29 (2015) 200–204. <https://doi.org/10.1021/ef501922t>.
- [186] Isroi, M.M. Ishola, R. Millati, S. Syamsiah, M.N. Cahyanto, C. Niklasson, M.J. Taherzadeh, Structural changes of oil palm empty fruit bunch (OPEFB) after fungal and phosphoric acid pretreatment, *Molecules.* 17 (2012) 14995–15012. <https://doi.org/10.3390/molecules171214995>.
- [187] A.M. Falih, Impact of heavy metals on cellulolytic activity of some soil fungi, *Kuwait Journal of Science and Engineering.* 25 (1998) 397–407.
- [188] S.J. Stohs, D. Bagchi, Oxidative mechanisms in the toxicity of metal ions, *Free Radic Biol Med.* 18 (1995) 321–336. [https://doi.org/10.1016/0891-5849\(94\)00159-H](https://doi.org/10.1016/0891-5849(94)00159-H).
- [189] R.S. Yehia, Aflatoxin detoxification by manganese peroxidase purified from *Pleurotus ostreatus*, *Brazilian Journal of Microbiology.* 45 (2014) 127–133. <https://doi.org/10.1590/S1517-83822014005000026>.
- [190] C. Wan, Y. Li, Effectiveness of microbial pretreatment by *Ceriporiopsis subvermispora* on different biomass feedstocks, *Bioresour Technol.* 102 (2011) 7507–7512. <https://doi.org/10.1016/J.BIORTECH.2011.05.026>.

- [191] H. Yu, G. Guo, X. Zhang, K. Yan, C. Xu, The effect of biological pretreatment with the selective white-rot fungus *Echinodontium taxodii* on enzymatic hydrolysis of softwoods and hardwoods, *Bioresour Technol.* 100 (2009) 5170–5175. <https://doi.org/10.1016/j.biortech.2009.05.049>.
- [192] W. Wang, T. Yuan, B. Cui, Biological pretreatment with white rot fungi and their co-culture to overcome lignocellulosic recalcitrance for improved enzymatic digestion, *Bioresources.* 9 (2014) 3968–3976. <https://doi.org/10.15376/biores.9.3.3968-3976>.
- [193] W. Wang, T. Yuan, B. Cui, Y. Dai, Pretreatment of *Populus tomentosa* with *Trametes velutina* supplemented with inorganic salts enhances enzymatic hydrolysis for ethanol production, *Biotechnol Lett.* 34 (2012) 2241–2246. <https://doi.org/10.1007/s10529-012-1031-3>.
- [194] W. Wang, T. Yuan, B. Cui, Y. Dai, Investigating lignin and hemicellulose in white rot fungus-pretreated wood that affect enzymatic hydrolysis, *Bioresour Technol.* 134 (2013) 381–385. <https://doi.org/10.1016/j.biortech.2013.02.042>.
- [195] A.L. Pometto, J. (Hans) van Leeuwen, P. Shrestha, S.K. Khanal, M. Rasmussen, S.K. Khanal, A.L. Pometto, J. (Hans) van Leeuwen, Solid-Substrate Fermentation of Corn Fiber by *Phanerochaete chrysosporium* and Subsequent Fermentation of Hydrolysate into Ethanol, *J Agric Food Chem.* 56 (2008) 3918–3924. <https://doi.org/10.1021/jf0728404>.
- [196] N. Wittner, W. Broos, J. Bauwelinck, J. Slezsák, S.E. Vlaeminck, I. Cornet, Enhanced fungal delignification and enzymatic digestibility of poplar wood by combined CuSO<sub>4</sub> and MnSO<sub>4</sub> supplementation, *Process Biochemistry.* 108 (2021) 129–137. <https://doi.org/10.1016/J.PROCBIO.2021.06.002>.
- [197] K. Hayer, M. Stratford, D.B. Archer, Structural Features of Sugars That Trigger or Support Conidial Germination in the Filamentous Fungus *Aspergillus niger*, *Appl Environ Microbiol.* 79 (2013) 6924. <https://doi.org/10.1128/AEM.02061-13>.
- [198] N. Wittner, J. Slezsák, W. Broos, J. Geerts, S. Gergely, S.E. Vlaeminck, I. Cornet, Rapid lignin quantification for fungal wood pretreatment by ATR-FTIR spectroscopy, *Spectrochim Acta A Mol Biomol Spectrosc.* 285 (2023) 121912. <https://doi.org/10.1016/J.SAA.2022.121912>.
- [199] V. Ashokkumar, R. Venkatkarthick, S. Jayashree, S. Chuetor, S. Dharmaraj, G. Kumar, W.-H. Chen, C. Ngamcharussrivichai, Recent advances in lignocellulosic biomass for biofuels and value-added bioproducts - A critical review, *Bioresour Technol.* 344 (2022) 126195. <https://doi.org/10.1016/j.biortech.2021.126195>.

- [200] R. Kumar, C.E. Wyman, Key features of pretreated lignocelluloses biomass solids and their impact on hydrolysis, *Bioalcohol Production: Biochemical Conversion of Lignocellulosic Biomass*. (2010) 73–121. <https://doi.org/10.1533/9781845699611.1.73>.
- [201] V. Sharma, J. Yadav, R. Kumar, D. Tesarova, A. Ekielski, P.K. Mishra, On the rapid and non-destructive approach for wood identification using ATR-FTIR spectroscopy and chemometric methods, *Vib Spectrosc*. 110 (2020) 103097. <https://doi.org/10.1016/J.VIBSPEC.2020.103097>.
- [202] G. Toscano, V. Maceratesi, E. Leoni, P. Stipa, E. Laudadio, S. Sabbatini, FTIR spectroscopy for determination of the raw materials used in wood pellet production, *Fuel*. 313 (2022) 123017. <https://doi.org/10.1016/J.FUEL.2021.123017>.
- [203] M. Manfredi, E. Robotti, F. Quasso, E. Mazzucco, G. Calabrese, E. Marengo, Fast classification of hazelnut cultivars through portable infrared spectroscopy and chemometrics, *Spectrochim Acta A Mol Biomol Spectrosc*. 189 (2018) 427–435. <https://doi.org/10.1016/J.SAA.2017.08.050>.
- [204] S. Sarkar, U. Taraphder, S. Datta, S.P. Swain, D. Saikhom, Multivariate Statistical Data Analysis-Principal Component Analysis (PCA), *International Journal of Livestock Research*. 7 (2017) 60–78. <https://doi.org/10.5455/ijlr.20170415115235>.
- [205] S. Wold, M. Sjöström, L. Eriksson, PLS-regression: a basic tool of chemometrics, *Chemometrics and Intelligent Laboratory Systems*. 58 (2001) 109–130. [https://doi.org/10.1016/S0169-7439\(01\)00155-1](https://doi.org/10.1016/S0169-7439(01)00155-1).
- [206] B.S. Gupta, B. Shankar Gupta, B.P. Jelle, T. Gao, Application of ATR-FTIR Spectroscopy to Compare the Cell Materials of Wood Decay Fungi with Wood Mould Fungi, *Article in International Journal of Spectroscopy*. 2015 (2015) 1–7. <https://doi.org/10.1155/2015/521938>.
- [207] A. Naumann, M. Navarro-González, S. Peddireddi, U. Kües, A. Polle, Fourier transform infrared microscopy and imaging: Detection of fungi in wood, *Fungal Genetics and Biology*. 42 (2005) 829–835. <https://doi.org/10.1016/J.FGB.2005.06.003>.
- [208] D.M. Rudakiya, A. Gupte, Assessment of white rot fungus mediated hardwood degradation by FTIR spectroscopy and multivariate analysis, *J Microbiol Methods*. 157 (2019) 123–130. <https://doi.org/10.1016/j.mimet.2019.01.007>.



- [209] J. Ma, H. Yue, H. Li, J. Zhang, Y. Zhang, X. Wang, S. Gong, G.Q. Liu, Selective delignification of poplar wood with a newly isolated white-rot basidiomycete *Peniophora incarnata* T-7 by submerged fermentation to enhance saccharification, *Biotechnol Biofuels*. 14 (2021) 1–15. <https://doi.org/10.1186/s13068-021-01986-y>.
- [210] G.C. Santos, C.R. Corso, Comparative analysis of azo dye biodegradation by *Aspergillus oryzae* and *Phanerochaete chrysosporium*, *Water Air Soil Pollut*. 225 (2014) 1–11. <https://doi.org/10.1007/s11270-014-2026-6>.
- [211] B. Kiss, S. Gergely, A. Salgó, Á. Németh, Investigation of differences in the cultivation of nanochloropsis and chlorella species by fourier-transform infrared spectroscopy, *Periodica Polytechnica Chemical Engineering*. 62 (2018) 388–395. <https://doi.org/10.3311/PPCH.12863>.
- [212] A. Barth, Infrared spectroscopy of proteins, *Biochimica et Biophysica Acta (BBA) - Bioenergetics*. 1767 (2007) 1073–1101. <https://doi.org/10.1016/J.BBABIO.2007.06.004>.
- [213] C. Krishna, Solid-state fermentation systems - An overview, *Crit Rev Biotechnol*. 25 (2005) 1–30. <https://doi.org/10.1080/07388550590925383>.
- [214] T. Mehmood, K.H. Liland, L. Snipen, S. Sæbø, A review of variable selection methods in Partial Least Squares Regression, *Chemometrics and Intelligent Laboratory Systems*. 118 (2012) 62–69. <https://doi.org/10.1016/J.CHEMOLAB.2012.07.010>.
- [215] J. Shi, D. Xing, J. Li, FTIR studies of the changes in wood chemistry from wood forming tissue under inclined treatment, *Energy Procedia*. 16 (2012) 758–762. <https://doi.org/10.1016/j.egypro.2012.01.122>.
- [216] C.G. Yoo, X. Meng, Y. Pu, A.J. Ragauskas, The critical role of lignin in lignocellulosic biomass conversion and recent pretreatment strategies: A comprehensive review, *Bioresour Technol*. 301 (2020) 122784. <https://doi.org/10.1016/J.BIORTECH.2020.122784>.
- [217] J.L. Rahikainen, J.D. Evans, S. Mikander, A. Kalliola, T. Puranen, T. Tamminen, K. Marjamaa, K. Kruus, Cellulase–lignin interactions—The role of carbohydrate-binding module and pH in non-productive binding, *Enzyme Microb Technol*. 53 (2013) 315–321. <https://doi.org/10.1016/J.ENZMICTEC.2013.07.003>.
- [218] A. Pandey, Solid-state fermentation, *Biochem Eng J*. 13 (2003) 81–84. [https://doi.org/10.1016/S1369-703X\(02\)00121-3](https://doi.org/10.1016/S1369-703X(02)00121-3).

- [219] A. Kartakoullis, J. Comaposada, A. Cruz-Carrión, X. Serra, P. Gou, Feasibility study of smartphone-based Near Infrared Spectroscopy (NIRS) for salted minced meat composition diagnostics at different temperatures, *Food Chem.* 278 (2019) 314–321. <https://doi.org/10.1016/J.FOODCHEM.2018.11.054>.
- [220] A. Savitzky, M.J.E. Golay, Smoothing and Differentiation of Data by Simplified Least Squares Procedures, *Anal Chem.* 36 (1964) 1627–1639. [https://doi.org/10.1021/AC60214A047/ASSET/AC60214A047.FP.PNG\\_V03](https://doi.org/10.1021/AC60214A047/ASSET/AC60214A047.FP.PNG_V03).
- [221] W.F. McClure, Analysis Using Fourier Transforms, in: *Handbook of Near-Infrared Analysis*. 3rd Ed. (Ed. Burns, D.A., Ciurczak, E.W.), 3rd Editio, CRC Press, 2008: pp. 93–121. <https://doi.org/10.1201/9781420007374-11>.
- [222] T. Næs, T. Isaksson, T. Fearn, T. Davies, Scatter correction of spectroscopic data, in: *A User-Friendly Guide to Multivariate Calibration and Classification*, NIR Publications, 2002: pp. 105–125. <https://doi.org/10.1255/978-1-906715-25-0>.
- [223] J.S. Shenk, M.O. Westerhaus, *The Application of near Infrared Reflectance Spectroscopy (NIRS) to Forage Analysis*, John Wiley & Sons, Ltd, 1994. <https://doi.org/10.2134/1994.foragequality.c10>.
- [224] M.A. Czarnecki, Resolution enhancement in second-derivative spectra., *Appl Spectrosc.* 69 (2015) 67–74. <https://doi.org/10.1366/14-07568>.
- [225] Z. Yang, Y. Liu, X. Pang, K. Li, Preliminary Investigation into the Identification of Wood Species from Different Locations by Near Infrared Spectroscopy, *Bioresources.* 10 (2015) 8505–8517. <https://doi.org/10.15376/biores.10.4.8505-8517>.
- [226] M. Schwanninger, J.C. Rodrigues, K. Fackler, M. Schwanninger, J.C. Rodrigues, K. Fackler, A review of band assignments in near infrared spectra of wood and wood components Special Issue on Wood and Wood products, *J. Near Infrared Spectrosc.* 19 (2011) 287–308. <https://doi.org/10.1255/jnirs.955>.
- [227] D. Cozzolino, The Ability of Near Infrared (NIR) Spectroscopy to Predict Functional Properties in Foods: Challenges and Opportunities, *Molecules.* 26 (2021). <https://doi.org/10.3390/MOLECULES26226981>.
- [228] J.S. Shenk, J.J.J. Workman, M.O. Westerhaus, *Application of NIR spectroscopy to agricultural products*, CRC Press, 2008. <https://doi.org/10.1201/9781420007374-24>.

- [229] A. Cogulet, P. Blanchet, V. Landry, Wood degradation under UV irradiation: A lignin characterization, *J Photochem Photobiol B*. 158 (2016) 184–191. <https://doi.org/10.1016/J.JPHOTOBIO.2016.02.030>.
- [230] W.R. Hruschka, Spectral Reconstruction, in: *Handbook of Near-Infrared Analysis*. 3rd Ed. (Ed. Burns, CRC Press, 2008: pp. 333–344. <https://doi.org/10.1201/9781420007374-22>.
- [231] L. Ou, H. Kim, S. Kelley, S. Park, Impacts of feedstock properties on the process economics of fast-pyrolysis biorefineries, *Biofuels, Bioproducts and Biorefining*. 12 (2018) 442–452. <https://doi.org/10.1002/BBB.1860>.
- [232] R. Agrawal, P. Kumari, P. Sivagurunathan, A. Satlewal, R. Kumar, R.P. Gupta, S.K. Puri, Pretreatment process and its effect on enzymatic hydrolysis of biomass, *Current Status and Future Scope of Microbial Cellulases*. (2021) 145–169. <https://doi.org/10.1016/B978-0-12-821882-2.00012-0>.
- [233] D. Humbird, R. Davis, L. Tao, C. Kinchin, D. Hsu, A. Aden, P. Schoen, J. Lukas, B. Olthof, M. Worley, D. Sexton, D. Dudgeon, *Process Design and Economics for Biochemical Conversion of Lignocellulosic Biomass to Ethanol: Dilute-Acid Pretreatment and Enzymatic Hydrolysis of Corn Stover*, (2011). <https://www.nrel.gov/docs/fy11osti/47764.pdf> (accessed March 16, 2023).
- [234] W. Broos, N. Wittner, J. Geerts, J. Dries, S.E. Vlaeminck, N. Gunde-Cimerman, A. Richel, I. Cornet, Evaluation of Lignocellulosic Wastewater Valorization with the Oleaginous Yeasts *R. kratochvilovae* EXF7516 and *C. oleaginosum* ATCC 20509, *Fermentation*. 8 (2022) 204. <https://doi.org/10.3390/FERMENTATION8050204>.
- [235] P. Shrestha, M. Rasmussen, S.K. Khanal, A.L. Pometto, J. Van Leeuwen, Solid-substrate fermentation of corn fiber by *Phanerochaete chrysosporium* and subsequent fermentation of hydrolysate into ethanol, *J Agric Food Chem*. 56 (2008) 3918–3924. <https://doi.org/10.1021/JF0728404>.
- [236] C. del Cerro, E. Erickson, T. Dong, A.R. Wong, E.K. Eder, S.O. Purvine, H.D. Mitchell, K.K. Weitz, L.M. Markillie, M.C. Burnet, D.W. Hoyt, R.K. Chu, J.-F. Cheng, K.J. Ramirez, R. Katahira, W. Xiong, M.E. Himmel, V. Subramanian, J.G. Linger, D. Salvachúa, Intracellular pathways for lignin catabolism in white-rot fungi, *Proceedings of the National Academy of Sciences*. 118 (2021). <https://doi.org/10.1073/pnas.2017381118>.
- [237] M.Á. Pallín, S. González-Rodríguez, G. Eibes, M. López-Abelairas, M.T. Moreira, J.M. Lema, T.A. Lú-Chau, Towards industrial application of fungal pretreatment in 2G biorefinery: scale-up of solid-state fermentation of wheat straw, *Biomass Convers Biorefin*. 1 (2022) 1–13. <https://doi.org/10.1007/S13399-022-02319-1>.

- [238] F.P. Casciadori, A. Bück, J.C. Thoméo, E. Tsotsas, Two-phase and two-dimensional model describing heat and water transfer during solid-state fermentation within a packed-bed bioreactor, *Chemical Engineering Journal*. 287 (2016) 103–116. <https://doi.org/10.1016/J.CEJ.2015.10.108>.
- [239] The Chemical Engineering Plant Cost Index - Chemical Engineering, 2021. <https://www.chemengonline.com/pci-home> (accessed March 18, 2023).
- [240] M.S. Peters, K.D. Timmerhaus, *Plant Design and Economics for Chemical Engineers*. 3rd Edition, McGraw-Hill., 1991.
- [241] U.S. Bureau of Labor Statistics. Producer Price Index by Commodity: Chemicals and Allied Products [WPU06], (2023). <https://alfred.stlouisfed.org/series?seid=WPU06> (accessed March 18, 2023).
- [242] Eurostat Average full time adjusted salary per employee, (2021). [https://ec.europa.eu/eurostat/databrowser/view/NAMA\\_10\\_FTE\\_\\_custom\\_4232263/bookmark/table?lang=en&bookmarkId=fafb4e3b-f3aa-4907-9102-16be8df6f775](https://ec.europa.eu/eurostat/databrowser/view/NAMA_10_FTE__custom_4232263/bookmark/table?lang=en&bookmarkId=fafb4e3b-f3aa-4907-9102-16be8df6f775) (accessed March 18, 2023).
- [243] R. Sinnott, G. Towler, Costing and Project Evaluation, *Chemical Engineering Design*. (2020) 275–369. <https://doi.org/10.1016/B978-0-08-102599-4.00006-0>.
- [244] W. Moomaw, P. Burgherr, G. Heath, M. Lenzen, A. Nyboer, J; VerbruggeEdenhofer, Annex II: Methodology. In IPCC Special Report on Renewable Energy Sources and Climate Change Mitigation, 2012. [https://archive.ipcc.ch/pdf/special-reports/srren/SRREN\\_FD\\_SPM\\_final.pdf](https://archive.ipcc.ch/pdf/special-reports/srren/SRREN_FD_SPM_final.pdf).
- [245] M. Van Dael, T. Kuppens, S. Lizin, S. Van Passel, *Techno-economic Assessment Methodology for Ultrasonic Production of Biofuels*, (2015) 317–345. [https://doi.org/10.1007/978-94-017-9624-8\\_12](https://doi.org/10.1007/978-94-017-9624-8_12).
- [246] D. Klein-Marcuschamer, P. Oleskowicz-Popiel, B.A. Simmons, H.W. Blanch, The challenge of enzyme cost in the production of lignocellulosic biofuels, *Biotechnol Bioeng*. 109 (2012) 1083–1087. <https://doi.org/10.1002/BIT.24370>.
- [247] M.H. Cheng, H. Huang, B.S. Dien, V. Singh, The costs of sugar production from different feedstocks and processing technologies, *Biofuels, Bioproducts and Biorefining*. 13 (2019) 723–739. <https://doi.org/10.1002/BBB.1976>.

- [248] J. Littlewood, R.J. Murphy, L. Wang, Importance of policy support and feedstock prices on economic feasibility of bioethanol production from wheat straw in the UK, *Renewable and Sustainable Energy Reviews*. 17 (2013) 291–300. <https://doi.org/10.1016/J.RSER.2012.10.002>.
- [249] C.E.R. Reis, N. Libardi Junior, H.B.S. Bento, A.K.F. de Carvalho, L.P. de S. Vandenberghe, C.R. Soccol, T.M. Aminabhavi, A.K. Chandel, Process strategies to reduce cellulase enzyme loading for renewable sugar production in biorefineries, *Chemical Engineering Journal*. 451 (2023) 138690. <https://doi.org/10.1016/J.CEJ.2022.138690>.
- [250] L. Ou, C. Dou, J.H. Yu, H. Kim, Y.C. Park, S. Park, S. Kelley, E.Y. Lee, Techno-economic analysis of sugar production from lignocellulosic biomass with utilization of hemicellulose and lignin for high-value co-products, *Biofuels, Bioproducts and Biorefining*. 15 (2021) 404–415. <https://doi.org/10.1002/BBB.2170>.
- [251] E. Miliotti, S. Dell’Orco, G. Lotti, A.M. Rizzo, L. Rosi, D. Chiaramonti, Lignocellulosic Ethanol Biorefinery: Valorization of Lignin-Rich Stream through Hydrothermal Liquefaction, *Energies* 2019, Vol. 12, Page 723. 12 (2019) 723. <https://doi.org/10.3390/EN12040723>.
- [252] S. V. Obydenkova, P.D. Kouris, E.J.M. Hensen, H.J. Heeres, M.D. Boot, Environmental economics of lignin derived transport fuels, *Bioresour Technol*. 243 (2017) 589–599. <https://doi.org/10.1016/J.BIORTECH.2017.06.157>.
- [253] A. Lago, H. Hernando, J.M. Moreno, D.P. Serrano, J. Feroso, Valorisation of a lignin-rich residue via catalytic pyrolysis over ZrO<sub>2</sub>/ZSM-5 technical catalyst, *Fuel Processing Technology*. 215 (2021) 106746. <https://doi.org/10.1016/J.FUPROC.2021.106746>.
- [254] P. Chairattanamakorn, T. Imai, R. Kondo, M. Ukita, P. Prasertsan, Screening thermotolerant white-rot fungi for decolorization of wastewaters, *Appl Biochem Biotechnol*. 128 (2006) 195–204. <https://doi.org/10.1385/ABAB:128:3:195>.
- [255] M. Couturier, D. Navarro, D. Chevret, B. Henrissat, F. Piumi, F.J. Ruiz-Dueñas, A.T. Martinez, I. V. Grigoriev, R. Riley, A. Lipzen, J.G. Berrin, E.R. Master, M.N. Rosso, Enhanced degradation of softwood versus hardwood by the white-rot fungus *Pycnoporus coccineus*, *Biotechnol Biofuels*. 8 (2015) 1–16. <https://doi.org/10.1186/S13068-015-0407-8>.

- [256] V. Mishra, A.K. Jana, M.M. Jana, A. Gupta, Fungal pretreatment of sweet sorghum bagasse with supplements: improvement in lignin degradation, selectivity and enzymatic saccharification, *3 Biotech.* 7 (2017) 110. <https://doi.org/10.1007/s13205-017-0719-4>.
- [257] Y.H.P. Zhang, J. Hong, X. Ye, Cellulase Assays, in: *Methods Mol Biol*, Humana Press, Totowa, NJ, 2009: pp. 213–231. [https://doi.org/10.1007/978-1-60761-214-8\\_14](https://doi.org/10.1007/978-1-60761-214-8_14).
- [258] M.D. Asemoloye, M.A. Marchisio, V.K. Gupta, L. Pecoraro, Genome-based engineering of ligninolytic enzymes in fungi, *Microbial Cell Factories* 20:1. 20 (2021) 1–18. <https://doi.org/10.1186/S12934-021-01510-9>.
- [259] C. Zhang, X. Meng, X. Wei, L. Lu, Highly efficient CRISPR mutagenesis by microhomology-mediated end joining in *Aspergillus fumigatus*, *Fungal Genetics and Biology.* 86 (2016) 47–57. <https://doi.org/10.1016/J.FGB.2015.12.007>.
- [260] J.E. Kowalczyk, S. Saha, M.R. Mäkelä, Application of crispr/cas9 tools for genome editing in the white-rot fungus *dichomitus squalens*, *Biomolecules.* 11 (2021). <https://doi.org/10.3390/BIOM11101526>.
- [261] T. Boontawon, T. Nakazawa, C. Inoue, K. Osakabe, M. Kawauchi, M. Sakamoto, Y. Honda, Efficient genome editing with CRISPR/Cas9 in *Pleurotus ostreatus*, *AMB Express.* 11 (2021) 1–11. <https://doi.org/10.1186/S13568-021-01193-W>.

## Curriculum vitae



Name: **Nikolett Wittner**  
E-mail: [nikolettwittner@gmail.com](mailto:nikolettwittner@gmail.com)  
Linkedin: <https://be.linkedin.com/in/nikolett-wittner-b9762a155>  
ResearchGate: <https://www.researchgate.net/profile/Nikolett-Wittner-2>

### Education

2015-2017 Budapest University of Technology and Economics- Master of Science in Chemical Engineering, specialising in Analytical Chemistry. Graduated with highest honours in July 2017  
*Master's thesis: Solid-phase synthesis of molecularly imprinted nanoparticles for protein recognition*

February-June 2017 University of Antwerp- Erasmus student  
*Master's thesis: Evaluation of measuring techniques for microbial growth during solid-state fermentation*

2011-2015 Budapest University of Technology and Economics Bachelor in Chemical Engineering  
*Bachelor's thesis: Synthesis of molecularly imprinted nanoparticles in lateral-flow immunoassay membranes*

## Research experience

Oct 2018-Sept 2022    PhD student-BioWAVE (Bio-Chemical Wastewater Valorisation and Engineering)

Project: Improving and characterizing solid-state fungal pretreatment by *Phanerochaete chrysosporium* for sugar production from poplar wood

Feb 2018-Sept 2018    Researcher-BioGEM (Bio-Chemical Green Engineering & Materials)

Project: Determination of volatile aroma compounds in fruit juice using gas chromatography coupled with solid phase microextraction

Aug 2017-Dec 2017    Researcher-BioGEM

Project: Evaluation of measuring techniques (such as FTIR, oxygen uptake rate measurement, glucosamine assay) to follow up solid-state fermentation

## Conference attendance (poster/oral presentation)

**EFIB 2020** - European Forum for Industrial Biotechnology and the Bioeconomy. Poster presentation | Online | October 5-6, 2020

Poster: *Enhanced fungal delignification and enzymatic digestibility of poplar wood by combined CuSO<sub>4</sub> and MnSO<sub>4</sub> supplementation.*

**BIORESTEC 2021** - 3rd International Conference on Bioresource Technology for Bioenergy, Bioproducts & Environmental Sustainability. Poster presentation | Online | May 17-19, 2021.

Poster Award Winner with the poster: *Enhanced fungal delignification and enzymatic digestibility of poplar wood by combined CuSO<sub>4</sub> and MnSO<sub>4</sub> supplementation.*

**RRB 2022** - 18th International Conference on Renewable Resources and Biorefineries. Poster presentation | Brugge (Belgium) | June 1-3, 2022

Poster: *Rapid lignin quantification for fungal wood pretreatment by ATR-FTIR spectroscopy*



**WasteEng2022** - 9th International Conference on Engineering for Waste and Biomass Valorisation. Oral presentation | Copenhagen (Denmark) | June 27-30, 2022

Oral presentation: *Successful elimination of substrate sterilization during solid-state fungal pretreatment of poplar wood*

### List of publications

#### First authored (obtained during the doctoral education)

N. Wittner, W. Broos, J. Bauwelinck, J. Slezsák, S.E. Vlaeminck, I. Cornet, Enhanced fungal delignification and enzymatic digestibility of poplar wood by combined CuSO<sub>4</sub> and MnSO<sub>4</sub> supplementation, *Process Biochem.* 108 (2021) 129–137.

<https://doi.org/10.1016/J.PROCBIO.2021.06.002>

N. Wittner, J. Slezsák, W. Broos, J. Geerts, S. Gergely, S.E. Vlaeminck, I. Cornet, Rapid lignin quantification for fungal wood pretreatment by ATR-FTIR spectroscopy, *Spectrochim. Acta Part A Mol. Biomol. Spectrosc.* 285 (2023) 121912.

<https://doi.org/10.1016/J.SAA.2022.121912>

N. Wittner, S. Gergely, J. Slezsák, W. Broos, S.E. Vlaeminck, I. Cornet, Follow-up of solid-state fungal wood pretreatment by a novel near-infrared spectroscopy-based lignin calibration model, *J Microbiol Methods.* 208 (2023) 106725.

<https://doi.org/10.1016/J.MIMET.2023.106725>

#### Other publications

I. Cornet, N. Wittner, G. Tofani, S. Tavernier, FTIR as an easy and fast analytical approach to follow up microbial growth during fungal pretreatment of poplar wood with *Phanerochaete chrysosporium*, *J. Microbiol. Methods.* 145 (2018) 82–86.

<https://doi.org/10.1016/J.MIMET.2018.01.004>

J. Bauwelinck, N. Wittner, W. Broos, M. Wijnants, S. Tavernier, I. Cornet, Kinetic modelling of the biochemical 9-octadecenedioic acid production and lipid accumulation using differently functionalised C18:1 substrates, *Biochem. Eng. J.* 166 (2021) 107872. <https://doi.org/10.1016/J.BEJ.2020.107872>

J. Bauwelinck, M. Caluwé, M. Wijnants, N. Wittner, W. Broos, J. Dries, V. Akkermans, S. Tavernier, I. Cornet, Chocolate industry side streams as a valuable feedstock for microbial long-chain dicarboxylic acid production, *Biochem. Eng. J.* 167 (2021). <https://doi.org/10.1016/J.BEJ.2020.107888>

W. Broos, N. Wittner, J. Geerts, J. Dries, S.E. Vlaeminck, N. Gunde-Cimerman, A. Richel, I. Cornet, Evaluation of Lignocellulosic Wastewater Valorisation with the Oleaginous Yeasts *R. kratochvilovae* EXF7516 and *C. oleaginosum* ATCC 20509, *Fermentation*. 8 (2022) 204. <https://doi.org/10.3390/FERMENTATION8050204/S1>